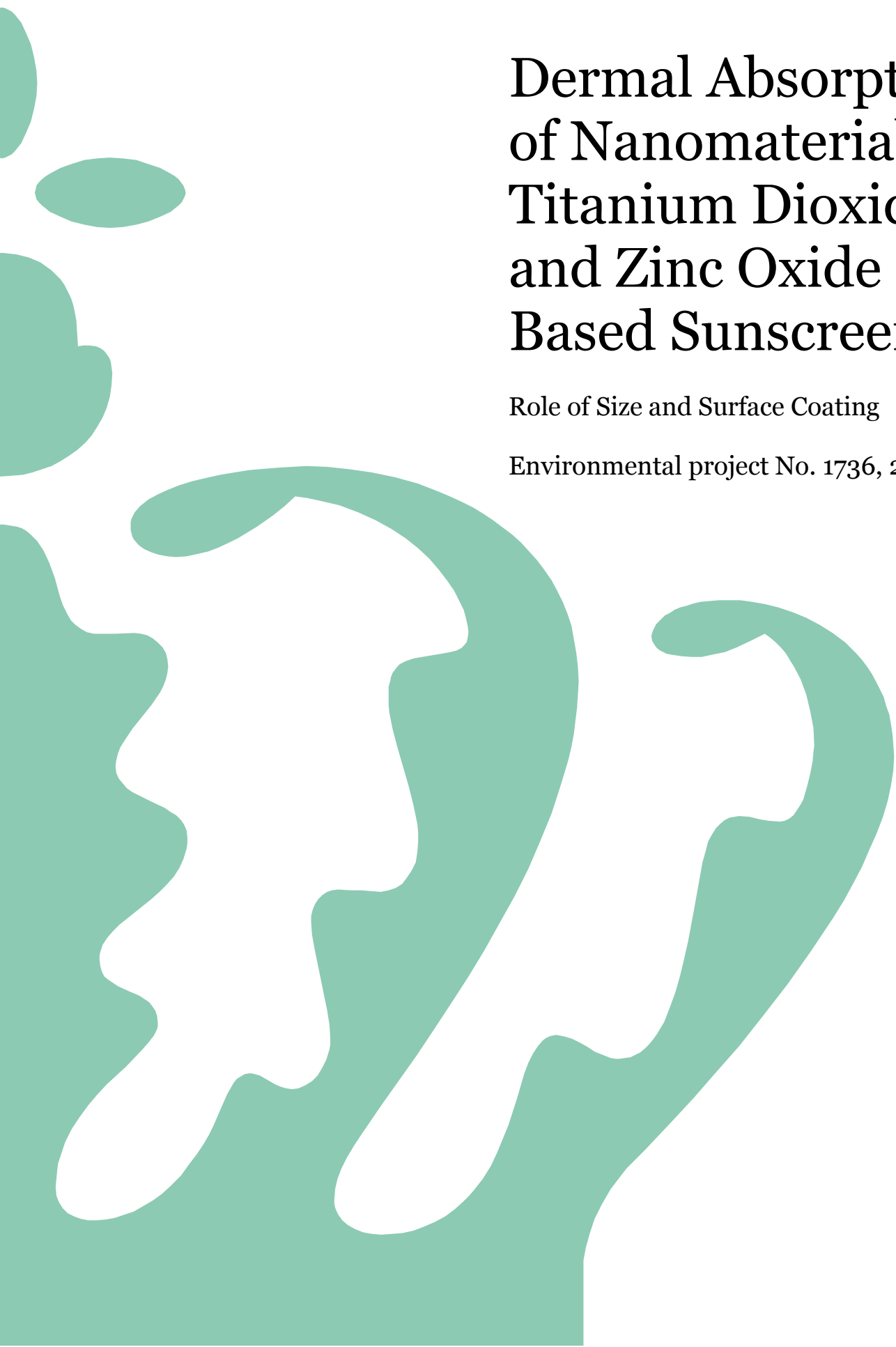


Dermal Absorption of Nanomaterials Titanium Dioxide and Zinc Oxide Based Sunscreen

Role of Size and Surface Coating

Environmental project No. 1736, 2015



Title:

Dermal Absorption of Nanomaterials Titanium Dioxide and Zinc Oxide Based Sunscreen

Editing:

Christiane Beer, Department of Public Health, Aarhus University, Denmark

Karin Stenderup, Department of Dermatology, Aarhus University Hospital, Denmark

Jing Wang, iNANO Center, Aarhus University, Denmark

Duncan S. Sutherland, iNANO Center, Aarhus University, Denmark

Jens R. Nyengaard, Department of Clinical Medicine, Aarhus University, Denmark

Published by:

The Danish Environmental Protection Agency

Strandgade 29

1401 Copenhagen K

Denmark

www.mst.dk/english

Year:

2015

ISBN no.

978-87-93352-53-7

Disclaimer:

When the occasion arises, the Danish Environmental Protection Agency will publish reports and papers concerning research and development projects within the environmental sector, financed by study grants provided by the Danish Environmental Protection Agency. It should be noted that such publications do not necessarily reflect the position or opinion of the Danish Environmental Protection Agency.

However, publication does indicate that, in the opinion of the Danish Environmental Protection Agency, the content represents an important contribution to the debate surrounding Danish environmental policy.

Sources must be acknowledged.

Contents

Foreword	5
Executive Summary	6
Resumé	11
1. Introduction	16
1.1 Scientific background	16
1.2 Objective of the project.....	17
1.3 Experimental methods	18
1.4 Structure of the report	18
2. Material and Methods	19
2.1 Overview of the experimental setup.....	19
2.2 Nanoparticles	19
2.3 Sunscreen formulation	21
2.4 Preparation of nanoparticle containing sunscreen	21
2.5 Nanoparticle characterization	23
2.5.1 TEM and EDX analysis of nanoparticle dry powders.....	23
2.5.2 Dynamic light scattering (DLS) analysis of the nanoparticle size and surface charge in MilliQ water.....	23
2.5.3 <i>In situ</i> observation of Nanoparticles in sunscreen using an optical microscope	23
2.5.4 Acoustic attenuation spectroscopy (AAS)	24
2.6 <i>In vitro</i> and <i>in vivo</i> skin models	24
2.6.1 Treated surface area.....	24
2.6.2 Time of exposure.....	24
2.6.3 Dosage of nanoparticles.....	24
2.6.4 <i>In vitro</i> EpiDerm™ system (MatTek) – normal, human 3D epidermis model	26
2.6.5 <i>In vivo</i> mouse model for acute irritant contact dermatitis (ICD).....	31
2.6.6 <i>In vivo</i> xenograft human skin model	32
2.6.7 Statistical analysis	37
3. Results	38
3.1 Nanoparticle preparation and characterization	38
3.1.1 Characterization of the pre-dispersant	38
3.1.2 Characterization of sunscreen	38
3.1.3 Characterization of the nanoparticle powders.....	39
3.1.4 Particle size distribution of nanoparticles dispersed in MilliQ water, pre- dispersant C12-C15 alkyl benzoate and sunscreen	42
3.1.5 Acoustic attenuation spectroscopy (AAS) measurement of the particle size distribution in sunscreen	46
3.1.6 Conclusion nanoparticle characterization	48
3.2 Dermal absorption/penetration of TiO ₂ and ZnO NPs in <i>in vitro</i> EpiDerm™ skin model.....	48
3.2.1 Effect of sunscreen on skin model permeability – TEER measurements	48

3.2.2	Investigation of the transport of TiO ₂ and ZnO NPs through EpiDerm™ skin models using ICP-MS.....	49
3.2.3	Cell viability.....	52
3.2.4	Cytokine analysis.....	53
3.2.5	Histology and transmission electron microscopy.....	58
3.2.6	Conclusion <i>in vitro</i> EpiDerm™ skin model.....	60
3.3	<i>In vivo</i> skin models.....	61
3.3.1	<i>In vivo</i> TPA irritant contact dermatitis (ICD) mouse model	61
3.3.2	Xenograft human skin model	69
3.3.3	Conclusion <i>in vivo</i> skin models.....	72
4.	Discussion.....	73
5.	Conclusion	79
	References	80
Appendix 1:	Nanoparticle information as provided by the manufacturer.....	85
Appendix 2:	Transmission electron microscopy	89
Appendix 3:	Weight and ear thickness in <i>in vivo</i> mouse model for acute irritant contact dermatitis after exposure to sunscreen with or without nanoparticles	105
Appendix 4:	Weight measurements in <i>in vivo</i> human xenograft skin model	112
Appendix 5:	ICP-MS measurement data of medium below <i>in vitro</i> EpiDerm skin models and TEER of the tissues after 20h of exposure.....	114
Appendix 6:	Cytokine release of <i>in vitro</i> EpiDerm skin models after 20h exposure (AE) and 3 days after ended exposure.....	117
Appendix 7:	Test report ICP-MS measurements of the <i>in vitro</i> and <i>in vivo</i> skin models: cell culture medium, mice ears and human skin.....	131
Appendix 8:	Certificate of analysis for the used lots of EpiDerm™ skin model	136

Foreword

In 2011 the Danish government and the Red-Green Alliance (a.k.a. Enhedslisten) decided on an initiative called “Bedre styr på nano” (“Better control of nano”) for the Danish Finance Act of 2012. This initiative is running for four years (2012-2015) and includes several projects for the use of nanomaterials in products on the Danish market and their consequences on consumers and the environment. Furthermore, the aim is to clarify possible risks that might be associated with nanomaterials for consumers and the environment.

The current project ‘Dermal Absorption of Nanomaterials Titanium Dioxide and Zinc Oxide in Sunscreen’ is part of this “Better control of nano” initiative and was started in March 2014 and ended in June 2015. The aim of this project was to generate new knowledge on physicochemical properties that may influence dermal absorption of nanomaterials.

The project was carried out at Aarhus University and has been headed by Ass.Prof. Christiane Beer as project leader and scientific manager with significant contributions by the project collaborates and associated scientists Ass.Prof. Karin Stenderup, Dr. Jing Wang, Prof. Jens Randel Nyengaard, and Ass.Prof. Duncan S. Sutherland.

The associated steering committee for this project had the following members:

Anne Mette Zenner Boisen, Danish Environmental Protection Agency, Copenhagen, Denmark

Craig Poland, Institute of Occupational Medicine, Edinburgh, Great Britain

The project was financed by the Danish Finance Act, Agreement 2012-2015 on Better Control of Nanomaterials and their Safety (“Bedre styr på nano”).

Executive Summary

Under the Agreement "Better Control of Nanomaterials" ("Bedre styr på nanomaterialer"), the Danish Environmental Protection Agency (EPA) has initiated a series of projects with the aim of further clarifying possible risks to consumers and the environment. These projects will also help to generate new knowledge on the impact of nanomaterials on consumers and the environment in selected areas of research. The current experimental project on dermal absorption of nanomaterials is part of this series.

The absorption of nanomaterials into or through the skin may result in topical or systemic effects such as inflammation, allergy and cancer. Knowledge concerning dermal penetration and absorption of nanomaterials is limited. The recent evaluation of the existing scientific literature on dermal absorption commissioned by the Danish EPA [Poland CA et al., 2013] has shown that the interpretation of results on this endpoint is hampered by non-harmonized testing approaches, insufficient characterization of test materials and the alteration of multiple experimental parameters in a non-systematic way. To further ensure that results from dermal absorption studies can be used in a wider setting the "Dermal absorption of nanomaterials" report [Poland CA et al., 2013] recommends that future studies focus on the alteration of a single physicochemical property (such as size, surface charge, hydrophobicity e.g.) in order to help identify potential structure activity relationships between nanomaterials and their dermal penetration efficiency.

It is widely accepted that the excessive exposure to sunlight significantly increases the risk of developing skin cancers such as malignant melanoma. This risk is efficiently reduced by use of sunscreens and sun blockers as they, depending on their protection properties, reduce or prevent the UV-A and UV-B radiation penetrating the skin [Green et al., 2011]. With the development of nanotechnology, titanium dioxide nanoparticles (TiO₂ NPs) and zinc oxide nanoparticles (ZnO NPs) are increasingly used as physical sunscreens. At present, TiO₂ is included in Annex VI of the Cosmetics Regulation, which is a positive list of permitted UV filters. ZnO is currently not included in Annex VI, but it is expected to be allowed in both the nano- and non-nano form in up to 25% in the near future. The purity, crystallinity, size and coating are predefined, when these UV filters are used in the nano-form. The Nordic eco-label 'Svanen' has not allowed the use of nanomaterials in cosmetics as of 2011. TiO₂ NPs and zinc oxide nanoparticles are an effective filter against UV-radiation and are at the same time non-irritating and more compatible with sensitive skin than chemical sunscreens. In addition, compared to micro-sized titanium dioxide or zinc oxide particles the nano-sized form of these particles have more consumer-friendly characteristics that allow an easy application of the sunscreens. Both, TiO₂ NPs and ZnO NPs do not leave an unsightly whitish tint on the skin. However, due to their small size there have been concerns that TiO₂ NPs and ZnO NPs might penetrate the skin thereby interacting with lower, living layers of the epidermis and dermis, and be absorbed into the blood stream leading to potential systemic health risks [Donaldson et al., 2004; Maynard et al., 2011; Nel et al., 2006; Oberdorster et al., 2005; Singh et al., 2009; Tetley, 2007]. From *in vitro* studies in cell cultures it is known that nanoparticles can induce, e.g., oxidative stress and genotoxicity [Nel et al., 2006; Singh et al., 2009]. Therefore, there are concerns that dermal absorption and penetration of nanomaterials may result in topical or systemic effects such as cardiovascular disease and cancer. For titanium dioxide nanoparticles this might be of special concern as they are chemically inert and could theoretically accumulate within the body. Although most of the scientific studies that have been performed to date show that TiO₂ NPs and ZnO NPs are not absorbed through the skin to any great extent [Poland CA et al., 2013; SCCS (Scientific Committee on Consumer Safety), 2012; SCCS (Scientific Committee on Consumer Safety), 2014], there have been concerns that TiO₂ NPs can penetrate the skin through hair follicles

where they have been found [Senzui et al., 2010]. However, it might be questioned if this leads to penetration. If a nanoparticles moves down into a hair follicle towards the base of the hair shaft, it is still external as there still is a dermal barrier between the nanoparticle and the replicating skin cells and vasculature. Another issue is the possible absorption through damaged skin, e.g., due to sun burns, skin diseases or skin injuries.

In their “Opinion on titanium dioxide (nano form)” the Scientific Committee on Consumer Safety (SCCS) concluded: “*From the limited relevant information provided in the submission, and the information from open literature, the SCCS considers that TiO₂ nanomaterials in a sunscreen formulation are unlikely to lead to: systemic exposure to nanoparticles through human skin to reach viable cells of the epidermis, dermis, or other organs.*” [SCCS (Scientific Committee on Consumer Safety), 2014]. However, the SCCS also state that: “*Although there is no conclusive evidence at present to indicate penetration of TiO₂ nanoparticles through the skin to viable cells of the epidermis, a number of studies have shown that they can penetrate into the outer layers of the stratum corneum, and can also enter hair follicles and sweat glands.*” [SCCS (Scientific Committee on Consumer Safety), 2014]. For ZnO NPs the SCCS stated that there is no indication for dermal penetration of ZnO NPs based on the available scientific literature. However, a very small proportion of Zn ions that are released from the ZnO NPs may be available for systemic exposure after dermal application [SCCS (Scientific Committee on Consumer Safety), 2012]. In addition, the Danish EPA stated in the recently published report that knowledge on the dermal penetration and absorption of nanomaterials is still limited. They recommended that future studies should not only have a specific research question or hypothesis but also focus on the alteration of a single physicochemical property (e.g. such as size, surface charge, hydrophobicity) instead of change multiple physicochemical properties at a time to be able to identify properties that are critical for a dermal penetration of the skin. Furthermore, the application of the nanoparticles should occur in commercially-relevant formulations as well as detailed characterization of the particles in situ should be performed (i.e. within the test formulation). The report also noted that several studies report a considerable lag time between the application of the test substance and an appearance in the circulation.

We addressed the research question if the size or surface coating of TiO₂ NPs and ZnO NPs has an effect on the dermal penetration/absorption of the nanoparticles following these recommendations in this project by:

- Using a commercially available sunscreen as test formulation
- Including a lag time of several days after application of the nanoparticle containing sunscreen as well as repeated application of the nanoparticle containing sunscreen in case of *in vivo* experiments in mice models for inflamed skin and human skin
- Use of a newly available method, acoustic attenuation spectroscopy, to determine the particle size distribution directly in sunscreen.

Based on these recommendations we investigated in this project:

- 1) the dermal absorption and penetration of the test nanomaterials titanium dioxide and ZnO NPs in *in vitro* EpiDerm™ system (MatTek) for normal, human 3D epidermis, *in vivo* mouse model for acute irritant contact dermatitis, and xenograft human skin model.
- 2) the effect of size and surface coating on dermal absorption and penetration of the test nanomaterials TiO₂ NPs (size and coating) and ZnO NPs (coating).
- 3) the test nanomaterials in OECD validated models for skin corrosion and skin irritation as human health hazard endpoints according to the OECD test guidelines #431 and #439, respectively.
- 4) the physicochemical properties of the used nanomaterials with special focus on the particle size distribution in sunscreen.

An overview of the experimental design is shown in Figure 1. The *in vitro* skin models were used in OECD validated models for skin corrosion and skin irritation as human health hazard endpoints according to the OECD test guidelines #431 and #439, respectively. In addition, this *in vitro* model was used to investigate the inflammatory potential of nanomaterial containing sunscreen using multiplex cytokine assays. Preparation and analysis of samples from the treated *in vitro* 3D epidermis models and biopsies from the *in vivo* skin models were evaluated for dermal absorption and penetration of TiO₂ NPs and ZnO NPs using transmission electron microscopy (TEM), inductively coupled plasma mass spectrometry (ICP-MS), and hematoxylin and eosin (H&E) staining. The project was performed in three stages:

- 1) Production of 8 different nanoparticle containing sunscreens and characterization of the nanoparticles
- 2) Exposure of *in vitro* and *in vivo* skin models to these sunscreens
- 3) Analysis of the dermal penetration of the skin models as well as of the effect on the *in vitro* skin model.

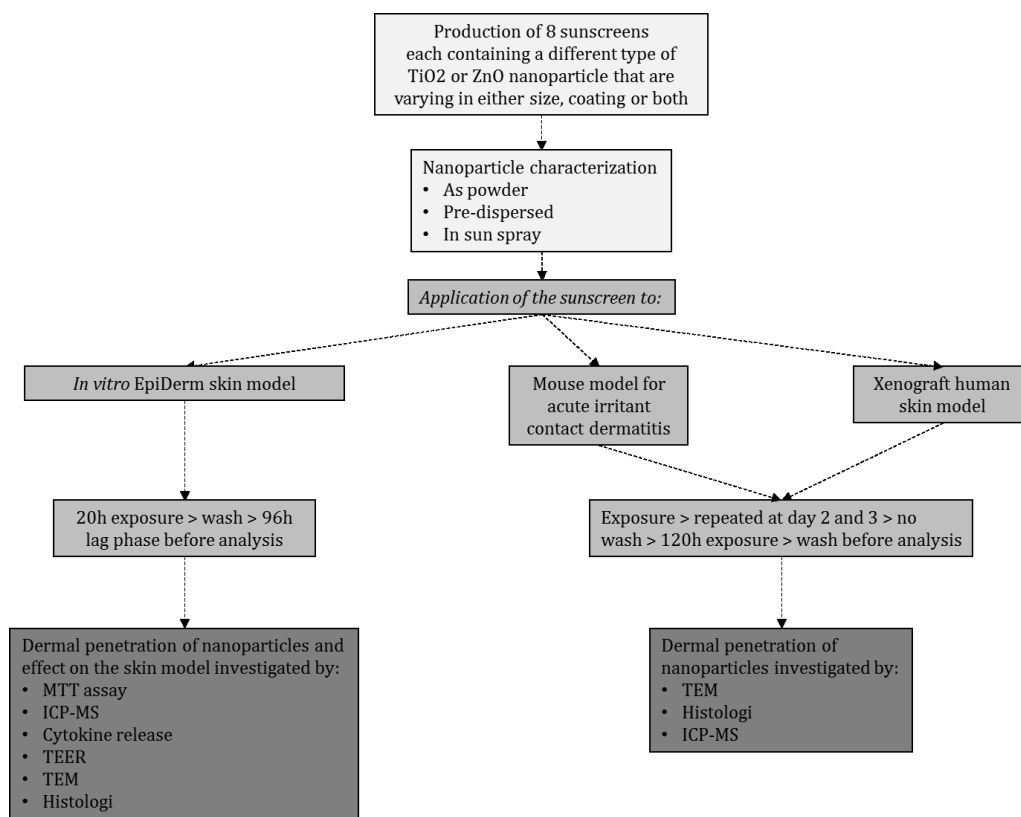


FIGURE 1: OVERVIEW OF THE EXPERIMENTAL DESIGN OF THE PROJECT

It is assumed that a large part of the Danish population, including children, use sunscreen during the summer. In a recommendation by the European Commission, it has been calculated that using 36 g of sunscreen per day offers sufficient protection [European Commission, 2006]. The quantities we used in the *in vitro* and *in vivo* tissue models are higher and correspond to a realistic "worst case" scenario in order to ensure that the results from this project reflect a real life situation as closely as possible.

One important part of this project was the characterization of the nanoparticles in sunscreen, especially their size distribution. Due to the complexity of a system like sunscreen (viscosity, oil in water emulsion) the characterization was difficult to perform. However, a new method, acoustic attenuation spectroscopy, could be used to measure the particle size distribution directly in sunscreen. With this method we could show that in most of the prepared sunscreens, the nanoparticles have a particle size distribution where 50% of the particles are around 200 nm. In two of the prepared sunscreens the particle size distribution was noticeable larger with of 393 nm and 661 nm, respectively. Furthermore, at least 90% of the particles had a size of larger than 100 nm. But, as these data are based on the weight of the nanoparticles and nanoparticle agglomerations, there could be a high number of particles below 100 nm. This is due to the fact that larger particles weight more and thereby mask for the small particles in the analysis. A way to explain this phenomenon is by looking at three particles with either 1 μm , 2 μm , or 3 μm in diameter, respectively. When looking at the number size distribution for these particles each particle size accounts for one third of the total. Converted to a volume ($4/3\pi r^3$) or weight size distribution, 75% of the total volume would come from the 3 μm particles, and less than 3% comes from the 1 μm particles. It becomes obvious that the majority of the total particle mass or volume comes from the larger particles. Even if 90% of the particles are larger than 100 nm based on their weight there could still be more than 50% of the particles smaller than 100 nm based on their number. This limitation of this study should be addressed in future studies investigating the number size distribution of nanoparticles in commercially available sunscreens.

When investigating the dermal penetration in the EpiDerm™ skin model; the ICP-MS analysis results show that in the case of zinc oxide nanoparticle containing sunscreen, dermal penetration of ZnO was clearly apparent whereas for TiO₂ the result was more uncertain and not clear. However, none of the other used methods can confirm this result. Both, TiO₂ NPs and ZnO NPs have no effect on skin corrosion and skin penetration and do not induce secretion of cytokines and inflammatory responses. Furthermore, no nanoparticles were detected by electron microscopy beneath the upper surface of the skin model although based on the ICP-MS analysis several hundred ZnO NPs should be present in the electron microscopy thin sections. As ZnO NPs are known to be dissolved in biological systems [SCCS (Scientific Committee on Consumer Safety), 2012], we conclude that ZnO NPs are not transported in their particulate form but as zinc ions through the cell layer. This is in agreement with the available literature as no ZnO NPs were found in viable skin layers [Cross et al., 2007; Durand et al., 2009; Dussert et al., 1997; Filipe et al., 2009; Gamer et al., 2006; Kuo et al., 2009; Song et al., 2011a; Szikszai et al., 2010]. Only a few studies could show minimal transdermal absorption [Monteiro-Riviere et al., 2011; Gulson et al., 2010; Gulson et al., 2012]. However, it is not clear if this absorption occurred as ZnO NPs or Zn ions and the SCCS concluded that *“Considering the dissolution of ZnO, it is most likely that the zinc was absorbed in ionic form.”* [SCCS (Scientific Committee on Consumer Safety), 2012] supporting the conclusion of our study. For TiO₂ NPs we conclude that penetration of the EpiDerm™ skin model did not occur at or above the limit of detection.

Within the *in vivo* skin models (mouse model for acute irritant contact dermatitis, xenograft human skin model) that were used to investigate the dermal penetration/absorption of TiO₂ NPs, titanium was detected in skin biopsies using ICP-MS. The investigation of dermal absorption/penetration was limited to TiO₂ NPs in the *in vivo* skin models as TiO₂ NPs are the only nanomaterials [Poland CA et al., 2013] use as physical UV-filter in sunscreens in Denmark.

The amount of titanium in the skin of the mice ears varied considerably between 3.2 and 121.56 mg/kg dry weight corresponding to 0.0011% to 0.12% of the amount of the originally added TiO₂ NPs. The measured concentration of titanium in the human xenograft skin varies between <0.11 and 2.51 mg/kg dry weight and therefore does not reach the amount of the originally added TiO₂ NPs (0.015% to 0.00014% of the originally added TiO₂ NPs). Especially for the mouse model for acute irritant contact dermatitis, the possibility of the penetration of the skin by TiO₂ NPs could be excluded as no nanoparticles were detected in the deeper skin layers by transmission electron

microscopy (TEM). Based on our estimations from the ICP-MS results at least several hundred TiO₂ NPs should be present per TEM thin section with the exception of the largest investigated TiO₂ NPs with a size of 100 nm. Here only a few particles would be present per thin section making a detection of the particles more unlikely. For the xenograft skin model dermal penetration/absorption of TiO₂ NPs did not occur at or above the limit of detection. In both skin models nanoparticle like structures that were observed in the samples were also found in the controls and were identified to be either melanin vesicles of the skin or polysomes. TiO₂ NPs were only observed in stratum corneum. For both *in vivo* skin models, an incomplete washing off of the sunscreen from the skin after the end of the experiment could be an explanation for the detection of titanium in the skin biopsies by ICP-MS but not by TEM.

Based on our results using *in vitro* and *in vivo* mouse and human skin models we conclude that dermal penetration of TiO₂ and ZnO NPs did not occur at or above the limit of detection of the used experimental methods. Should absorption of TiO₂ and ZnO nanoparticles occur at levels below the detection limit of the assays used herein, the systemic dose would be very small (far lower than the doses used in the studies discussed above) and so highly unlikely to cause systemic toxicity based on toxicological evidence in rodents. This is in accordance with the conclusions that were made by the SCCS that stated that both kind of nanoparticles are safe to use for dermal applications up to a concentration of 25% in cosmetic products [SCCS (Scientific Committee on Consumer Safety), 2012; SCCS (Scientific Committee on Consumer Safety), 2014].

Resumé

I henhold til aftalen "Bedre Styr på nanomaterialer" har Miljøstyrelsen igangsat en række projekter med det formål yderligere at tydeliggøre eventuelle risici for forbrugerne og miljøet. Disse projekter vil også bidrage til at skabe ny viden om virkningen af nanomaterialer for forbrugerne og miljøet på udvalgte forskningsområder. Det nuværende forsøgsprojekt om hudabsorption af nanomaterialer er en del af denne serie.

Absorption af nanomaterialer ind i eller gennem huden, kan resultere i topiske eller systemiske virkninger såsom inflammation, allergi og cancer. Viden om hudpenetration og -absorption af nanomaterialer er begrænset. Den seneste evaluering af den eksisterende videnskabelige litteratur om absorption gennem huden, som blev foranlediget af Miljøstyrelsen [Poland CA et al., 2013], har vist, at fortolkningen af resultaterne på dette område hæmmes af ikke-harmoniserede testmetoder, utilstrækkelig karakterisering af testmaterialer og ved at flere testparametre ændres samtidig på en ikke-systematisk måde. For yderligere at sikre, at resultaterne fra undersøgelser af hudabsorption af nanomaterialer kan sige noget generelt anbefaler Miljøstyrelsens tidligere rapport "Dermal absorption af nanomaterialer" [Poland CA et al., 2013], at fremtidige studier fokuserer på ændring af en enkelt fysisk-kemisk egenskab (såsom størrelse, overfladebelægning (coating), hydrofobicitet etc.) ad gangen for at kunne identificere potentielle struktur-aktivitetsforhold mellem nanomaterialer og deres evne til at trænge ind i eller gennem huden.

Det er almindeligt accepteret, at overdreven udsættelse for direkte sollys øger risikoen for at udvikle hudkræft i form af almindelig hudkræft og modermærkekræft. Denne risiko reduceres væsentligt ved brug af solcreme og solblokker, som, afhængigt af deres beskyttelsesegenskaber, reducerer eller forhindrer UV-A og UV-B-stråling i at trænge ind i huden [Green et al., 2011]. I nanoteknologiens kølvand anvendes titaniumdioxid- og zinkoxidnanopartikler nu i stigende grad som fysiske solfiltre verden over. På nuværende tidspunkt er TiO₂ opført i bilag VI til Kosmetikforordningen, hvilket er en positivliste over tilladte UV-filtre. ZnO er i øjeblikket ikke opført i bilag VI, men det forventes at blive tilladt i både nano- og ikke-nano formen med op til 25% i den nærmeste fremtid. Renhed, krystallinitet, størrelse og overfladebelægning (coating) er prædefinerede, når disse UV-filtre anvendes i nano-form. Det nordiske Svanemærke 'Svanen' har ikke tilladt brug af nanomaterialer i kosmetik siden 2011. Titaniumdioxid- og zinkoxidnanopartikler er effektive filtre mod UV-stråling og er, på samme tid, ikke-irriterende og således mere skånsomme overfor følsom hud sammenlignet med kemiske solfiltre. Desuden er titaniumdioxid- og zinkoxidpartikler i nanostørrelse mere brugervenlige i forhold til større titaniumdioxid- eller zinkoxidpartikler (i mikrometer størrelse). Ydermere efterlader hverken titaniumdioxid- eller zinkoxidnanopartikler et skæmmende hvidligt lag på huden efter påføring. Men, på grund af deres reducerede størrelse, har der været bekymring for, om titaniumdioxid- og zinkoxidnanopartikler kan trænge ind i huden og derved påvirke de lavere liggende lag af over- og underhuden, og om en eventuel optagelse i blodbanen kan føre til potentielle systemiske sundhedsrisici [Donaldson et al., 2004; Maynard et al., 2011; Nel et al., 2006; Oberdorster et al., 2005; Singh et al., 2009; Tetley, 2007]. Fra *in vitro* undersøgelser i cellekulturer er det kendt, at nanopartikler kan fremkalde, f. eks. oxidativ stress (dannelse af frie radikaler) og DNA skader [Nel et al., 2006; Singh et al., 2009] og dermed føre til forskellige sygdomme så som hjerte-kar-sygdomme og kræft. For titaniumdioxidnanopartikler kunne dette være af særlig bekymring, da de ikke nedbrydes i kroppen og derfor teoretisk set kunne ophobes. Selvom de fleste, af de til dato, udførte videnskabelige undersøgelser viser, at titaniumdioxid- og zinkoxidnanopartikler ikke absorberes i huden [Poland CA et al., 2013; SCCS (Scientific Committee on Consumer Safety), 2012; SCCS (Scientific Committee on Consumer Safety), 2014], har der været bekymring for, om titaniumdioxidnanopartikler kan trænge ind i huden via hårsækkene [Senzui et al., 2010]. Det er dog tvivlsomt om hårsækken kan føre til optagelse igennem huden, da en

nanopartikel, som bevæger sig ned i en hårsæk, stadig er uden på huden og der er stadig er en hudbarriere mellem nanopartiklen og de underliggende hudceller og blodkar. Et andet problem er mulig absorption i beskadiget hud, opstået pga. solskoldning, diverse hudsygdomme eller hudlæsioner.

I rapporten "Opinion on titanium dioxide (nano form)" konkluderer "The Scientific Committee on Consumer Safety (SCCS)" følgende: "Ud fra de begrænsede eksisterende relevante oplysninger og oplysninger fra den tilgængelige litteratur, mener SCCS, at det er usandsynligt at titaniumdioxidnanopartikler i solcreme fører til systemisk eksponering via menneskehuden og at partiklerne når de levedygtige celler i epidermis, dermis, og andre organer" [SCCS (Scientific Committee on Consumer Safety), 2014]. På den anden side siger SCCS også, at: "Selvom der ikke er noget afgørende bevis for, på nuværende tidspunkt, at titaniumdioxidnanopartikler kan gennemtrænge huden og nå de levedygtige celler i overhuden, har en række undersøgelser vist, at de kan trænge ind i de ydre lag af stratum corneum (skællaget), og kan trænge ind i hårsække og svedkirtler." [SCCS (Scientific Committee on Consumer Safety), 2014]. For zinkoxidnanopartikler erklærer SCCS, at der, baseret på den tilgængelige videnskabelige litteratur, ikke er nogen indikation på dermal penetrering af zinkoxidnanopartikler. Den meget lille andel af Zn-ioner, der frigives fra zinkoxidnanopartikler kan dog give ophav til systemisk eksponering efter dermal applikation [SCCS (Scientific Committee on Consumer Safety), 2012]. Miljøstyrelsen i Danmark konkluderede i rapporten fra 2013, at viden om hudoptag af nanomaterialer stadig er begrænset [Poland CA et al., 2013]. Rapporten anbefaler, at fremtidige studier ikke blot bør have en specifik forskningshypotese, men også bør have fokus på kun at ændre en enkelt fysisk-kemisk egenskab (såsom størrelse, overflade ladning eller hydrofobicitet af nanopartiklerne) ad gangen i stedet for samtidig at ændre flere egenskaber på en gang. Kun på denne måde kan egenskaber, der er afgørende for en dermal penetrering af huden, identificeres. Desuden bør undersøgelser af nanopartikler foretages med f.eks. kommercielt relevante solcremeprodukter og indeholde en detaljeret karakterisering af nanopartiklerne *in situ* (dvs. direkte i selve solcremen). Rapporten bemærker også, at flere undersøgelser rapporterer om en betydelig forsinkelsestid mellem anvendelsen af teststoffet og en eventuel tilstedeværelse i blodbanen.

I dette projekt har vi adresseret nogle af de hidtidige begrænsninger i den foreliggende litteratur, som er nævnt af miljøstyrelsen, og har undersøgt, på systematisk vis, om titaniumdioxid- og zinkoxidnanopartiklers størrelse og overfladebelægning (coating) spiller en rolle for en eventuel dermal penetrering/absorption. Dette har vi gjort ved at:

- benytte en kommercielt tilgængelig solcreme
- indføre en latenstid på flere dage efter påføring af solcreme, som indeholder nanopartikler, inden målinger i huden
- gentagne påføring af solcreme, som indeholder nanopartikler
- anvende en ny tilgængelig metode (acoustic attenuation spectroscopy) til at bestemme partikelstørrelsesfordeling direkte i solcremen.

Baseret på miljøstyrelsens anbefalinger, undersøgte vi således:

- 1) den dermale absorption og penetrering af titaniumdioxid- og zinkoxidnanopartikler i normal human hud i en 3D model (*in vitro* EpiDerm™ -system (Mattek)), i inflammeret musehud *in vivo* (musemodel for akut irritativ kontakt dermatitis) og i human hud *in vivo* (human hud xenotransplanteret til mus).
- 2) effekten af størrelse og overfladebelægning (coating) af titaniumdioxid- og zinkoxidnanopartiklerne på en eventuel dermal absorption og penetration.
- 3) effekten af titaniumdioxid- og zinkoxidnanopartikler i en OECD valideret model for hudirritation
- 4) de fysisk-kemiske egenskaber af de anvendte nanopartikler med særlig fokus på partikelstørrelsesfordelingen i solcremen.

En oversigt over det eksperimentelle design er vist i Figure 2. *In vitro* hudmodellen er OECD valideret og blev brugt til undersøgelse af hudirritation, som et mål for mulige sundhedseffekter, i overensstemmelse med OECDs retningslinjer # 431 og # 439. Endvidere blev *in vitro* hudmodellen anvendt til at undersøge titaniumdioxid- og zinkoxidnanopartiklernes inflammatoriske potentiale ved hjælp af multiplex cytokinanalyser. Prøver fra *in vitro* hudmodellen og biopsier fra *in vivo* hudmodellerne blev evalueret for dermal absorption og penetrering af titaniumdioxid- og zinkoxidnanopartikler ved hjælp af transmission elektronmikroskopi (TEM), induktivt koblet plasma massespektrometri (ICP- MS) og hematoxylin og eosin (H&E) farvning. Projektet blev udført i tre faser som følger:

- 1) Fremstilling af solcremer indeholdende 8 forskellige nanopartikler samt karakterisering af nanopartiklerne.
- 2) Eksponering af *in vitro* og *in vivo* hudmodellerne for disse solcremer.
- 3) Analyse af dermal penetrering i hudmodellerne samt effekten i *in vitro*-hudmodellen.

Det antages, at en stor del af den danske befolkning, herunder børn, bruger solcreme i løbet af sommeren. I en henstilling fra Europa-Kommissionen er det beregnet, at der bør anvendes 36 g solcreme per dag for at opnå tilstrækkelig solbeskyttelse [European Commission, 2006]. De mængder vi har brugt i *in vitro* og *in vivo* hudmodellerne ligger over denne mængde og svarer til et realistisk "worst case" scenarie. Dermed er det sikret at resultaterne afspejler virkeligheden så godt som muligt.

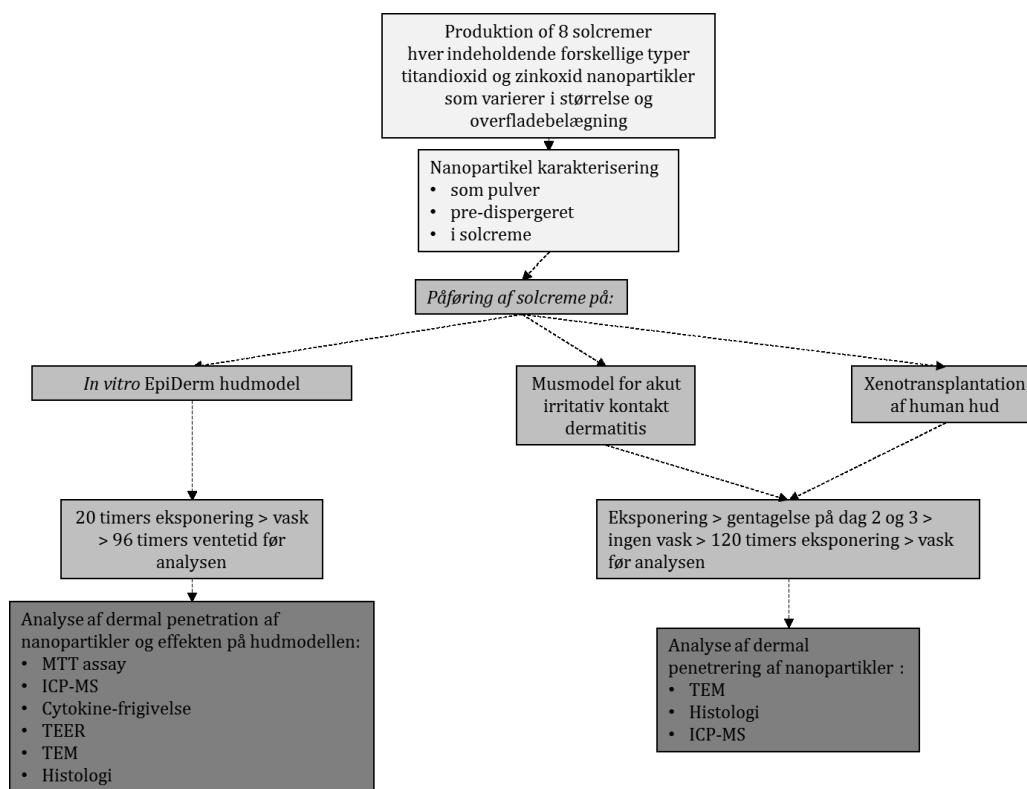


FIGURE 2: OVERSICHT OVER PROJEKTETS EKSPERIMENTELLE DESIGN

En vigtig del af dette projekt er nanopartiklernes karakterisering i solcremen, især deres størrelsesfordeling. På grund af kompleksiteten i et system som solcreme (viskositet, olie i vand-

emulsion) var karakteriseringen vanskelig at udføre. Imidlertid kunne en ny metode: 'acoustic attenuation spectroscopy', anvendes til måling af partikelstørrelsesfordelingen direkte i solcremen. Med denne metode kunne vi vise, at nanopartiklerne har en partikelstørrelsesfordeling, hvor 50% af partiklerne har en diameter på omkring 200 nm i de fleste af de fremstillede solcremer. I to af de fremstillede solcremer var partikelstørrelsesfordelingen mærkbar større (393 nm og 661 nm i diameter). Desuden havde mindst 90% af partiklerne en størrelse på mere end 100 nm i diameter. Men, da disse data er baseret på nanopartiklernes vægt, kan der ligeledes være et stort antal partikler til stede på under 100 nm i diameter. Dette skyldes, at større partikler vejer mere og derved maskerer for de små partikler i analysen. En måde at forklare dette fænomen på, er ved at se på tre partikler med enten 1 µm, 2 µm, eller 3 µm i diameter. Når man ser på antallet så tegner hver partikelstørrelse sig for en tredjedel af det samlede antal. Kigger man derimod kun på volumen ($4/3\pi r^3$) eller den vægt baserede størrelsesfordeling, vil 75% af det samlede volumen komme fra partiklen med 3 µm i diameter, og mindre end 3% fra partiklen med 1 µm i diameter. På den måde bliver det tydeligt, at størstedelen af den samlede partikelmasse eller volumen kommer fra de større partikler. Denne begrænsning af undersøgelsen bør behandles i fremtidige studier for at undersøge størrelsesfordelingen af nanopartikler i kommercielt tilgængelige solcremer.

I ICP-MS undersøgelsen af dermal penetrering i *in vitro* hudmodellen viser analyseresultaterne en klar penetrering af zinkoxid, hvorimod resultaterne for titaniumdioxid er mere usikre. Det skal understreges, at ingen af de andre anvendte metoder, til måling af penetrering, kan bekræfte dette resultat. Både titaniumdioxid- og zinkoxidnanopartikler har ingen effekt på hudirritation og fremkalder heller ikke øget udtryk af cytokiner og dermed et inflammatorisk respons. Endvidere blev der ikke påvist nanopartikler ved TEM analysen under den øvre overflade af *in vitro* hudmodellen, selvom der, ifølge ICP-MS analysen, burde være adskillige hundrede zinkoxidnanopartikler til stede. Zinkoxidnanopartikler er kendt for at dissociere i biologiske systemer [SCCS (Scientific Committee on Consumer Safety), 2012] og derfor konkluderer vi at zinkoxidnanopartikler ikke penetrerer huden i partikelform, men som zinkioner. Dette er i overensstemmelse med den tilgængelige litteratur, da der ikke er fundet zinkoxidnanopartikler i de nederste hudlag [Cross et al., 2007; Durand et al., 2009; Dussert et al., 1997; Filipe et al., 2009; Gamer et al., 2006; Kuo et al., 2009; Song et al., 2011b; Szikszai et al., 2010]. Kun få undersøgelser kan vise en minimal transdermal absorption [Gulson et al., 2010; Gulson et al., 2012; Monteiro-Riviere et al., 2011]. Det er dog ikke klart om zink, i disse studier, penetrerede som nanopartikler eller zinkioner og SCCS konkluderer, at "I betragtning af ZnOs dissociering er det mest sandsynligt, at zink penetrerer på ion form." [SCCS (Scientific Committee on Consumer Safety), 2012] hvilket understøtter konklusionen af vores undersøgelse.

For titaniumdioxidnanopartikler kan vi ud fra analysernes resultaterne konkludere, at der ingen penetration er i *in vitro* hudmodellen over metodernes detektionsgrænse.

Ved hjælp af ICP-MS analysen blev titanium også detekteret i hudbiopsier fra *in vivo* hudmodellerne (musmodellen for akut irritativ kontakt dermatitis og den humane xenotransplantationshudmodel). Undersøgelsen var begrænset til titaniumdioxidnanopartikler i *in vivo* hudmodellerne, da titaniumdioxidnanopartikler er de eneste nanopartikler, der på nuværende tidspunkt anvendes, som fysisk UV-filter, i solcremer solgt i Danmark.

Mængden af titanium i musenes hud varierede betydeligt (mellem 3,2 og 121,6 mg/kg tørvægt)svarende til 0.0011% til 0.12% af den oprindeligt tilsatte mængde titaniumdioxidnanopartikler. Den målte koncentration af titanium i den humane xenotransplanterede hud varierede mellem mindre end 0,11 og 2,5 mg / kg tørvægt og nåede derfor ikke op på mængden af den oprindeligt tilsatte mængde titaniumdioxidnanopartikler (0.015% to 0.00014% af den oprindeligt tilsatte mængde titaniumdioxidnanopartikler) . Baseret på ICP-MS resultaterne burde der være mindst flere hundrede titaniumdioxidnanopartikler til stede per TEM snit. I begge hudmodeller blev der fundet nanopartikel-lignende strukturer, som dog også blev observeret i kontrollerne. Disse strukturer blev identificerede som enten melanin vesikler i huden eller polysomer. Titaniumdioxidnanopartikler blev kun observeret i stratum corneum (skællaget).

For begge *in vivo* hudmodeller, kunne en ufuldstændig afvaskning af solcreme fra huden efter afslutningen af forsøget være en mulig forklaring på påvisning af titanium i hudbiopsier ved ICP-MS, men ikke TEM analysen.

Baseret på vores resultater fra *in vitro* og *in vivo* hudmodellerne konkluderer vi, at dermal penetrering af titaniumdioxid- og zinkoxidnanopartikler ikke kan måles over detektionsgrænsen for de anvendte eksperimentelle metoder. Hvis dermal penetrering af TiO₂ og ZnO nanopartikler forekommer ved værdier under detektionsgrænsen for de anvendte testmetoder ville den systemiske dosis være så lille, at det baseret på det nuværende datagrundlag ikke vil være skadeligt. Dette er i overensstemmelse med de konklusioner, der blev foretaget af SCCS, som erklærede, at begge slags nanopartikler er sikre at bruge i hudprodukter i en koncentration på op til 25% [SCCS (Scientific Committee on Consumer Safety), 2012; SCCS (Scientific Committee on Consumer Safety), 2014].

1. Introduction

1.1 Scientific background

Under the Agreement "Better Control of Nanomaterials" ("Bedre styr på nanomaterialer"), the Danish Environmental Protection Agency (EPA) has initiated a series of projects with the aim of further clarifying possible risks to consumers and the environment. These projects will also help to generate new knowledge on the impact of nanomaterials on consumers and the environment in selected areas of research. The current experimental project on dermal absorption of nanomaterials is part of this series.

The absorption of nanomaterials into or through the skin may result in topical or systemic effects such as inflammation, allergy and cancer. Knowledge concerning dermal penetration and absorption of nanomaterials is limited. The recent evaluation of the existing scientific literature on dermal absorption commissioned by the Danish EPA¹ has shown that the interpretation of results on this endpoint is hampered by non-harmonized testing approaches, insufficient characterization of test materials and the alteration of multiple experimental parameters in a non-systematic way as well as a lack of benchmark comparators within studies. To further ensure that results from dermal absorption studies can be used in a wider setting the "Dermal absorption of nanomaterials" report¹ recommends that future studies focus on the alteration of a single physicochemical property (such as size, surface charge, hydrophobicity e.g.) in order to help identify potential structure activity relationships between nanomaterials and their dermal penetration efficiency.

It is well established that excessive exposure to UV-A and UV-B radiation is correlated to an increased risk of malignant melanoma. This risk is efficiently lowered by use of sunscreens [Green et al., 2011]. Titanium dioxide nanoparticles (TiO₂ NPs) and zinc oxide nanoparticles (ZnO NPs) are examples of nanomaterials that are used as physical UV-filters in sunscreen. At present, TiO₂ is included in Annex VI of the Cosmetics Regulation, which is a positive list of permitted UV filters. ZnO is currently not included in Annex VI, but it is expected to be allowed in both the nano- and non-nano form in up to 25% in the near future. The purity, crystallinity, size and coating are predefined, when these UV filters are used in the nano-form. The Nordic Eco-label 'Svanen' does not allow nanomaterials as of 2011. It can be assumed that most of the Danish population including children are using sunscreen during the summer. In a recommendation of the European Commission it is calculated that 36 g sunscreen are used per dag [European Commission, 2006]. Based on the definition of a nanomaterial by the European Commission from the 18th October 2011 where the Recommendation on the definition of a nanomaterial was adopted a "nanomaterial" means: "*A natural, incidental or manufactured material containing particles, in an unbound state or as an aggregate or as an agglomerate and where, for 50 % or more of the particles in the number size distribution, one or more external dimensions is in the size range 1 nm - 100 nm. In specific cases and where warranted by concerns for the environment, health, safety or competitiveness the number size distribution threshold of 50 % may be replaced by a threshold between 1 and 50 %.*" [European Commission, 2011]. TiO₂ NPs and, in some countries outside the EU ZnO NPs, are used in sunscreens as they are not only an effective filter against UV-radiation but at the same time are non-irritating and more compatible with sensitive skin than chemical sunscreens. Compared to micro-sized titanium dioxide or ZnO particles TiO₂ NPs and ZnO NPs have more consumer-friendly characteristics that allow a more easy application of the sunscreens. In addition, TiO₂ NPs and ZnO NPs do not leave an unsightly whitish tint on the skin. However,

¹ [Dermal absorption of nanomaterials \(2013\). Environmental Project number 1504, http://www.mst.dk/Publikationer/Publications/2013/October/978-87-93026.html.](http://www.mst.dk/Publikationer/Publications/2013/October/978-87-93026.html)

although there have been a number of toxicological investigations it is still not clear if TiO₂ NPs and ZnO NPs can penetrate the skin and be absorbed into the blood stream leading to potential systemic health risks.

As these nanoparticles are some of the most used nanoparticles for dermal applications - they are not only used in sunscreens but also in other cosmetic products - they are, in relation to dermal absorption, also the most intensively studied nanoparticles [Nohynek and Dufour E. K., 2012]. Although most of the studies show that TiO₂ NPs and ZnO NPs cannot be absorbed through the skin [Monteiro-Riviere et al., 2011; Nohynek and Dufour E. K., 2012; Poland CA et al., 2013; SCCS (Scientific Committee on Consumer Safety), 2012; SCCS (Scientific Committee on Consumer Safety), 2014] there are also reports that suggest that TiO₂ NPs can penetrate the skin through hair follicles and pores [Bennat and Muller-Goymann C. C., 2000]. In addition, although it is not clear if the dermal absorption occurs as nanoparticle or in dissolved form, dermal absorption was shown after application of ZnO NPs to human skin [Gulson et al., 2010; Gulson et al., 2012; Monteiro-Riviere et al., 2011]. Another issue is the possible absorption through damaged skin, e.g., due to sun burns, skin diseases or skin injuries. From *in vitro* studies in cell cultures it is known that TiO₂ NPs can induce, e.g., oxidative stress and genotoxicity [Botelho et al., 2014; Chen et al., 2014; Kansara et al., 2015; Srivastava et al., 2013]. However, dermal exposure to TiO₂ NPs does not seem to lead to these cytotoxic effects due to the low level of dermal penetration. But although there have been a number of studies concerning the dermal absorption of TiO₂ NPs it is difficult to draw a final conclusion at this time and the same is true for ZnO NPs. This is due to the either insufficient physicochemical characterization of the used particles or changes in the experimental settings in an unsystematic way in the studies. Both reasons make it hard to directly compare studies made during the past decade and there are still a number of knowledge gaps [Poland CA et al., 2013].

1.2 Objective of the project

In theory, dermal absorption and penetration of nanomaterials may result in topical or systemic effects such as inflammation, allergy or cancer.

In their "Opinion on titanium dioxide (nano form)" the Scientific Committee on Consumer Safety (SCCS) concluded: "*From the limited relevant information provided in the submission, and the information from open literature, the SCCS considers that TiO₂ nanomaterials in a sunscreen formulation are unlikely to lead to: systemic exposure to nanoparticles through human skin to reach viable cells of the epidermis, dermis, or other organs.*" [Scientific Committee on Consumer Safety), Opinion on titanium dioxide (nano form), 22 July 2013, revision of 22 April 2014].

However, the SCCS also state that: "*Although there is no conclusive evidence at present to indicate penetration of TiO₂ nanoparticles through the skin to viable cells of the epidermis, a number of studies have shown that they can penetrate into the outer layers of the stratum corneum, and can also enter hair follicles and sweat glands. It is therefore recommended not to use TiO₂ with substantially high photocatalytic activity (e.g. S75-F, S75-G, S75-O) in sunscreen formulations. Other TiO₂ nanomaterials that have a relatively lower but still significant level of photocatalytic activity (e.g. S75-C, S75-D, S75-E) may be used, but further investigations over longer post-application periods taking into account the potential photocatalytic activity post-application, whilst allowing for appropriate lag-time and using realistic application scenarios may be necessary to ascertain that they do not pose a risk due to photocatalytic activity.*" [Scientific Committee on Consumer Safety), Opinion on titanium dioxide (nano form), 22 July 2013, revision of 22 April 2014]. Also the Danish EPA stated in a recently published report that knowledge on the dermal penetration and absorption of nanomaterials is still limited. They concluded that this is mainly due to non-harmonized testing approaches, insufficient characterization of test materials and the alteration of multiple experimental parameters in a non-systematic way as well as a lack of benchmark comparators within studies [Poland CA et al., 2013]. It was recommended in this report that future studies should not only have a specific research question but also focus on the alteration of a single physicochemical property (such as size, surface charge, hydrophobicity e.g.) instead of change multiple physicochemical properties at a time to be able to identify properties that are

critical for a dermal penetration of the skin. Furthermore, the application of the nanoparticles should occur in commercially-relevant formulations as well as particle characterizations should be performed in this test formulation. The report also noted that several studies report a considerable lag time between the application of the test substance and an appearance in the circulation. We addressed these recommendations in this project by:

- Using a commercially available sunscreen as test formulation
- Including a lag time of several days after application of the nanoparticle containing sunscreen as well as repeated application of the nanoparticle containing sunscreen in case of *in vivo* experiments
- Use of a newly available method, acoustic attenuation spectroscopy, to determine the particle size distribution directly in sunscreen.

Based on these recommendations, the aim of this project was to investigate:

- 1) the dermal absorption and penetration of the test nanomaterials TiO₂ NPs and ZnO NPs in *in vitro* EpiDerm™ system (MatTek) for normal, human 3D epidermis,
- 2) the dermal absorption and penetration of the test nanomaterials TiO₂ NPs in *in vivo* mouse model for acute irritant contact dermatitis, and xenograft human skin model.
- 3) the effect of size and surface coating on dermal absorption and penetration of the test nanomaterials TiO₂ NPs (size and coating) and ZnO NPs (coating).
- 4) the test nanomaterials in OECD validated models for skin corrosion and skin irritation as human health hazard endpoints according to the OECD test guidelines #431 and #439, respectively.
- 5) the physicochemical properties of the used nanomaterials with special focus on the particle size distribution in sunscreen.

The investigation of dermal absorption/penetration was limited to TiO₂ NPs in the *in vivo* skin models as TiO₂ NPs are the only nanomaterials currently in use as physical UV-filter in sunscreens that are available on the Danish market.

1.3 Experimental methods

In this project the dermal absorption and penetration of TiO₂ NPs and ZnO NPs with different particle sizes and surface coating were investigated in a commercial sunscreen formulation. For these investigations, the Organisation for Economic Co-operation and Development (OECD) validated *in vitro* EpiDerm™ system (MatTek) for normal, human 3D epidermis and *in vivo* mouse models for acute irritant contact dermatitis and xenograft human skin model were used. The *in vitro* skin models were used in OECD validated tests for skin corrosion and skin irritation as human health hazard endpoints according to the OECD test guidelines #431 and #439, respectively. In addition, this *in vitro* model was used to investigate the inflammatory potential of nanomaterial containing sunscreen using multiplex cytokine assays. Preparation and analysis of samples from the treated *in vitro* 3D epidermis models and biopsies from the *in vivo* skin models were evaluated for dermal absorption and penetration of TiO₂ NPs and ZnO NPs using transmission electron microscopy (TEM), inductively coupled plasma mass spectrometry (ICP-MS), and hematoxylin and eosin (H&E) staining.

1.4 Structure of the report

The report is structured as a scientific report where in chapter 2 the used materials and methods are described, in chapter 3 a detailed description of the results is given that are discussed in chapter 4 and concluded in chapter 5. Furthermore, supplementary data and information are given in the appendixes at the end of the document.

2. Material and Methods

2.1 Overview of the experimental setup

The project was performed in three stages and a graphical overview over these three stages is given in Figure 3. These stages were:

- 1) Production of 8 different nanoparticle containing sunscreens and characterization of the nanoparticles
- 2) Exposure of *in vitro* and *in vivo* skin models to these sunscreens
- 3) Analysis of the dermal penetration of the skin models as well as of the effect on the *in vitro* skin model.

In the chapters of the Material and Methods section, the used methods are described in detail.

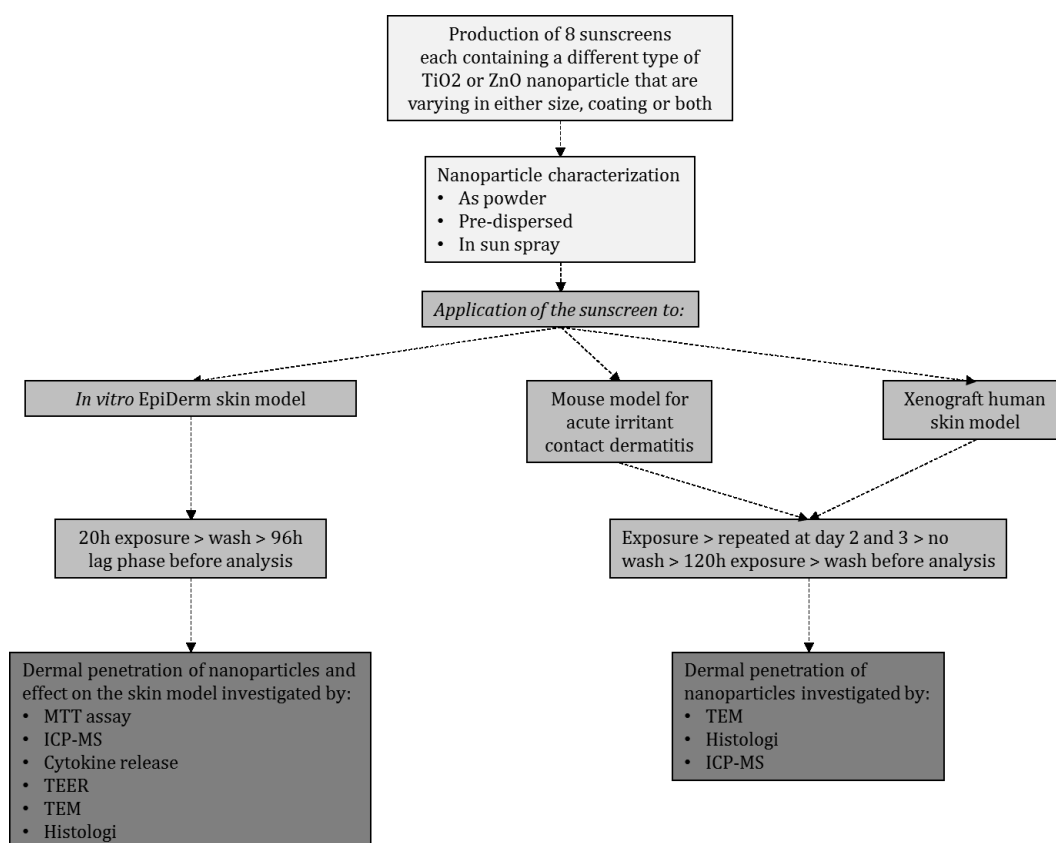


FIGURE 3: OVERVIEW OF THE EXPERIMENTAL DESIGN. LIGHT GRAY: EXPERIMENTAL STAGE 1); MIDDLE GRAY: EXPERIMENTAL STAGE 2); DARK GRAY: EXPERIMENTAL STAGE 3).

2.2 Nanoparticles

Nanoparticles of titanium dioxide and zinc oxide were chosen as test materials as a dermal exposure of workers as well as consumers is very likely to have occurred due to their extensive use in, e.g., sunscreen products and painting. Furthermore, the risk assessment of TiO₂ NPs and ZnO NPs is of

high importance as they can substantially protect the population for UV-A and UV-B exposure as UV filter in sunscreens, thereby minimizing the risk of skin cancer such as malignant melanoma. Titanium dioxide and zinc oxide based particles have the advantage over chemical UV filters that they are much less irritant and less allergenic. However, micro-sized titanium dioxide and zinc oxide particles are hard to distribute on the skin and leave a whitish cover on the skin. This disadvantage is not found for TiO₂ NPs and ZnO NPs, which appear transparent.

The most significant changes of the test nanomaterials TiO₂ NPs and ZnO NPs with respect to their possible ability for dermal absorption and penetration are changes of their size and surface coating. It is known that changes of the size of nanoparticles can change their physicochemical properties and their reactivity due the increased surface to volume ratio. In the report on Dermal absorption of nanomaterials by the Danish Environmental Protection Agency (Danish EPA) it is shown that TiO₂ NPs of around 30 nm size penetrate into the dermis whereas TiO₂ NPs of more than 80 nm penetrate at maximum into the stratum corneum [Poland CA et al., 2013]. Furthermore, in this report it is concluded that several studies indicate that the surface chemistry is an important factor for the ability of the nanoparticles to penetrate into the skin. Changes of the surface coating of nanoparticles can lead to modified surface charges and altered hydrophobicity or hydrophilicity thereby eventually leading to a higher possibility of dermal absorption and penetration [Poland CA et al., 2013]. Therefore, the choice of the nanoparticles were made based on size (17 to 100 nm TiO₂ NPs; 18 and 20 nm ZnO NPs) and coating (uncoated and several coatings used for nanoparticles for cosmetic products) (Table 1) thereby giving the possibility to investigate if size and/or surface coating has an influence on the dermal absorption and penetration of nanomaterials. In addition, in the case of TiO₂ NPs the crystalline form of TiO₂ NPs was limited to rutile particles as this is the crystalline form that is used in sunscreens due to its low photo-activity [Jacobs et al., 2010; Kubac et al., 2015].

Differently coated and sized TiO₂ NPs and ZnO NPs were purchased from US Research Nanomaterials Inc. that are commercially available for use in sunscreen products. In addition, BioNord A/S donated two kinds of TiO₂ NPs (UV-Titan M161 and M262) produced by KEMIRA PIGMENTS OY, Finland. These nanoparticles have been used by BioNord A/S for the production of sunscreens with physical UV filters. The used nanoparticles are listed in Table 1.

TABLE 1: OVERVIEW OF THE USED NANOPARTICLES

Sample code	Description
C)	TiO ₂ , rutile, uncoated high purity 99.9%, 30 nm
D)	TiO ₂ , rutile, uncoated high purity 99.9%, 100 nm
E)	TiO ₂ , rutile, coated with silicon and alumina (hydrophilic), 30 nm
F)	TiO ₂ , rutile, coated with silicone oil (lipophilic), 30 nm
G)	UV-Titan M161: TiO ₂ , rutile, coated with alumina and stearic acid, 17 nm
H)	UV-Titan M262: TiO ₂ , rutile, coated with Alumina, Silicone, ~20 nm
I)	ZnO, uncoated high purity 99.95%, 18 nm
K)	ZnO, coated with 3-aminopropyltriethoxysilane (KH550) (hydrophilic/oleophilic), 20 nm

2.3 Sunscreen formulation

BioNord A/S donated a sunscreen that does not contain any physical UV-filter. This sunscreen was chosen as it had a compared to other sunscreens a low viscosity that allowed an easy application of the sunscreen (with or without added nanoparticles) to the *in vitro* and *in vivo* skin models and it allowed for adding up to 10 v/v% oil. The latter was important, as pre-dispersed nanoparticles had to be added to the pre-produced sunscreen.

The sunscreen contains the following ingredients and is produced by BioNord A/S as follows:

TABLE 2: SUNSCREEN FORMULATION

Trade name	Phase	INCI
Water	1	Aqua
Keltrol AP	1	Xanthan Gum
Dermofeel PA-3	1	Sodium Phytate, Aqua, Alcohol
Verstatil PC	1	Phenoxyethanol, Caprylyl Glycol
Propylen Glycol	1	Propylene Glycol
Glycerin	1	Glycerin
Waglinol AB 1215	2	C12-C15 Alkyl Benzoate
Parsol 340	2	Octocrylene
Parsol MCX	2	Ethylhexyl Methoxycinnamate
Parsol 1789	2	Butyl Methoxydibenzoylmethane
Mulsifan RT 11	2	Ceteareth-22
Soldoc EB 29	2	Isostearyle Isostearate

The ingredients that are marked in Table 2 with 1 are mixed and heated to 75°C while stirring making phase 1. The ingredients that are marked in table 2 with 2 are mixed separately and heated to 75°C while stirring making phase 2. Phase 2 is added to phase 1 while stirring. The pH is adjusted to ~pH 6.

Furthermore, BioNord A/S donated C12-C15 alkylbenzoate that is used to pre-disperse the different nanoparticles before adding them to the sunscreen.

2.4 Preparation of nanoparticle containing sunscreen

The Scientific Committee on Consumer Safety (SCCS) concluded in their opinion on Titanium Dioxide (nano form) COLIPA n° S75 that: “*On the basis of the available evidence, the SCCS has concluded that the use of TiO₂ nanomaterials with the characteristics as indicated below, at a concentration up to 25% as a UV-filter in sunscreens, can be considered to not pose any risk of adverse effects in humans after application on healthy, intact or sunburnt skin.*” [SCCS (Scientific Committee on Consumer Safety), 2014]. For ZnO NPs the SCCS state that: “*In summary, it is concluded on the basis of available evidence that the use of ZnO nanoparticles with the characteristics as indicated below, at a concentration up to 25% as a UV-filter in sunscreens, can be considered not to pose a risk of adverse effects in humans after dermal application.*” [SCCS (Scientific Committee on Consumer Safety), 2012]. However, these conclusions are only valid for the kind of TiO₂ NPs and ZnO NPs that were included in the opinions. The interested readers are

referred to the SCCS opinions for more details on that subject [SCCS (Scientific Committee on Consumer Safety), 2012; SCCS (Scientific Committee on Consumer Safety), 2014].

In most sunscreen products containing physical UV-filters, the concentration varies between 1 and 5%. In a personal communication Søren Sneholt, BioNord A/S Denmark, wrote (Danish translated to English): “When we launched sunscreens with pigments in the mid 90's they contained the most of the time 5% of the UV - Titan powder. Whether they were coated with Dimethylpolysiloxane or stearic acid. The reason for this was that we could get about sun protection factor (SPF) 25 with this amount. As I recall, we had a protection of approximately 93 % at this amount. Most formulations were made as W / O emulsions = water in oil, they were very water resistant and therefore suitable for babies / children. For adults the most sunscreens were a mixture of UV - Titan and chemical filters in order to get less whitening of the skin.”

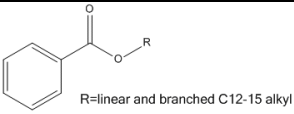
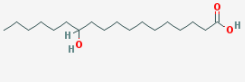
For this project it was necessary to go down to 2.5 wt% nanoparticles in the sunscreen for practical reasons. Pre-dispersion of the nanoparticles with 50 wt% nanoparticles resulted in extremely high viscosities. Therefore, the nanoparticle concentration in the pre-dispersions had to be adjusted to 25 wt% or 33.3 wt% to be able to disperse the particles properly. This decision was made as it is better to have the physicochemical properties of the particles correct and the concentration in the product incorrect rather than the other way around. If the concentration of the nanoparticles is correct but their properties incorrect then the experiment is confounded, and the results are meaningless. On the other hand, if the properties are correct then a higher dose can be extrapolated. Furthermore, as the by BioNord A/S premade sunscreen only allows for the addition of 10 v/v % oil without disturbing the emulsion, which would lead to a separation of the water and oil phase, the concentration of the nanoparticles in the sunscreen had to be adjusted to 2.5 wt%. The final preparation of the sunscreen was stable during the whole project period with no phase separation.

The preparation of the sunscreen was performed in two steps:

- 1) pre-dispersion of nanoparticles in C12-C15 alkylbenzoate/polyhydroxystearic acid;
- 2) mixing of pre-dispersed nanoparticles with sunscreen.

An overview of information on the components of the pre-dispersant is given in Table 3.

TABLE 3: INFORMATION ON THE INGREDIENTS IN THE PRE-DISPERSANT

	C12-C15 alkyl benzoate	Polyhydroxystearic acid
Structure		
wt%	90	10
Molecular weight (g/mol)	290.44-332.52	300.48
Density (g/cm ³)	0.915 – 0.935	/
Aspect	Clear liquid	/
Viscosity (25°C, mPas)	~ 12	/
Refractive index	1.4830-1.4850	/

To prepare the C12-C15 alkylbenzoate/polyhydroxystearic acid mixture polyhydroxystearic acid (10wt%) was mixed with C12-C15 alkylbenzoate (90wt%). The mixture was warmed to 40°C and stirred until polyhydroxystearic acid is completely dissolved. Titanium dioxide or zinc oxide powder was added for pre-dispersion as follows (including the sample codes C) to K) used throughout the project):

- C) 5g TiO₂, rutile, high purity 99.9%, 30 nm + 10g mixture of polyhydroxystearic acid (10wt%) with C12-C15 alkylbenzoate (90wt%)
- D) 5g TiO₂, rutile, high purity 99.9%, 100 nm + 15g mixture of polyhydroxystearic acid (10wt%) with C12-C15 alkylbenzoate (90wt%)
- E) 5g TiO₂ coated with Silicon and Aluminium, rutile, 30 nm (hydrophilic) + 10g mixture of polyhydroxystearic acid (10wt%) with C12-C15 alkylbenzoate (90wt%)
- F) 5g TiO₂ coated with Silicone Oil, rutile, 30 nm (lipophilic) + 10g mixture of polyhydroxystearic acid (10wt%) with C12-C15 alkylbenzoate (90wt%)
- G) 5g UV-Titan M 161: TiO₂ NPs, rutile, 17 nm, coated with alumina and stearic acid + 15g mixture of polyhydroxystearic acid (10wt%) with C12-C15 alkylbenzoate (90wt%)
- H) 5g UV-Titan M 262: TiO₂ NPs, rutile, ~20 nm, coated with Alumina, Silicone + 10g mixture of polyhydroxystearic acid (10wt%) with C12-C15 alkylbenzoate (90wt%)
- I) 5g ZnO NPs / Nanopowder (high purity 99.95%, uncoated), 18 nm + 10g polyhydroxystearic acid (10wt%) with C12-C15 alkylbenzoate (90wt%)
- K) 5g ZnO NPs coated with 1 wt% KH550 (3-aminopropyltriethoxysilane), 20 nm + 10g polyhydroxystearic acid (10wt%) with C12-C15 alkylbenzoate (90wt%)

These pre-dispersions contained therefore 33.3wt% TiO₂ NPs and ZnO NPs with the exception of samples C) and G). Both had to be diluted more (25wt%) as they were too viscous. All samples were dispersed using a Ultra-Turrax T25 (IKA Labortechnik) with 24.000 rpm for 2 minutes on ice.

In step 2) the pre-dispersed nanoparticles were added to the sunscreen to 2.5wt% end concentration. The mixture was dispersed using a Ultra-Turrax T25 (IKA Labortechnik) with 24.000 rpm for 1 minute.

2.5 Nanoparticle characterization

Chapters 2.5.1 to 2.5.4 describe the methods that were used to characterize the nanoparticles either as powders, pre-dispersed in C12-C15 alkylbenzoate/polyhydroxystearic acid mixture or finally dispersed in sunscreen. Particle size distribution of the nanoparticles in sunscreen was of special interest due to a possible categorization of the used sunscreens as nanomaterial containing product. The particle size distribution was also investigated for powders and pre-dispersed nanoparticles.

2.5.1 TEM and EDX analysis of nanoparticle dry powders

The nanoparticle powders were dispersed in MilliQ water to approximately 10 µg/mL using 10 seconds ultrasonication in a water-bath sonicator, dropped on to copper grids with carbon film and left to dry at room temperature. TEM (FEI CM20) was applied to observe the grids with nanoparticles at 200 keV. A CCD camera was used to record images.

For energy dispersive X-ray analysis (EDX), singles were collected and analyzed using the EDAX genesis software (EDAX Inc.).

2.5.2 Dynamic light scattering (DLS) analysis of the nanoparticle size and surface charge in MilliQ water

The nanoparticle powders were dispersed in MilliQ water to approximately 50 µg/mL by ultrasonication in a water-bath sonicator for 30 minutes. Size distribution of the particles were detected in a 173° backscatter angle, high-resolution model, while zeta-potential distributions were measured in the Smoluchowski model ($F(Ka) = 1.5$). Data were recorded and analyzed using the Zetasizer 6.02 software (Malvern, DK).

2.5.3 *In situ* observation of Nanoparticles in sunscreen using an optical microscope

The final-dispersed nanoparticles were dropped directly onto 2 cm x 6 cm glass slides. A 1.5 cm x 1.5 cm cover glass was carefully put on top of the droplet and left still for 10 minutes. The slides were observed by an optical microscope (Leica). A CCD camera was used to record images.

2.5.4 Acoustic attenuation spectroscopy (AAS)

Acoustic attenuation spectroscopy (AAS) was regarded a useful method for the characterization of the particle size distribution in sunscreen. The samples were sent to and analysed by QUANTACHROME GmbH & Co. KG, Odelzhausen, Germany.

In a first step the background signal was measured before the measurements of the samples. The samples have been measured generally without further dilution. However, sample C and Sample D had to be diluted 1:1 with sunscreen due to a too small sample volume that had been left for analysis. The suspensions were dispersed by shaking and filled in the measurement chamber. The samples were measured by a pulse technique device that measures the electroacoustic signal at frequencies from 1 to 10 MHz for either pure liquids or colloids.

2.6 *In vitro* and *in vivo* skin models

The following skin models were chosen for the investigation of dermal absorption and penetration of nanomaterials:

- *In vitro*: EpiDerm™ system (MatTek) – normal, human 3D epidermis model;
- *In vivo*: mouse model for acute irritant contact dermatitis, and xenograft human skin model for dermal absorption of nanomaterials.

The exposed surface area, time of exposure and dosage of nanoparticles are described for these three skin models in chapters 2.6.1 to 2.6.3 followed by a detailed description of the experimental setup for the three skin models as well as the used analysis methods for dermal absorption/penetration of the nanoparticles as well as the effect on the *in vitro* skin model.

2.6.1 Treated surface area

The EpiDerm™ system of MatTek covers a surface area of 0.6 cm² per tissue. For *in vivo* experiments the average area of the mouse ears is between 39.8 ± 1.3 mm² (6 weeks of age) and 50.5 ± 2.3 mm² (36 weeks of age). Per ear, 2 biopsies are taken with a diameter of 3 mm for further investigations. The xenotransplanted human skin tissue has a surface area of approximately 1.5 cm².

2.6.2 Time of exposure

According to the OECD guideline for the testing of chemicals, skin absorption: *in vitro* method #428, a period of 24 hours for skin exposure is normally required for investigating the absorption of test substances. However, for test substances that penetrate slowly longer times may be required. Therefore, the experiments included a 96 hours lag phase for the *in vitro* experiments and a 120 hours lag phase for the *in vivo* experiments after the last exposure before samples/biopsies were taken. The lag phase for the *in vitro* system was chosen based on the viability of the EpiDerm skin model. The skin model could be cultivated without problems up to one week. However, as the skin model is designed for immediate use we chose not to cultivate the cells longer to avoid eventual effects due to the long cultivation period of the skin model. In the *in vivo* experiments the application of the test nanomaterials were repeated three times with 24 hours intervals to simulate the repeated use of sunscreen products. As mentioned before, after the last application there was a lag phase of 120 hours before samples/biopsies were taken. However, in comparison to the *in vitro* experiments, the applied sunscreen was not washed off. To avoid systemic absorption due to oral uptake, the mice were single housed and were dressed with collars throughout the experiment.

2.6.3 Dosage of nanoparticles

According to the OECD guideline for the testing of chemicals, skin absorption: *in vitro* method #428 the amount of applied sunscreen containing nanoparticles were at least 10 µl/cm². The amount of added nanoparticles per cm² were calculated as follows:

In vitro EpiDerm™ Skin Model

30 µl sunscreen containing 2.5wt% nanoparticles (wt/wt) $\hat{=}$ 21.7 mg sunscreen containing 0.54 mg nanoparticles per 0.6 cm² = 0.9 mg nanoparticles/cm² skin. An estimate of the number of nanoparticles that is added per cm² skin is given in Table 4.

In vivo mouse model for acute irritant contact dermatitis (ICD)

Per mouse:

10 µl sunscreen containing 2.5wt% nanoparticles topically onto the anterior and the posterior surfaces of both ears on three days $\hat{=}$ Σ 30 µl sunscreen containing 2.5wt% nanoparticles onto the anterior as well as onto the posterior surface of both ears $\hat{=}$ 0.54 mg nanoparticles per 38.5 to 52.8 mm² = 1.02 to 1.4 mg nanoparticles/cm² skin. An estimate of the number of nanoparticles that is added per cm² skin is given in Table 4.

In vivo xenograft human skin model

Per mouse:

15 µl sunscreen containing 2.5wt% nanoparticles applied on three days onto the xenograft $\hat{=}$ Σ 45 µl sunscreen containing 2.5wt% nanoparticles $\hat{=}$ 0.81 mg nanoparticles per ~1.5 cm² = 0.54 mg nanoparticles/cm² skin. An estimate of the number of nanoparticles that is added per cm² skin is given in Table 4.

TABLE 4: ESTIMATED NUMBER OF NANOPARTICLES ADDED PER CM² SKIN OF THE DIFFERENT SKIN MODELS

Sample code	Size [nm]	Particle volume [cm ³]	Bulk density [g/cm ³]	Weight of one particle [g]	Dosage [#particles/cm ² skin]		
					<i>in vitro</i> EpiDerm skin model	<i>in vivo</i> ICD model	<i>in vivo</i> xenograft model
C)	30	1.41E-17	0.25	3.53E-18	2.55E+14	2.89E+14	1.53E+14
D)	100	5.24E-16	0.37	1.94E-16	4.65E+12	5.27E+12	2.79E+12
E)	30	1.41E-17	0.54	7.63E-18	1.18E+14	1.34E+14	7.07E+13
F)	30	1.41E-17	0.58	8.20E-18	1.10E+14	1.24E+14	6.59E+13
G)	17	2.57E-18	0.15	3.86E-19	2.33E+15	2.64E+15	1.40E+15
H)	20	4.19E-18	0.15	6.28E-19	1.43E+15	1.62E+15	8.59E+14
I)	18	3.05E-18	0.53	1.62E-18	5.56E+14	---	---
K)	20	4.19E-18	0.53	2.22E-18	4.05E+14	---	---

Based on the size of the used nanoparticles (area of the circle corresponding to the diameter of the nanoparticle) and the estimated number that were applied to 1 cm² skin we estimated the surface a single layer of nanoparticles would cover. The results are presented in Table 5 and show that the with the sunscreen applied nanoparticles were several orders of magnitude over sufficient to completely cover the skin model.

It has of course to be kept in mind that the particle numbers and occupied areas are estimates that are merely based on the size of the nanoparticles given by the manufacturer and are not based on measurements of the particle size distribution. This was not done as the particle size distribution was weight based and not a number size distribution. The use of weight based particle size distributions for these calculations would lead to an unacceptable level of error.

TABLE 5: ESTIMATION OF THE SURFACE OCCUPIED BY A SINGLE LAYER OF NANOPARTICLES

Sample code	Estimated surface occupied of a single layer nanoparticles [cm ²]		
	<i>in vitro</i> EpiDerm™ skin model	<i>in vivo</i> TPA model	<i>in vivo</i> xenograft model
C)	1800.10	2040.12	1080.06
D)	364.68	413.30	218.81
E)	832.91	943.96	499.75
F)	775.47	878.86	465.28
G)	5291.52	5997.05	3174.91
H)	4497.71	5097.40	2698.62
I)	1414.39	---	---
K)	1272.94	---	---

2.6.4 *In vitro* EpiDerm™ system (MatTek) – normal, human 3D epidermis model

The EpiDerm™ Skin Model was chosen for this project as it is validated by the OECD for evaluating the skin corrosion and skin irritation potential of chemicals and other drugs. A schematic overview of the EpiDerm™ Skin Model is given in Figure 4.

The MatTek's patented EpiDerm™ System is described by the manufacturer as follows: “*MatTek's patented EpiDerm™ System consists of normal, human-derived epidermal keratinocytes (NHEK) which have been cultured to form a multilayered, highly differentiated model of the human epidermis. These "ready-to-use" tissues, also known generically as reconstructed human epidermis (RhE), are cultured on specially prepared cell culture inserts using serum free medium, attain levels of differentiation on the cutting edge of in vitro skin technology. Ultrastructurally, the EpiDerm™ Skin Model closely parallels human skin, thus providing a useful in vitro means to assess dermal irritancy and toxicology.*

The EpiDerm™ Skin Model exhibits in vivo-like morphological and growth characteristics which are uniform and highly reproducible. EpiDerm™ consists of organized basal, spinous, granular, and cornified layers analogous to those found in vivo. EpiDerm™ is mitotically and metabolically active. Markers of mature epidermis-specific differentiation such as pro-filaggrin, the K1/K10 cytokeratin pair, involucrin, and type I epidermal transglutaminase have been localized in the model.

Ultrastructural analysis has revealed the presence of keratohyalin granules, tonofilament bundles, desmosomes, and a multi-layered stratum corneum containing intercellular lamellar lipid layers arranged in patterns characteristic of *in vivo* epidermis.”

[<http://www.mattek.com/EpiDerm/data-sheet>].

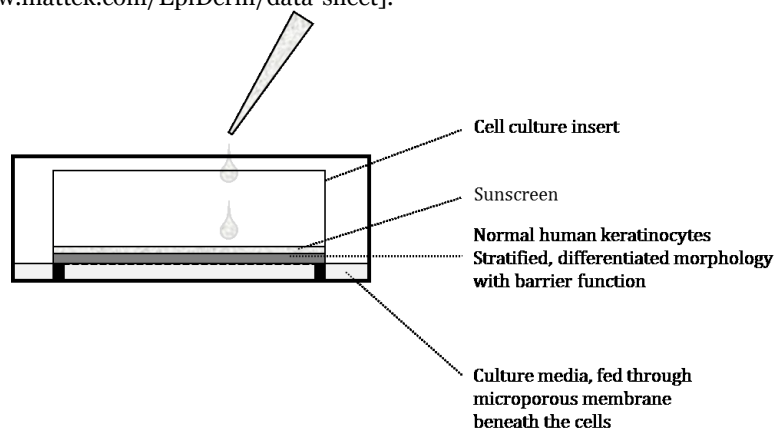


FIGURE 4: *IN VITRO* EPIDERM™ SYSTEM (MATTEK) – NORMAL, HUMAN 3D EPIDERMIS MODEL

The disadvantage of the EpiDerm™ system is that it is an artificially constructed skin model that most likely does not behave exactly as normal skin. However, it is sufficient to allow for the investigation of dermal absorption and penetration of nanoparticles as a proof of principle. The experiments with the EpiDerm™ system were accompanied by *in vivo* experiments with mice and human skin. Thereby, the experimental design gives a great opportunity to compare the *in vitro* and *in vivo* which is important when considering that it is otherwise forbidden to undertake specific animal testing for cosmetics (including sunscreen).

2.6.4.1 Exposure and sample taking of *in vitro* EpiDerm™ system (MatTek)

Besides the analysis of the potential of nanoparticle containing sunscreen to induce skin corrosion and skin irritation the EpiDerm™ Skin Model was also used to investigate the induction of the release of cyto- and chemokines as marker for their inflammatory potential as well as the adsorption and penetration of nanoparticles by the cells of the EpiDerm™ skin model by transmission electron microscopy (TEM). Furthermore, the effect on the structure of the skin model was investigated by histological H&E staining of selected samples (Figure 5 and Table 6).

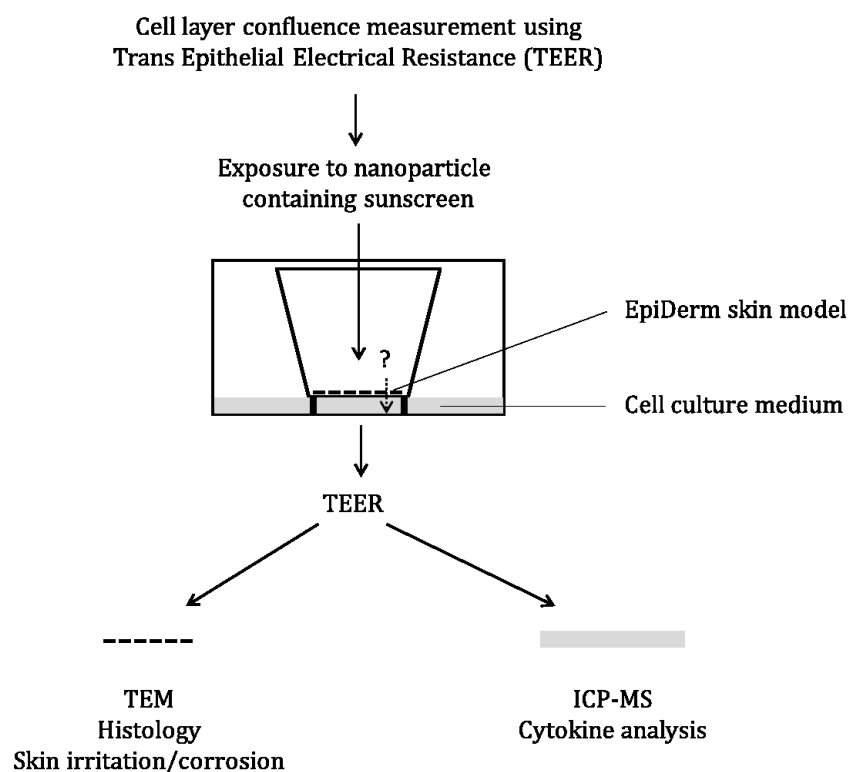


FIGURE 5: OVERVIEW OF THE EXPERIMENTAL DESIGN FOR THE EPIDERM™ SKIN MODEL

Although the production of the EpiDerm™ skin model is standardized and done following GMP procedures there might be variations from lot to lot and between the single tissues. Therefore, all experiments were performed on three different EpiDerm™ skin model lots (lots #19645, #19650, #19661) with three tissues per treatment (A) to (K) per lot (Table 6). The exposure and cultivation of the tissues were performed based on the manual provided by the manufacturer with modifications of the exposure time and cultivation period. Both, the exposure time and cultivation period, were tested before the actual experiment was performed with no effect on the cell viability (data not shown). The experimental timeline was as follows:

Day 0 Day of arrival of EpiDerm™ skin model and Trans Epithelial Electrical Resistance (TEER) measurement

Six-well plates were pre-filled with 0.9 ml of cell culture medium in each well. The EpiDerm™ skin model tissues were prepared for further cultivation by removing any remaining shipping agarose that might adhere to the outer sides of the culture insert. The tissues were transferred into the prepared 6-well plates and incubated for 60 ± 5 min at 37°C in a humidified incubator with 5% CO_2 . After this incubation period, TEER measurements were performed and the culture inserts with the tissues transferred into new culture medium. The tissues were cultivated overnight at 37°C in a humidified incubator with 5% CO_2 .

Day 1 Exposure

Before exposure, TEER measurements were performed. Subsequently the tissues were transferred into fresh culture medium and 30 μl of nanoparticle containing sunscreen was added on top of the tissues. The application of the sunscreen was done by pipetting. In addition, untreated tissues were used as negative control and sunscreen without nanoparticles as vehicle control. A cotton mesh was added on top of the sunscreen for even distribution. The tissues were incubated for 20 hours at 37°C in a humidified incubator with 5% CO_2 .

Day 2 End of exposure and TEER measurements

After 20 h the exposure was ended by rinsing the tissues with PBS 15 times using a washing bottle as described by the manufacturer. The cotton mesh was carefully removed and TEER measurements were performed. The culture inserts with the tissues were transferred into new culture medium. The tissues were cultivated at 37°C in a humidified incubator with 5% CO₂ for two days.

Cell culture medium from below the culture insert was stored at -80°C for later ICP-MS and cytokine analysis.

Day 4 Medium exchange

TEER measurements were performed and the culture inserts with the tissues were transferred into new culture medium. The tissues were cultivated at 37°C in a humidified incubator with 5% CO₂ for two days.

Cell culture medium from below the culture insert was stored for later cytokine analysis at -80°C.

Day 6 TEER measurements, MTT Viability Assay, Sample preparation

TEER measurements were performed and cell culture medium from below the culture insert was stored for later cytokine analysis at -80°C.

From the three tissues that were treated with the same sample one tissue was prepared for TEM, one tissue was prepared for histology, and one tissue was used for skin corrosion and skin irritation analysis using the MTT assay.

TABLE 6: OVERVIEW OF THE EXPOSURE AND SAMPLE TAKING OF *IN VITRO* EPIDERM™ SYSTEM

Sample (Sample code)	Tissue	Medium analysis	Medium analysis	Tissue analysis
Negative control (A)	1	Cytokine	ICP-MS pooled	Skin irritation, skin corrosion
	2	Cytokine		TEM
	3	Cytokine		Histology
Sunscreen control (B)	1	Cytokine	ICP-MS pooled	Skin irritation, skin corrosion
	2	Cytokine		TEM
	3	Cytokine		Histology
TiO₂ NP 30nm uncoated (C)	1	Cytokine	ICP-MS pooled	Skin irritation, skin corrosion
	2	Cytokine		TEM
	3	Cytokine		Histology
TiO₂ NP 100nm uncoated (D)	1	Cytokine	ICP-MS pooled	Skin irritation, skin corrosion
	2	Cytokine		TEM
	3	Cytokine		
TiO₂ NP 30nm Silicone Oil coat (E)	1	Cytokine	ICP-MS pooled	Skin irritation, skin corrosion
	2	Cytokine		TEM
	3	Cytokine		
TiO₂ NP 30nm Silicone, Al coat (F)	1	Cytokine	ICP-MS pooled	Skin irritation, skin corrosion
	2	Cytokine		TEM
	3	Cytokine		
TiO₂ NP 17nm stearic acid, Al coat (G)	1	Cytokine	ICP-MS pooled	Skin irritation, skin corrosion
	2	Cytokine		TEM
	3	Cytokine		
TiO₂ NP 20nm Silicone, Al coat (H)	1	Cytokine	ICP-MS pooled	Skin irritation, skin corrosion
	2	Cytokine		TEM
	3	Cytokine		
ZnO NP 18nm uncoated (I)	1	Cytokine	ICP-MS pooled	Skin irritation, skin corrosion
	2	Cytokine		TEM
	3	Cytokine		Histology
ZnO NP 20 nm KH550 coated (K)	1	Cytokine	ICP-MS pooled	Skin irritation, skin corrosion
	2	Cytokine		TEM
	3	Cytokine		

An overview over the workflow for the exposure of the *in vitro* EpiDerm™ system and the subsequent sample taking is given in Table 7.

TABLE 7: WORKFLOW OF THE EXPOSURE AND SAMPLE TAKING OF THE *IN VITRO* EPIDERM™ SYSTEM

	Workflow	Sample taking
Day 0	Arrival of <i>in vitro</i> EpiDerm™ system	
Day 1 (before exposure)	- TEER measurement - Exposure to sunscreen ± TiO ₂ NPs and ZnO NPs (3 tissues per sample)	
Day 2 (after exposure)	- End of exposure (20h) - Washing off the sunscreen from EpiDerm™ system - TEER measurement	100 µl of culture media for cytokine analysis from each tissue 500 µl of culture media from each tissue pooled for ICP-MS measurements
Day 3	---	---
Day 4 (48h after ended exposure)	- Medium exchange - TEER measurement	Storage of medium for cytokine analysis
Day 5	---	---
Day 6 (96h after ended exposure)	- TEER measurement - Skin corrosion and skin irritation assay	Sample preparation for transmission electron microscopy and histology

2.6.5 *In vivo* mouse model for acute irritant contact dermatitis (ICD)

When investigating a potential dermal absorption and penetration of nanoparticles that are present in sunscreen, one of the important questions is whether sun burned skin allows for greater absorption and penetration of the particles. As sun burned skin is inflamed, the acute irritant contact dermatitis mouse model was used to investigate the effect of inflammation in parallel to normal skin. The use of a mouse model for these investigations allows for very controlled experimental settings. In the acute irritant contact dermatitis mouse model, inflammation in mouse ear skin is induced by the application of 12-O-tetradecanoylphorbol-13-acetate (TPA) simulating acute irritant contact dermatitis. The experiments were performed for TiO₂ NPs only.

For the experiment 36 C57BL/6J mice (6-10 weeks old) were used. The animals were divided randomly into six separate treatment groups with two subgroups each. Per group, both ears of one subgroup were treated with TPA and the other subgroup was treated with vehicle (acetone) on day 1, 2 and 3 (2 x 10 µl topically onto the anterior and the posterior surfaces of both ears). The use of the second ear as direct internal control was considered to be problematic as a systemic effect of TPA on the mice could not entirely be excluded. See also Figure 6 for the experimental setup. Group 1 was left untreated. Groups 2-6 were treated once daily, on day 2, 3 and 4, with sunscreen in a volume of 10 µL onto the anterior and 10 µL on the posterior surfaces of both ears (30 min. post TPA challenge on day 2 and 3). Group 2 received sunscreen alone, group 3 received sunscreen mixed with 30 nm TiO₂ NPs (Sample C: TiO₂, rutile, high purity 99.9%, US Research Nanomaterials Inc.), group 4 received sunscreen mixed with 100 nm TiO₂ NPs (Sample D, rutile,

high purity 99.9%, US Research Nanomaterials Inc.), group 5 received sunscreen mixed with 30 nm TiO₂ NPs coated with silicone (Sample E, rutile, high purity 99.9%, US Research Nanomaterials Inc.) and group 6 received sunscreen mixed with 30 nm TiO₂ NPs coated with silicone and aluminum (Sample F, rutile, high purity 99.9%, 30 nm, US Research Nanomaterials Inc.). Mice were anaesthetized with isoflurane prior to sunscreen application. To prevent oral uptake of nanoparticles, all mice, treated with sunscreen, were single housed and dressed with collars (Elizabethan Collars, Kent Scientific, Torrington, CT, U.S.A.). Ear thickness is measured on day 1, 2, 3, 4 and 8 to measure the effect of TPA, vehicle (acetone) and sunscreen treatment. On day 8, retro-orbital blood samples were collected in lithium-heparin containing tubes, snap frozen in liquid N₂ and stored at -80°C until further use. Following, mice were killed by cervical dislocation. Each ear is removed and washed 3 times in 1 ml C12-15 alkyl benzoate (undiluted) followed by 3 times in 1 ml 1% Triton X-100 (diluted in PBS) followed by 3 times in 1 ml PBS. Washing occurs by vortexing at highest speed for 10 seconds. The ear is transferred into a new tube with fresh washing agent after each washing step. Two 3 mm punch biopsies were taken per ear and fixed in phosphate buffered 2% glutaraldehyde. Leftover skin was stored at -80°C until further use. Additionally, from each mouse, the liver, the spleen and auricular node was removed, snap frozen in liquid N₂ and stored at -80°C until further use. However, analysis of these samples were not part of this project. Mice were fed standard rodent laboratory diet, given water ad libitum and housed under standard conditions with a 12-h light/dark cycle and controlled temperature. All animal experimental procedures were approved by the Danish Experimental Animal Inspectorate.

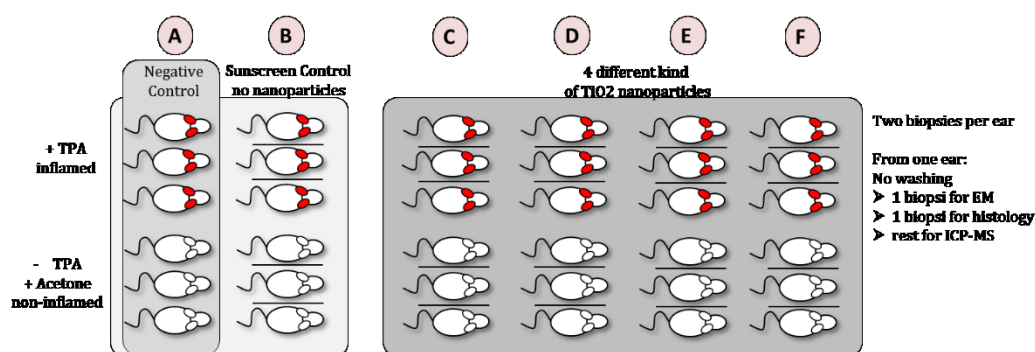


FIGURE 6: OVERVIEW OVER THE EXPERIMENTAL DESIGN FOR ACUTE IRRITANT CONTACT DERMATITIS (ICD) MOUSE MODEL

2.6.6 *In vivo* xenograft human skin model

Mouse skin is different from human skin. Mouse skin lacks apocrine sweat glands and rete ridges/dermal papillae, is covered with dense hair with differences in the hair cycle (about three weeks compared to hair cycles of the human scalp of several years). Additionally, human hair can penetrate into deep dermis [Wong et al., 2011]. These differences could therefore lead to different results for the dermal absorption and penetration of nanoparticles. Due to the rules of the Danish EPA for experimental projects, it was not allowed to use human volunteers within this project. To be able to investigate the absorption and penetration of nanoparticle containing sunscreen on human skin a xenograft human skin model was used. Normal human skin was provided by a healthy donor (27 years, female) undergoing corrective surgery. Informed consent was obtained and the study was approved by the Central Ethical Committee and conducted in accordance with the Declaration of Helsinki protocols. A keratome skin biopsy (containing both epidermis and dermis) was obtained from the normal skin and cut into smaller grafts (~1.5 cm²) before transplantation onto the back of 16 C.B-17 severe combined immunodeficient (SCID) mice (female, 6-8 weeks of age, Taconic, Ry, Denmark), as described [Dam et al., 1999; Rosada et al., 2010; Stenderup et al., 2009; Stenderup et al., 2011]. Prior to surgery, mice were anesthetized by a subcutaneous injection

of Ketaminol (ketamine, 100mg/kg, Intervet) and Narcoxyl (xylazine, 10 mg/kg, Intervet). The back was shaved and part of the exposed skin was removed. The grafts were sutured with an absorbable 6-0 suture (Caprosyn, Tyco) and covered with Xeroform dressings (Sherwood Medical Company) for 1 week. Analgesic (9 µg/ml, buprenorphin, Temgesic, Reckitt Benckiser Healthcare International) was provided in the drinking water. After a healing period of seven weeks, the animals were divided randomly into six separate treatment groups. Group 1 was left untreated. Groups 2-6 were treated once daily, on day 1, 2 and 3, with sunscreen (see chapter 2.3) in a volume of 15 µL covering the grafted human skin. Group 2 received sunscreen alone, group 3 received sunscreen mixed with 30 nm titanium oxide nanoparticles (Sample C, TiO₂, rutile, high purity 99.9%, US Research Nanomaterials Inc.), group 4 received sunscreen mixed with 100 nm TiO₂ (Sample D, rutile, high purity 99.9%, US Research Nanomaterials Inc.), group 5 received sunscreen mixed with 30 nm TiO₂ coated with silicone (Sample E, rutile, high purity 99.9%, US Research Nanomaterials Inc.) and group 6 received sunscreen mixed with 30 nm TiO₂ coated with silicone and aluminum (Sample F, rutile, high purity 99.9%, 30 nm, US Research Nanomaterials Inc.). Mice were anaesthetized with isoflurane prior to sunscreen application. To prevent oral uptake of nanoparticles, all mice treated with sunscreen were single housed and dressed with collars (Elizabethan Collars, Kent Scientific, Torrington, CT, U.S.A.).

On day 8, retro-orbital blood samples were collected in lithium-heparin containing tubes, snap frozen in liquid N₂ and stored at -80°C until further use. Following this, mice were killed by cervical dislocation and the grafted human skin washed three times in each of the following solutions, to remove remaining sunscreen: C12-15 alkyl benzoate, triton X-100 (1% diluted in PBS) and PBS. The grafted human skin was removed and two 3 mm punch biopsies were taken and fixed in phosphate buffered 2% glutaraldehyde. Leftover skin was stored at -80°C until further use. Additionally, from each mouse, the liver and the spleen was removed, snap frozen in liquid N₂ and stored at -80°C until further use. However, analysis of these samples were not part of this project. Mice were fed standard rodent laboratory diet, given water ad libitum and housed under standard conditions with a 12-h light/dark cycle and controlled temperature. All animal experimental procedures were approved by the Danish Experimental Animal Inspectorate.

2.6.6.1 Trans Epithelial Electrical Resistance (TEER) measurement

For the Trans Epithelial Electrical Resistance (TEER) the Millicell® ERS (Electrical Resistance System) were used that measures membrane potential and resistance of epithelial cells in culture and can be used to measure the resistance of cells grown on microporous membranes. With this system, membrane capacitance does not affect resistance readings.

This method allows for the qualitatively investigation of cell monolayer health and measures quantitatively cell confluence. An increase in TEER is an indication of cell monolayer health, growth and confluence whereas a decrease indicates a loss in confluence and possible problems with the health of the cell culture. A silver/silver chloride (Ag/AgCl) pellet on each electrode tip measures voltage.

For the TEER measurement the inserts with the *in vitro* EpiDerm™ skin models were transferred into a 6 well filled with 900 µl PBS, and 300 µl PBS were added on top of the cells in the insert. Subsequently, the resistance was measured. The measurement occurred during the whole period of the experiment on the days indicated in Table 7.

2.6.6.2 Skin corrosion and skin irritation analysis – MTT assay

The skin corrosion and skin irritation analysis is based on the MTT assay, which is a colorimetric assay where the cell viability is measured. In this assay tetrazolium dye MTT 3-(4,5-dimethylthiazol-2-yl)-2,5-diphenyltetrazolium bromide is reduced by the NAD(P)H-dependent cellular oxidoreductase enzyme to insoluble formazan, which has a purple color. Reduction of MTT depends on the cellular metabolic activity and may reflect, under defined conditions, the number of viable cells or at least the metabolic activity of the cells. Thereby, this assay is used to investigate changes of the cell viability or metabolic activity that are due to the exposure to a test substance, in this project, nanoparticle containing sunscreen. Furthermore, this assay is used to perform the skin

corrosion and skin irritation analysis. The EpiDerm™ system has been validated by the OECD for skin corrosion and skin irritation test (OECD test guidelines #431 and #439). As stated by the OECD: "... reconstructed human epidermis (RhE), which in its overall design closely mimics the biochemical and physiological properties of the upper parts of the human skin. ... Depending on the regulatory framework and the classification system in use, this procedure may be used to determine the skin irritancy of test substances as a stand-alone replacement test for *in vivo* skin irritation testing, or as a partial replacement test, within a tiered testing strategy."

Here, this was performed as described by the manufacturer (MatTek). Essentially, each tissue was incubated with 300 µl of 1 mg/ml MTT solution for 3 hours (37 °C, 5% CO₂, 95 % RH). After washing with PBS the tissues were incubated with 2 ml isopropanol overnight. For each tissue, three 200 µL aliquots of the purple formazan solution were transferred into a 96-well flat bottom microtiter plate. For blanks, use isopropanol. The optical density (OD) was read in a 96-well plate spectrophotometer using a wavelength of 570 nm (540-580).

2.6.6.3 ICP-MS

The samples were weighed into a Teflon tube and 2 ml half concentrated nitric acid added. The Teflon tube was sealed and heated in a microwave oven at temperatures around 120 to 140 degrees under high pressure. Thereby the samples were completely dissolved and used for ICP-MS measurements that were performed by DCE/Department of Environmental Science and Department of Bioscience, Aarhus University that is accredited to a selection of analysis, including test sampling and *in situ* measurements. The accreditation means that the institutes are annually controlled by DANAK, the Danish Accreditation Body of laboratories which ensures that the institutes and the testing (analysis, test samples and *in situ* measurements) follow the international standard ISO 17025 for General Requirements for Competence and Calibration Laboratories.

2.6.6.4 Cytokine analysis

Cytokines are important mediators in inflammatory responses. Secretion of cytokines as cellular response upon exposure to a test substance might therefore be a sign for the induction of inflammatory responses.

The release of cytokines in the cell culture medium beneath the *in vitro* EpiDerm™ skin model was investigated using the Bio-Plex® Pro™ Human Cytokine 27-Plex kit from BioRad and the Bio-Plex® MAGPIX™ Multiplex Reader. Medium samples were taken directly after 20 h exposure and on day 3 after ended exposure (48 hours after ended exposure). The cytokines that were released into the medium were quantified for all tissues of the three *in vitro* EpiDerm™ skin model lots resulting in data for nine independent *in vitro* EpiDerm™ skin model tissues. The analyses were performed. For the analysis 50 µL of undiluted medium was used and the assay was performed exactly as described by the manufacturer.

2.6.6.5 Transmission electron microscopy (TEM)

The investigation of the dermal absorption and penetration of the nanoparticles in sunscreen was done by transmission electron microscopy (TEM) for the *in vitro* and *in vivo* skin models. Although it is a very time consuming and only a qualitative method, this method can show directly the dermal absorption and penetration of the nanoparticles as well as the localization of the particles within the skin layers and the cells. The investigated TEM sections were 70 to 100 nm thick. For a section of 50 µm length the estimated particle number exposure of a surface area corresponding to a TEM section of 50µm x 70nm was calculated and is shown in Table 8 below. Although these are estimates, except for sample D) a detection of particles in deeper skin layer should be possible based on these numbers. A general detection limit cannot be given as this is dependent on the number of sections at time that is used for analysis. However, the used system of a FEI Morgagni transmission electron microscope with SISIII digital camera has a 0.45 nm point - point resolution and is able to detect the used nanoparticles.

TABLE 8: ESTIMATED PARTICLE NUMBER EXPOSURE TO A 50 µM X 70 NM UPPER SURFACE AREA OF A TEM SECTION

Sample code	Estimated particles per 50 µm x 70 nm area [particle number]		
	<i>in vitro</i> EpiDerm skin model	<i>in vivo</i> TPA model	<i>in vivo</i> xenograft model
C)	890,000	1,010,000	530,000
D)	16,000	18,000	9,800
E)	410,000	470,000	250,000
F)	380,000	435,000	230,000
G)	8,160,000	9,250,000	4,900,000
H)	5,010,000	5,680,000	3,000,000
I)	1,950,000	---	---
K)	1,420,000	---	---

The samples were prepared for electron microscopy as follows:

Sample preparation of *in vitro* EpiDerm™ skin model:

The inserts were transferred into a 24-well plate. To fix the tissues 1.5 ml phosphate buffered 2% glutaraldehyde in PBS were added and the tissues stored at 4°C. The inserts with the cells were transferred into 12-well boxes and dehydrated therein by the following incubations: 3 x 5 min 0.1 M phosphate buffer pH 7.2, 1 hour 1% OsO₄ in 0.1 M phosphate buffer, 2 x 5 min 0.1 M phosphate buffer, 2 x 5 min 0.05 M maleate buffer pH 5.2. At this point the membrane was cut free from the plastic cylinder of the insert with a pointed scalpel; the cylinder was removed and proceeded with the dehydration by 2 x 5 min 50% ethanol, 2 x 10 min 70% ethanol, 2 x 10 min 90% ethanol, 2 x 10 min 96% ethanol, 2 x 15 min 99% ethanol, 2 x 15 min isopropanol (2-propanol). The tissues were embedded by incubation in isopropanol / EPON 1:1 overnight and 8 hours incubation in pure EPON. The membrane where then placed in capsules and filled up with EPON. Polymerization was at least 24 hours at 60°C.

Sample preparation of *in vivo* mouse model for acute irritant contact dermatitis

Mice ear biopsies were fixated adding 1.5 ml phosphate buffered 2% glutaraldehyde in PBS. The biopsies were then stored at 4°C. The biopsies were dehydrated and embedded by the following incubation sequence: 3 x 5 min 0.1 M phosphate buffer, 60 min 1% Osmium in phosphate buffer, 2 x 15 min 0.1 M Phosphate Buffer, 2 x 15 min 0.05M maleate, 2 x 15 min 70% ethanol, 2 x 15 min 90% ethanol, 2 x 15 min 96% ethanol, 3 x 15 min 99% ethanol, 2 x 30 min propylene oxide, 1 day propylene oxide / Epon 3:1, 4 days propylene oxide / Epon 1:1, 2 days propylene oxide / Epon 1:3, 1 day pure Epon. The biopsies where then placed in capsules and filled up with EPON. Polymerization was at least 24 hours at 60°C.

Sample preparation of *in vivo* xenograft human skin model

Xenograft human skin biopsies were fixated adding 1.5 ml phosphate buffered 2% glutaraldehyde in PBS. The biopsies were then stored at 4°C. The biopsies were dehydrated and embedded as described for *in vitro* EpiDerm™ skin model.

TEM digital images

The TEM samples were screened in a standardized way to ensure that all samples were treated exactly the same and pictures were taken using a FEI Morgagni transmission electron microscope with a SISIII digital camera with a 0.45 nm point - point resolution.

Step 1) The morphology of the *in vitro* EpiDerm™ system, *in vivo* mouse model for acute irritant contact dermatitis, and *in vivo* xenograft human skin model samples were investigated using a magnification of 7100x. Images were taken from the surface and further down in the direction of the membrane the tissue was cultivated on or in the direction of deeper skin layers in the case of the *in vivo* models. Approximately four images are taken for each morphological different tissue layer.

Step 2) The whole surface of the TEM sample was systematic scanned for residual nanoparticles at the surface that were not washed off. If nanoparticles can be found at the surface, images are taken with a magnification of 22.000x (final magnification 71.000x) and 44.000x (final magnification 142.000x).

Step 3) Three regions with nanoparticles at the surface are identified and here the samples are investigated through all tissue layers and images are taken from all cellular structures that could be nanoparticles. Images were taken with 22.000x (final magnification 71.000x) and 44.000x (final magnification 142.000x) magnification. For negative controls (no sunscreen and sunscreen without nanoparticles) the samples are systematically screened for structures similar to nanoparticles.

2.6.6.6 H&E staining - Histology

In vitro EpiDerm™ skin model tissues, mice ear biopsies, xenograft human skin biopsies were fixated adding 1.5 ml phosphate buffered 2% glutaraldehyde. The biopsies were then stored at 4°C before they underwent the following H&E staining procedure. Given are the incubation times and the reagents the tissues were incubated in:

Infiltration paraffin:

70% alc.	2h
96% alc.	1h + 2h
99% alc.	1h + 1h + 2h
Xylene	1h + 1h + 2h
Paraffin	2h + 2h

Dehydration before staining:

Xylene	3 x 5 min.
99% alc.	3 x 4 min.
96% alc.	3 x 4 min.
70% alc	2 x 5 min.
Dest. Water	1 – 2 min.

Staining:

Mayers Hæmatoxylin	8 min.
Running tap water	10 min.
Eosin	4 min.
96% alc.	3 x 1 min.
99% alc.	3 x 2 min.
Xylene	3 x 3 min.

Eosin:

Eosin 1%	50 ml.
96% alc.	200 ml.
Acetic acid 100%	2.5 ml.

5 µm sections were cut at a Leica RM 2255 and the cuts were investigated using light microscopy (Leica) and picture were taken using a color LCD camera.

2.6.7 Statistical analysis

Data are expressed as mean +/- standard deviation (SD). The statistical significance was determined by Student's t-test ($p < 0.05$) or one way analysis of variance (ANOVA) followed by Dunnett test. Statistical analysis was performed in SigmaPlot ver. 11.

3. Results

3.1 Nanoparticle preparation and characterization

The aim of this project was to evaluate if nanoparticles in sunscreen are able to penetrate the skin. This was done by application of nanoparticle containing sunscreen to *in vitro* skin models as well as mouse and human skin. Throughout the project, the following controls were used: negative control - untreated skin models that received no sunscreen, and sunscreen control – skin models that received sunscreen that did not contain nanoparticles as test formulation control.

In an opinion of the Scientific Committee on Consumer Safety (SCCS) on nano form titanium dioxide the investigation of the particle size distribution was an important lack of information for a number of studies (SCCS (Scientific Committee on Consumer Safety), Opinion on titanium dioxide (nano form), 22 July 2013, revision of 22 April 2014). A number of different toxicological studies and investigations were therefore considered as of limited use for a risk assessment. The particle size distribution of the particles in sunscreen is therefore an important information for the evaluation of the experimental results – are the nanoparticles present in sunscreen as single nanoparticles, nano-sized aggregates of nanoparticles or as micro-sized aggregates. The TiO₂ and ZnO NPs that were used for this project were dispersed in sunscreen similar to a protocol used by the cosmetic industry. The nanoparticles were characterized at different stages: as nanoparticle powders, pre-dispersed and final dispersed in sunscreen. Especially the particle size distribution in sunscreen was of interest as it is the product the consumers are applying to their skin.

3.1.1 Characterization of the pre-dispersant

Before adding the different TiO₂ and ZnO NPs to the sunscreen the nanoparticle powders were pre-dispersed in a mixture of polyhydroxystearic acid (10 wt%) and C₁₂-C₁₅ alkyl benzoate (90 wt%). To evaluate if the pre-dispersant affects the measurement of the particle size distribution the pre-dispersant was investigated by dynamic light scattering analysis (DLS). The pre-dispersant showed no signal (data not shown).

3.1.2 Characterization of sunscreen

Pre-dispersed nanoparticles were diluted with sunscreen to a final concentration of 2.5% wt/wt. The used sunscreen is an oil-in-water emulsion with different ingredients, but mainly C₁₂-C₁₅ alkyl benzoate and water.

The size distribution of the oil droplets of the sunscreen was analyzed by DLS after 1000 times dilution in MilliQ water and is shown in Figure 7. The DLS analysis showed two peaks, one at around 180 nm and one at around 450 nm.

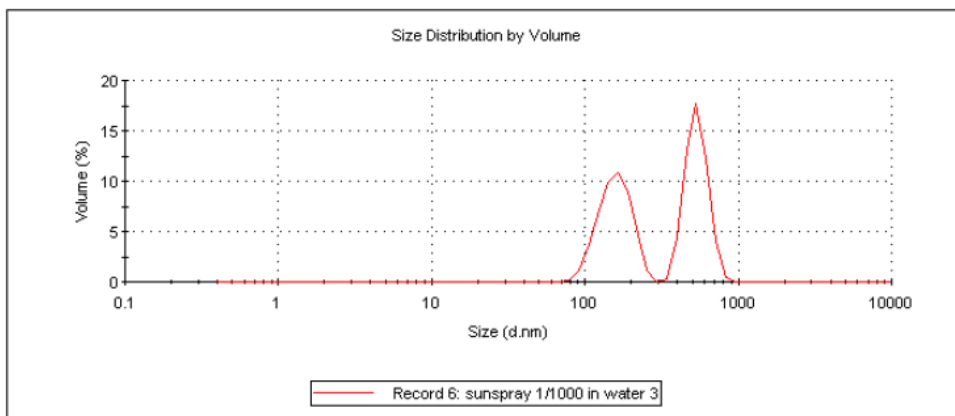


FIGURE 7: SIZE DISTRIBUTION OF THE OIL DROPLETS OF THE SUNSCREEN. ANALYSIS BY DLS AFTER 1000X DILUTION IN DEMINERALIZED (MILLIQ) WATER.

The different sizes of the oil droplets was confirmed by optical microscope and is shown in Figure 8.

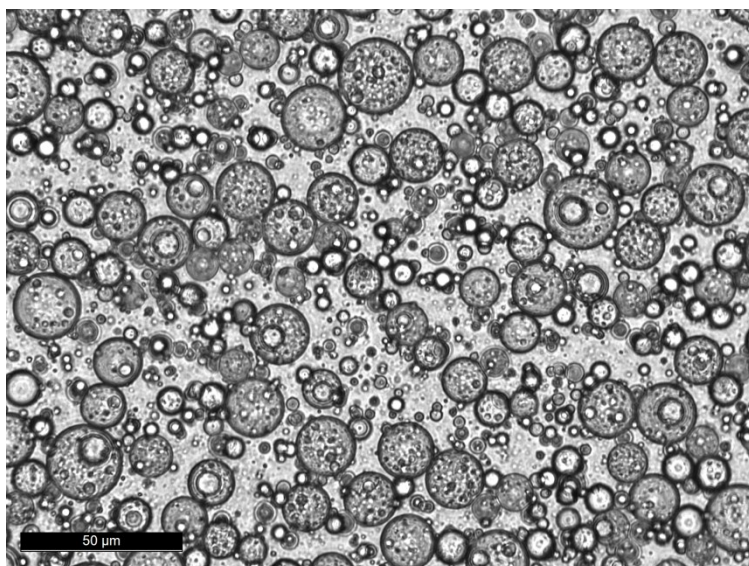


FIGURE 8: SIZE DISTRIBUTION OF THE OIL DROPLETS OF THE SUNSCREEN ANALYZED BY OPTICAL MICROSCOPE.

3.1.3 Characterization of the nanoparticle powders

The nanoparticle powders were investigated by transmission electron microscopy (TEM) and energy dispersive X-ray analysis (EDX). A detailed description of the investigated nanoparticles are given in the Material and Methods section. TEM pictures of the different nanoparticle powders are shown in Figure 9. Besides samples C) and G), which have a more needle-shaped form, all nanoparticles had a spherical form. The EDX analysis showed a clear signal for, depending on the nanoparticle type, either Ti or Zn (Figure 10). The single of Cu is due to the copper grid used for sample preparation.

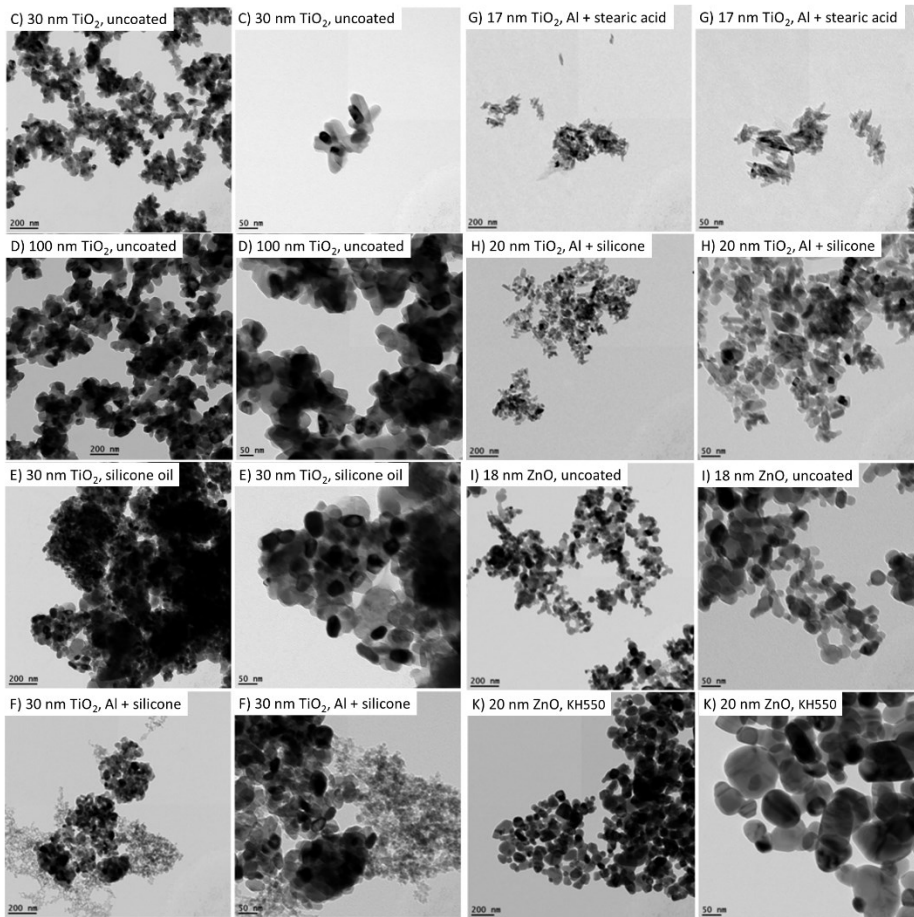


FIGURE 9: TRANSMISSION ELECTRON MICROSCOPY OF THE USED NANOPARTICLE POWDERS SAMPLES C) TO K)

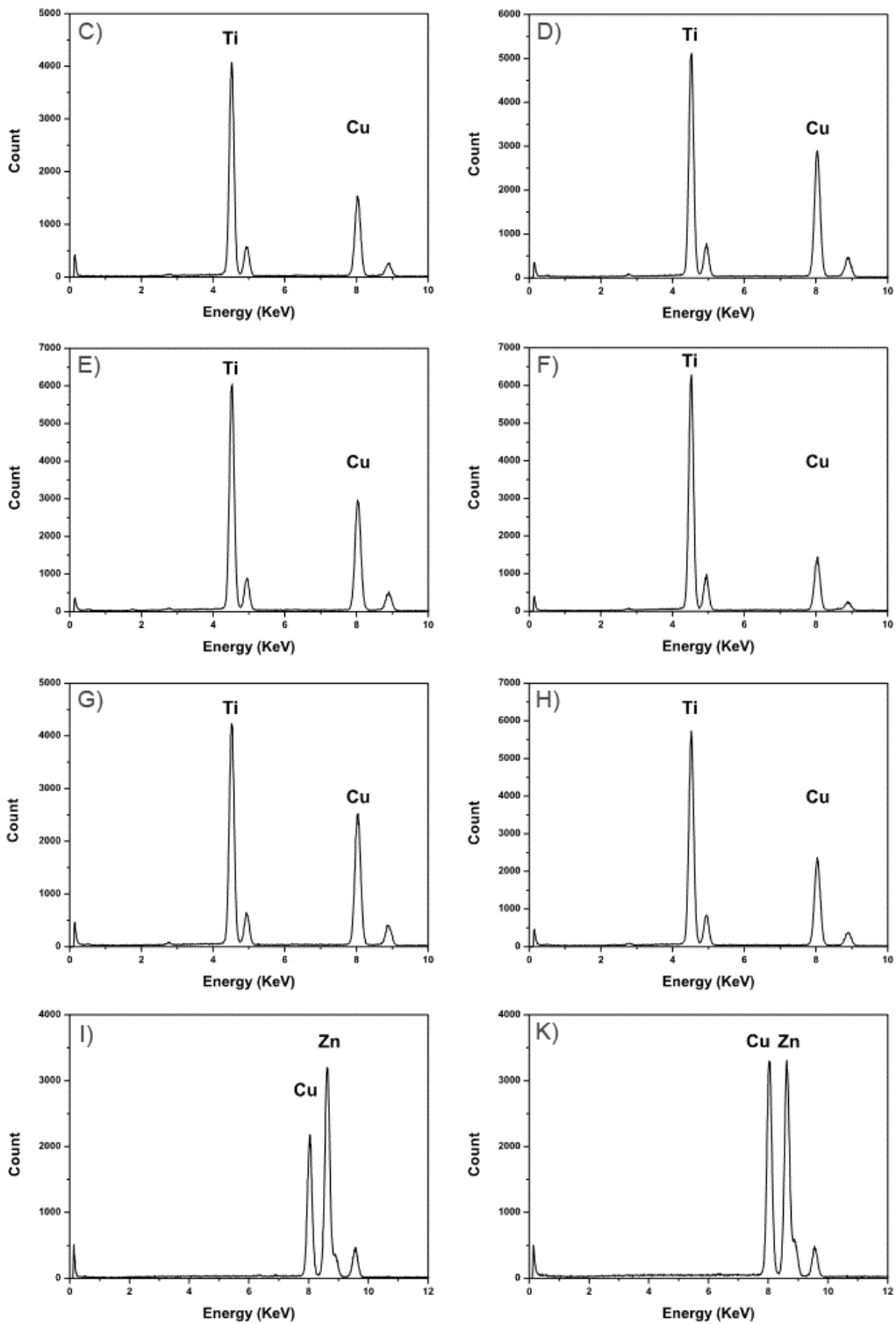


FIGURE 10: TEM-EDX OF THE NANOPARTICLE POWDERS, SAMPLES C) TO K). THE SINGLE OF CU IS DUE TO THE COPPER GRID.

3.1.4 Particle size distribution of nanoparticles dispersed in MilliQ water, pre-dispersant C12-C15 alkyl benzoate and sunscreen

Dynamic light scattering (DLS) analysis were used to determine the size of the nanoparticles and their surface charge (ζ -potential or electrokinetic potential in colloidal dispersions) in MilliQ water. The results are shown in Figure 11, and Z-average size, polydispersity index (PDI), and zeta potential are summarized in Table 9.

As can be seen from Figure 11, the nanoparticles are highly aggregated in MilliQ water. However, as the pre-dispersion of the nanoparticles occurred in C12-C15 alkyl benzoate before adding to the sunscreen, the aggregation in sunscreen might be different. The ζ -potential shows that all TiO₂ NPs have an anionic, negative surface charge whereas ZnO NPs are neutral to fairly positively charged in water (Table 9). However, it has to be kept in mind that the ζ -potential measurement occurred in water and that the ζ -potential in sunscreen might be different.

TABLE 9: SUMMARY OF Z-AVERAGE SIZE, POLYDISPERSITY INDEX (PDI), AND ZETA POTENTIAL FOR THE NANOPARTICLES IN MILLIQ WATER

Sample code	Z-average size [nm]	PDI	Zeta potential [mV]	Surface charge in MilliQ water
C)	250	0.190	-51.9	negative
D)	363	0.196	-57.1	negative
E)	537	0.305	-58.4	negative
F)	623	0.240	-48.9	negative
G)	714	0.507	-32.9	negative
H)	1030	0.469	-15.8	negative
I)	440	0.245	+9.35	neutral/fairly positive
K)	976	0.269	-1.44	neutral

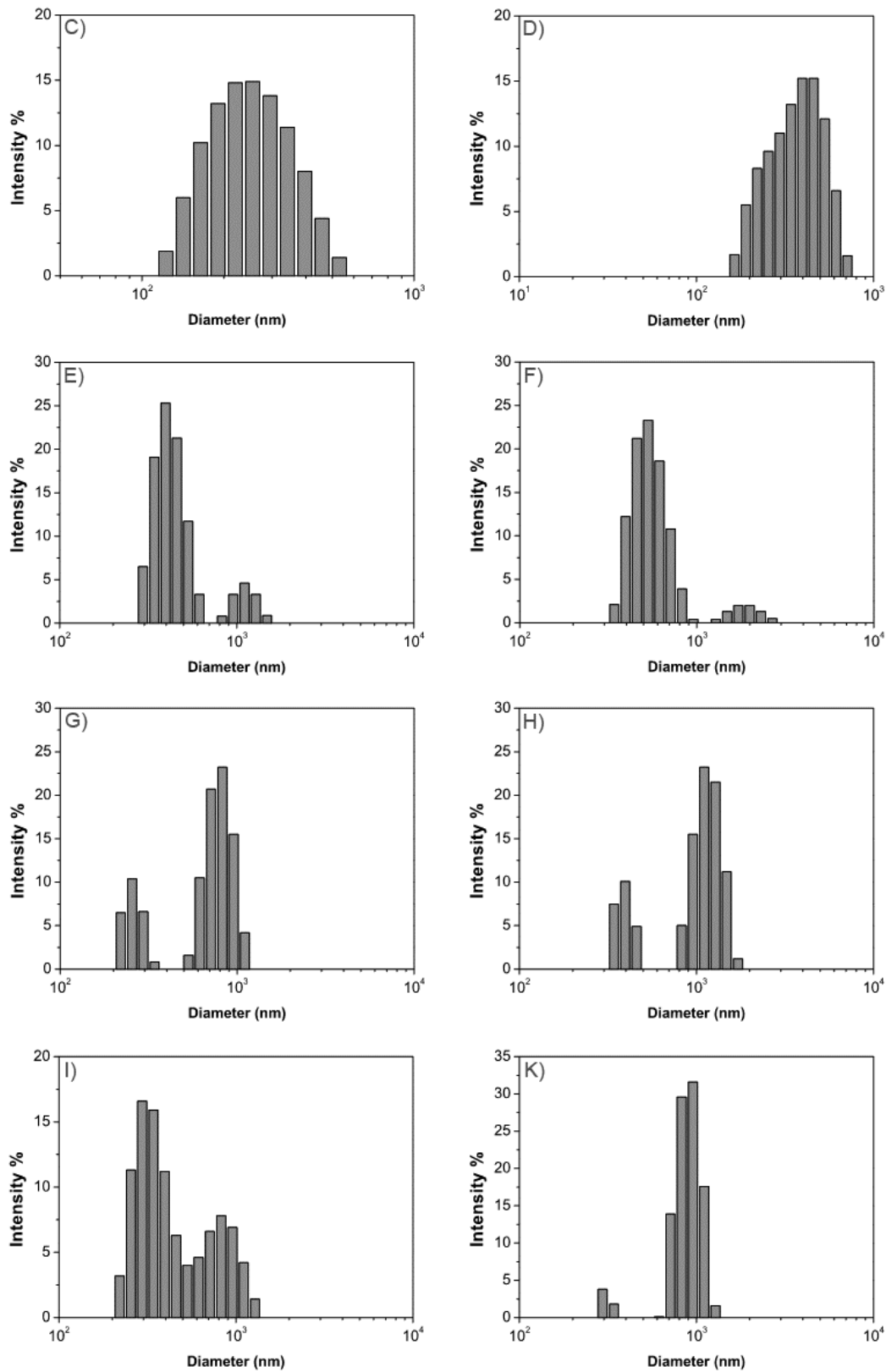


FIGURE 11: DYNAMIC LIGHT SCATTERING (DLS) ANALYSIS OF THE PARTICLE SIZE DISTRIBUTION OF THE NANOPARTICLES IN MILLIQ WATER

As DLS was not applicable for the investigation of the particle size distribution of nanoparticles in C12-C15 alkyl benzoate the pre-dispersion of the eight different nanoparticles were observed by an optical microscope (Figure 12). CCD camera recorded images were used to analyze size distributions using Software ImageJ 2.0. For all nanoparticles there is a major group of small aggregates around 250nm in diameter. TiO₂ NPs without surface coating (samples C and D)) or with silicone oil coating (sample F)) show larger aggregation groups around 2µm, indicating a less stable dispersion in C12-C15 alkyl benzoate. Within the nanoparticles with similar Al coating (samples E), G) and H)), the nanoparticle samples E) and G) have similar size distributions where about 20% of the total population are smaller aggregates (250 nm), while sample H) has about 50% of the smaller aggregates. This might be due to the shape differences, since G) is more spindle-shaped with a length close to 40nm according to TEM. Coated ZnO NPs are better dispersed compared to uncoated ones, as a greater population of small aggregates and smaller size of larger aggregates are detected. However, it should be mentioned that the limit of resolution for an optical microscope under oil is ~200nm.

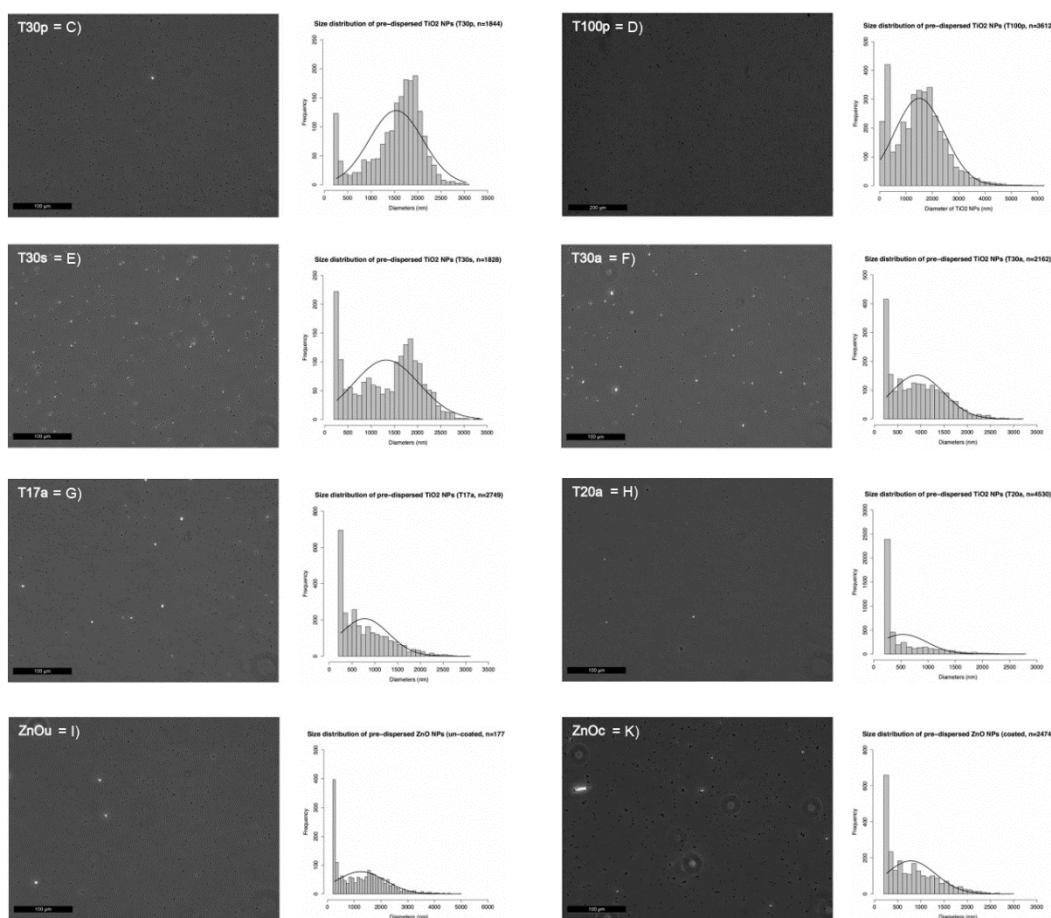


FIGURE 12: ANALYSIS OF THE PARTICLE SIZE DISTRIBUTION OF PRE-DISPersed NANOPARTICLES BY OPTICAL MICROSCOPY

Optical microscopy was also used in a first attempt to investigate the particle size distribution of the nanoparticles in sunscreen (Figure 13). TiO₂ NPs without surface coating (samples C and D)) or with silicone oil coating (sample F)) were found to aggregate on the outside surface of oil droplets in sunscreen. With similar Al coating (samples E), G), H)), TiO₂ NPs were found to aggregate on the inner side of emulsions, while sample G) seems to evenly coat the inner layer of the emulsion. Both

ZnO NPs look similar to G). However, this could also indicate the dissolution of ZnO NPs , as ZnO NPs are known to dissolve and since the sample were observed more than 24 h post preparation.

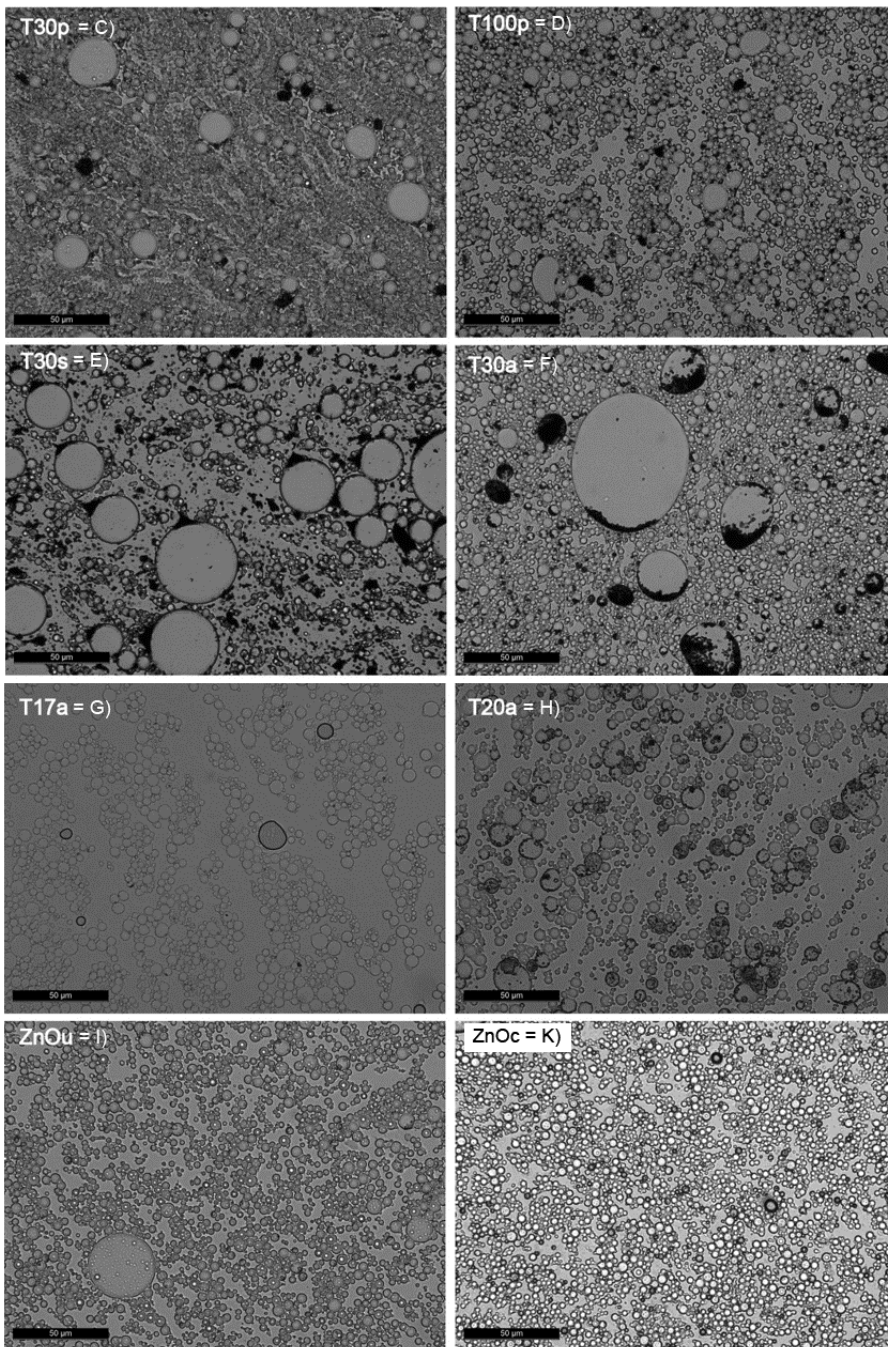


FIGURE 13: OPTICAL MICROSCOPY OF NANOPARTICLES IN SUNSCREEN

Because of the resolution limit, optical microscopy is not a very reliable method to investigate the particle size distribution of nanoparticles in sunscreen. However, due to the viscosity of sunscreen and the extremely high amount of nanoparticles (2.5%wt/wt) the methods to investigate the particle size distribution are very limited. One possibility to overcome these problems is the use of acoustic attenuation spectroscopy (AAS).

3.1.5 Acoustic attenuation spectroscopy (AAS) measurement of the particle size distribution in sunscreen

The Electroacoustic method can be used for the determination of ζ -potential related properties like the iso-electric point of concentrated dispersions and is a technique that is applicable to investigate the particle size distribution in sunscreen. A pulse technique device measures the electroacoustic signal at frequencies from 1 to 10 MHz for either pure liquids or colloids. Ultrasound induces a motion of particles relative to the liquid. This motion disturbs the double layer, shifting a screening cloud of counter-ions. This displacement of the ionic cloud with respect to the particle surface creates a dipole moment. The sum of these dipole moments over many particles creates an electric field, which is measured as the electroacoustic vibration current (CVI). This field depends on the value of ζ -potential, which is calculated applying an appropriate theory. Furthermore, other colloidal parameter like dynamic mobility, Debye length and surface charge can be determined. The measured particle sizes are shown in Table 10. Samples C), E), F), I), and K) have particle size distribution where 50% of the particles are around 200 nm. Samples G) and H) show a noticeable larger size of 661 nm and 393 nm, respectively. With this method it was possible to reliably measure the particle size distribution in sunscreen. The graphs of the measured size distribution are shown in Figure Figure 14. As already seen from the data presented in Table 10, the samples C), E), F), I), and K) have a very narrow standard variation. This means that the particles in these samples have nearly the same size.

TABLE 10: ACOUSTIC ATTENUATION SPECTROSCOPY (AAS) MEASUREMENT OF THE PARTICLE SIZE DISTRIBUTION IN SUNSCREEN

Sample code	NP type	Size [nm]	Surface coating	d10* [nm]	d50** [nm]	d90*** [nm]	SD [nm]
C	TiO ₂	30	Uncoated	192	197	204	11
D	TiO ₂	100	Uncoated	263	359	458	112
E	TiO ₂	30	Silicone oil	251	258	266	11
F	TiO ₂	30	Silicone and alumina	230	236	244	11
G	TiO ₂	17	Alumina, stearic acid	310	661	1410	274
H	TiO ₂	20	Alumina, silicone	186	393	828	270
I	ZnO	18	Uncoated	178	184	189	11
K	ZnO	20	KH550	205	212	218	11

* 10% of the particles have a size below this diameter; ** 50% of the particles have a size below this diameter; *** 90% of the particles have a size below this diameter (or 10% of the particles have a size larger then this diameter)

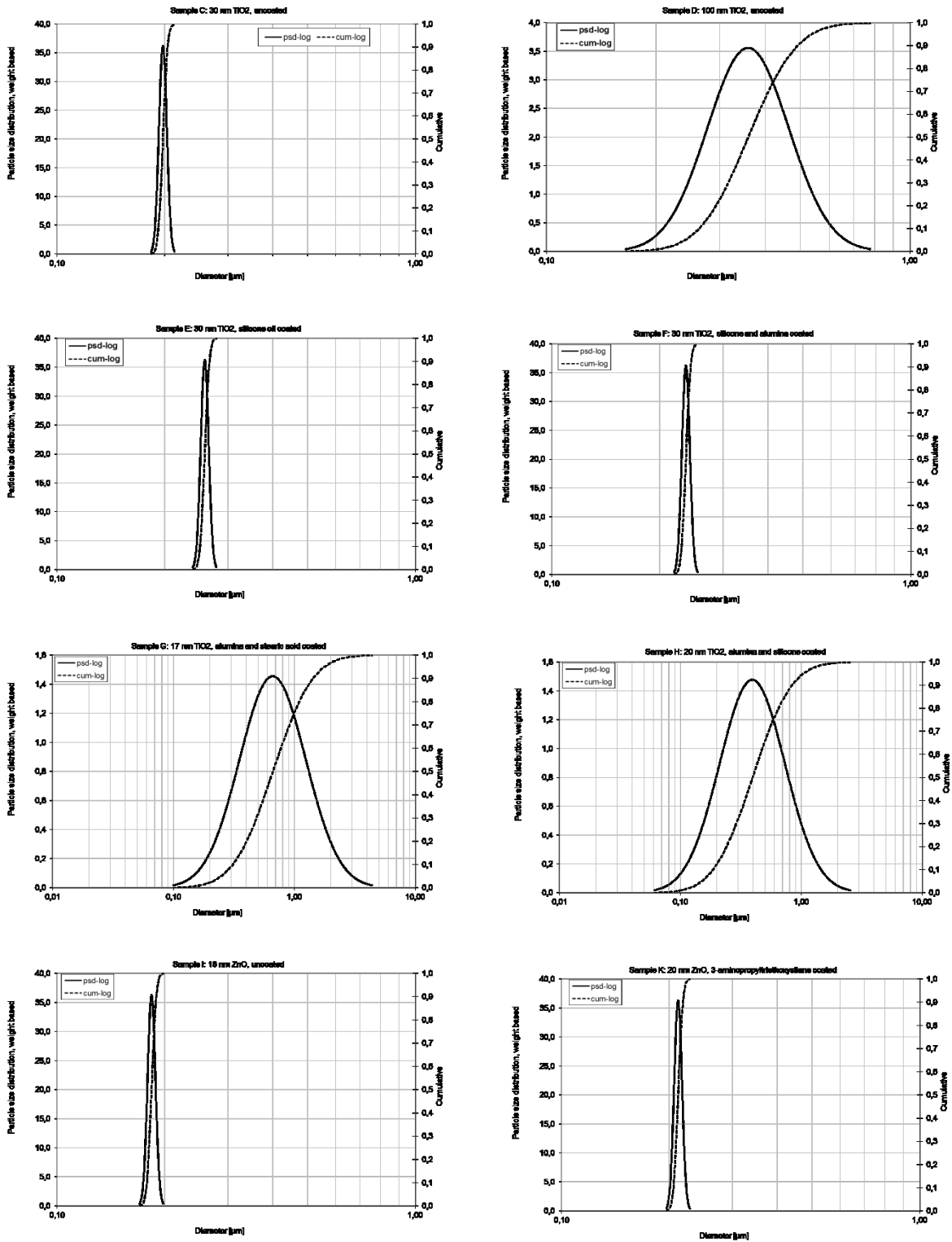


FIGURE 14: WEIGHT BASED PARTICLE SIZE DISTRIBUTION OF TiO₂ AND ZnO NANOPARTICLES IN SUNSCREEN

3.1.6 Conclusion nanoparticle characterization

Our characterization data suggest a strong agglomeration/aggregation tendency of the nanoparticles in sunscreen. However, as we are only able to determine the weight based particle size distribution and not the number size distribution for these particles there could be a high number of particles below 100 nm present in our samples that were not detected.

3.2 Dermal absorption/penetration of TiO₂ and ZnO NPs in *in vitro* EpiDerm™ skin model

The *in vitro* EpiDerm™ skin model was used in the first set of experiments, as it is a skin model that is validated by the OECD for the investigation of skin corrosion and skin irritation. Furthermore, this model allowed us to directly measure the potential transport of the on top of the skin model applied nanoparticles through the EpiDerm™ skin model into the medium beneath by elemental analysis using ICP-MS. With this spectroscopy method it is possible to detect titanium and zinc that originates from nanoparticles that have penetrated the skin model into the medium below. In addition, the medium beneath the skin model was investigated in parallel for released cytokines that are a measure for inflammatory responses as a reaction to the exposure and/or the uptake of the particles by the cells. After a lag-phase of several days after the exposure to nanoparticle containing sunscreen, the EpiDerm™ skin models were analyzed for skin corrosion and skin irritation and samples for transmission electron microscopy and histology were prepared. During the whole duration of the experiment, the confluence of the skin model was measured by TEER. This was especially important before samples were taken for ICP-MS as a leaky skin model would lead to a direct migration of TiO₂ or ZnO NPs into the medium beneath the skin model thereby leading to false positive Ti and Zn signals. An overview of the experimental setup using the *in vitro* EpiDerm™ skin model is shown in Figure 15 and the results from the different analysis are described in detail in chapters 3.2.1 to 3.2.5. The different analyses were chosen, as none of them can stand alone to analyze the dermal absorption and penetration of nanoparticles.

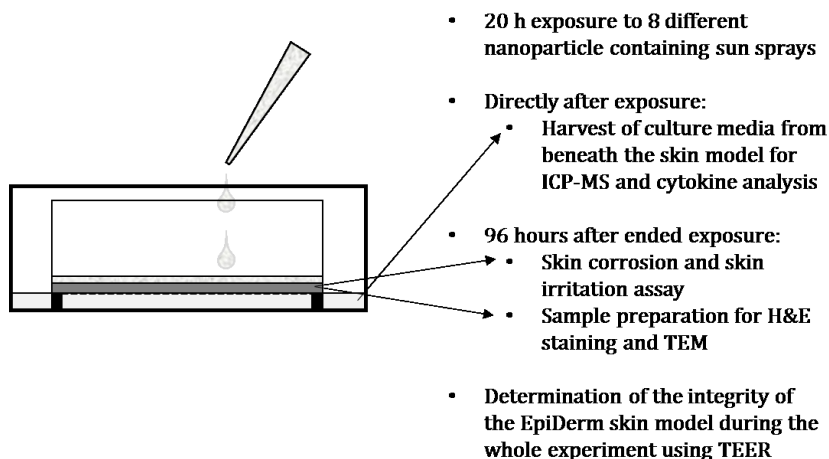


FIGURE 15: OVERVIEW OF THE EXPERIMENTAL SETUP USING THE *IN VITRO* EPIDERM™ SKIN MODEL

3.2.1 Effect of sunscreen on skin model permeability – TEER measurements

The integrity and confluence of the EpiDerm™ skin model is of uppermost importance for the investigation of a potential dermal absorption and penetration. Therefore, Trans Epithelial Electrical Resistance (TEER) measurements were performed at several time points during the experiments. The resistance of the skin model is a measure for how dense the skin model is and if exposure to sunscreen, with or without nanoparticles, is disturbing the integrity of the cell layers. If this would be the case, the detection of TiO₂ or ZnO NPs in the medium beneath the skin model would not necessarily originate from the transport of these particles through the skin. Thereby it

would not be possible to draw a definite conclusion on the dermal penetration of TiO₂ or ZnO nanoparticle. Figure 16 shows that the application of sunscreen, independent if TiO₂ or ZnO NPs were present, leads to a clear and significant decrease in the resistance of the skin models (compare before and after 20h exposure columns). After a first drastic decrease no further significant decrease in TEER were observed during the rest of the experiment. For untreated EpiDerm skin models TEER of 510 ± 120 Ω/cm² have been reported [Kandarova H, 2006]. As these reported measurements were performed on untreated EpiDerm™ skin models, we consider TEER with at least 390 Ω/cm² as confluent and tissues with a TEER below 390 Ω/cm² (510 Ω/cm² – 120 Ω/cm²) were considered as leaky. After an exposure of 20h, this was only the case in one tissue (sample E), experiment 2, tissue 2; see table A5.2 in appendix 5). Further 5 tissues (two tissues that received sunscreen control and one tissue that received sample C, D), and K)) were below the mean value of 510 Ω/cm² (see table A5.2 in appendix 5). It can be concluded that the skin model is getting less dense due to the addition of sunscreen. The presence of TiO₂ or ZnO NPs in the sunscreen has no further effect on the TEER. This decline will be further discussed in connection with the analysis of the presence of Ti and Zn below the ICP-MS EpiDerm™ skin models in chapter 3.2.2.

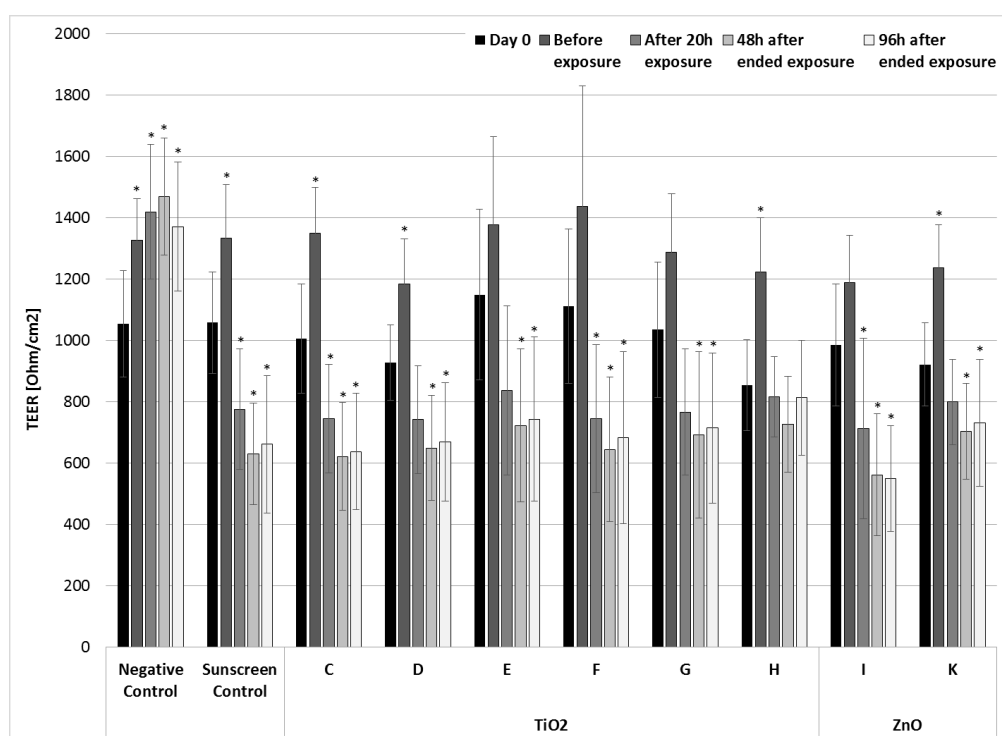


FIGURE 16: TEER MEASUREMENT OF EPIDERM™ SKIN MODELS DURING THE COURSE OF THE EXPERIMENT. DATA ARE THE MEAN OF NINE INDEPENDENT TISSUES SHOWN WITH STANDARD VARIATIONS. DAY 0 SHOW THE TEER AFTER ARRIVAL OF THE TISSUES. DATA ARE EXPRESSED AS MEAN ± SD OF NINE INDEPENDENT TISSUES. STATISTICAL SIGNIFICANCE COMPARED TO CONTROL WAS CALCULATED BY ONE-WAY ANALYSIS OF VARIANCE (ANOVA) FOLLOWED BY DUNNETT TEST AND * DEPICTS P<0.05.

3.2.2 Investigation of the transport of TiO₂ and ZnO NPs through EpiDerm™ skin models using ICP-MS

Inductively coupled plasma–mass spectrometry (ICP-MS) is one of the most frequently used method to detect trace metals. The detection limit for Ti and Zn is 1 µg/L. Based on our calculation of the numbers of nanoparticles that were added to the EpiDerm™ skin model, this corresponds to between 2.83x10⁹ particles (sample D) and 1.59x10¹² particles (sample G) depending on the mass of the nanoparticles. These particle numbers are reached if 0.06% of the applied nanoparticles

penetrate the skin model and reach the medium below. Due to the high content of Ca^{2+} , Na^+ , and Cl^- in cell culture medium titanium could not be measured properly as the high content of these elements lead to interferences with the analysis. Therefore, the titanium content was estimated by assuming that there is no titanium in the lowest reagent blank (DMEM cell culture medium) and that the interference is proportional to the calcium content. The estimated concentrations are the highest the titanium content can be; however, the concentration might also be lower than that. This becomes clear when looking at the results for samples that were not treated with TiO_2 NPs containing sunscreen (Negative Control, sunscreen control, samples I) and K) in Table 11 and table in appendix 7). Between 0.47 and 1.10 $\mu\text{g}/\text{L}$ titanium were detected in average in these samples with 0.1 $\mu\text{g}/\text{L}$ as the lowest and 1.5 $\mu\text{g}/\text{L}$ as the highest detected concentration after 20h exposure (Table 11, Figure 17). Due to the washing of the tissues after ended exposure, a contamination of the cell culture medium beneath the skin model could not entirely be excluded. As there was no possibility to check for eventual contaminations, we decided that no ICP-MS analysis was performed at later time points. The titanium content in the samples that received TiO_2 NPs containing sunscreen exceeded in nearly all cases these concentrations of the controls, although they were close to the concentrations measured for the controls. However, it has to be kept in mind that these data are estimations and the highest the titanium content can be. Therefore, we cannot conclude from these measurements if or if not TiO_2 NPs have penetrated the skin model. Zinc measurements are all well above the detection limit of 1 $\mu\text{g}/\text{L}$ (Figure 18, Table 11) and as the measured concentrations exceed in some cases the added amount of ZnO NPs it can be assumed that all added ZnO NPs were transported through the skin model. However, although these values clearly show a transport through the EpiDerm™ skin model it is not clear if this occurs as ZnO nanoparticle or Zn ion.

TABLE 11: ICP-MS MEASUREMENTS OF TITANIUM AND ZINC IN CELL CULTURE MEDIUM FROM BENEATH THE EPIDERM™ SKIN MODEL; TITANIUM CONCENTRATIONS ARE ESTIMATES AND THE HIGHEST THE TITANIUM CONTENT CAN BE

	Ti [µg/L]	Zn [µg/L]
Negative Control	1.00 ± 0.36	25.00 ± 1.73
Sunscreen Control	0.47 ± 0.47	37.00 ± 4.36
C	1.40 ± 0.00	36.67 ± 3.06
D	1.40 ± 0.20	36.67 ± 5.51
E	1.03 ± 0.35	35.33 ± 1.53
F	2.03 ± 0.84	41.33 ± 11.02
G	1.60 ± 1.13	36.33 ± 5.13
H	1.57 ± 0.12	36.67 ± 3.79
I	0.77 ± 0.58	2744.67 ± 308.80
K	1.10 ± 0.36	2439.00 ± 905.38

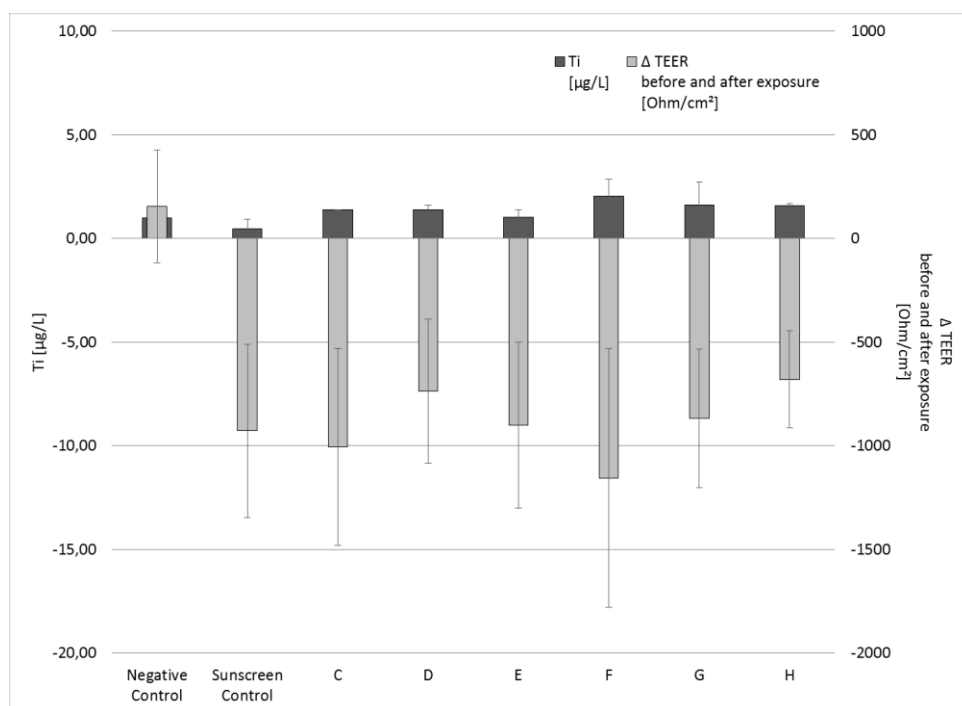


FIGURE 17: ICP-MS MEASUREMENTS OF TITANIUM IN CELL CULTURE MEDIUM FROM BENEATH THE EPIDERM™ SKIN MODEL AFTER 20h EXPOSURE AND CHANGES IN TEER DURING THE EXPOSURE PERIOD. SHOWN ARE THE MEAN VALUES OF THREE INDEPENDENT EXPERIMENTS. MEDIUM FOR ICP-MS WAS POOLED FROM THREE TISSUES PER EXPERIMENT. DATA ARE EXPRESSED AS MEAN ± SD OF THREE INDEPENDENT TISSUES. STATISTICAL SIGNIFICANCE COMPARED TO CONTROL WAS

CALCULATED BY ONE-WAY ANALYSIS OF VARIANCE (ANOVA) FOLLOWED BY DUNNETT TEST. TI CONCENTRATIONS OF THE SAMPLES WERE NOT STATISTICALLY DIFFERENT FROM THE NEGATIVE CONTROL.

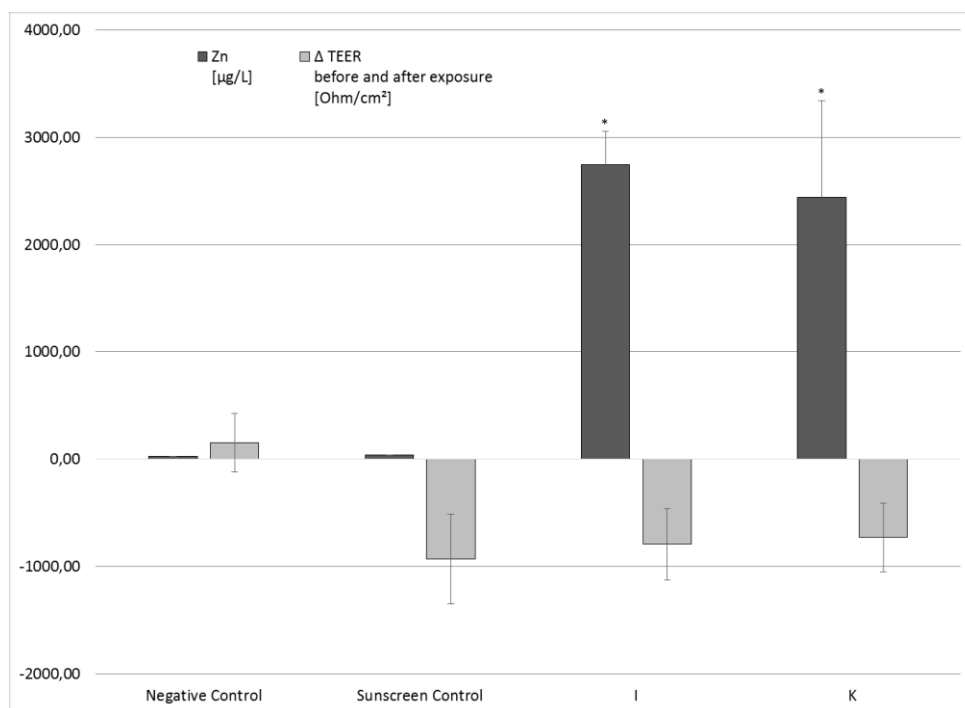


FIGURE 18: ICP-MS MEASUREMENTS OF ZINC IN CELL CULTURE MEDIUM FROM BENEATH THE EPIDERM™ SKIN MODEL AFTER 20H EXPOSURE AND CHANGES IN TEER DURING THE EXPOSURE PERIOD. DATA ARE EXPRESSED AS MEAN \pm SD OF THREE INDEPENDENT TISSUES. STATISTICAL SIGNIFICANCE COMPARED TO CONTROL WAS CALCULATED BY ONE-WAY ANALYSIS OF VARIANCE (ANOVA) FOLLOWED BY DUNNETT TEST AND * DEPICTS $P < 0.05$.

3.2.3 Cell viability

The decline in TEER could be a sign for that exposure to sunscreen has an effect on the cell health and on the confluence of the EpiDerm™ skin model. This skin corrosion and skin irritation can be measured using the MTT assay, which is a colorimetric assay where the cell viability is measured. From Figure 19 it can be seen that the application of sunscreen, independent of if TiO₂ or ZnO NPs were present, has no or only a minimal effect on the cell viability. Importantly, sunscreen alone gives the same decrease in cell viability as nanoparticle containing sunscreen independent of whether or not TiO₂ or ZnO NPs were present.

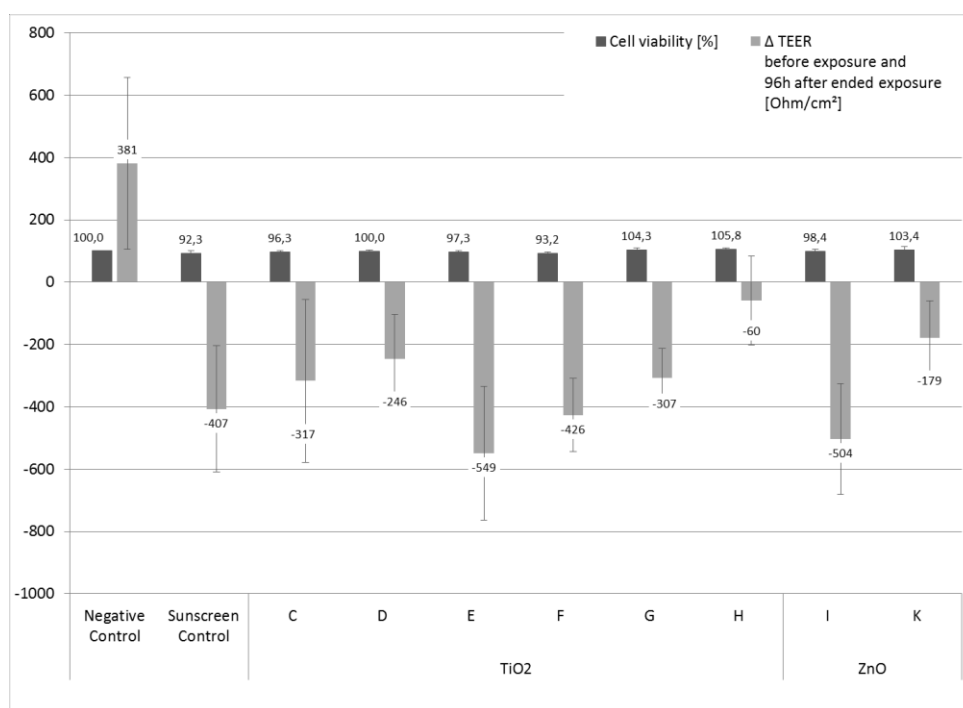


FIGURE 19: SKIN CORROSION AND SKIN IRRITATION MEASURED AS CELL VIABILITY USING THE MTT ASSAY AND CHANGES IN TEER DURING THE EXPOSURE PERIOD. DATA ARE EXPRESSED AS MEAN ± SD OF THREE INDEPENDENT EXPERIMENTS OF FIVE EPIDERM TISSUES. STATISTICAL SIGNIFICANCE COMPARED TO CONTROL WAS CALCULATED BY ONE-WAY ANALYSIS OF VARIANCE (ANOVA) FOLLOWED BY DUNNETT TEST. THE CELL VIABILITY OF THE SAMPLES WERE NOT STATISTICALLY DIFFERENT FROM THE NEGATIVE CONTROL.

3.2.4 Cytokine analysis

For the quantification of secreted cytokines a 27-plex system was used that covers 27 of the most important cytokines. A summary of the results are shown in Table 12, Table 13 and Table 14 and in the figures in appendix 6. Only for few investigated cytokines a significant change of the released cytokine concentration was detected. Importantly, exposure to sunscreen that did not contain nanoparticles induced a significantly changed release of eight cytokines (Table 13). Directly after 20h exposure only for two cytokines (monocyte chemotactic protein 1 (MCP1) and Vascular endothelial growth factor (VEGF)) a significant increase in their concentration was measured; however only for some of the sunscreens containing TiO₂ NPs (Table 13). For VEGF this increase was still present 48 h after ended exposure. In the case of ZnO NPs only a decrease of the cytokine release was detected.

TABLE 12: EFFECT OF 20H EXPOSURE TO SUNSCREEN CONTAINING TiO₂ AND ZNO NPS ON THE CYTOKINE RELEASE

Cytokine	Result	Comments
Basic FGF	No effect of TiO ₂ NPs and ZnO NPs	Concentrations around or below LLOQ
Ecotaxin	No effect of TiO ₂ NPs and ZnO NPs directly after 20h exposure, 48h after ended exposure effect for sample K)	Concentrations just above LLOQ
G-CSF	No effect of TiO ₂ NPs and ZnO NPs directly after 20h exposure, 48h after ended exposure	Concentrations just above LLOQ

effect for sample F)

GM-CSF	No effect of TiO ₂ NPs and ZnO NPs	Concentrations below LLOQ
IFN-γ	No effect of TiO ₂ NPs and ZnO NPs	Concentrations below LLOQ
IL-10	No effect of TiO ₂ NPs and ZnO NPs	Concentrations above LLOQ
IL-12p70	No effect of TiO ₂ NPs and ZnO NPs	Concentrations above LLOQ
IL-13	No effect of TiO ₂ NPs and ZnO NPs	Concentrations above LLOQ
IL-15	No effect of TiO ₂ NPs and ZnO NPs	Concentrations below LLOQ
IL-17	No effect of TiO ₂ NPs and ZnO NPs	Concentrations below detection limit
IL-1β	No effect of TiO ₂ NPs and ZnO NPs directly after 20h exposure, 48h after ended exposure effect for samples C), H), I), K)	Concentrations above LLOQ
IL-1ra	No effect of TiO ₂ NPs and ZnO NPs directly after 20h exposure, 48h after ended exposure effect for samples C), I), K)	Concentrations above LLOQ
IL-2	No effect of TiO ₂ NPs and ZnO NPs	Concentrations below or just above LLOQ
IL-4	No effect of TiO ₂ NPs and ZnO NPs	Concentrations below LLOQ
IL-5	No effect of TiO ₂ NPs and ZnO NPs	Concentrations below LLOQ
IL-6	No effect of TiO ₂ NPs and ZnO NPs	Concentrations below or just above LLOQ
IL-7	No effect of TiO ₂ NPs and ZnO NPs	Concentrations below LLOQ
IL-8	No effect of TiO ₂ NPs and ZnO NPs directly after 20h exposure, 48h after ended exposure effect for samples G), H)	Concentrations above LLOQ
IL-9	No effect of TiO ₂ NPs and ZnO NPs	Concentrations above LLOQ
IP-10	No effect of TiO ₂ NPs and ZnO NPs	Concentrations above LLOQ
MCP-1	No effect of TiO ₂ NPs and ZnO NPs directly after 20h exposure except for sample H), 48h after ended exposure effect for sample G)	Concentrations above LLOQ
MIP-1α	No effect of TiO ₂ NPs and ZnO NPs directly after 20h exposure, 48h after ended exposure effect for sample K)	Concentrations around LLOQ
MIP-1β	No effect of TiO ₂ NPs and ZnO NPs	Concentrations around LLOQ
PDGF-BB	No effect of TiO ₂ NPs and ZnO NPs	Concentrations above LLOQ
RANTES	No effect of TiO ₂ NPs and ZnO NPs	Concentrations above LLOQ
TNF-α	No effect of TiO ₂ NPs and ZnO NPs	Concentrations above LLOQ
VEGF	No effect of ZnO NPs; effect of TiO ₂ NPs directly after 20h exposure for samples C), G), H), 48h after ended exposure effect for samples C), F), G), H),	Concentrations above LLOQ

TABLE 13: FOLD CHANGE OF SIGNIFICANTLY ALTERED CYTOKINE RELEASE

Significantly changed release of cytokines				
	induced by sunscreen alone (no nanoparticles)		induced by sunscreen +nanoparticles (compared to sunscreen control)	
	After 20h exposure	48h after ended exposure	After 20h exposure	48h after ended exposure
Basic FGF	No	No	No	No
Ecotaxin	No	No	No	Yes for K) ↓ 1.32x
G-CSF	No	Yes, ↓ 1.43x	No	Yes for F) ↑ 1.86x
IL-10	Yes, ↑ 1.45x	No	No	No
IL-12 p70	Yes, ↑ 1.48x	No	No	No
IL-13	No	No	No	No
IL-1beta	No	No	No	Yes for C) ↓ 1.54x H) ↓ 1.89x I) ↓ 4.33x K) ↓ 4.27x
IL-1ra	Yes, ↑ 2.22x	No	No	Yes for C) ↑ 1.42x I) ↓ 1.83x K) ↓ 2.42x
IL-8	Yes, ↓ 1.28x	Yes, ↓ 1.45x	No	Yes for G) ↓ 1.35x H) ↓ 1.31x
IL-9	Yes, ↑ 1.72x	No	No	No
IP-10	No	No	No	No
MCP-1	No	No	Yes for H) ↑ 1.27x	Yes for G) ↑ 1.35x
MIP-1alpha	Yes, ↑ 1.37x	No	No	Yes for K) ↓ 1.21x
PDGF BB	No	Yes, ↓ 1.53x	No	No
RANTES	No	No	No	No
TNF alpha	Yes, ↑ 1.68x	No	No	No
VEGF	Yes, ↑ 1.84x	No	Yes for C) ↑ 1.25x G) ↑ 1.24x H) ↑ 1.24x	Yes for C) ↑ 1.20x F) ↑ 1.22x G) ↑ 1.30x H) ↑ 1.21x

TABLE 14: CONCENTRATION OF CYTOKINES RELEASED INTO THE CELL CULTURE MEDIUM AFTER 20H EXPOSURE TO SUNSCREEN CONTAINING NANOPARTICLES AND 48H AFTER ENDED EXPOSURE FOR SIGNIFICANTLY CHANGED CYTOKINE CONCENTRATIONS

Cytokine concentration after 20h exposure [pg/mL]											
Cytokine	LLOQ [pg/mL]	Untreated control	Sunscreen control	C) TiO ₂ 30nm uncoated	D) TiO ₂ 100nm uncoated	E) TiO ₂ 30nm silicone oil	F) TiO ₂ 30nm Al/Silicone	G) TiO ₂ 17nm Al/stearic acid	H) TiO ₂ 20nm Al/Silicone	I) ZnO 18nm uncoated	K) ZnO 20nm KH550
MCP-1	1.848	3.01 ±1.59	3.76 ±1.53	n.s.	n.s.	n.s.	n.s.	n.s.	5.92 ±2.79	n.s.	n.s.
VEGF	39.902	1756.37 ±431.29	3235.70 ±513.49	4059.07 ±832.19	n.s.	n.s.	n.s.	4002.22 ±861.23	4002.29 ±314.95	n.s.	n.s.

Cytokine concentration 48h after ended exposure [pg/mL]											
Cytokine	LLOQ [pg/mL]	Untreated control	Sunscreen control	C) TiO ₂ 30nm uncoated	D) TiO ₂ 100nm uncoated	E) TiO ₂ 30nm silicone oil	F) TiO ₂ 30nm Al/Silicone	G) TiO ₂ 17nm Al/stearic acid	H) TiO ₂ 20nm Al/Silicone	I) ZnO 18nm uncoated	K) ZnO 20nm KH550
Ecotaxin	5.183	7.06 ±2.04	6.68 ±2.13	n.s.	n.s.	n.s.	n.s.	n.s.	n.s.	n.s.	5.05 ±2.70
G-CSF	3.281	15.18 ±5.80	7.81 ±3.10	n.s.	n.s.	n.s.	14.54 ±10.71	n.s.	n.s.	n.s.	n.s.
IL-1beta	0.480	4.80 ±2.92	5.58 ±4.26	3.62 ±0.5	n.s.	n.s.	n.s.	n.s.	2.95 ±0.95	1.29 ±0.93	1.31 ±1.36
IL-1ra	5.297	128.89 ±16.18	151.52 ±55.43	214.75 ±166.14	n.s.	n.s.	n.s.	n.s.	n.s.	82.67 ±28.56	62.57 ±23.36
IL-8	2.471	334.02 ±75.31	230.76 ±65.51	n.s.	n.s.	n.s.	n.s.	208.81 ±51.20	175.70 ±26.21	n.s.	n.s.
MCP-1	1.848	6.60 ±2.00	5.80 ±1.58	n.s.	n.s.	n.s.	n.s.	7.84 ±2.34	n.s.	n.s.	n.s.
MIP-1alpha	0.522	0.67 ±0.08	0.65 ±0.11	n.s.	n.s.	n.s.	n.s.	n.s.	n.s.	n.s.	0.54 ±0.11
VEGF	39.902	4179.12 ±741.67	3849.44 ±767.47	4609.29 ±979.91	n.s.	n.s.	4678.27 ±693.80	5017.70 ±1154.95	4659.38 ±567.63	n.s.	n.s.

LLOQ – lower limit of quantification; n.s. – not significant

3.2.5 Histology and transmission electron microscopy

Transmission electron microscopy (TEM) was used to investigate the dermal absorption and penetration of TiO₂ or ZnO NPs directly. However, no TiO₂ or ZnO NPs could be detected beneath the upper surface of the skin model using this method (Figure 21, Figure 22, Figures in Appendix 2). Nanoparticle-like structures were also present in the negative controls and did not resemble the appearance of nanoparticles at higher magnifications (Figure 20). ICP-MS analysis detects Zn concentrations beneath the cell layer that correspond to the applied amount of ZnO NPs. Therefore, this negative result for TEM would suggest either that there is no transport of Zn in particulate form through the cell layer or that this transport occurs so fast that it is not possible to detect any ZnO NPs in the cell layer 96h after ended exposure to ZnO nanoparticle containing sunscreen (Appendix 2). For TiO₂ NPs we estimated that between 16,000 (for the largest nanoparticle, sample D) and 8,160,000 nanoparticles (for the smallest nanoparticle, sample G) could theoretically be on top of the upper surface of a TEM section of 50 μm x 70 nm. Using ICP-MS the detected titanium was close to the detection limit of 1 μg/mL which corresponds to 0.00006% of the added particle numbers. Therefore, for a surface area of a TEM section between 9.6 (sample D) and 4.900 nanoparticles (sample G) could be expected to have crossed the cell layer. These numbers show that in case of sample D it would be difficult to detect nanoparticles using TEM. Despite that, we found TiO₂ NPs at the surface of the tissues but not in deeper skin layers (Figure 22). However, for sample G a detection of nanoparticles within the cell layers could be possible as TiO₂ NPs are inert and the ICP-MS data do not point to a fast transport through the cell layer. An overview over the H&E staining of selected EpiDerm tissues are shown in Figure 23. No difference was visible independent if the cells were untreated (negative control) or exposed to sunscreen or sunscreen containing nanoparticles.

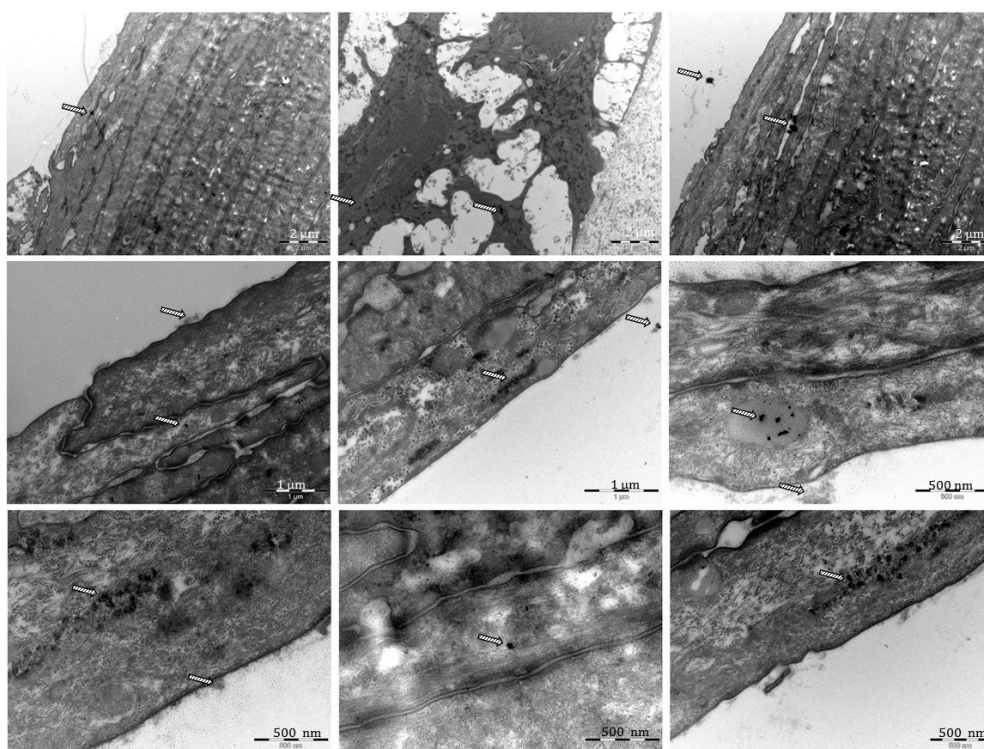


FIGURE 20: TRANSMISSION ELECTRON MICROSCOPY OF SUNSCREEN CONTROL EPIDERM SKIN MODEL; NANOPARTICLE-LIKE STRUCTURES ARE MARKED WITH A WHITE ARROW

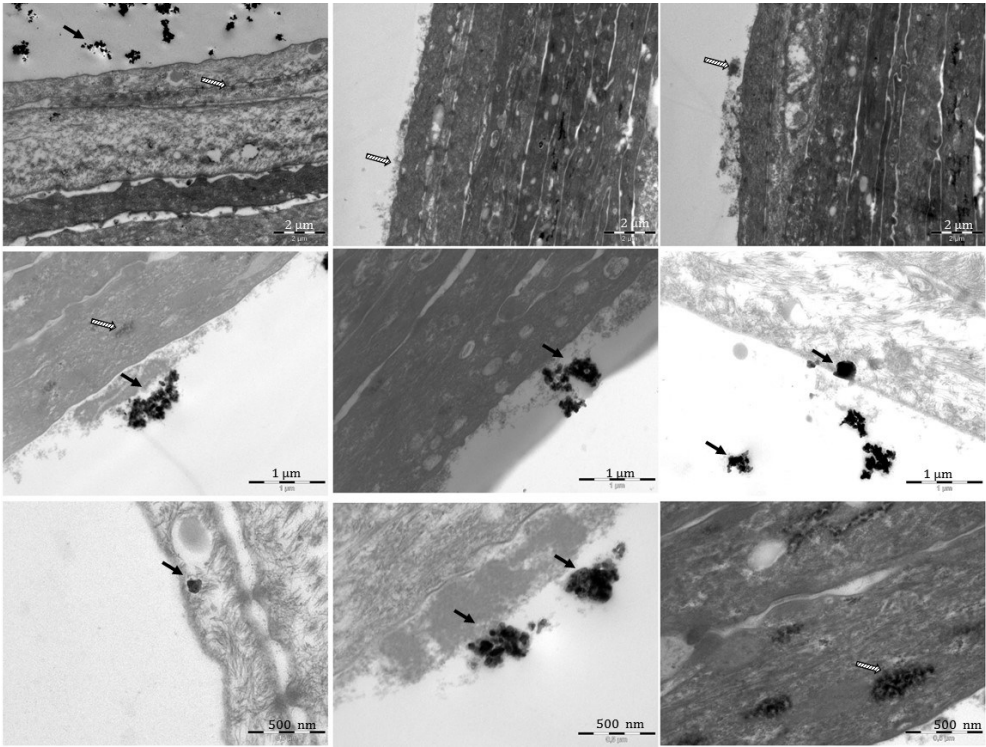


FIGURE 21: TRANSMISSION ELECTRON MICROSCOPY OF EPIDERM SKIN MODEL EXPOSED TO SAMPLE C; NANOPARTICLE-LIKE STRUCTURES ARE MARKED WITH A WHITE ARROW, TiO_2 NPS ARE MARKED WITH A BLACK ARROW

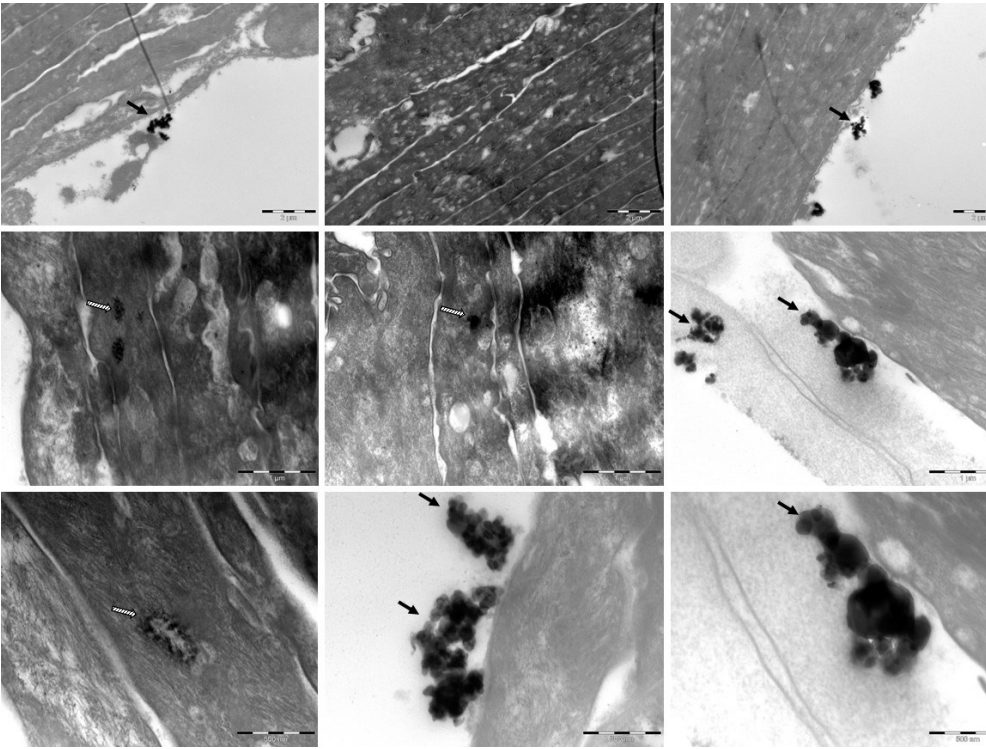


FIGURE 22: TRANSMISSION ELECTRON MICROSCOPY OF EPIDERM SKIN MODEL EXPOSED TO SAMPLE D; NANOPARTICLE-LIKE STRUCTURES ARE MARKED WITH A WHITE ARROW, TiO₂ NPS ARE MARKED WITH A BLACK ARROW

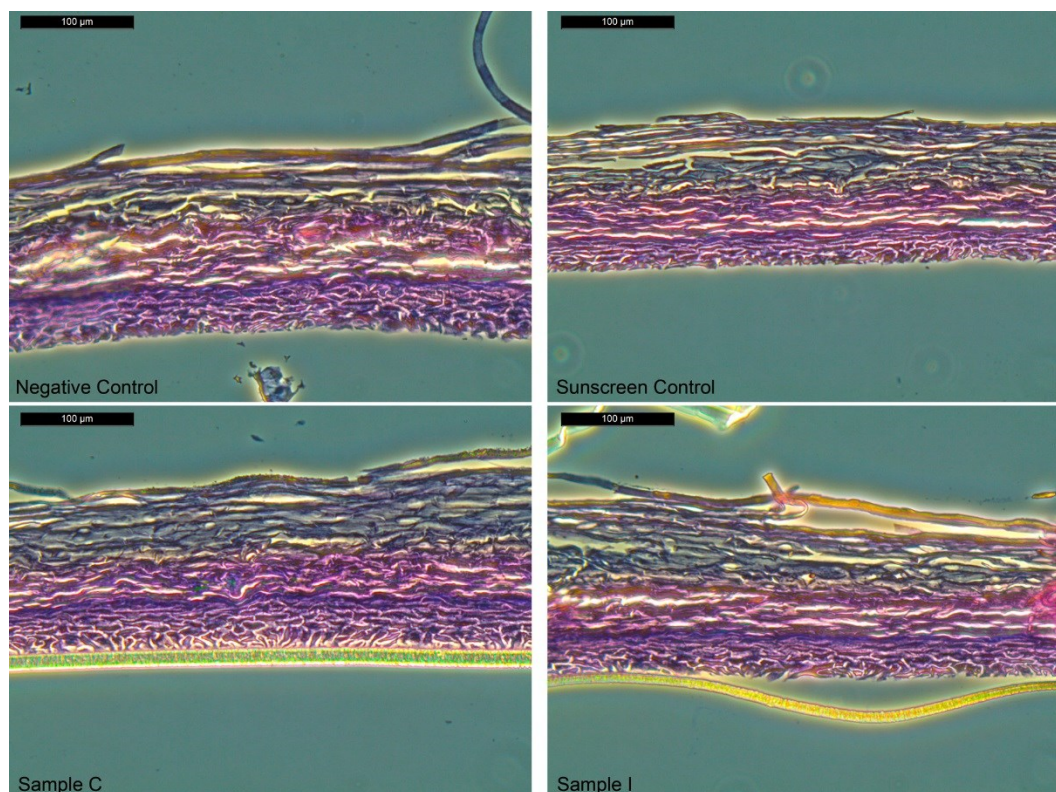


FIGURE 23: H&E STAINING OF SELECTED EPIDERM™ SKIN MODELS, MAGNIFICATION 200X

3.2.6 Conclusion *in vitro* EpiDerm™ skin model

The results from the ICP-MS analysis show in the case of ZnO nanoparticle containing sunscreen clearly dermal penetration of the EpiDerm™ skin model whereas for TiO₂ NPs the result was more uncertain as the Ti measurement was complicated through the high salt content of the cell culture medium. But the estimated concentrations were estimated as the highest Ti concentrations that there could be and were around the values for the controls. And even if we assume that the ICP-MS analysis also in the case of TiO₂ NPs show dermal penetration, electron microscopy could not confirm this result. No nanoparticles were detected by electron microscopy beneath the upper surface of the skin model. In addition, the nanoparticles have no effect on skin corrosion and skin penetration and have only minimal effects on inflammatory responses. In the case of ZnO nanoparticle containing sunscreen the presence of ZnO might even have a protective effect. As ZnO NPs are known to be dissolved in biological systems, we conclude that ZnO NPs are not transported in their particulate form but as Zn ions through the cell layer. For TiO₂ NPs we conclude, based on all the results from the different used methods, that there is no dermal penetration/absorption at or above the detection limit of the used methods. In addition, these results were independent on the size and coating of the nanoparticles.

3.3 *In vivo* skin models

A possible dermal penetration and absorption by the different nanoparticles in sunscreen is also investigated *in vivo* in a mouse model for acute irritant contact dermatitis and a xenograft human skin model. The mouse model for acute irritant contact dermatitis gives the possibility to investigate the effect of skin irritation and inflammation on the dermal absorption and penetration of the test nanomaterials. This was considered to be an important analysis as sunscreens are often applied to irritated and inflamed skin. The rationale behind this is the concern that nanomaterials might be taken up by damaged skin more easily due to an impaired protection capacity toward foreign materials. Although the structure of the mouse epidermis is different from the human skin, it is a suitable system to show the general ability of the test nanomaterials to penetrate skin tissue. However, a xenograft human skin model is used to overcome this problem. Here, xenotransplanted human skin is investigated for dermal absorption of the test nanomaterials giving the possibility to investigate dermal absorption on human skin *in vivo* without making direct studies on human volunteers.

Both *in vivo* models and the experimental details are described in the material and methods section. Briefly, both *in vivo* models were repeatedly exposed to TiO₂ NPs containing sunscreen (3 times with 24h time-lag in between) and biopsies were taken 4 days after the last application of sunscreen. As the sunscreen were not washed off the mice after application this corresponds to an exposure time of 120 h. This exposure setup was chosen to not only simulate repeated exposure but also to analyze the dermal absorption and penetration in a worst case scenario with extreme long exposure times. Long exposure times were requested in the report published by the Danish EPA [Poland CA et al., 2013] and is also a requirement for slowly absorbed substances in OECD guidelines. The biopsies were investigated by ICP-MS for the presence of titanium and by TEM to detect particles within the dermal cell layers. Histology was performed for selected samples to show an overall picture of the dermal structure with and without exposure to nanoparticle containing sunscreen.

3.3.1 *In vivo* TPA irritant contact dermatitis (ICD) mouse model

During the experiment the weight of the mice were monitored routinely as a measure for the health of the animals. From Figure 24 it can be seen that the weight dropped on day 3 for all sunscreen treated animals independently of the nanoparticle content. The reason for this decrease in body weight is most likely due to the wearing of a collar, which is supported by the fact that the mice gained their original weight at day 8.

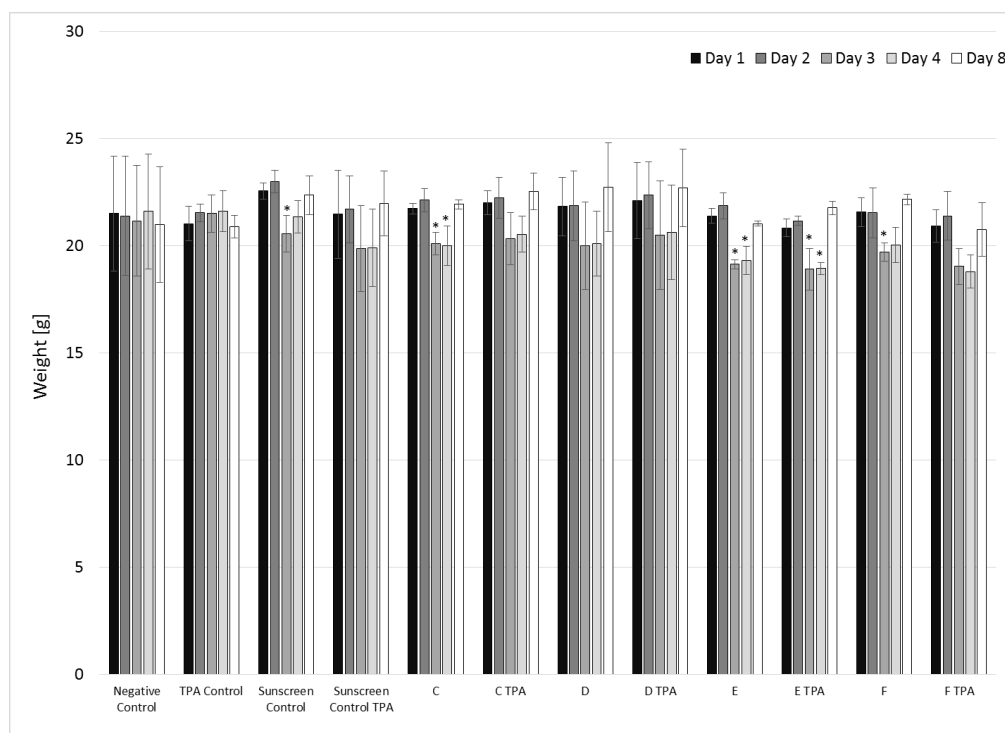


FIGURE 24: WEIGHT OF THE MICE USED FOR THE TPA IRRITANT CONTACT DERMATITIS (ICD) MOUSE MODEL DURING THE EXPERIMENT; N = 3 ANIMALS PER GROUP. DATA ARE EXPRESSED AS MEAN ± SD. STATISTICAL SIGNIFICANCE COMPARED TO CONTROL WAS CALCULATED BY ONE-WAY ANALYSIS OF VARIANCE (ANOVA) FOLLOWED BY DUNNETT TEST AND * DEPICTS P<0.05.

Besides the weight of the mice the ear thickness was monitored during the experiment. As TPA induces inflammation, treatment with TPA leads to an increase in the ear thickness. Therefore, an increase of the ear thickness is a measure for a successful induction of inflammatory processes. Figure 25 shows the effect of the TPA treatment on the ear thickness. Interestingly, the addition of sunscreen to the ears gave also an increase in the ear thickness. This effect was observed independently from if there were nanoparticles present in the sunscreen or not and the presence of TiO₂ NPs did not lead to a further increase in the ear thickness.

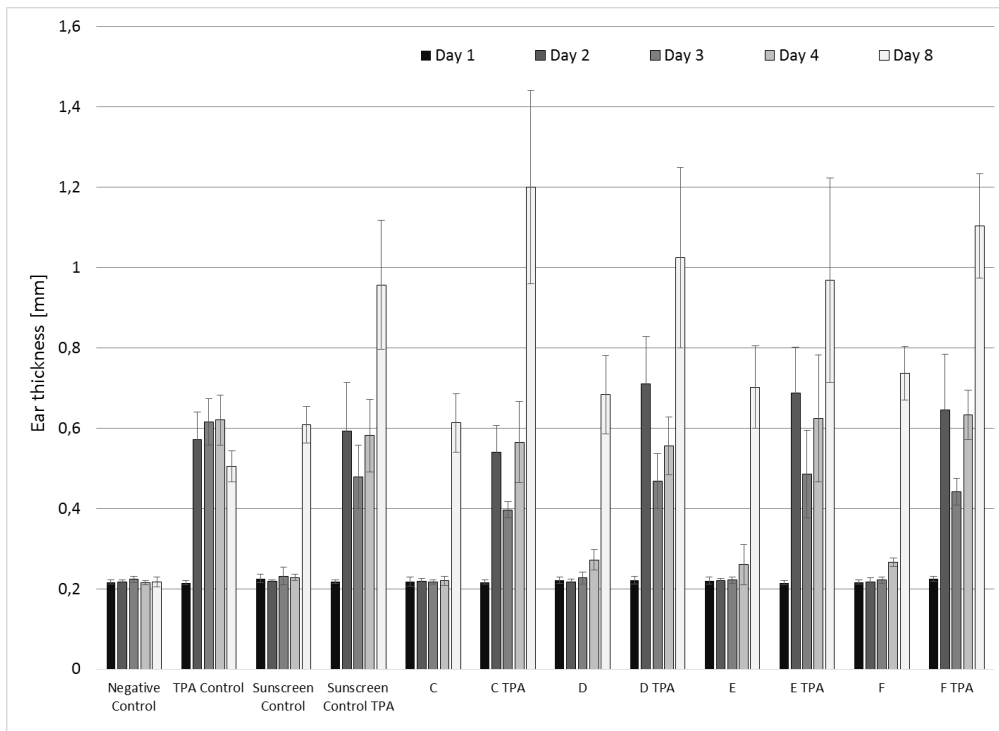


FIGURE 25: EAR THICKNESS DURING THE EXPERIMENT AS RESULT OF TPA AND SUNSCREEN TREATMENT; N = 3 ANIMALS PER GROUP. DATA ARE EXPRESSED AS MEAN ± SD.

After the exposure period had ended, two mice ear biopsies of two randomly selected animals were investigated for the amount of titanium using ICP-MS. The data are given as mg titanium per kg dry weight tissue. Therefore, the maximum amount of titanium that could have been detected, assuming complete absorption and penetration of the nanoparticles was calculated. Per ear 1.08 mg TiO₂ NPs were added (0.54 mg per side) and the dry weight of the analyzed ear biopsies varied between 0.0036 and 0.0106 g. Therefore, between 102 and 300 g titanium per kg dry weight would be the maximal amount of titanium that could have been detected. The amount of titanium on the skin of the mice ears varies considerably between 3.2 and 121.56 mg/kg dry weight (Table 15) corresponding to 0.0011% to 0.12% of the amount of the originally added TiO₂ NPs.

TABLE 15: ICP-MS MEASUREMENTS OF TITANIUM OF MICE EAR BIOPSIES (DETECTION LIMIT IS 0.6 MG/KG DRY WEIGHT)

	Ti [mg/kg dry weight]	
	Animal 1	Animal 2
Negative control	4.49	<2.3
TPA control	<1.6	<1.0
Sunscreen control	1.6	<0.5
Sunscreen TPA	<1	<0.4
C	12.97	29.6
C TPA	17.62	19.04
D	19.54	15.96
D TPA	6.4	3.2
E	57.92	100.33
E TPA	16.42	121.56
F	27.1	43
F TPA	32.04	17.96

The detection of Ti on the mice ear could be explained by an incomplete washing off the sunscreen from the mice skin after the ended experiment (Figure 28). Especially for TPA treated mice, the complete removal of TiO₂ NPs was impossible due to the inflammation that led to the formation of slough at the ear. Only mild washing steps and no mechanical forces to remove the TiO₂ NPs were used as this would have led to the disturbance of the upper most skin layers. Due to the few skin layers of the mice, the use of tape-stripping was also disregarded. Another possibility, the penetration of the skin by TiO₂ NPs could be excluded as no nanoparticles were detected in the deeper skin layers by electron microscopy. Based on our estimations (see material and methods section) at least several thousand TiO₂ NPs should be present per TEM thin section should unimpeded penetration have occurred. However, TiO₂ NPs were only observed at stratum corneum and not in deeper skin layers. Shown are examples of non-inflamed mice ear skin (Figure 28, Figure 29) but the same was true for inflamed mice ear skin (see figures in appendix 2). Nanoparticle-like structures that were observed in the samples were also found in the controls independent if inflammation was induced or not and were identified to be either melanin vesicles of the skin or polysomes (Figure 26, Figure 27). From the ICP-MS data and the TEM pictures, we could not detect any difference for normal and inflamed mice skin although the H&E staining show a clear effect of the TPA treatment leading to inflammation (notice the much thicker tissue and increased amounts of cell layers). Interestingly, sunscreen itself is leading to an increased ear thickness (Figure 30). Based on our findings from the cytokine analysis in EpiDerm™ skin models showing an increased release of cytokines after sunscreen exposure we suggest that this increased thickness of the ears is due to an inflammatory response to the sunscreen. Furthermore, size and surface coating of the TiO₂ NPs did not have an influence on the dermal penetration into deeper skin layers and dermal absorption.

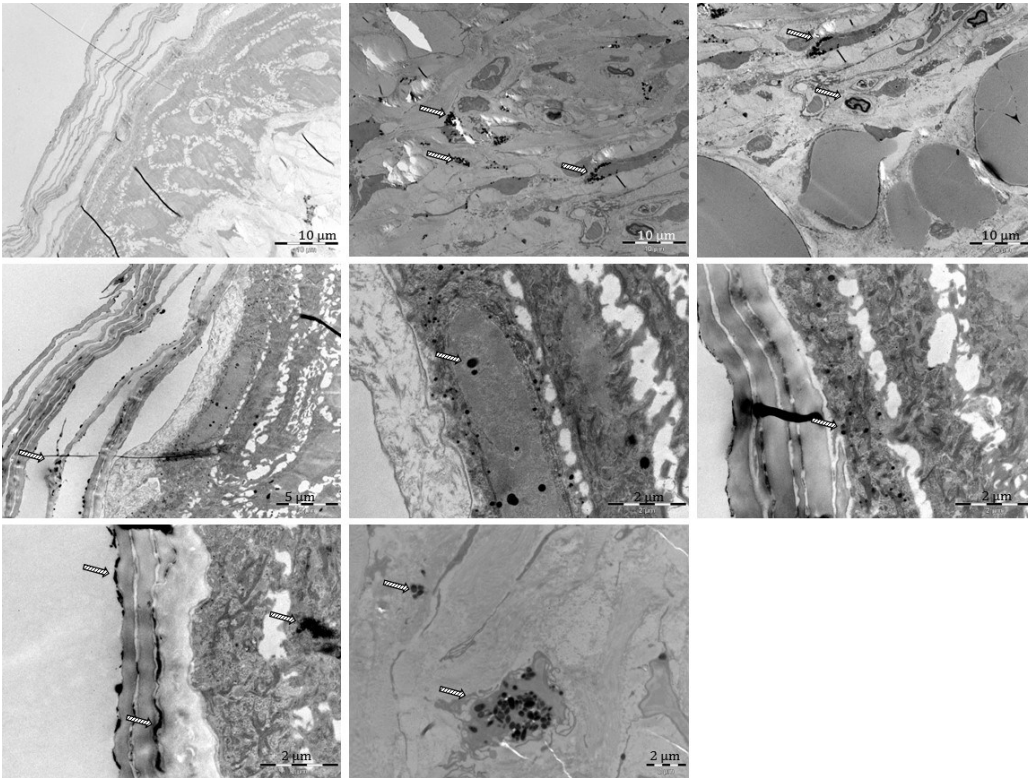


FIGURE 26: TRANSMISSION ELECTRON MICROSCOPY OF NON-INFLAMED (ACETONE TREATED) MICE EAR EXPOSED TO SUNSCREEN CONTROL; NANOPARTICLE-LIKE STRUCTURES ARE MARKED WITH A WHITE ARROW

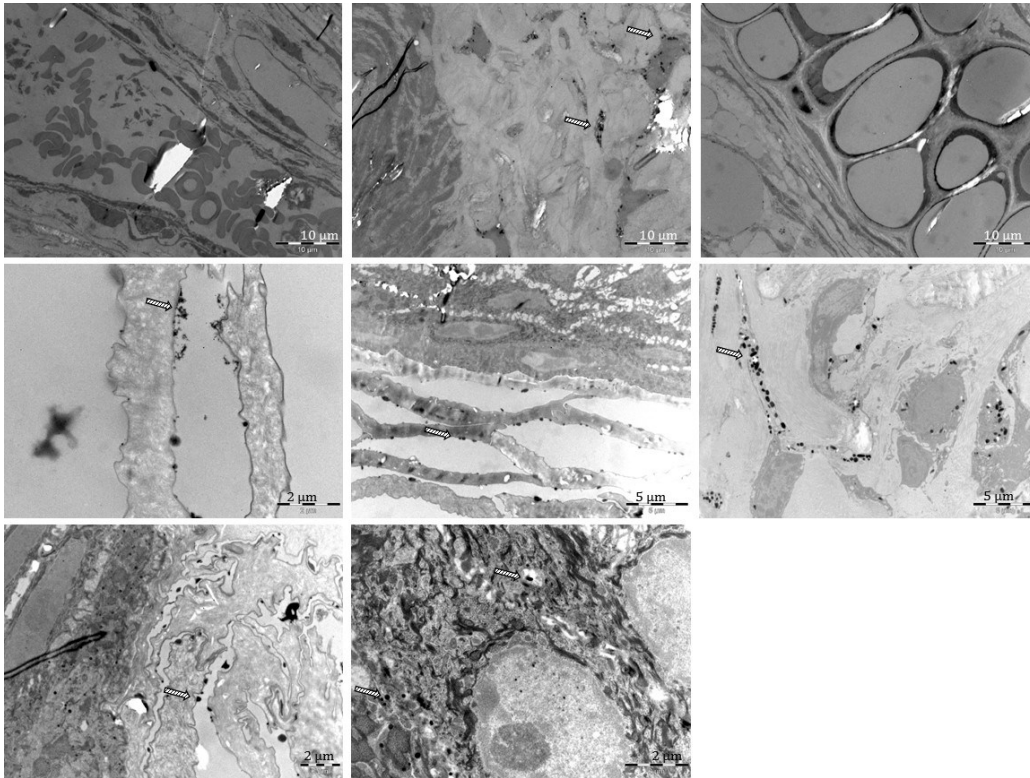


FIGURE 27: TRANSMISSION ELECTRON MICROSCOPY OF INFLAMED (TPA TREATED) MICE EAR EXPOSED TO SUNSCREEN CONTROL; NANOPARTICLE-LIKE STRUCTURES ARE MARKED WITH A WHITE ARROW

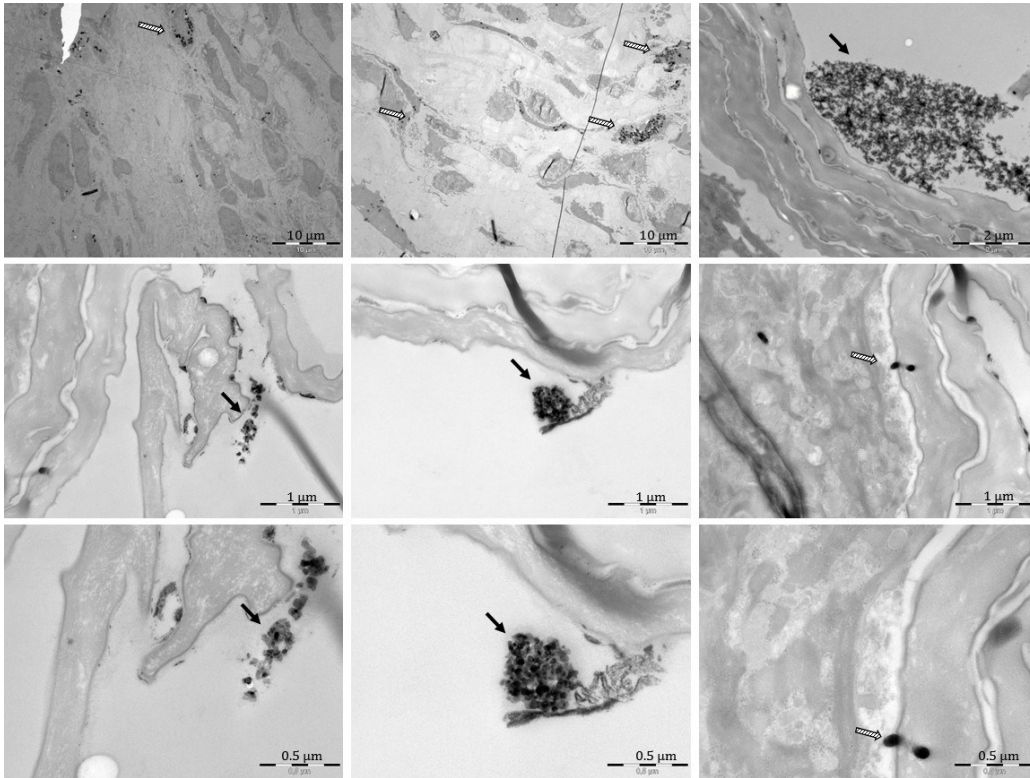


FIGURE 28: TRANSMISSION ELECTRON MICROSCOPY OF NON-INFLAMED (ACETONE TREATED) MICE EAR EXPOSED TO SAMPLE E; NANOPARTICLE-LIKE STRUCTURES ARE MARKED WITH A WHITE ARROW, TIO₂ NPS ARE MARKED WITH A BLACK ARROW

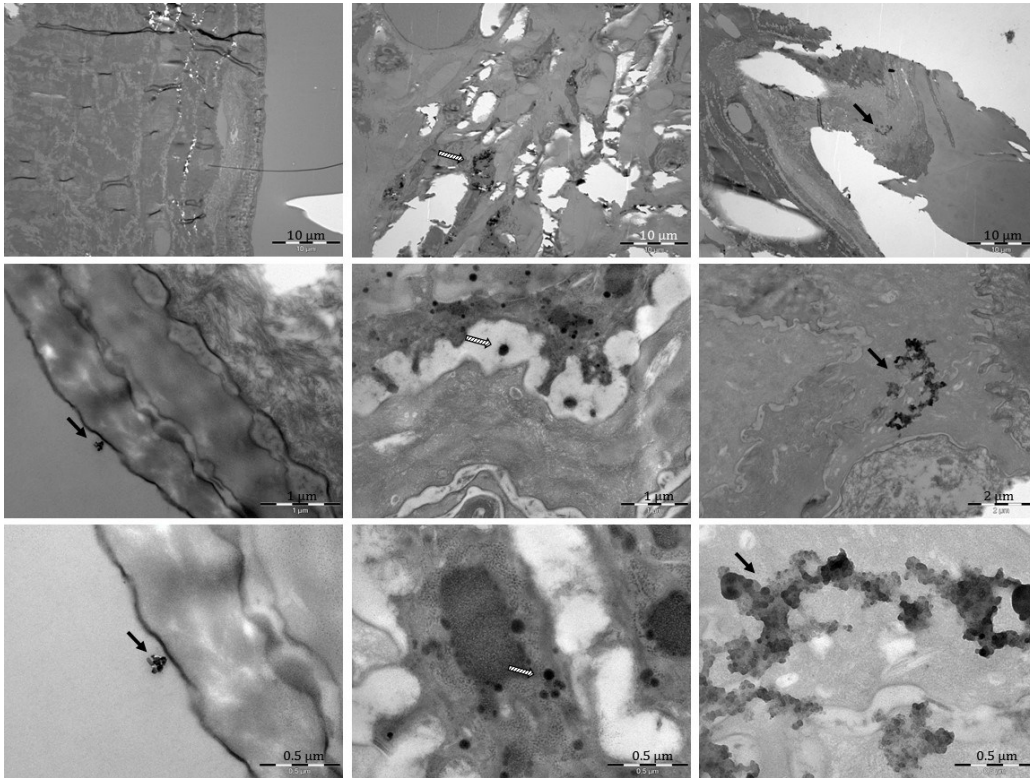


FIGURE 29: TRANSMISSION ELECTRON MICROSCOPY OF NON-INFLAMED (ACETONE TREATED) MICE EAR EXPOSED TO SAMPLE F; NANOPARTICLE-LIKE STRUCTURES ARE MARKED WITH A WHITE ARROW, TIO₂ NPS ARE MARKED WITH A BLACK ARROW

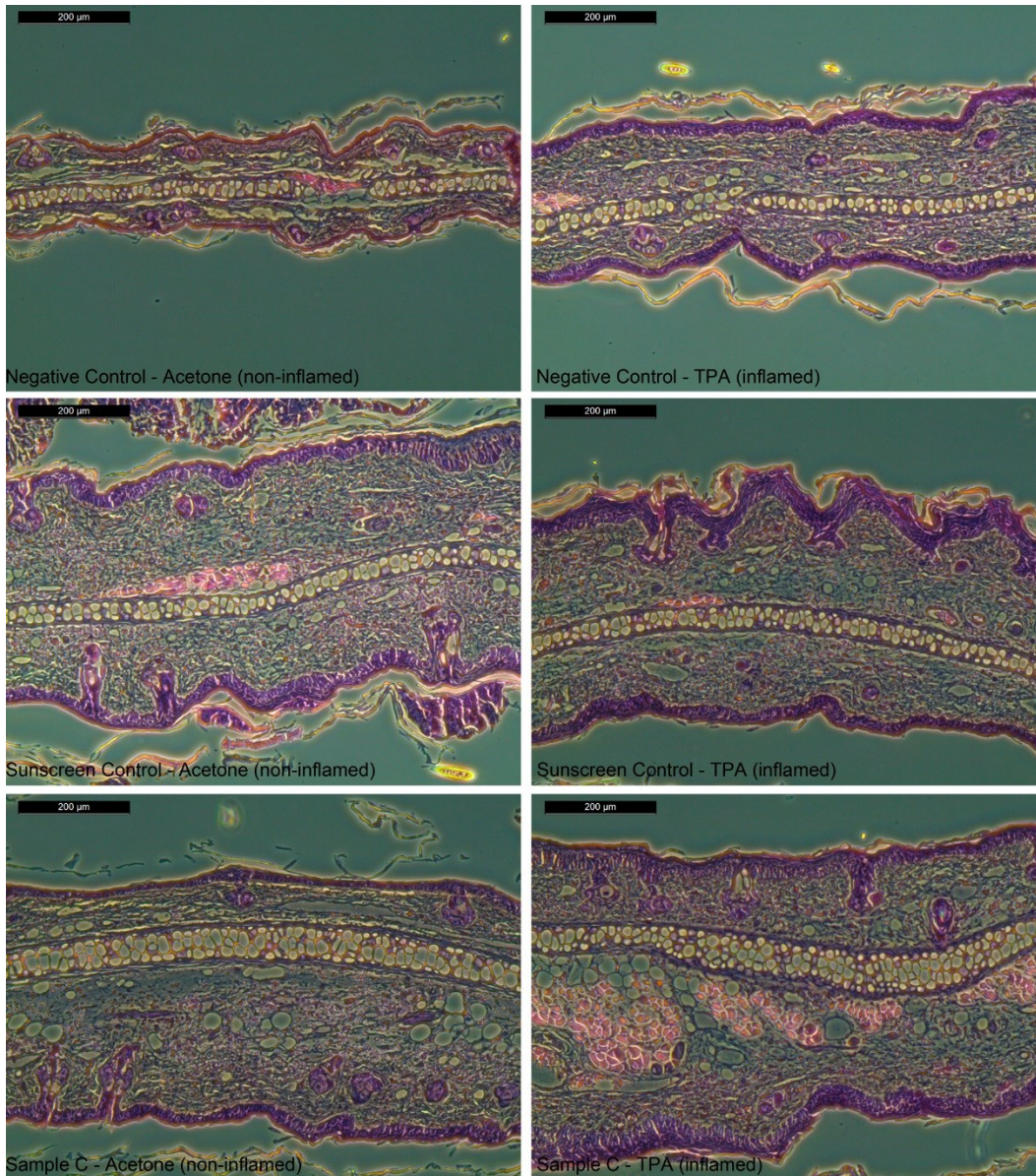


FIGURE 30: H&E STAINING OF SELECTED MOUSE EAR BIOPSIES, MAGNIFICATION 100X

3.3.2 Xenograft human skin model

During the experiment the weight of the mice were monitored routinely as a measure for the health of the animals. From Figure 31 it can be seen that the weight dropped slightly on day 2 for samples C to F. However, this drop was not significant compared to the controls and the weight measured on day 1.

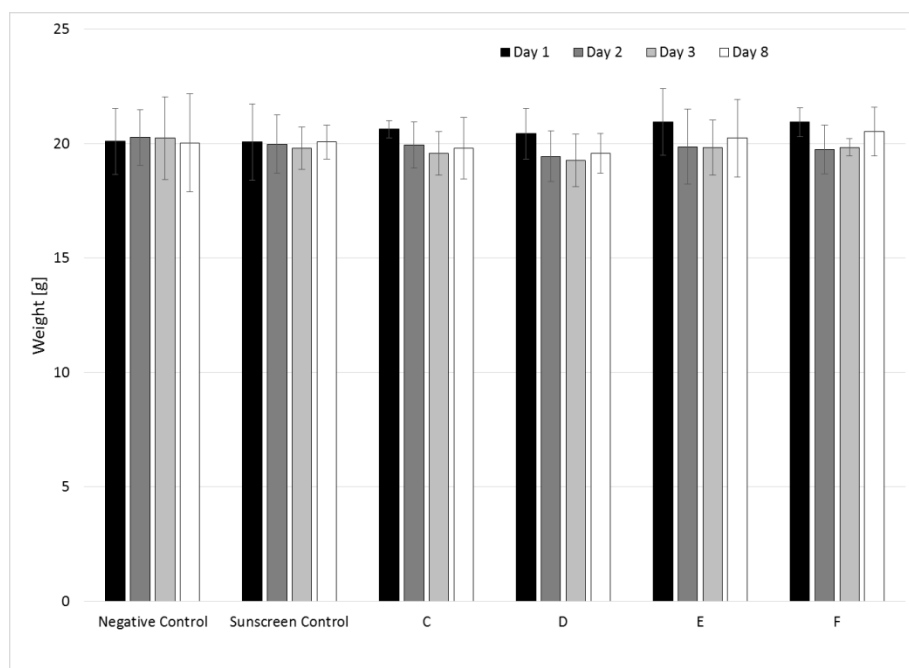


FIGURE 31: WEIGHT OF THE MICE DURING THE EXPERIMENT; N = 3 ANIMALS PER GROUP. DATA ARE EXPRESSED AS MEAN ± SD OF THREE ANIMALS. STATISTICAL SIGNIFICANCE COMPARED TO CONTROL WAS CALCULATED BY ONE-WAY ANALYSIS OF VARIANCE (ANOVA) FOLLOWED BY DUNNETT TEST. THE WEIGHT CHANGES WERE NOT STATISTICALLY DIFFERENT FROM THE NEGATIVE CONTROL.

After the exposure period had ended, the xenograft biopsies of two of maximal three successfully transplanted mice were investigated for titanium content using ICP-MS. The data are given as mg titanium per kg dry weight tissue. Therefore, the maximum amount of titanium that could have been detected assuming complete absorption and penetration of the nanoparticles was calculated. The dry weight of the analyzed xenografts varied between 0.0071 and 0.0316 g to which 0.54 mg TiO₂ NPs were added. Therefore, between 17 and 76 g titanium per kg dry weight would be the maximal amount of titanium that could have been detected by ICP-MS. The measured concentration of titanium on the skin of the xenograft varies between <0.11 and 2.51 mg/kg dry weight (Table 16) and reaches therefore not the amount of the originally added TiO₂ NPs (0.015% to 0.00014% of the originally added TiO₂ NPs). Six of the twelve investigated xenografts had titanium concentrations below the detection limit, amongst others the four control samples. The other two were one xenograft of sample C and D, respectively. Two xenografts had titanium concentrations slightly above the detection limit (samples D and E) whereas four xenografts had more clearly detectable titanium concentrations (samples C, E and F). However, an incomplete washing off the sunscreen from the human skin after the ended experiment could be an explanation for this result (see Figure 33). Nanoparticle-like structures that were observed in the samples were also found in the controls and were identified to be either melanin vesicles of the skin or polysomes (Figure 32). TiO₂ NPs were only observed at stratum corneum but not in deeper skin layers (Figure 33) although there seems to be a small change of the skin morphology due to exposure to sunscreen (Figure 34). Furthermore, size and surface coating of the TiO₂ NPs did not have an influence on the dermal penetration into deeper skin layers and dermal absorption.

TABLE 16: ICP-MS MEASUREMENTS OF TITANIUM ON XENOGRAFTED HUMAN SKIN (DETECTION LIMIT IS 0.3 MG/KG DRY WEIGHT)

Ti [mg/kg dry weight]		
	Xenograft 1	Xenograft 2
Negative control	<0.15	<0.34
Sunscreen control	<0.15	<0.11
C	0.87	0.21
D	0.25	0.32
E	0.94	0.3
F	2.51	1.8

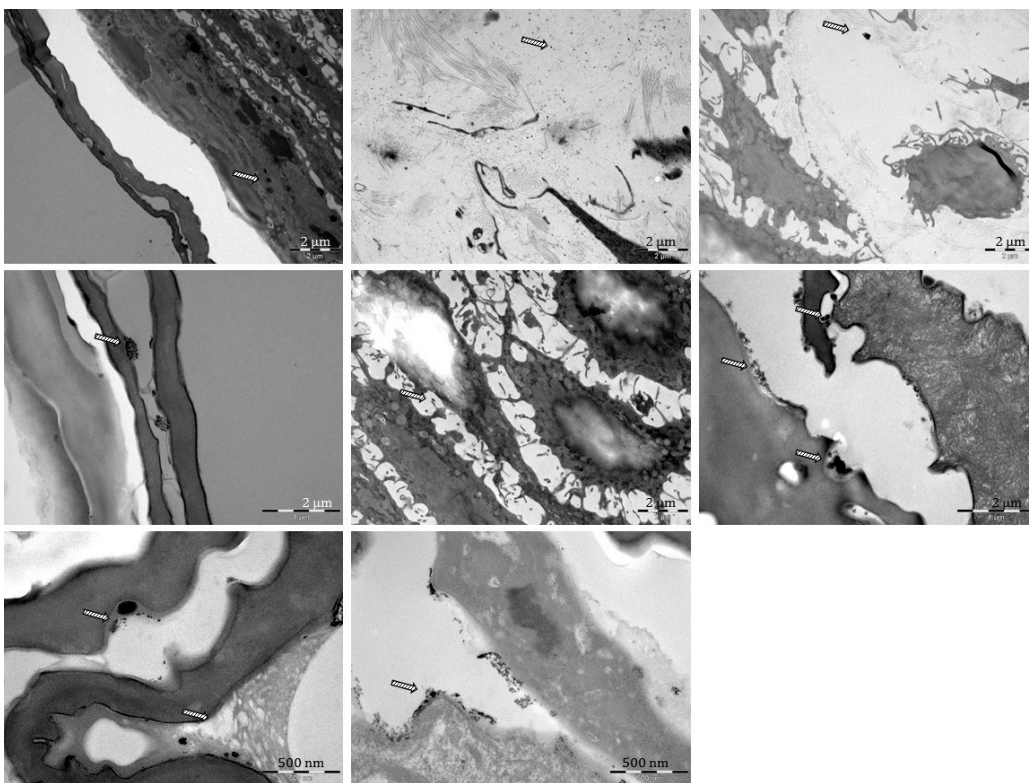


FIGURE 32: TRANSMISSION ELECTRON MICROSCOPY OF XENOGRAFTED HUMAN SKIN EXPOSED TO SUNSCREEN CONTROL; NANOPARTICLE-LIKE STRUCTURES ARE MARKED WITH A WHITE ARROW

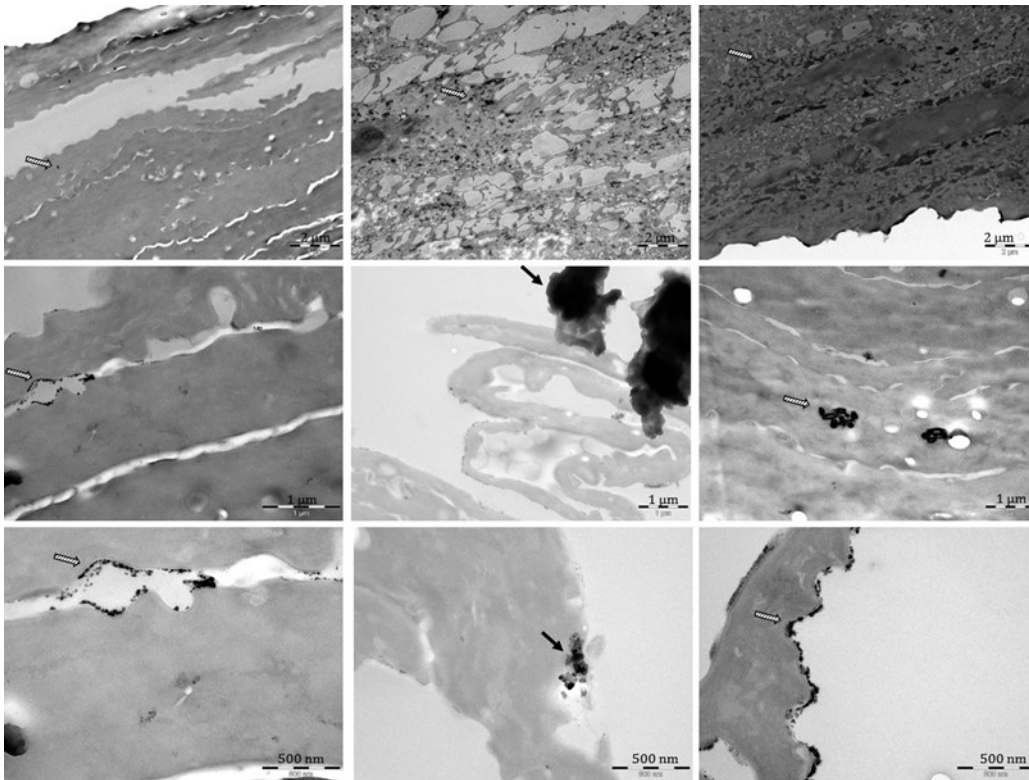


FIGURE 33: TRANSMISSION ELECTRON MICROSCOPY OF XENOGRAFTED HUMAN SKIN EXPOSED TO SAMPLE E; NANOPARTICLE-LIKE STRUCTURES ARE MARKED WITH A WHITE ARROW, TiO_2 NPS ARE MARKED WITH A BLACK ARROW

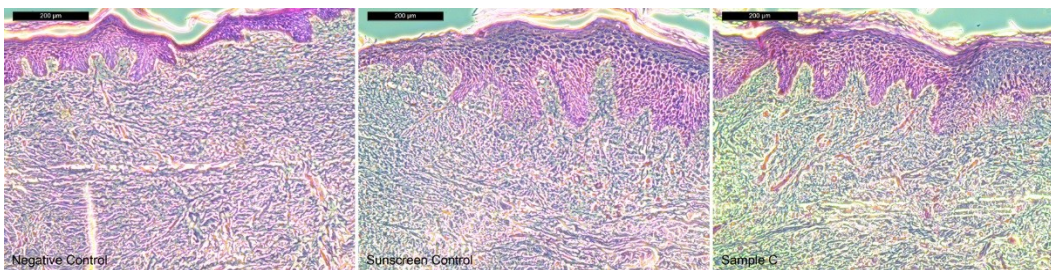


FIGURE 34: H&E STAINING OF SELECTED HUMAN XENOGRAFT SKIN MODELS, MAGNIFICATION 200X

3.3.3 Conclusion *in vivo* skin models

Although in both *in vivo* skin models titanium was detected in skin biopsies using ICP-MS a dermal penetration/absorption could not be confirmed using transmission electron microscopy. TiO_2 NPs were only observed at stratum corneum and not within deeper skin layers. In both skin models nanoparticle like structures that were observed in the samples were also found in the controls and were identified to be either melanin vesicles of the skin or polysomes. In addition, these results were independent of the size and coating of the nanoparticles.

4. Discussion

In the project “Dermal Absorption of Titanium Dioxide and Zinc Oxide Based Sunscreen: Role of Size and Surface Coating” we investigated the dermal penetration/absorption of differently sized and coated TiO₂ NPs and ZnO NPs in a commercial sunscreen in the *in vitro* human EpiDerm™ skin model. For TiO₂ NPs the experiments performed with the EpiDerm™ system were accompanied by *in vivo* skin models for mouse and human skin (mouse model for acute irritant contact dermatitis and xenograft human skin model, respectively). Thereby, for TiO₂ NPs the experimental design gave a great opportunity to compare the results from *in vitro* and different *in vivo* experiments. This is especially important when considering that it is otherwise forbidden to undertake specific animal testing for cosmetics (including sunscreen). ZnO NPs were only investigated *in vitro* as these nanoparticles are at the time of this project not allowed as UV-filters in the EU.

When designing the experiments for this project the focus was on three points: the type of nanoparticles that should be used; the type of skin models that the dermal penetration/absorption should be investigated in; and the methods that should be used for nanoparticle characterization and detection in the skin models.

TiO₂ NPs and ZnO NPs were chosen as test materials as a dermal exposure of workers as well as consumers is very likely to have occurred due to their extensive use in, e.g., sunscreen products and paint. It can be assumed that most of the Danish population including children are using sunscreen during the summer. It is assumed that in average 2 x 18 g sunscreen (36 g sunscreen) are used per dag when we are exposed to the sun [European Commission, 2006]. This corresponds to a dosage of 1 mg sunscreen per cm² skin and 0.257 mg nanoparticles/cm² skin when it is calculated with the highest approved TiO₂ NPs concentration in cosmetic products [Larsen et al., 2015]. Depending on the skin model we applied 0.54 mg nanoparticles/cm² skin (xenograft human skin model), 0.9 mg nanoparticles/cm² skin (*in vitro* human EpiDerm™ skin model), and up to 1.4 mg nanoparticles/cm² (mouse model for acute irritant contact dermatitis). This means that in our experiments we applied between 2.1 to 5.4 fold more sunscreen to the skin models than in the scenarios of the European Commission and the Danish EPA [European Commission, 2006; Larsen et al., 2015]. Although the dosage of sunscreen used by us is higher than what is assumed for the risk assessment scenarios described above we are still within a concentration that is not unrealistic and would cover worst case scenarios.

The risk assessment for TiO₂ NPs and ZnO NPs is in this connection of course of high importance as they substantially can protect the population for UV-A and UV-B exposure as UV filter in sunscreens, thereby minimizing the risk of skin cancer such as malignant melanoma. TiO₂ NPs and ZnO NPs have the advantage over chemical UV filters that they are much less irritant and less allergenic [Uter et al., 2014]. The most significant changes of the test nanomaterials TiO₂ NPs and ZnO NPs with respect to their possible ability for dermal absorption and penetration are changes of their size and surface coating. It is known that changes of the size of nanoparticles can change their physicochemical properties and their reactivity due to the increased surface to volume ratio. In the report on Dermal absorption of nanomaterials by the Danish EPA it is shown that TiO₂ NPs of around 30 nm size penetrate into the dermis whereas TiO₂ NPs of more than 80 nm penetrate maximal into the stratum corneum [Poland CA et al., 2013]. Furthermore, in the report of the Danish EPA it is concluded that several studies indicate that the surface chemistry is an important factor for the ability of the nanoparticles to penetrate into the skin. Changes of the surface coating

of nanoparticles can lead to modified surface charges and altered hydrophobicity or hydrophilicity thereby eventually leading to a higher possibility of dermal absorption and penetration [Poland CA et al., 2013]. Therefore, the choice of the nanoparticles for this project here were made based on size (17 to 100 nm TiO₂ NPs; 18 to 20 nm ZnO NPs) and coating (uncoated and several coatings used for nanoparticles for cosmetic products) (Table 1 in Material and Methods) thereby giving the possibility to investigate if size and/or surface coating has an influence on the dermal absorption and penetration of nanomaterials. In addition, in the case of TiO₂ NPs the crystalline form of TiO₂ NPs was limited to rutile particles as this is the crystalline form that is primarily used in sunscreens due to its low photo-activity [Jacobs et al., 2010; Kubac et al., 2015]. However, despite the reports showing the role for size and coating for dermal penetration/absorption, we were not able to find a connection. In our investigations we did not find dermal penetration/absorption of particles of the investigated TiO₂ NPs and ZnO NPs at or above the detection limits of the used methods. However, we did see absorption of ZnO ions in the EpiDerm™ skin model. This was independent of if the nanoparticles were 17 or 100 nm in size and of the coating the particles had. However, TiO₂ NPs and ZnO NPs might have been aggregated. Using DLS we showed that the nanoparticles were at least highly aggregated in MilliQ water. However, as the pre-dispersion of the nanoparticles occurred in C12-C15 alkyl benzoate before adding to the sunscreen, the aggregation in sunscreen might be different. Indeed, acoustic attenuation spectroscopy (AAS) showed smaller aggregates of the TiO₂ NPs and ZnO NPs. AAS is a new reliable method which makes a direct measurement of the particle size distribution in sunscreen possible [Dukhin and Goetz, 2010]. Something that is otherwise quite difficult to achieve [Tyner et al., 2009]. However, as we only measured the particle size distribution based on the weight of the particles and not as number size distribution we cannot for sure say how many of the TiO₂ NPs and ZnO NPs in number are within the nano-size range (<100 nm) and not aggregated/agglomerated. This is due to the fact that larger particles weigh more and thereby mask for the small particles in the analysis. For example a 200 nm TiO₂ NP weighs 296 fold more than a 30 nm TiO₂ NP. That means that for one 200 nm particle there could be 296 30 nm particles present. Another way to explain this phenomenon is by looking at three particles with either 1 µm, 2 µm, or 3 µm in diameter, respectively. When looking at the number size distribution for these particles, each particle size accounts for one third of the total. Converted to a volume or weight size distribution, 75% of the total volume would come from the 3 µm particles, and less than 3% comes from the 1 µm particles. It becomes obvious that the majority of the total particle mass or volume comes from the larger particles. Therefore, even if the particles that are larger than 100 nm make up 99% of the weight of all nanoparticles that are present in number the particles that are smaller than 100 nm could still be more than 50%. The number size distribution is important to know as the size obviously plays a large role in dermal penetration/absorption in general. Magnusson *et al.* who have recently shown that molecular weight and molecular volume are the most important parameters that determine if molecules penetrate into human skin or are absorbed. The maximal flux through human skin is logarithmically related to their molecular weight and size. 600 Dalton large molecules were shown to have molecular flux that is approximately 10⁻¹² mol/cm²/h [Magnusson et al., 2004]. Nohynek and Dufour estimated that a 30 nm diameter- TiO₂ NP has an approximate molecular weight of more than 100,000 Dalton (our estimation is that it could easily be more like 10 million Daltons) and has therefore a molecular weight and volume that are at least by three to four orders of magnitude larger. Therefore, Nohynek and Dufour concluded that it is inconceivable that such a particle could significantly penetrate into or through human skin, which supports our results on dermal penetration/absorption [Nohynek and Dufour E. K., 2012]. All TiO₂ NPs and ZnO NPs had a weight based particle size distribution where 90% of the particles were around 200 nm and larger showing an aggregation/agglomeration of the TiO₂ NPs and ZnO NPs in sunscreen. However, we cannot say if the particles were present as stable aggregates where no nanoparticles are released from after they become part of this complex. Another important physicochemical property is the surface charge of the nanoparticles. It has been identified to play an important role for the toxicity is the surface charge of nanoparticles, positively, negatively or neutral surface charge. Studies showed that positively charged nanoparticles induce higher levels of toxicity compared to negatively charged particles of the same chemical composition

and result in cytotoxicity, disruption of cellular membrane integrity, apoptosis, necrosis, loss of mitochondrial membrane potential [Frohlich, 2012]. The surface charge has an influence on the toxicity of nanoparticles also indirectly as it influences the efficiency of the uptake of the particles by the cells, the uptake pathways and the cellular distribution [Asati et al., 2010; Bhattacharjee et al., 2013; Frohlich, 2012]. The ζ -potential analysis showed that all TiO₂ NPs have an anionic, negative surface charge whereas ZnO NPs are neutral to fairly positively charged in water. The inability to detect dermal penetration/absorption of TiO₂ NPs and ZnO NPs could therefore also be due to the surface charge of the investigated nanoparticles. However, it has to be kept in mind that the ζ -potential measurement occurred in water and that the ζ -potential in sunscreen might be different.

The EpiDerm™ Skin Model was chosen for this project as it is validated by the OECD for evaluating the skin corrosion and skin irritation potential of chemicals and other drugs. Although this system has the disadvantage that it is an artificially constructed skin model that most likely does not behave exactly as normal skin it is feasible to investigate the dermal penetration/absorption of nanoparticles. When investigating the dermal penetration of the EpiDerm™ skin model; the results of the ICP-MS analysis show that in the case of ZnO NP containing sunscreen, dermal penetration was clearly apparent whereas for TiO₂ NPs the result was more uncertain and not clear as the detected concentrations were just above the negative control and high concentrations of salts in the cell culture medium only allowed for an estimation of the Ti concentrations. However, none of the other used methods could show a dermal penetration/absorption of the nanoparticles. For example, no nanoparticles were detected by electron microscopy beneath the upper surface of the skin model although based on the ICP-MS analysis several hundred ZnO NPs should be present in the electron microscopy thin section. As ZnO NPs are known to be dissolved in biological systems [SCCS (Scientific Committee on Consumer Safety), 2012], we conclude that ZnO NPs are not transported in their particulate form but as zinc ions through the cell layer. This is in agreement with the available literature as no ZnO NPs were found in viable skin layers [Cross et al., 2007; Durand et al., 2009; Dussert et al., 1997; Filipe et al., 2009; Gamer et al., 2006; Kuo et al., 2009; Song et al., 2011a; Szikszai et al., 2010]. Only a few studies could show minimal transdermal absorption [Monteiro-Riviere et al., 2011; Gulson et al., 2010; Gulson et al., 2012]. However, it is not clear if this absorption occurred as ZnO NPs or Zn ions and the SCCS concluded that “*Considering the dissolution of ZnO, it is most likely that the zinc was absorbed in ionic form.*” [SCCS (Scientific Committee on Consumer Safety), 2012] supporting the conclusion of our study. The same was true for TiO₂ NPs where we conclude that penetration of the EpiDerm™ skin model did not occur at or above the limit of detection. In contrast to ZnO NPs TiO₂ NPs are inert and do not dissolve in biological systems. But again, except for ICP-MS no other method point to a dermal penetration/absorption of TiO₂ NPs. This is in agreement with the conclusion the SCCS and the Danish EPA made in their reports on TiO₂ NPs and the within these reports discussed literature [Poland CA et al., 2013; SCCS (Scientific Committee on Consumer Safety), 2014]. However, it has to be noted that exposure to sunscreen that did not contain nanoparticles induced a significantly changed release of eight cytokines. This effect on the cytokine release is most likely due to the fact that the used sunscreen contained chemical UV-filters (Parsol 340, Parsol MCX, Parsol 1789) as Parsol MCX and Parsol 1789 as well as other chemical UV-filters have been associated with allergy [Ang et al., 1998; Parry et al., 1995; Uter et al., 2014]. Directly after 20 h exposure only for two cytokines (monocyte chemoattractant protein 1 (MCP1) and Vascular endothelial growth factor (VEGF)) a significant increase in their concentration was measured when the EpiDerm™ skin model was exposed to TiO₂ NPs containing sunscreen. However, this was true for only some of the sunscreens that contained TiO₂ NPs. For VEGF this increase was still present 48h after ended exposure. In the case of ZnO NPs only a decrease of the cytokine release was detected. This is in accordance with the literature reporting that ZnO NPs have an anti-inflammatory effect [Ilves et al., 2014].

It has to be mentioned that there was a high level of variability in some of the samples. This is most likely due to the fact that in most cases the cytokine concentration was near the detection limit of the analysis method explaining the high variability. For these low concentrations, just few

molecules more or less will give a quite high variation in the measurements. Based on these results that the release of only very few cytokines were changed, that this change was in most of the cases not consistent as well as there were no detectable effect of the nanoparticle size and coating we conclude that sunscreens that contain TiO₂ or ZnO NPs do not induce more inflammatory responses than sunscreen without nanoparticles.

Within the *in vivo* skin models (mouse model for acute irritant contact dermatitis, xenograft human skin model) that were used to investigate the dermal penetration/absorption of TiO₂ NPs, titanium was detected in skin biopsies using ICP-MS. The amount of titanium on the skin of the mice ears varied considerably between 3.2 and 121.56 mg/kg dry weight and reached in some cases the amount of the originally added TiO₂ NPs. The measured concentration of titanium on the human xenograft skin varies between <0.11 and 2.51 mg/kg dry weight and reaches therefore not the amount of the originally added TiO₂ NPs. For both *in vivo* skin models, an incomplete washing off of the sunscreen from the skin after the end of the experiment could be an explanation for the detection of titanium in the skin biopsies. For the xenograft human skin model this could be improved by using tape stripping which would remove the upper skin layers and also the attached nanoparticles. However, this would be a problem for the mice skin at the ears as here only a few dermal skin layers are present. Another problem with this method would be that one would not be able to look at the upper skin layers. Tape stripping is generally being used to study how deep nanoparticles can penetrate the skin [Iannuccelli et al., 2014] and can be analysed for nanoparticles. However, this leads to a quite limited sample volume. Based on the available literature that has been reviewed in reports by the SCCS and the Danish EPA it had to be assumed that the amount of penetrated or absorbed Ti, if any, would be close to the detection limit [Poland CA et al., 2013; SCCS (Scientific Committee on Consumer Safety), 2014]. Therefore, we chose to investigate as much as possible of the available tissues and to combine the results with the results from the transmission electron microscopy (TEM). Using TEM, the possibility of the penetration of the skin by TiO₂ NPs could be excluded as no nanoparticles were detected in the deeper skin layers. Based on our estimations from the ICP-MS results at least several hundred TiO₂ NPs should be present per TEM thin section. The same was true for the xenograft skin model where dermal penetration/absorption of TiO₂ NPs did not occur at or above the limit of detection. In both skin models nanoparticle like structures that were observed in the samples were also found in the controls and were identified to be either melanin vesicles of the skin or polysomes. TiO₂ NPs were only observed at stratum corneum which is in agreement with the present literature including reports from the SCCS and the Danish EPA [Nohynek and Dufour E. K., 2012; Poland CA et al., 2013; SCCS (Scientific Committee on Consumer Safety), 2014; Shi et al., 2013].

When considering the detection limit of the various approaches used within this study to detect absorption of TiO₂ and ZnO nanoparticles through the dermal layers, it is possible to conclude that absorption does not occur at levels above the detection limit. However, it is not possible to exclude the potential for dermal absorption to be occurring at levels below the limit of detection, only that should it occur it is only at very low levels. Should low levels of absorption occur, the nanoparticles would likely become systemically available and therefore to understand what such low levels may mean in toxicological terms, it is useful to consider the literature on systemic biodistribution, clearance and toxicity of TiO₂ and ZnO.

One such study considering the biodistribution and clearance of TiO₂ nanoparticles was recently published by Elgrabli *et al.* who used intravenous (IV) injection of TiO₂ nanoparticles as this route of administration allowed knowledge of the exact bioavailable dose of TiO₂ present in rat blood [Elgrabli et al., 2015]. The TiO₂ nanoparticles were anatase and therefore differed from the rutile form of TiO₂ used in this study, however as anatase is considered to be the more of a safety concern than the rutile form it could be considered as a sufficiently precautionary surrogate [SCCS (Scientific Committee on Consumer Safety), 2014]. The nanoparticles used were 25 nm in diameter although DLS measurements in saline showed them to be agglomerated and therefore similar in terms of size and agglomeration state as the smaller TiO₂ nanoparticles used in the present study.

The authors treated rats with a relatively high dose of 7.7 to 9.4 mg/kg of TiO₂ (1.7mg per rat, 333 µl of 5 mg/ml suspension) and then assessed the Ti content of the lungs, liver, kidneys, spleen, brain, lymph nodes, testis and blood at 10 min, 1h, 1, 7, 28, and 56 days later using ICP-OES. They found no increase in Ti within the brain, lymph nodes, kidneys or testis and a small and short increase of Ti in the blood 10 minutes after the injection (0.33 µg versus 0.12 µg for the control) although this was not statistically significant. A similar observation of a rapid decline of titanium in blood (<0.5hrs) was also noted in a separate study using a range of TiO₂ particles (including 20nm rutile nanoparticles which is of great relevance) at a dose of 2.3 mg/rat [Geraets et al., 2014]. Elgrabli did however find a significant increase of Ti in urine 1 day after injection [Elgrabli et al., 2015](also shown by [Xie et al., 2011]) demonstrating clearance and excretion although such clearance is not noted in all studies [Shinohara et al., 2014]. Within the body, the vast majority of injected Ti was found in the liver (92.1%), the spleen (3.5%) and the lungs (0.7%). A very similar distribution was also shown by Shinohara et al. and also Geraets et al. [Geraets et al., 2014; Shinohara et al., 2014], the later study showed the highest tissue distribution after single IV injection (in descending order) in liver, spleen and lung for all TiO₂ nanomaterials, with recovery per tissue of 60-92%, 1.5-2.4% and 0.5-2.6% respectively, at 24 hours after dosing.

Over the time course in the Elgrabli study, Ti levels were significantly higher than controls for all time points in the lungs yet within the liver and the spleen, Ti levels increased up to 1 day then, decreased regularly 7, 28 and 56 days after the injection [Elgrabli et al., 2015]. Interestingly, despite the presence of TiO₂ in these organs, histopathological analysis indicated no significant alterations of the tissue structures although TiO₂ agglomerates were observed in all organs. This lack of specific organ toxicity and that of overall systemic toxicity was also confirmed across a wide range of toxicological parameters (e.g. total protein content, IL-1β and IL-6 levels in serum, urea, γGT, glucose, lactate dehydrogenase, leucocytes etc.) which similarly showed a lack of effect of intravenously injected TiO₂ NPs on heart, spleen, liver, kidneys and overall inflammation [Elgrabli et al., 2015]. As the Elgrabli study investigated the clearance kinetics of the injected TiO₂, using mathematical models they established that the half-life in the body, corresponding to clearance of 50% of the initial amount of TiO₂, was 12.7 days. This differed from the Geraets et al. study which, across a range of different TiO₂ nanoparticles showed that elimination from the studied organs was very slow, indeed the liver elimination half time was estimated at 12.6 days in the Elgrabli study whilst was measured as 28-248 days in the Geraets study (differing durations reflected the different particles used) [Elgrabli et al., 2015; Geraets et al., 2014].

A similar lack of systemic toxicity was observed by Fabian *et al.* after intravenous injection of 5mg/kg of nano- TiO₂ as there were no changes in the cytokines and enzymes measured in blood samples, indicating that there was no detectable inflammatory response or organ toxicity [Fabian et al., 2008].

In contrast to the Elgrabli and Fabian study results, some studies have shown toxicity after intravenous injection of TiO₂. An example of which is the 2013 article by Xu *et al.* which described a dose response study in mice across a remarkably high dose range of 0, 140, 300, 645, or 1387 mg/kg when considered in comparison to the Elgrabli study or the potential levels of absorption below the ICP-MS detection limits (<1µg/L) of this dermal absorption study. Here 40nm anatase TiO₂ were injected into mice and the response assessed up to 14 days. They found dose dependent effects across a range of endpoints including death in some instances at the highest dose, significant increase in organ weights, increase in blood uric acid (although most biochemical parameters were unchanged) from 140mg/kg dose. They also found that injection did not cause modification of haematological parameters (except an increase in white blood cells at 645mg/kg) or genetic toxicity [Xu et al., 2013].

In relation to ZnO nanoparticles, similar distributions have been reported as seen with TiO₂ [Choi et al., 2015; Yeh et al., 2012] and it has been observed that after IV injection, Zn ions seem to have a longer half-life in the plasma, but ZnONPs show greater tissue accumulation [Yeh et al., 2012] likely due to nonspecific uptake of metallic nanoparticles by reticuloendothelial cells [Lin et al., 2015]. Due to the persistent accumulation in tissues (of ZnO and TiO₂), renal and biliary excretion has been said to be generally low for metallic nanoparticles although it is hypothesised that renal

elimination could be substantially increased with smaller sizes and specific coatings [Lin et al., 2015].

In relation to the toxicity of ZnO administered via the intravenous injection route, there are far fewer published studies than for TiO₂. A very recent study by Choi *et al.* investigated the toxicokinetics of ZnO nanoparticles in rats via a single IV injection or a single oral administration. They found that when rats were injected with a high dose of 30 mg/kg, mitotic figures in hepatocytes were significantly increased and multifocal acute injuries with dark brown pigment were noted in lungs, while no significant damage was observed in rats treated orally with the same dosage [Choi et al., 2015]. Another study using a similar dose of 25 mg/kg intravenously injected into rats indicated that ZnO nanoparticles did not alter the general health of the animals as no toxic signs or mortality was observed and no obvious significant differences were noted in the body weight and the relative brain weight of tested animals [Amara et al., 2014]. This difference in study conclusion may however reflect the depth of toxicological investigation as the aim of the Amara et al. study was not an in depth toxicological investigation but rather an assessment of the effect of acute exposure to ZnO nanoparticles on the cognitive capacity and neurotransmitters levels in adult rats. What was also interesting about the Amara et al study was that they found that intravenously administered ZnO altered blood and brain zinc distribution and that ZnO appear to be absorbed in the brain in an ionic form although this did not appear to affect the neurotransmitter contents, locomotor activity and spatial working memory in adult rats [Amara et al., 2014].

Overall the evidence suggests that systemically available (i.e. via the intravenous route of exposure) TiO₂ and ZnO at high doses are rapidly removed from the circulation and sequestered by the reticuloendothelial system, primarily accumulating in the liver, spleen and lung. Removal from the body via the renal and biliary excretion routes is relatively slow although it is not possible to draw conclusions on the relative excretion rates of TiO₂ compared to ZnO although for the latter this may be more rapid due to dissolution of ZnO. It has been suggested that due to the slow rate of removal from the body, repeated administration could lead to an accumulation in the body if exposure/absorption is sufficiently high.

Intravenous administration of even high doses of TiO₂ and ZnO are well tolerated and positive results showing toxicity from studies such as that of Xu et al. must be considered in relation to the very high doses used as well as the negative responses in other studies at lower doses. In conclusion, these studies suggest that should absorption of TiO₂ and ZnO nanoparticles occur at levels below the detection limit of the assays used herein, the systemic dose would be very small (far lower than the doses used in the studies discussed above) and so highly unlikely to cause systemic toxicity based on the toxicological evidence in rodents.

5. Conclusion

One important part of this project was the characterization of the nanoparticles in sunscreen, especially their size distribution. Due to the complexity of a system like sunscreen (viscosity, oil in water emulsion) the characterization was difficult to perform. However, a new method, acoustic attenuation spectroscopy (AAS), could be used to measure the particle size distribution directly in sunscreen. With this method we could show that in most of the prepared sunscreens, the nanoparticles have a particle size distribution where 50% of the particles are around 200 nm based on their weight. In two of the prepared sunscreens the particle size distribution was noticeable larger with of 661 nm and 393 nm, respectively. Furthermore, at least 90% of the particles had a size of larger than 100 nm.

Three skin models, namely the *in vitro* EpiDerm™ skin model and two *in vivo* skin models (mouse model for acute irritant contact dermatitis, xenograft human skin model), were used to investigate the dermal penetration/absorption of TiO₂ NPs and ZnO NPs.

When investigating the dermal penetration in the EpiDerm™ skin model; the ICP-MS analysis results show that in the case of ZnO NPs containing sunscreen, dermal penetration/absorption was clearly apparent whereas for TiO₂ NPs the result was more uncertain and not clear. However, none of the other used methods can confirm this result. Both, TiO₂ and ZnO NPs have no effect on skin corrosion and skin penetration and do not induce secretion of cytokines and inflammatory responses. Furthermore, no nanoparticles were detected by electron microscopy beneath the upper surface of the skin model although based on the ICP-MS analysis several hundred NPs should be present in the electron microscopy thin section.

Within the *in vivo* skin models (mouse model for acute irritant contact dermatitis, xenograft human skin model) that were used to investigate the dermal penetration/absorption of TiO₂ NPs, titanium was detected in skin biopsies using ICP-MS. However, for both *in vivo* skin models, an incomplete washing off of the sunscreen from the skin after the end of the experiment could be an explanation for the detection of titanium in the skin biopsies. Based on our estimations from the ICP-MS results at least several hundred TiO₂ NPs should be present per electron microscopy thin section. In both skin models nanoparticle-like structures that were observed in the samples were also found in the controls and were identified to be either melanin vesicles of the skin or polysomes. TiO₂ NPs were only observed at stratum corneum.

Based on our results from the *in vitro* and *in vivo* mouse and human skin models we conclude that dermal penetration of TiO₂ and ZnO NPs did not occur at or above the limit of detection of the used experimental methods. Our results further support the conclusions that were made by the SCCS that stated that both kind of nanoparticles are safe to use for dermal applications up to a concentration of 25% in cosmetic products [SCCS (Scientific Committee on Consumer Safety), 2012; SCCS (Scientific Committee on Consumer Safety), 2014].

References

Reference List

- Amara S, Ben-Slama I, Mrad I, Rihane N, Jeljeli M, El-Mir L, Ben-Rhouma K, Rachidi W, Seve M, Abdelmelek H, Sakly M. 2014. Acute exposure to zinc oxide nanoparticles does not affect the cognitive capacity and neurotransmitters levels in adult rats. *Nanotoxicology*. **8 Suppl 1:208-15**. doi: 10.3109/17435390.2013.879342. Epub; 2014 Feb 13. 208-215.
- Ang P, Ng S K, Goh C L. 1998. Sunscreen allergy in Singapore. *Am. J. Contact Dermat*. **9** 42-44.
- Asati A, Santra S, Kaittanis C, Perez J M. 2010. Surface-charge-dependent cell localization and cytotoxicity of cerium oxide nanoparticles. *ACS Nano*. **4** 5321-5331.
- Bennat C, Muller-Goymann C C. 2000. Skin penetration and stabilization of formulations containing microfine titanium dioxide as physical UV filter. *Int. J. Cosmet. Sci*. **22** 271-283.
- Bhattacharjee S, Ershov D, Gucht J, Alink G M, Rietjens I M, Zuilhof H, Marcelis A T. 2013. Surface charge-specific cytotoxicity and cellular uptake of tri-block copolymer nanoparticles. *Nanotoxicology* **7** 71-84.
- Botelho MC, Costa C, Silva S, Costa S, Dhawan A, Oliveira P A, Teixeira J P. 2014. Effects of titanium dioxide nanoparticles in human gastric epithelial cells in vitro. *Biomed. Pharmacother*. **68** 59-64.
- Chen T, Yan J, Li Y. 2014. Genotoxicity of titanium dioxide nanoparticles. *J. Food Drug Anal*. **22** 95-104.
- Choi J, Kim H, Kim P, Jo E, Kim H M, Lee M Y, Jin S M, Park K. 2015. Toxicity of zinc oxide nanoparticles in rats treated by two different routes: single intravenous injection and single oral administration. *J. Toxicol. Environ. Health A*. **78** 226-243.
- Cross SE, Innes B, Roberts M S, Tsuzuki T, Robertson T A, McCormick P. 2007. Human skin penetration of sunscreen nanoparticles: in-vitro assessment of a novel micronized zinc oxide formulation. *Skin Pharmacol. Physiol*. **20** 148-154.
- Dam TN, Kang S, Nickoloff B J, Voorhees J J. 1999. 1alpha,25-dihydroxycholecalciferol and cyclosporine suppress induction and promote resolution of psoriasis in human skin grafts transplanted on to SCID mice. *J. Invest Dermatol*. **113** 1082-1089.
- Donaldson K, Stone V, Tran C L, Kreyling W, Borm P J. 2004. Nanotoxicology. *Occup. Environ. Med*. **61** 727-728.
- Dukhin, Goetz. 2010. *Characterization of Liquids, Nano- and Microparticulates, and Porous Bodies using Ultrasound, 2nd Edition*. Elsevier.
- Durand L, Habran N, Henschel V, Amighi K. 2009. In vitro evaluation of the cutaneous penetration of sprayable sunscreen emulsions with high concentrations of UV filters. *Int. J. Cosmet. Sci*. **31** 279-292.

Dussert AS, Gooris E, Hemmerle J. 1997. Characterization of the mineral content of a physical sunscreen emulsion and its distribution onto human stratum corneum. *Int. J. Cosmet. Sci.* **19** 119-129.

Elgrabli D, Beaudouin R, Jbilou N, Floriani M, Pery A, Rogerieux F, Lacroix G. 2015. Biodistribution and Clearance of TiO₂ Nanoparticles in Rats after Intravenous Injection. *PLoS. One.* **10** e0124490.

European Commission. COMMISSION RECOMMENDATION of 22 September 2006 on the efficacy of sunscreen products and the claims made relating thereto. 2006/647/EC. OJ L 265/39. In European Commission.

European Commission. **COMMISSION RECOMMENDATION of 18 October 2011 on the definition of nanomaterial** (2011/696/EU) . In European Commission.

Fabian E, Landsiedel R, Ma-Hock L, Wiench K, Wohlleben W, van R B. 2008. Tissue distribution and toxicity of intravenously administered titanium dioxide nanoparticles in rats. *Arch. Toxicol.* **82** 151-157.

Filipe P, Silva J N, Silva R, Cirne de Castro J L, Marques G M, Alves L C, Santus R, Pinheiro T. 2009. Stratum corneum is an effective barrier to TiO₂ and ZnO nanoparticle percutaneous absorption. *Skin Pharmacol. Physiol.* **22** 266-275.

Frohlich E. 2012. The role of surface charge in cellular uptake and cytotoxicity of medical nanoparticles. *Int. J. Nanomedicine.* **7** 5577-5591.

Gamer AO, Leibold E, van R B. 2006. The in vitro absorption of microfine zinc oxide and titanium dioxide through porcine skin. *Toxicol. In Vitro.* **20** 301-307.

Geraets L, Oomen A G, Krystek P, Jacobsen N R, Wallin H, Laurentie M, Verharen H W, Brandon E F, de Jong W H. 2014. Tissue distribution and elimination after oral and intravenous administration of different titanium dioxide nanoparticles in rats. *Part Fibre. Toxicol.* **11:30. doi: 10.1186/1743-8977-11-30.** 30-11.

Green AC, Williams G M, Logan V, Stratton G M. 2011. Reduced melanoma after regular sunscreen use: randomized trial follow-up. *J. Clin. Oncol.* **29** 257-263.

Gulson B, McCall M, Korsch M, Gomez L, Casey P, Oytam Y, Taylor A, McCulloch M, Trotter J, Kinsley L, Greenoak G. 2010. Small amounts of zinc from zinc oxide particles in sunscreens applied outdoors are absorbed through human skin. *Toxicol. Sci.* **118** 140-149.

Gulson B, Wong H, Korsch M, Gomez L, Casey P, McCall M, McCulloch M, Trotter J, Stauber J, Greenoak G. 2012. Comparison of dermal absorption of zinc from different sunscreen formulations and differing UV exposure based on stable isotope tracing. *Sci. Total Environ.* **420:313-8. doi: 10.1016/j.scitotenv.2011.12.046. Epub; %2012 Feb 7.** 313-318.

Iannuccelli V, Bertelli D, Romagnoli M, Scalia S, Maretti E, Sacchetti F, Leo E. 2014. In vivo penetration of bare and lipid-coated silica nanoparticles across the human stratum corneum. *Colloids Surf. B Biointerfaces.* **122:653-61. doi: 10.1016/j.colsurfb.2014.07.046. Epub; %2014 Aug 12.** 653-661.

Ilves M, Palomaki J, Vippola M, Lehto M, Savolainen K, Savinko T, Alenius H. 2014. Topically applied ZnO nanoparticles suppress allergen induced skin inflammation but induce vigorous IgE

production in the atopic dermatitis mouse model. *Part Fibre. Toxicol.* **11:38**. doi: **10.1186/s12989-014-0038-4**. 38-0038.

Jacobs JF, van d P, I, Osseweijer P. 2010. Sunscreens with Titanium Dioxide (TiO₂) Nanoparticles: A Societal Experiment. *Nanoethics.* **4** 103-113.

Kandarova H. **Evaluation and Validation of Reconstructed Human Skin Models as Alternatives to Animal Tests in Regulatory Toxicology.** In PhD Thesis, Freie Universitaet Berlin.

Kansara K, Patel P, Shah D, Shukla R K, Singh S, Kumar A, Dhawan A. 2015. TiO₂ nanoparticles induce DNA double strand breaks and cell cycle arrest in human alveolar cells. *Environ. Mol. Mutagen.* **56** 204-217.

Kubac L, Akrman J, Kejlova K, Bendova H, Klanova K, Hladikova Z, Pikal P, Kovarikova L, Kasparova L, Jirova D. 2015. Characteristics of titanium dioxide microdispersions with different photo-activity suitable for sunscreen formulations. *Int. J. Pharm.* **481** 91-96.

Kuo TR, Wu C L, Hsu C T, Lo W, Chiang S J, Lin S J, Dong C Y, Chen C C. 2009. Chemical enhancer induced changes in the mechanisms of transdermal delivery of zinc oxide nanoparticles. *Biomaterials.* **30** 3002-3008.

Larsen PB, Christensen F, Jensen K A, Brinch A, Mikkelsen S H. Exposure assessment of nanomaterials in consumer products Environmental project No. 1636, 2015. In Danish Environmental Protection Agency.

Lin Z, onteiro-Riviere N A, Riviere J E. 2015. Pharmacokinetics of metallic nanoparticles. *Wiley Interdiscip Rev Nanomed Nanobiotechnol* **7** 189-217.

Magnusson BM, Anissimov Y G, Cross S E, Roberts M S. 2004. Molecular size as the main determinant of solute maximum flux across the skin. *J. Invest Dermatol.* **122** 993-999.

Maynard AD, Warheit D B, Philbert M A. 2011. The new toxicology of sophisticated materials: nanotoxicology and beyond. *Toxicol. Sci.* **120 Suppl 1** S109-S129.

Monteiro-Riviere NA, Wiench K, Landsiedel R, Schulte S, Inman A O, Riviere J E. 2011. Safety evaluation of sunscreen formulations containing titanium dioxide and zinc oxide nanoparticles in UVB sunburned skin: an in vitro and in vivo study. *Toxicol. Sci.* **123** 264-280.

Nel A, Xia T, Madler L, Li N. 2006. Toxic potential of materials at the nanolevel. *Science* **311** 622-627.

Nohynek GJ, Dufour E K. 2012. Nano-sized cosmetic formulations or solid nanoparticles in sunscreens: a risk to human health? *Arch. Toxicol.* **86** 1063-1075.

Oberdorster G, Oberdorster E, Oberdorster J. 2005. Nanotoxicology: An emerging discipline evolving from studies of ultrafine particles. *Environmental Health Perspectives* **113** 823-839.

Parry EJ, Bilsland D, Morley W N. 1995. Photocontact allergy to 4-tert.butyl-4'-methoxy-dibenzoylmethane (Parsol 1789). *Contact Dermatitis.* **32** 251-252.

Poland CA, Read SAK, Varet J, Carse G, Christensen FM, Hankin SM. Dermal absorption of nanomaterials. Environmental Project No. 1504. In The Danish Environmental Protection Agency: Denmark.

Rosada C, Stenderup K, de D E, Dagnaes-Hansen F, Kamp S, Dam T N. 2010. Valrubicin in a topical formulation treats psoriasis in a xenograft transplantation model. *J. Invest Dermatol.* **130** 455-463.

SCCS (Scientific Committee on Consumer Safety). **OPINION ON Zinc oxide (nano form) COLIPA S 76.** In Scientific Committee on Consumer Safety SCCS.

SCCS (Scientific Committee on Consumer Safety). Opinion on titanium dioxide (nano form), 22 July 2013, revision of 22 April 2014. In SCCS (Scientific Committee on Consumer Safety).

Senzui M, Tamura T, Miura K, Ikarashi Y, Watanabe Y, Fujii M. 2010. Study on penetration of titanium dioxide (TiO₂) nanoparticles into intact and damaged skin in vitro. *J. Toxicol. Sci.* **35** 107-113.

Shi H, Magaye R, Castranova V, Zhao J. 2013. Titanium dioxide nanoparticles: a review of current toxicological data. *Part Fibre. Toxicol.* **10** 15.

Shinohara N, Danno N, Ichinose T, Sasaki T, Fukui H, Honda K, Gamo M. 2014. Tissue distribution and clearance of intravenously administered titanium dioxide (TiO₂) nanoparticles. *Nanotoxicology.* **8** 132-141.

Singh N, Manshian B, Jenkins G J, Griffiths S M, Williams P M, Maffei T G, Wright C J, Doak S H. 2009. NanoGenotoxicology: The DNA damaging potential of engineered nanomaterials. *Biomaterials* **30** 3891-3914.

Song Z, Kelf T A, Sanchez W H, Roberts M S, Ricka J, Frenz M, Zvyagin A V. 2011a. Characterization of optical properties of ZnO nanoparticles for quantitative imaging of transdermal transport. *Biomed. Opt. Express.* **2** 3321-3333.

Song Z, Kelf T A, Sanchez W H, Roberts M S, Ricka J, Frenz M, Zvyagin A V. 2011b. Characterization of optical properties of ZnO nanoparticles for quantitative imaging of transdermal transport. *Biomed. Opt. Express.* **2** 3321-3333.

Srivastava RK, Rahman Q, Kashyap M P, Singh A K, Jain G, Jahan S, Lohani M, Lantow M, Pant A B. 2013. Nano-titanium dioxide induces genotoxicity and apoptosis in human lung cancer cell line, A549. *Hum. Exp. Toxicol.* **32** 153-166.

Stenderup K, Rosada C, Dam T N, Salerno E, Belinka B A, Kachlany S C. 2011. Resolution of psoriasis by a leukocyte-targeting bacterial protein in a humanized mouse model. *J. Invest Dermatol.* **131** 2033-2039.

Stenderup K, Rosada C, Worsaae A, Dagnaes-Hansen F, Steiniche T, Hasselager E, Iversen L F, Zahn S, Woldike H, Holmberg H L, Romer J, Kragballe K, Clausen J T, Dam T N. 2009. Interleukin-20 plays a critical role in maintenance and development of psoriasis in the human xenograft transplantation model. *Br. J. Dermatol.* **160** 284-296.

Szikszai Z, Kertész Z, Bodnár E, Major I, Borbély I, Kiss Á, Hunyadi J. 2010. Nuclear microprobe investigation of the penetration of ultrafine zinc oxide into intact and tape-stripped human skin. *Nuclear Instruments and Methods in Physics Research Section B: Beam Interactions with Materials and Atoms* **268** 2160-2163.

Tetley TD. 2007. Health effects of nanomaterials. *Biochem. Soc. Trans.* **35** 527-531.

- Tyner KM, Wokovich A M, Doub W H, Buhse L F, Sung L P, Watson S S, Sadrieh N. 2009. Comparing methods for detecting and characterizing metal oxide nanoparticles in unmodified commercial sunscreens. *Nanomedicine. (Lond)*. **4** 145-159.
- Uter W, Goncalo M, Yazar K, Kratz E M, Mildau G, Liden C. 2014. Coupled exposure to ingredients of cosmetic products: III. Ultraviolet filters. *Contact Dermatitis*. **71** 162-169.
- Wong VW, Sorkin M, Glotzbach J P, Longaker M T, Gurtner G C. 2011. Surgical approaches to create murine models of human wound healing. *J. Biomed. Biotechnol.* **2011:969618**. doi: **10.1155/2011/969618**. Epub; %2010 Dec 1. 969618.
- Xie G, Wang C, Sun J, Zhong G. 2011. Tissue distribution and excretion of intravenously administered titanium dioxide nanoparticles. *Toxicol. Lett.* **205** 55-61.
- Xu J, Shi H, Ruth M, Yu H, Lazar L, Zou B, Yang C, Wu A, Zhao J. 2013. Acute toxicity of intravenously administered titanium dioxide nanoparticles in mice. *PLoS. One.* **8** e70618.
- Yeh TK, Chen J K, Lin C H, Yang M H, Yang C S, Chou F I, Peir J J, Wang M Y, Chang W H, Tsai M H, Tsai H T, Lin P. 2012. Kinetics and tissue distribution of neutron-activated zinc oxide nanoparticles and zinc nitrate in mice: effects of size and particulate nature. *Nanotechnology.* **23** 085102-4484/23.

Appendix 1: Nanoparticle information as provided by the manufacturer

Titanium Oxide Nanopowder / Nanoparticles (TiO₂, rutile, high purity, 99.9+%, 30 nm)

\$45/25g
\$79/50g
\$138/100g
\$299/500g
\$489/1kg

Please [contact us](#) for quotes on larger quantities. [Need Dispersion?](#)

Stock #: US3520

Number of nanoparticles in 1 gram? Here comes an example from [stock# US1054](#):

For US1054, Number of nanoparticles in 1 gram = 2.929×10^{16}

Density of Au is 19.32 g/cm^3

Volume of 1 gram Au = $1/19.32 = 5.176 \times 10^{-2} \text{ cm}^3$

For spherical nanoparticles of 15 nm, volume of one particle = $4/3 \times \pi \times (7.5 \times 10^{-7})^3 \text{ cm}^3 = 1.767 \times 10^{-18} \text{ cm}^3$

Therefore, number of nanoparticles in 1 gram = $[5.176 \times 10^{-2}] / [1.767 \times 10^{-18}] = 2.929 \times 10^{16}$ nanoparticles

Titanium Oxide Nanopowder (TiO₂, rutile)-analytical pure chemical reagent as raw materials, and washed by distilled water.

TiO₂ Nanopowder Purity: 99.9+%

TiO₂ Nanopowder APS: 30 nm

TiO₂ Nanopowder SSA: ~35-60m²/g

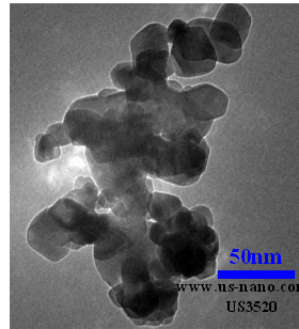
TiO₂ Nanopowder Color: white

TiO₂ Nanopowder Morphology: near spherical

TiO₂ Nanopowder Bulk Density: 0.25 g/cm³

TiO₂ Nanopowder True Density: 4.23 g/cm³

Electronic components based materials, such as multilayer chip ceramic capacitors (MLCC).



Order: 25g (add \$45) ▾

Quantity:

1

◀ Back

➤ Add To Cart

Titanium Oxide Nanopowder (TiO ₂) COA -- %												
TiO ₂	Al	Ca	Co	Cr	Fe	K+Na	Mo	Mg	P	S	Si	W
≥99.9	≤0.003	≤0.005	≤0.01	≤0.005	≤0.005	≤0.005	≤0.005	≤0.01	≤0.01	≤0.005	≤0.003	≤0.01

Titanium Oxide (TiO₂) Nanoparticles / Nanopowder (TiO₂ rutile HighPurity 99.9+% 100nm)

\$45/25g
\$79/50g
\$138/100g
\$299/500g
\$389/1kg

Please [contact us](#) for quotes on larger quantities. [Need Dispersion?](#)

Stock #: US3535

Number of nanoparticles in 1 gram? Here comes an example from [stock# US1054](#):

For US1054, Number of nanoparticles in 1 gram = 2.929×10^{16}

Density of Au is 19.32 g/cm^3

Volume of 1 gram Au = $1/19.32 = 5.176 \times 10^{-2} \text{ cm}^3$

For spherical nanoparticles of 15 nm, volume of one particle = $4/3 \times \pi \times (7.5 \times 10^{-7})^3 \text{ cm}^3 = 1.767 \times 10^{-18} \text{ cm}^3$

Therefore, number of nanoparticles in 1 gram = $[5.176 \times 10^{-2}] / [1.767 \times 10^{-18}] = 2.929 \times 10^{16}$ nanoparticles

Titanium Oxide Nanopowder (TiO₂, rutile)-analytical pure chemical reagent as raw materials, and washed by distilled water.

TiO₂ Nanopowder Purity: 99.9+%

TiO₂ Nanopowder APS: 100 nm

TiO₂ Nanopowder SSA: ~15-35m²/g

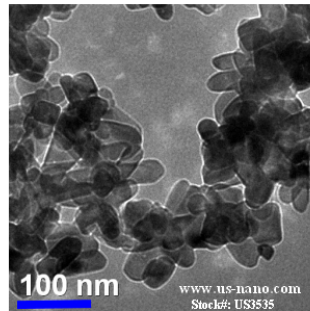
TiO₂ Nanopowder Color: white

TiO₂ Nanopowder Morphology: near spherical

TiO₂ Nanopowder Bulk Density: 0.37 g/cm³

TiO₂ Nanopowder True Density: 4.23 g/cm³

Electronic components based materials, such as multilayer chip ceramic capacitors (MLCC).



Order: 25g (add \$45) ▾

Quantity:

1

◀ Back

➤ Add To Cart

Titanium Oxide Nanopowder (TiO ₂) COA -- %												
TiO ₂	Al	Ca	Co	Cr	Fe	K+Na	Mo	Mg	P	S	Si	W
≥99.9	≤0.003	≤0.005	≤0.01	≤0.005	≤0.005	≤0.005	≤0.005	≤0.01	≤0.01	≤0.005	≤0.003	≤0.01

Titanium Dioxide Nanoparticles Coated with Silicon and Aluminum (TiO₂, Rutile, 30nm)

TiO₂, rutile, 92+wt%, 30 nm, coated with silicon and aluminum. Si and Al about 6.0-7.5 wt%. Super Hydrophilic with UV-protection!!

\$45/25g
\$75/50g
\$125/100g
\$299/500g
\$489/1kg

Please [contact us](#) for quotes on larger quantities.

Stock #: US3524

Titanium Oxide Nanoparticles (TiO₂, rutile, surface coated with silicon and aluminum, better paint color, stronger resistance to ultraviolet light, super hydrophilic and easier to be dispersed...)

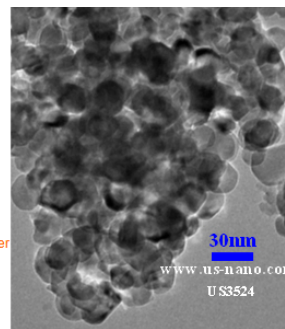
Titanium Oxide Nanoparticle Rutile: 92+wt%; Al and Si 6-7.5wt%

Titanium Oxide Nanoparticle APS: 30 nm

Titanium Oxide Nanoparticle SSA: >55m²/g

Titanium Oxide Nanoparticle Color: white

Titanium Oxide Nanoparticle Bulk Density: 0.58g/ml



Order: 25g (add \$45) ▾

Quantity:

1

◀ Back

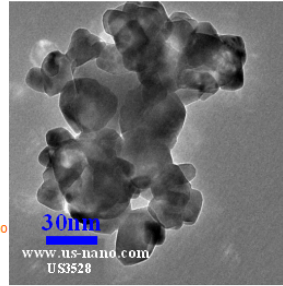
➤ Add To Cart

Titanium Dioxide Nanoparticles Coated with Silicon and Aluminum Certificate of Analysis				
TiO ₂ rutile : Al and Si	Fe	Mg	K+Na	Ca
92wt% : 6-7.5wt%	<11ppm	<55ppm	<160ppm	<75ppm

Titanium Dioxide Nanoparticles Coated with Silicone Oil (TiO2, Rutile, 30nm)

TiO2, rutile, 92+wt%, 30 nm, coated with silicone oil with 7wt%. Super Hydrophobic, Stronger Lipophilic (oleophilic) with UV-protection!
 \$45/25g
 \$75/50g
 \$125/100g
 \$299/500g
 \$489/1kg
 Please [contact us](#) for quotes on larger quantities.
 Stock #: US3528

Titanium Oxide Nanopowder (TiO2, rutile, surface coated with silicone oil, better paint color, stronger resistance to ultraviolet light and super hydrophobic, lipophilic and easier to be dispersed...)
 Titanium Oxide Nanopowder Rutile: 92+wt%, Silicone Oil: 7wt%
 Titanium Oxide Nanopowder APS: 30 nm
 Titanium Oxide Nanopowder SSA: >55m²/g
 Titanium Oxide Nanopowder Color: white
 Titanium Oxide Nanopowder Bulk Density: 0.54 g/ml



Order: 25g (add \$45)

Quantity:

1

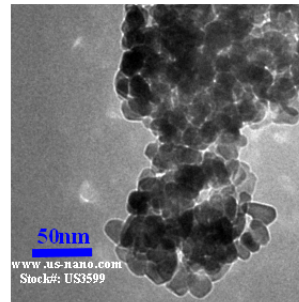
[Back](#) [Add To Cart](#)

Titanium Dioxide Nanoparticles Coated with Silicone Oil Certificate of Analysis				
TiO2rutile:Silicone Oil	SiO2	Mg	K+Na	Ca
92+wt%:7wt%	<55ppm	<45ppm	<160ppm	<60ppm

Zinc Oxide (ZnO) Nanoparticles / Nanopowder (ZnO, High Purity 99.95%, 18nm)

\$55/25g
 \$105/100g
 \$225/500g
 \$395/1kg
 Please [contact us](#) for quotes on larger quantities. (Need Dispersion?)
 Stock #: US3599

Zinc Oxide Nanopowder (ZnO)—analytical pure chemical reagent as raw materials, and washed by distilled water.
 Purity: 99.95%
 APS: 18 nm
 Color: milky white
 Crystal Phase: single crystal
 Morphology: nearly spherical
 SSA: 40-70 m²/g
 True Density: 5.606 g/cm³



Order: 25g (add \$55)

Quantity:

1

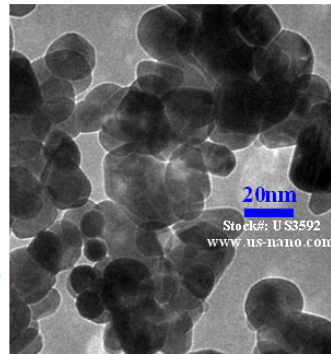
ZnO	Cu	Fe	Cd	Mn	K	Pb	Al
99.95%	2ppm	0.05ppm	5.3ppm	3.8ppm	0.03ppm	6.8ppm	0.08ppm

Note: The high-purity product was prepared by using analytically pure chemical reagent as raw materials.

Zinc Oxide Nanoparticles Coated with KH550 (ZnO, 99+%, 20nm, Coated with 1wt% Silane Coupling Agent)

Properties: Both hydrophilic and oleophilic and easier to be dispersed!
 \$55/5g
 \$95/25g
 \$165/50g
 \$255/100g
 \$435/500g
 \$699/1kg
 Please [contact us](#) for quotes on larger quantities.
 Stock #: US3592

Zinc Oxide Nanoparticles Coated with KH550=Silane Coupling Agent=3-Aminopropyltriethoxysilane=1wt%
 ZnO Purity: 99wt%
 APS: 20nm
 Color: white with very light yellow
 Crystal Phase: single crystal
 Morphology: nearly spherical
 SSA: 20-60 m²/g
 True Density: 5.606 g/cm³
 Bulk Density: 0.532 g/cm³
 Loss of weight in drying: 0.42
 Loss of weight on ignition: 2.1
 PH: 8.5-9.0



Order: 5g (add \$55)

Quantity:

1

[Back](#) [Add To Cart](#)

Zinc Oxide Nanoparticles Coated with KH550 Certificate of Analysis				
ZnO:KH550	TiO2	ZrO2	Fe2O3	AgO2
99%:1%	0.051%	0.017%	0.008%	0.027%

PRODUCT DATA SHEET

UV-TITAN M161

UV-TITAN M161 is a surface treated, hydrophobic ultrafine rutile titanium dioxide specifically developed to provide high Sun Protection Factor products in sun care and skin care cosmetic formulations. Small crystal size and controlled particle size distribution contributes to excellent dispersibility and transparency in emulsions.

TYPICAL PROPERTIES

Appearance		odourless, white powder
Crystal size, nm	ca.	17
Specific gravity	ca.	4
Specific surface area, m ² /g	ca.	70
Modifiers, compounds of		alumina, stearic acid
INCI name		titanium dioxide, alumina, stearic acid
Bulk density, kg/m ³		150
Packaging		10 kg paper bags/ 300 kg pallet

CLASSIFICATION

CAS no. (TiO ₂) 13463-67-7	Pigment White 6
EINECS no. (TiO ₂) 2366755	Components listed in TSCA, EINECS
Colour Index 77891	

The manufacture of UV-TITAN products is within the scope of the ISO 9001 certified Quality Management System. The Pori plant also has an ISO 14001 certified Environmental Management System.

SAFETY PRECAUTIONS

Please see the Material Safety Data Sheet before handling the material.

Warranty. This information herein is offered as a guide and is believed to be accurate and reliable as of the date of printing. The values given are not to be considered as a warranty and they are subject to change without prior notice. For additional information regarding our products or for information concerning current specifications, please contact our Technical Service. 07/2004

Kemira Pigments Oy

Sales & Technical Service
Titanite
FIN-28840 Pori
Finland

Tel. +358 (0)10 863 415
www.kemira.com

Fax numbers:
Industrial Pigments +358 10 863 1096
Specialty Products +358 10 863 1091
Co-products +358 10 863 1899
Technical Service +358 10 863 1812

Business ID 0948159-2
Registered office Helsinki
VAT FI 09481592

UV-Titan

PRODUCT DATA SHEET

UV-TITAN M262

UV-TITAN M262 is a surface treated, slightly hydrophobic ultrafine rutile titanium dioxide specifically developed for sun care, skin care and colour cosmetic formulations to give a broad spectrum UV radiation protection. UV-TITAN M262 can also be used in special skin treatment applications in which UVA/UVB protection is needed. UV-TITAN M262 possesses superior light stability, antioxidant resistance and excellent dispersibility in different vehicles.

TYPICAL PROPERTIES

Appearance	Odourless, white powder
Crystal size	ca. 20 nm
Specific gravity	ca. 4
Specific surface area	ca. 60 m ² /g
Modifiers, compounds of	Alumina, Silicone
INCI name	Titanium dioxide, Alumina, Dimethicone
Bulk density	150 kg/m ³
Packaging	10 kg paper bags/ 300 kg pallet

CLASSIFICATION

CAS No. (TiO ₂)	13463-67-7
EINECS (TiO ₂)	2366755
Colour Index	77891
Pigment White	6
Components listed in EINECS, TSCA	

The manufacture of UV-TITAN products is within the scope of the ISO 9001 certified Quality Management System. The Pori plant also has an ISO 14001 certified Environmental Management System.

SAFETY PRECAUTIONS

Please see the Material Safety Data Sheet before handling the material.

Warranty. This information herein is offered as a guide and is believed to be accurate and reliable as of date of printing. Values given are not to be considered as a warranty and they are subject to change without prior notice. For additional information regarding our products or for information concerning current specifications, please contact our Technical Service. 10/2000

KEMIRA

KEMIRA PIGMENTS OY
Helsinki

Reg.no 571.088. Registered office

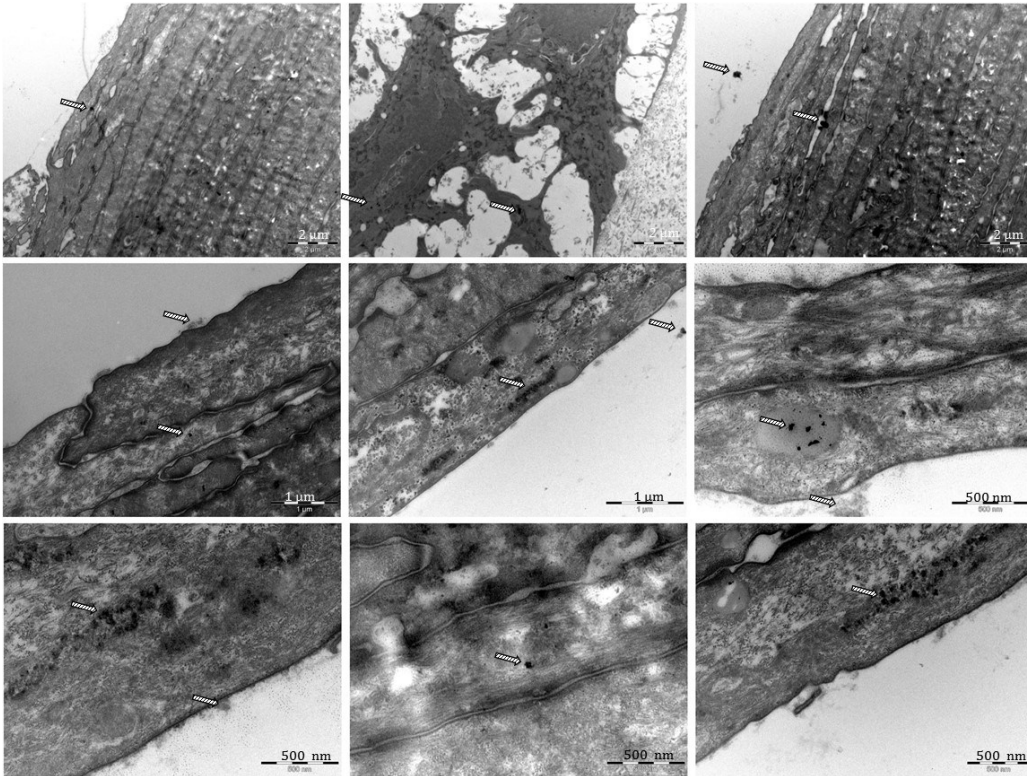
ADDRESS	TELEPHONE	TELEFAX
FIN-20940 Pori	+358 (0)10 841 415	+358 (0)10 842 1091
FINLAND		
http://www.kemira.com/pigments		

Appendix 2: Transmission electron microscopy

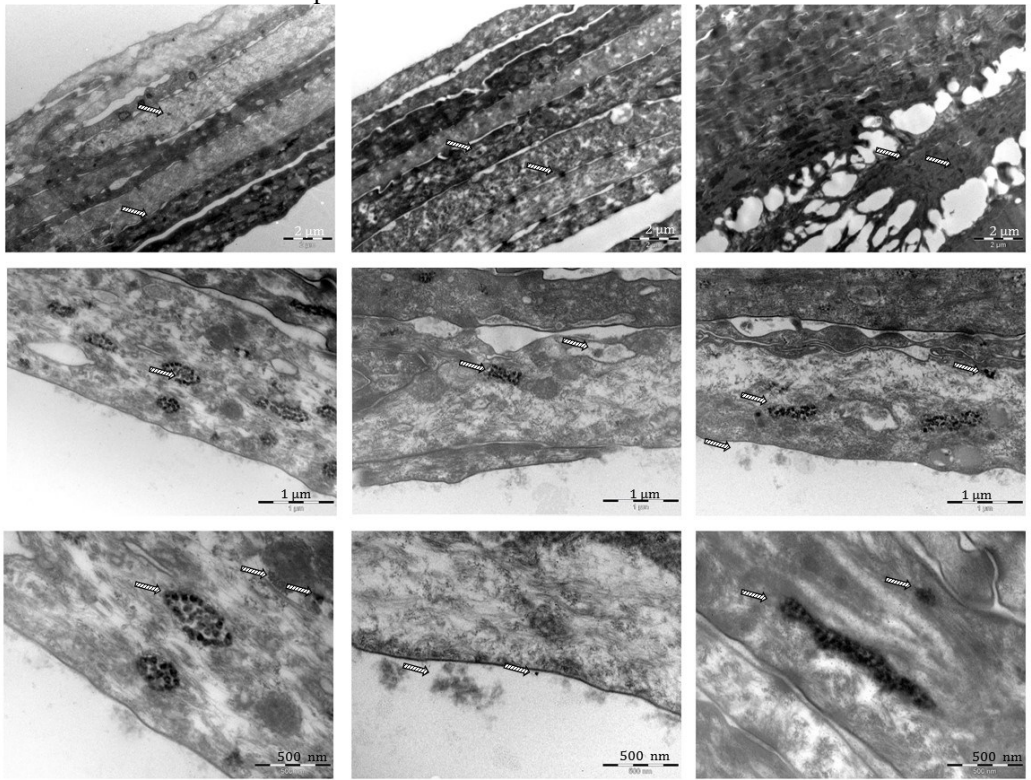
Cellular structures that could be mistaken for nanoparticles are marked with a white arrow. These structures are also marked in the samples where nanoparticles could be present in the TEM sections. Nano-sized structures we believe are nanoparticles are marked with a black arrow.

In vitro EpiDerm skin model

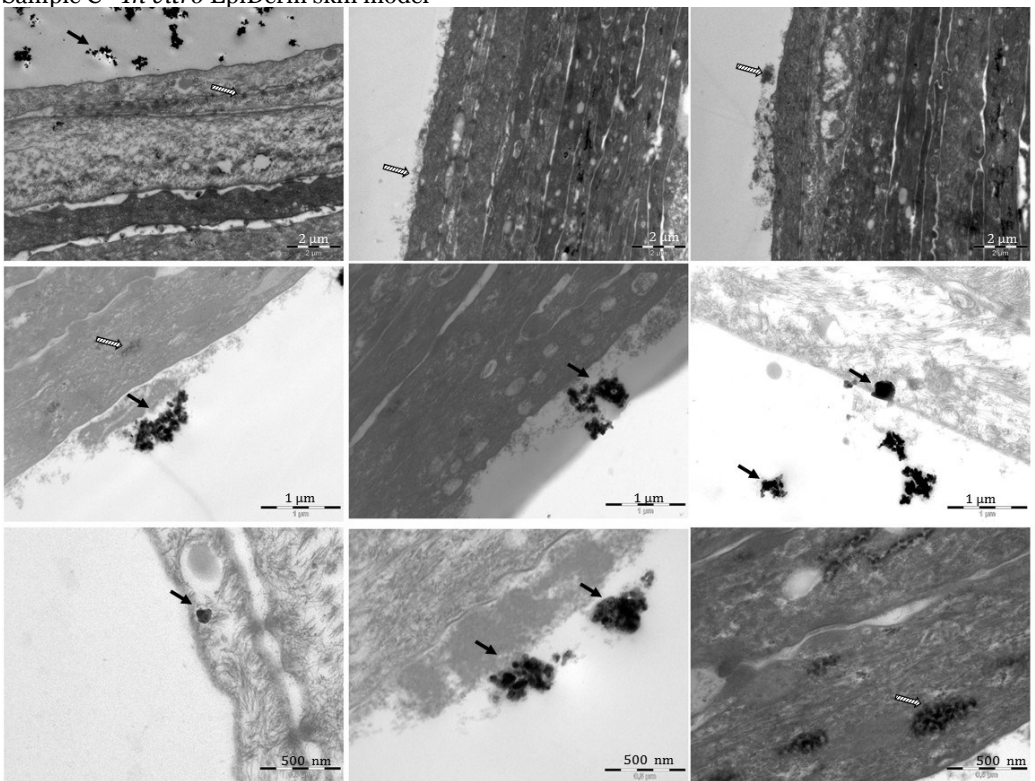
Negative control - *In vitro* EpiDerm skin model



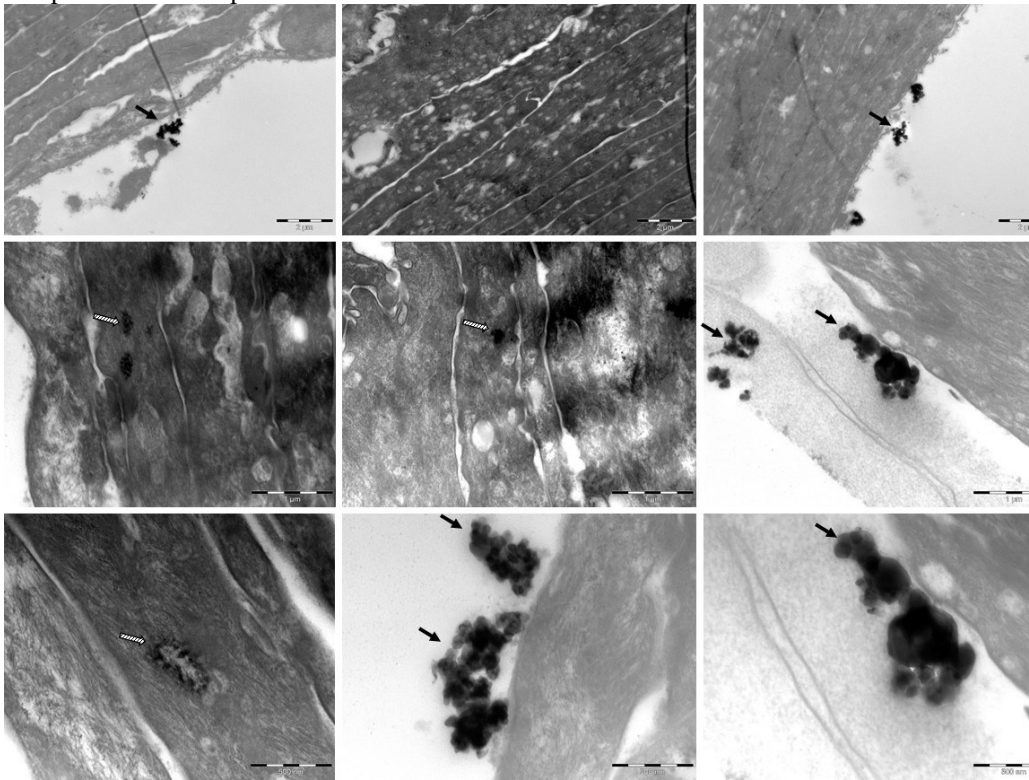
Sunscreen control - *In vitro* EpiDerm skin model



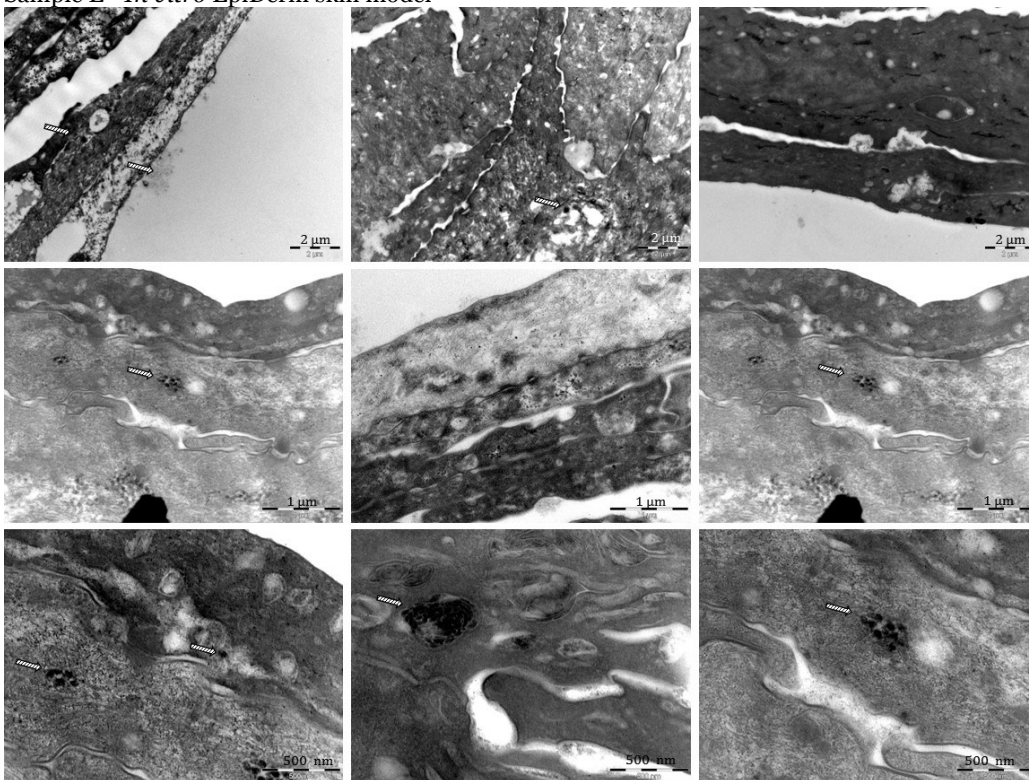
Sample C - *In vitro* EpiDerm skin model



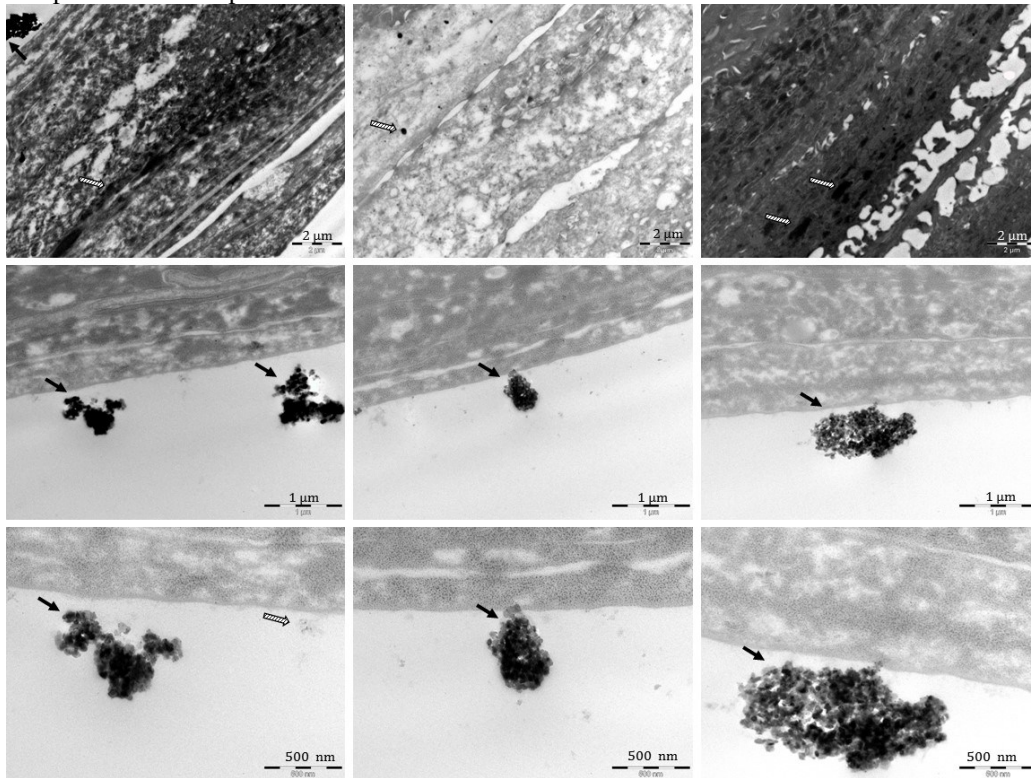
Sample D - *In vitro* EpiDerm skin model



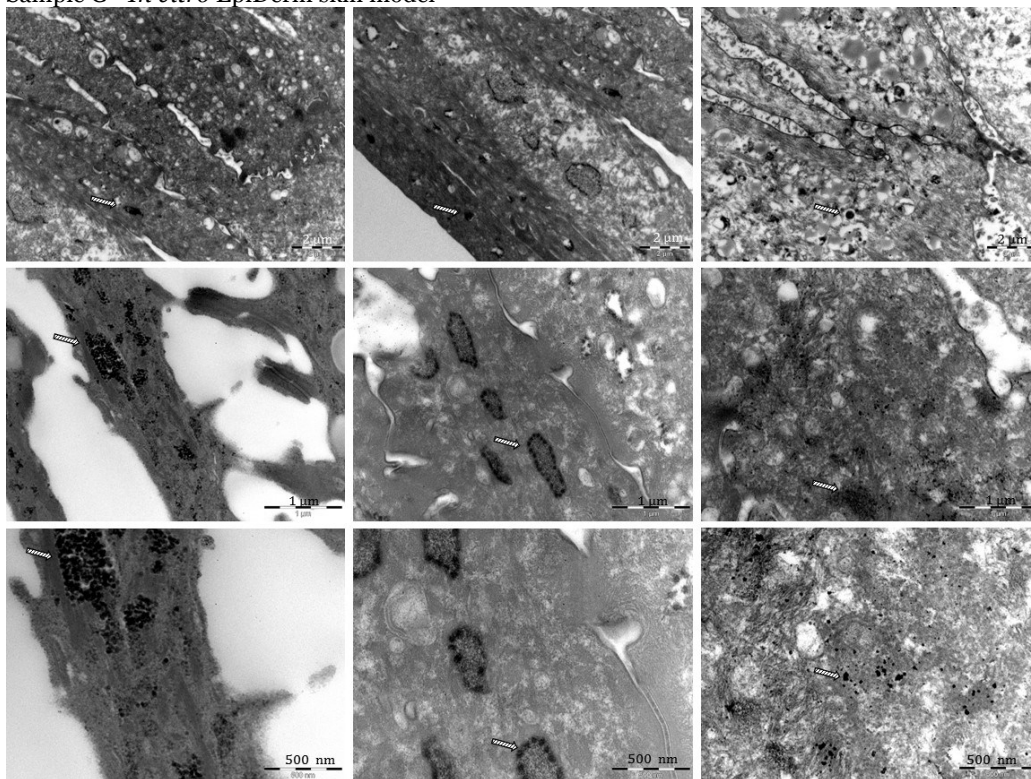
Sample E - *In vitro* EpiDerm skin model



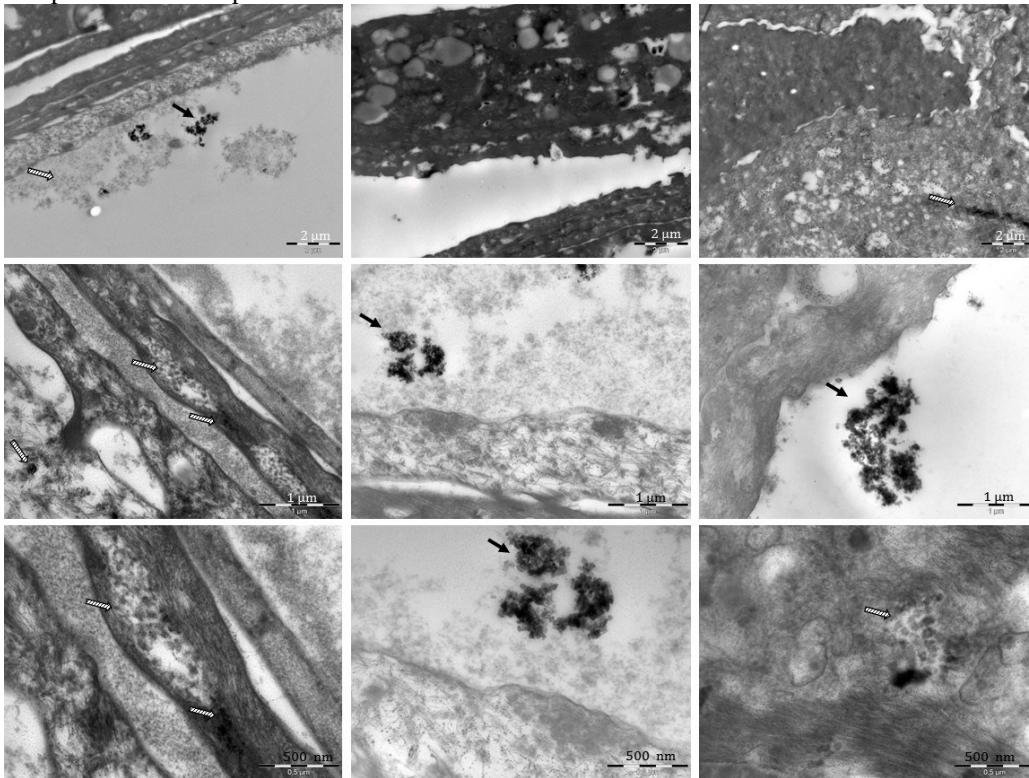
Sample F - *In vitro* EpiDerm skin model



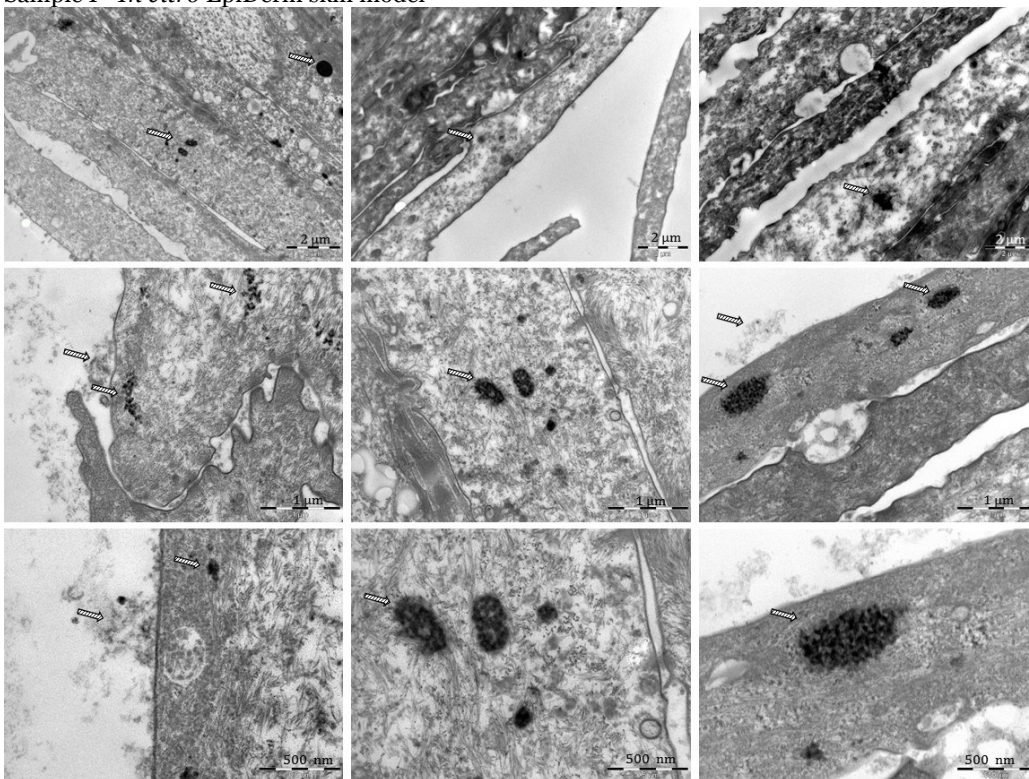
Sample G - *In vitro* EpiDerm skin model



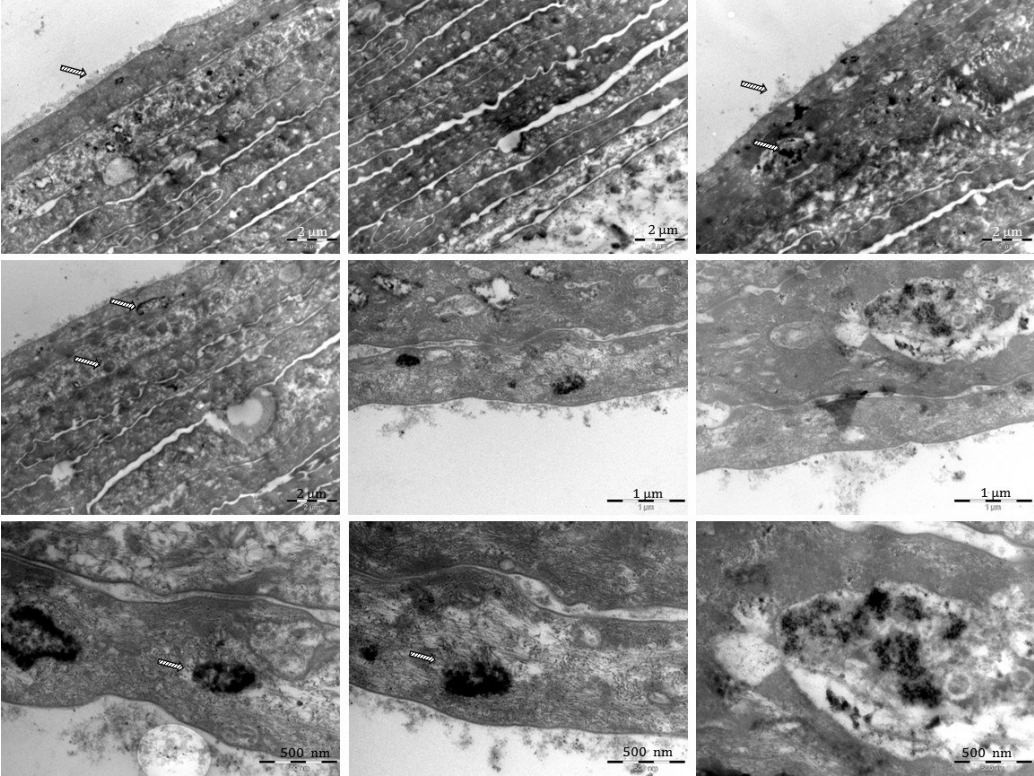
Sample H - *In vitro* EpiDerm skin model



Sample I - *In vitro* EpiDerm skin model

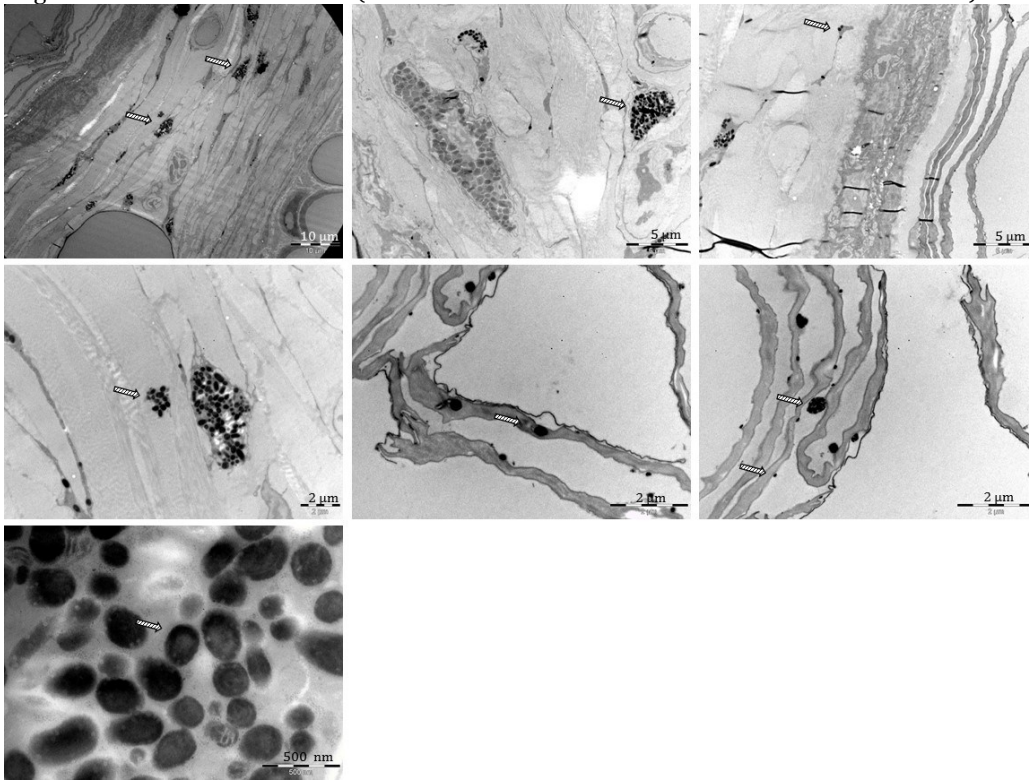


Sample K - *In vitro* EpiDerm skin model

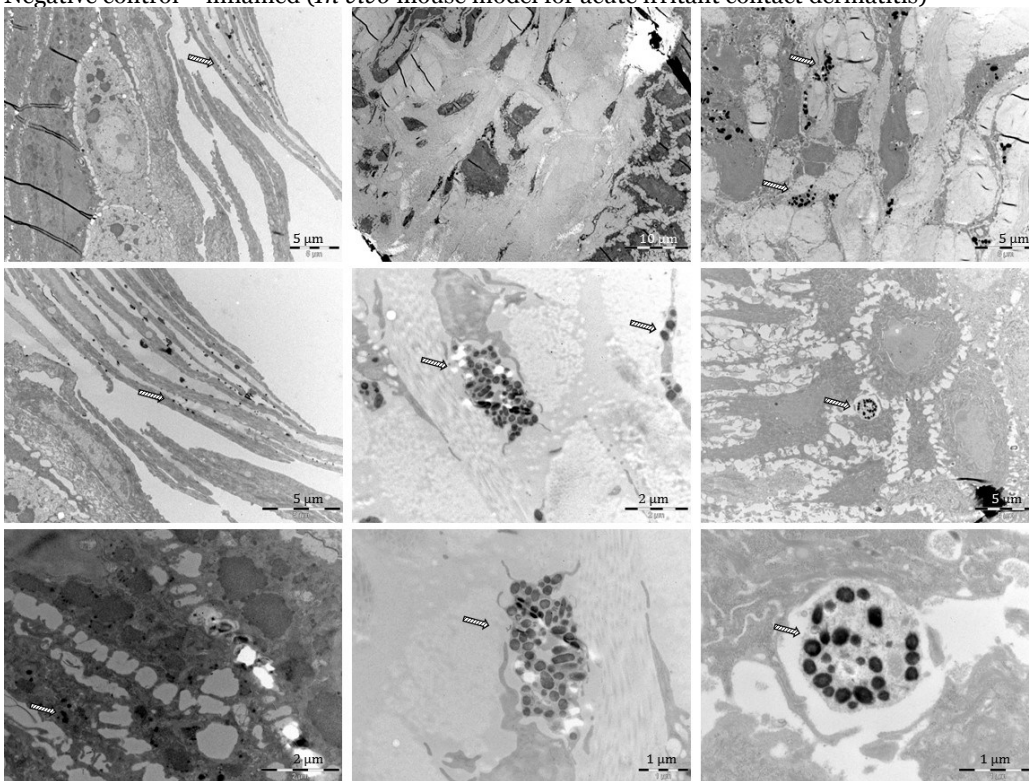


In vivo mouse model for acute irritant contact dermatitis

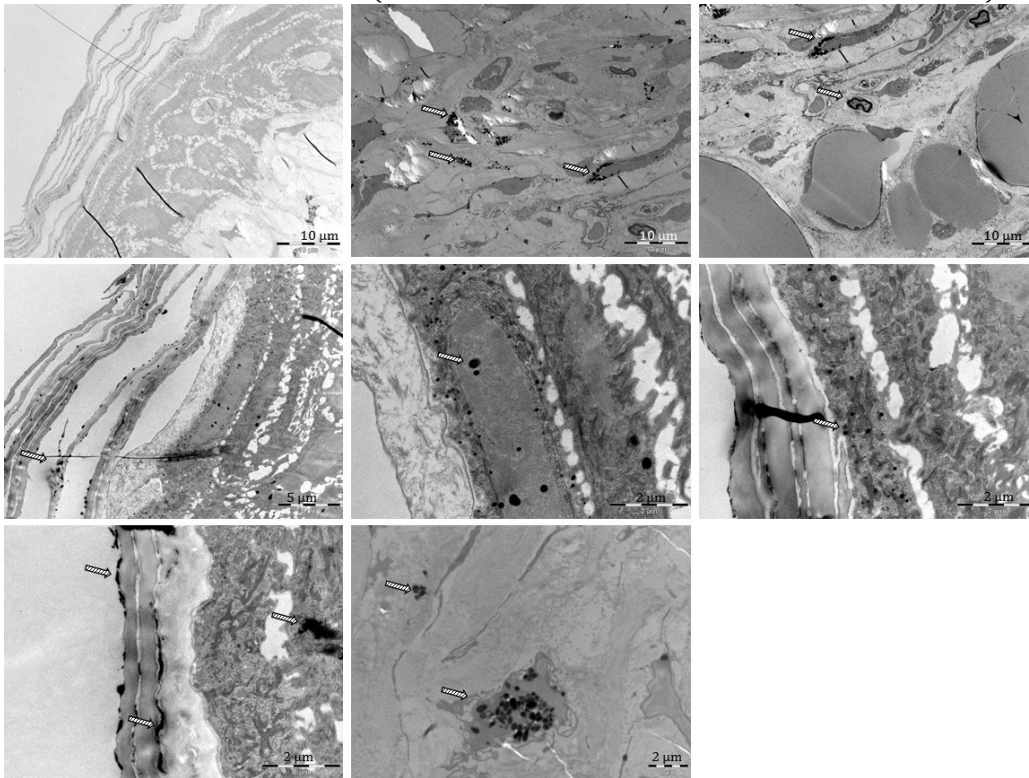
Negative control – non-inflamed (*In vivo* mouse model for acute irritant contact dermatitis)



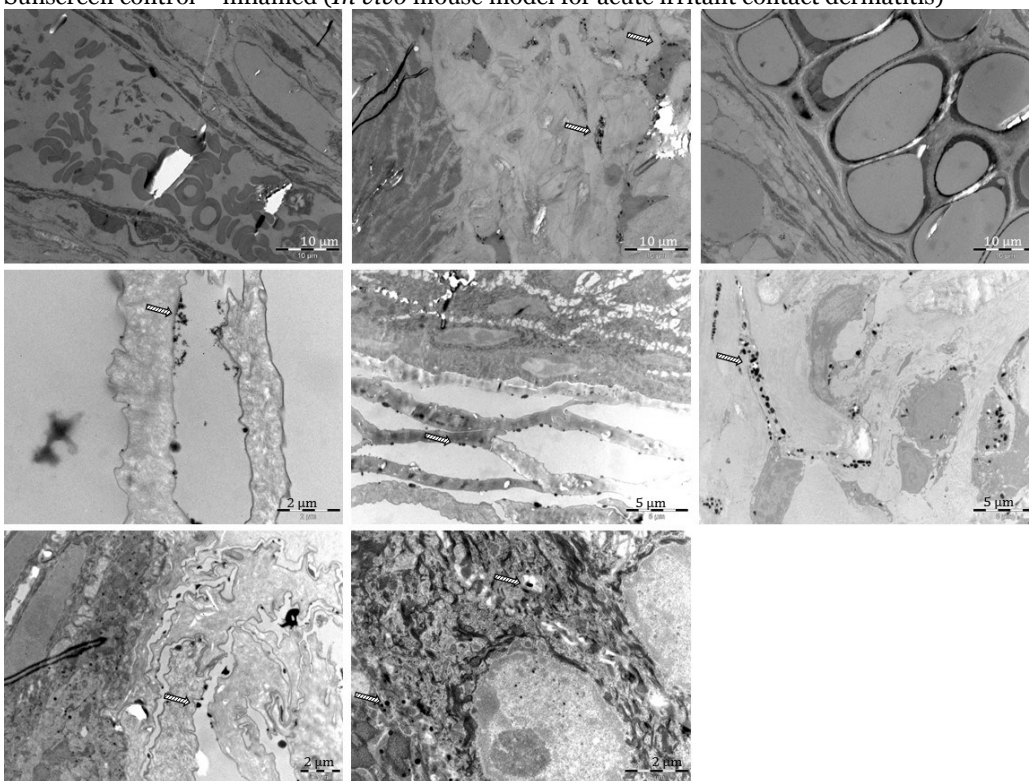
Negative control – inflamed (*In vivo* mouse model for acute irritant contact dermatitis)



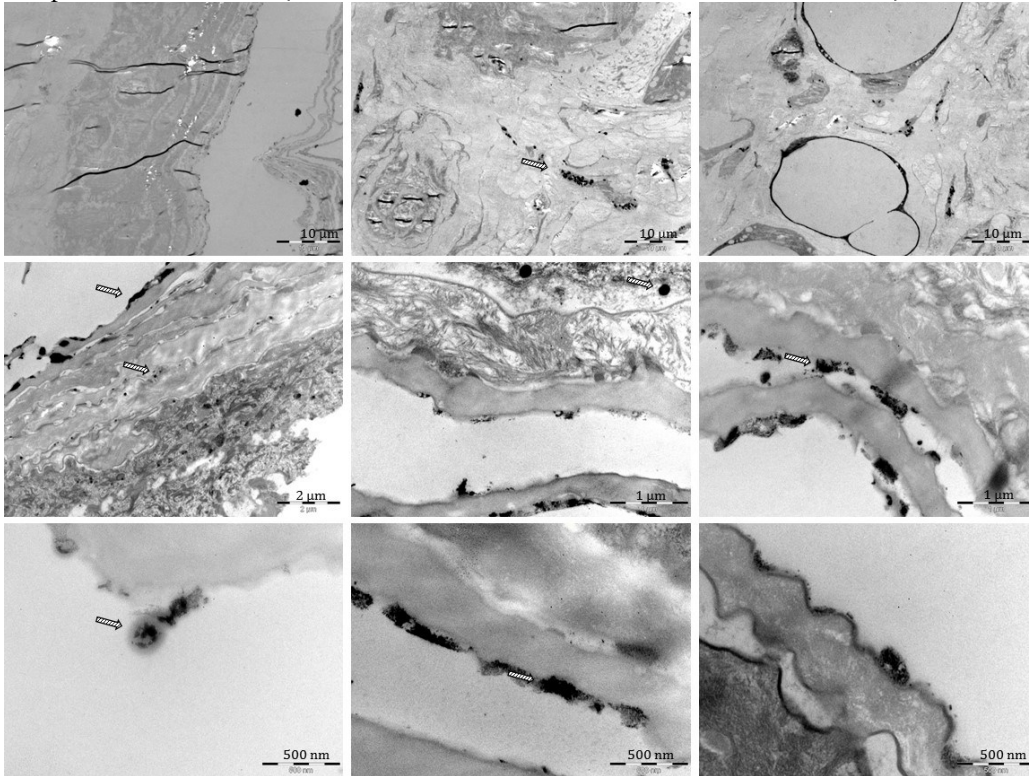
Sunscreen control – non-inflamed (*In vivo* mouse model for acute irritant contact dermatitis)



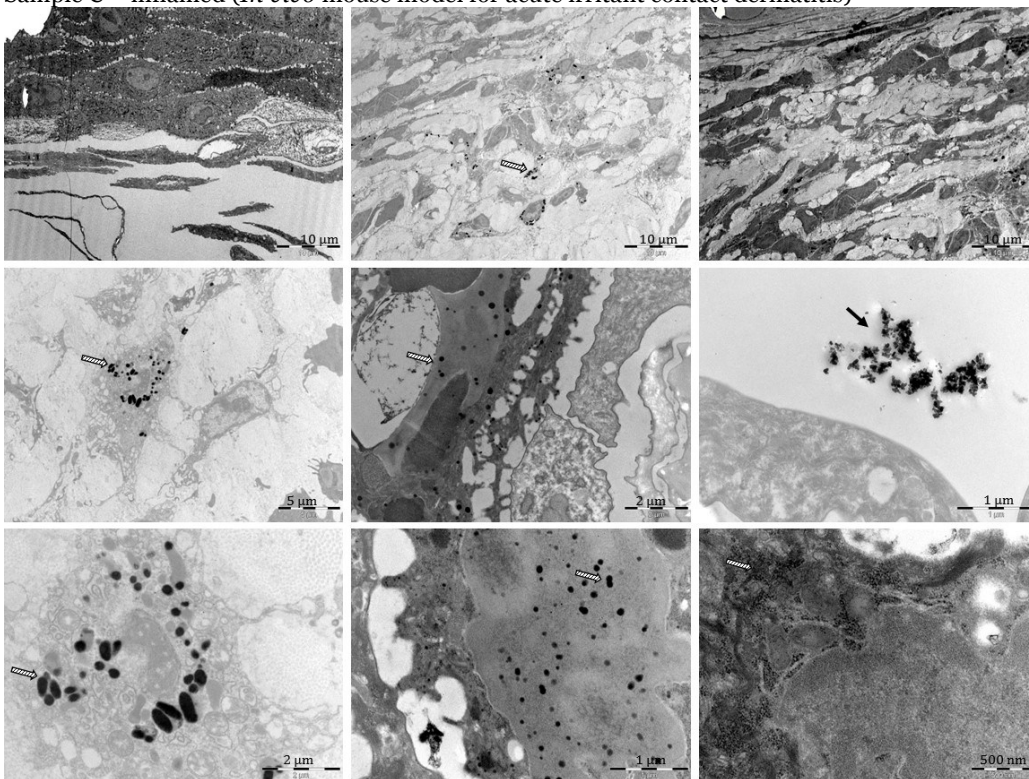
Sunscreen control – inflamed (*In vivo* mouse model for acute irritant contact dermatitis)



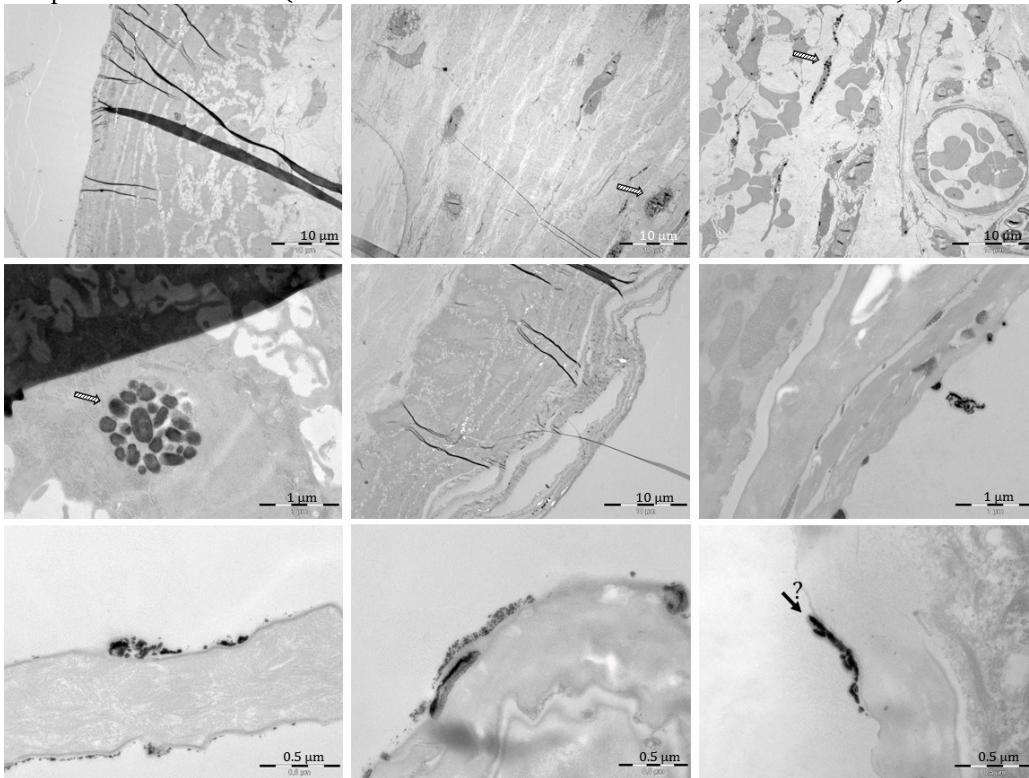
Sample C – non-inflamed (*In vivo* mouse model for acute irritant contact dermatitis)



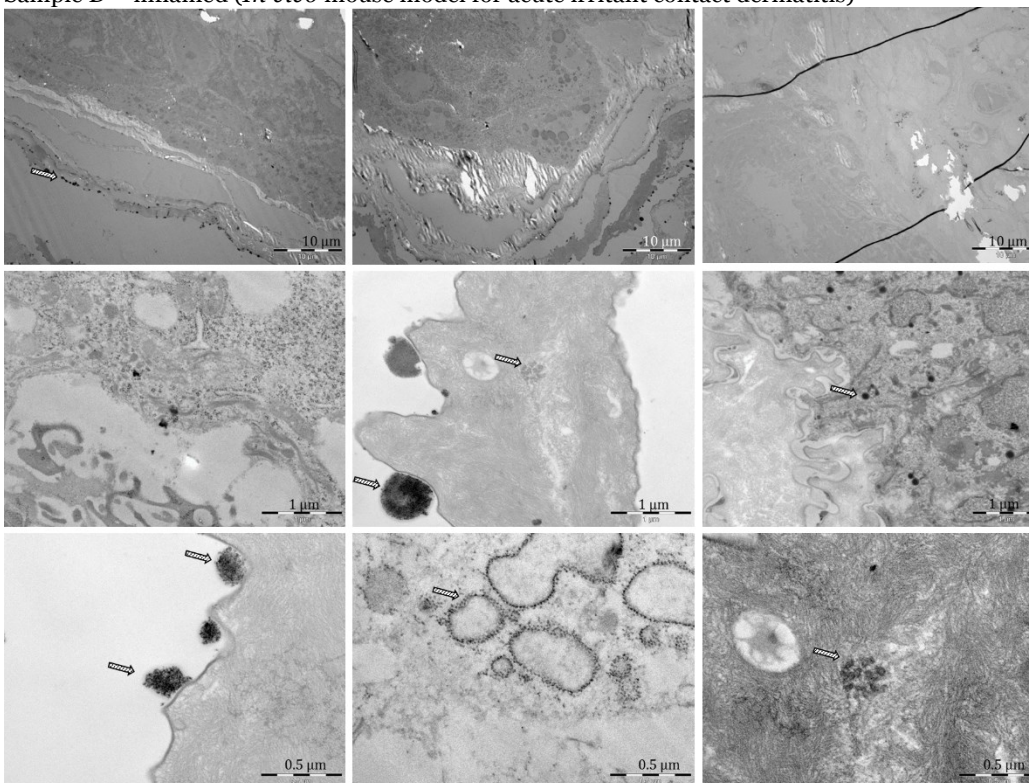
Sample C – inflamed (*In vivo* mouse model for acute irritant contact dermatitis)



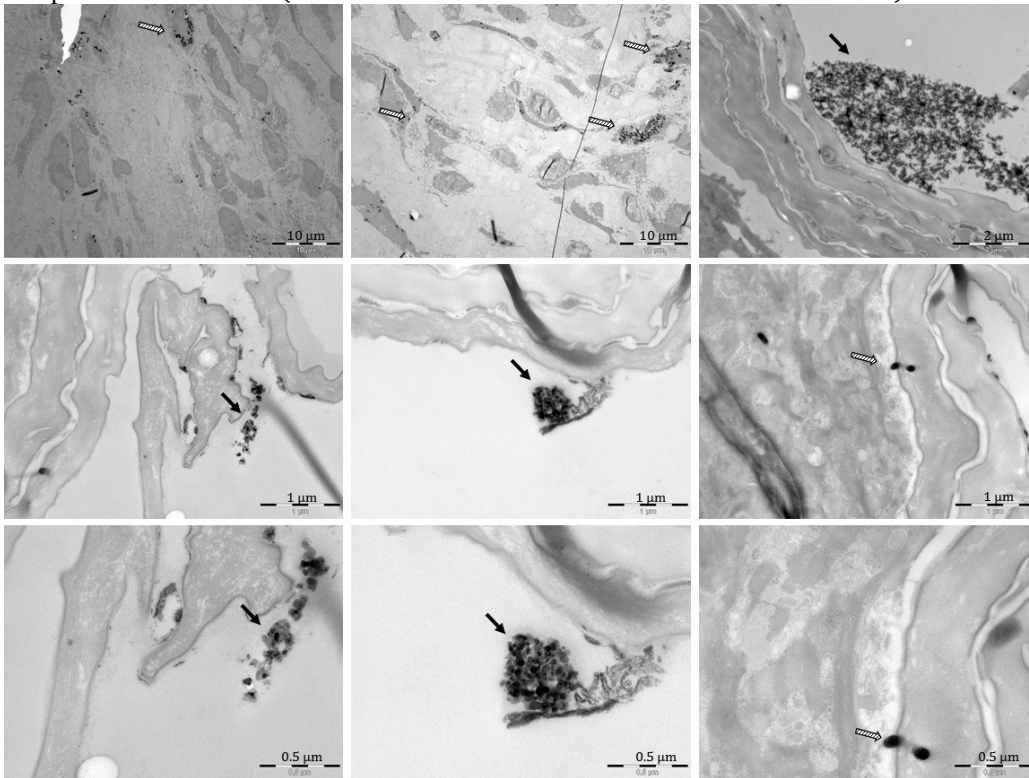
Sample D – non-inflamed (*In vivo* mouse model for acute irritant contact dermatitis)



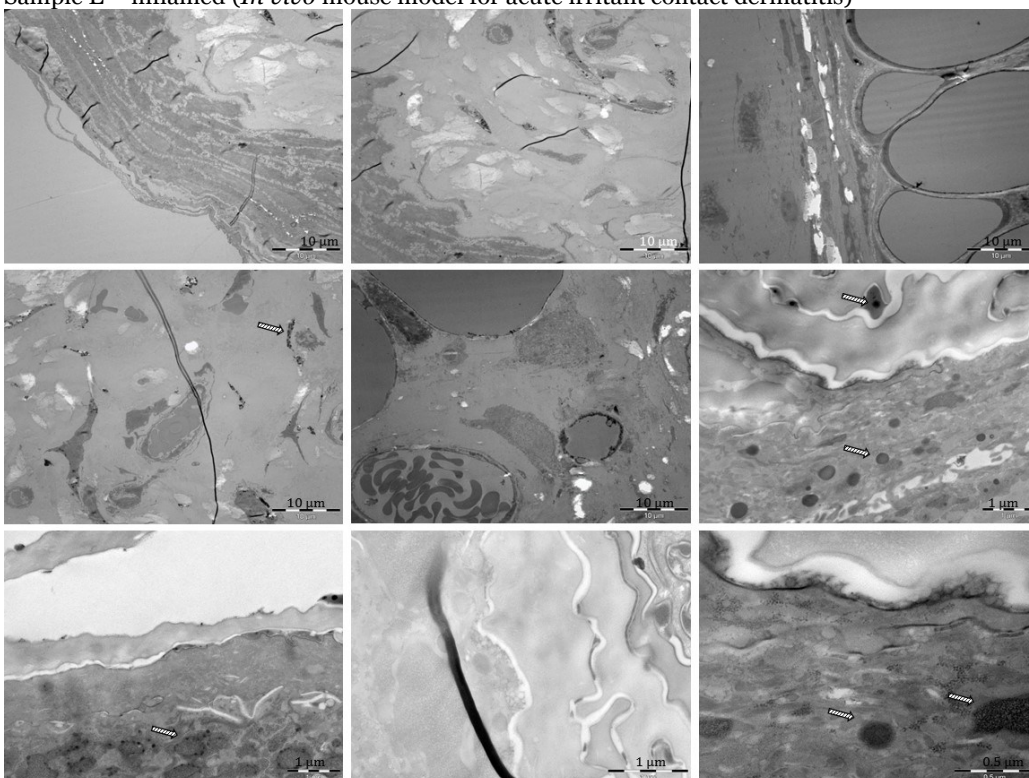
Sample D – inflamed (*In vivo* mouse model for acute irritant contact dermatitis)



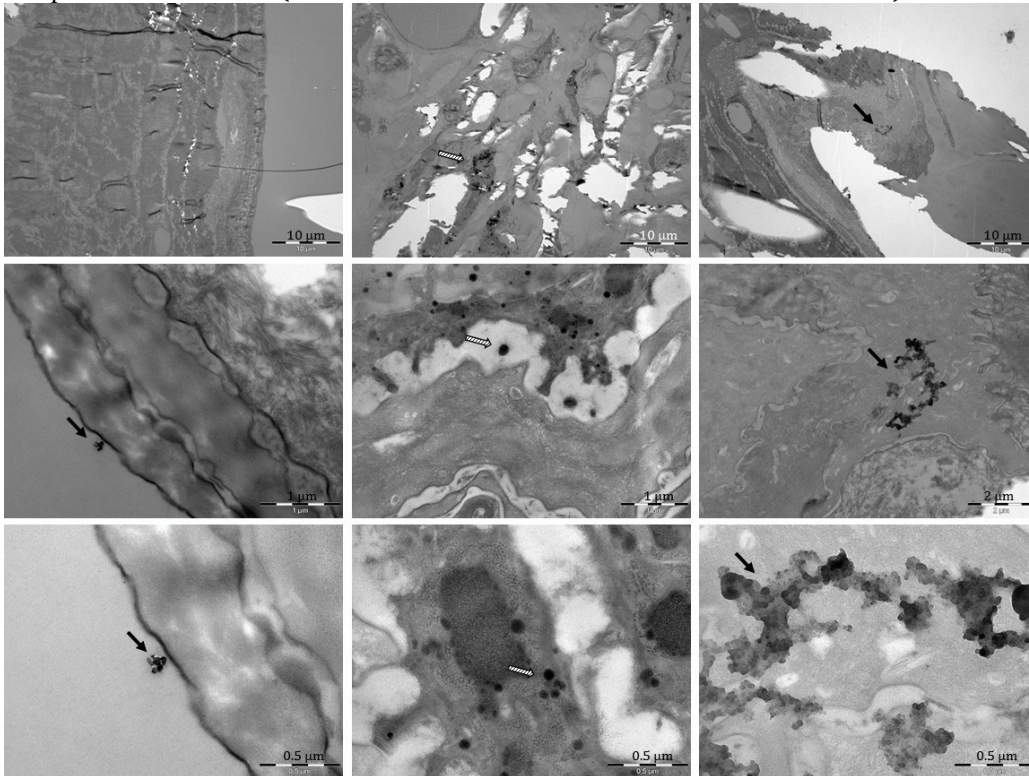
Sample E – non-inflamed (*In vivo* mouse model for acute irritant contact dermatitis)



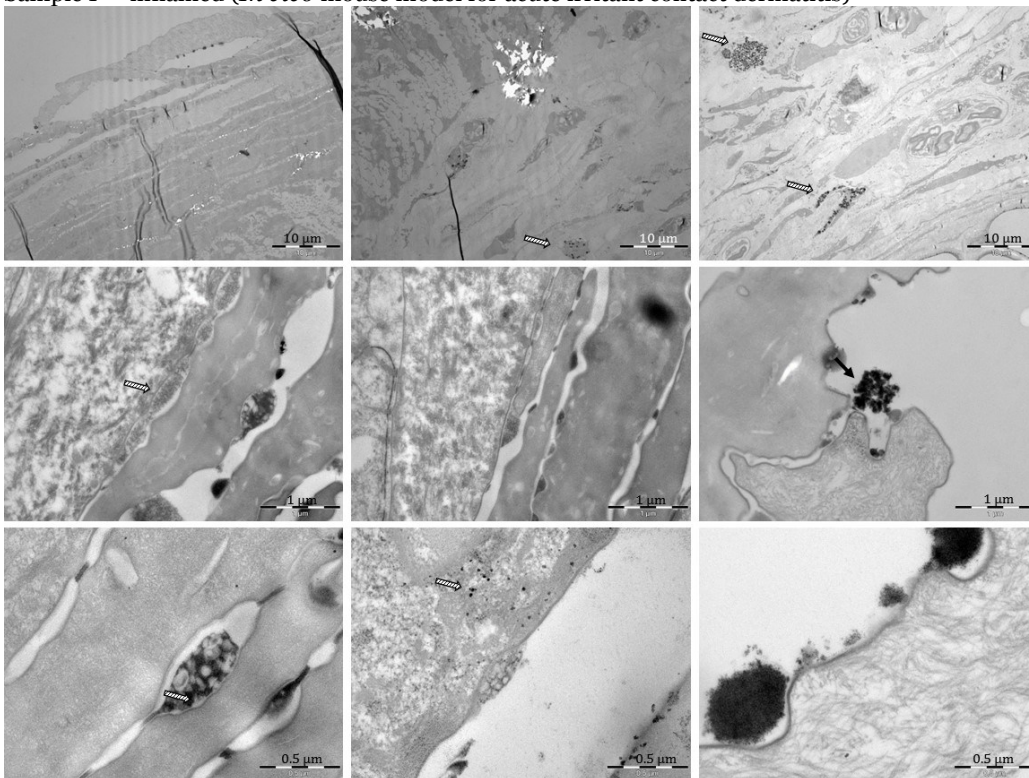
Sample E – inflamed (*In vivo* mouse model for acute irritant contact dermatitis)

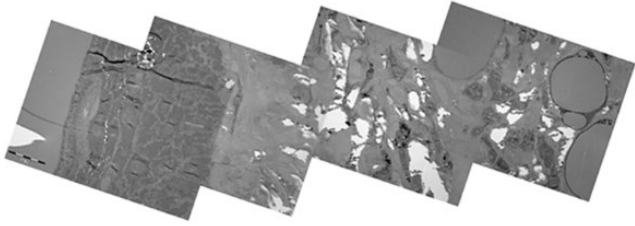


Sample F – non-inflamed (*In vivo* mouse model for acute irritant contact dermatitis)

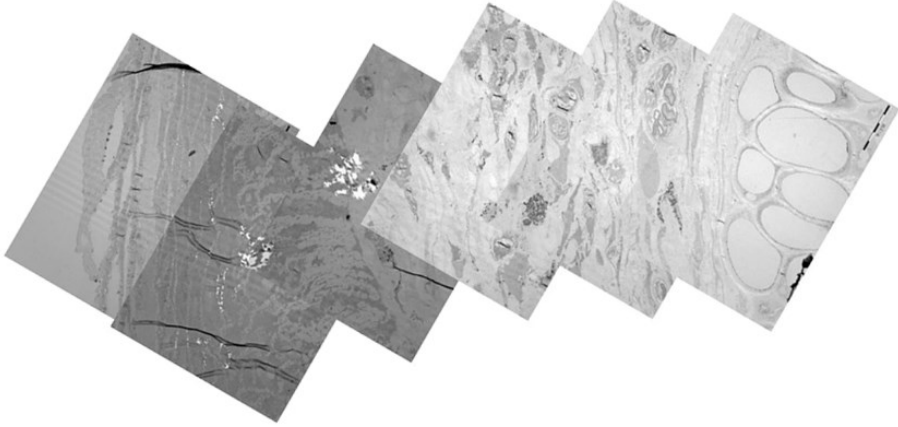


Sample F – inflamed (*In vivo* mouse model for acute irritant contact dermatitis)





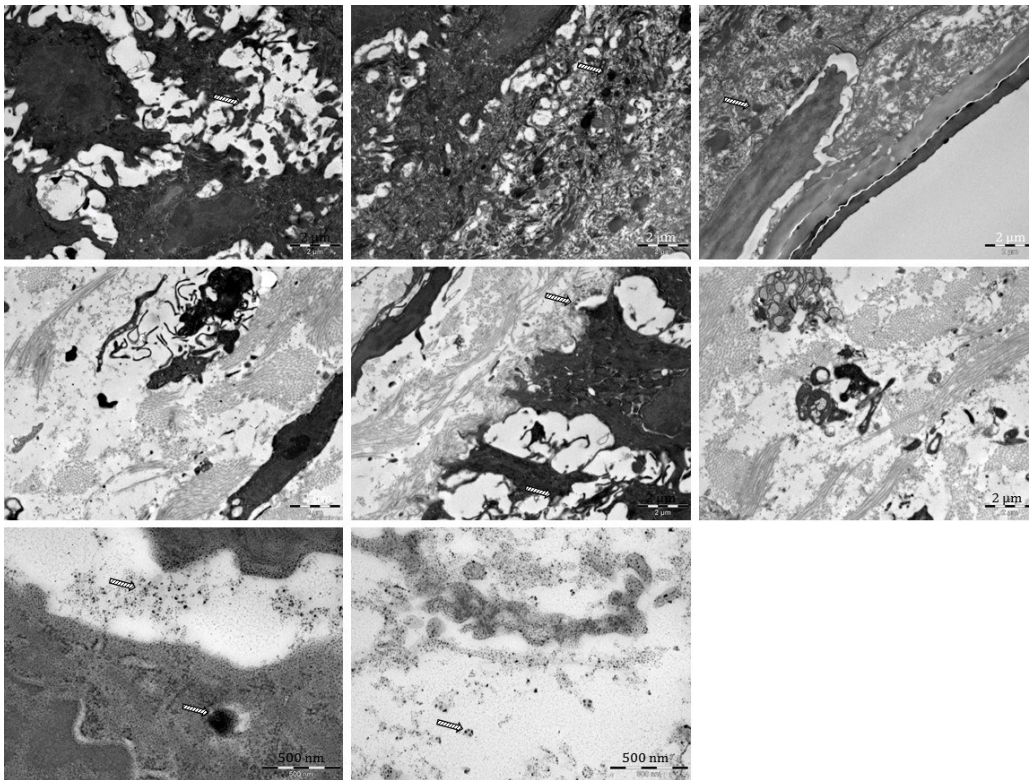
Acetone – non-inflamed



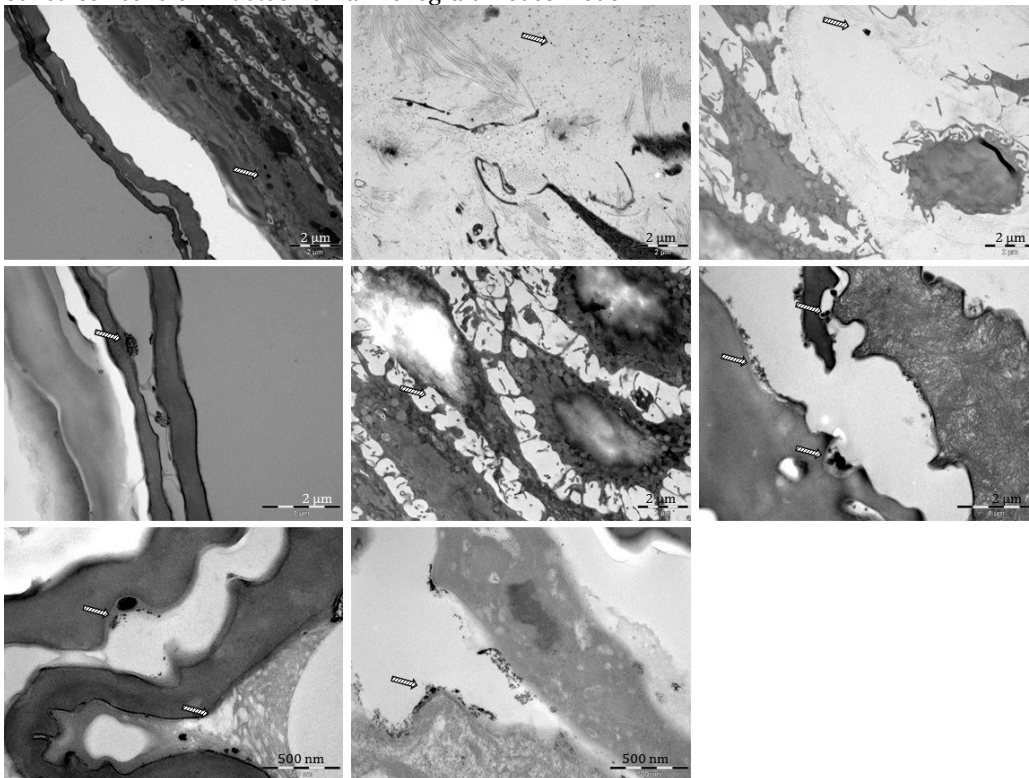
TPA inflamed

In vivo human xenograft mouse model

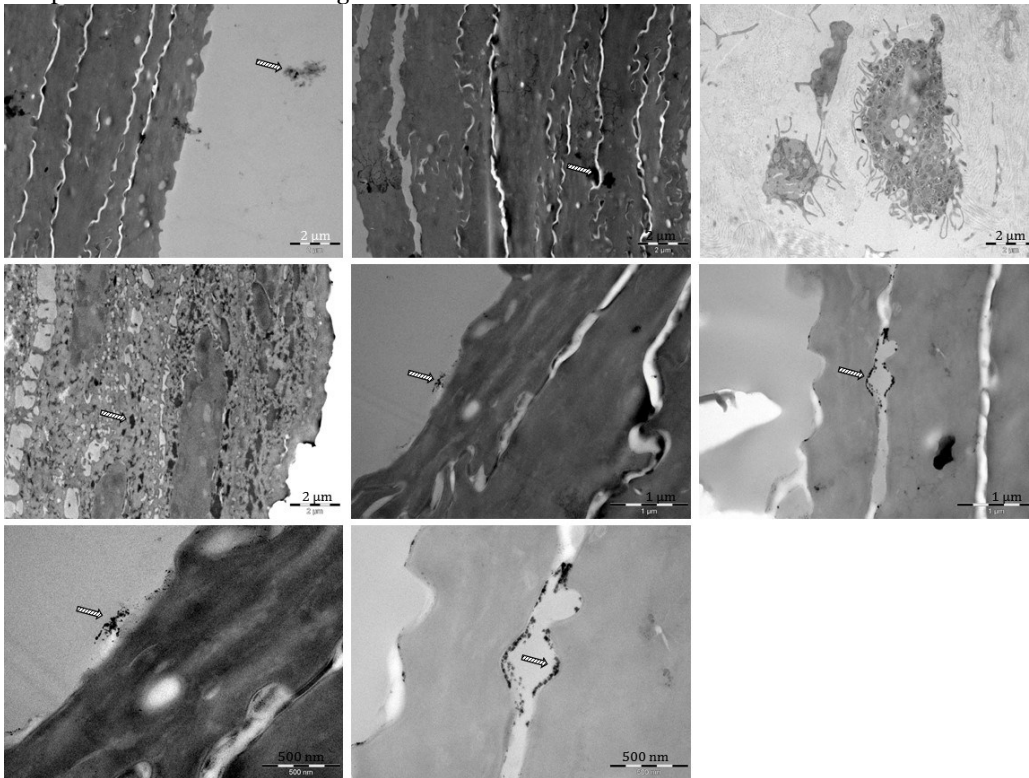
Negative control - *In vivo* human xenograft mouse model



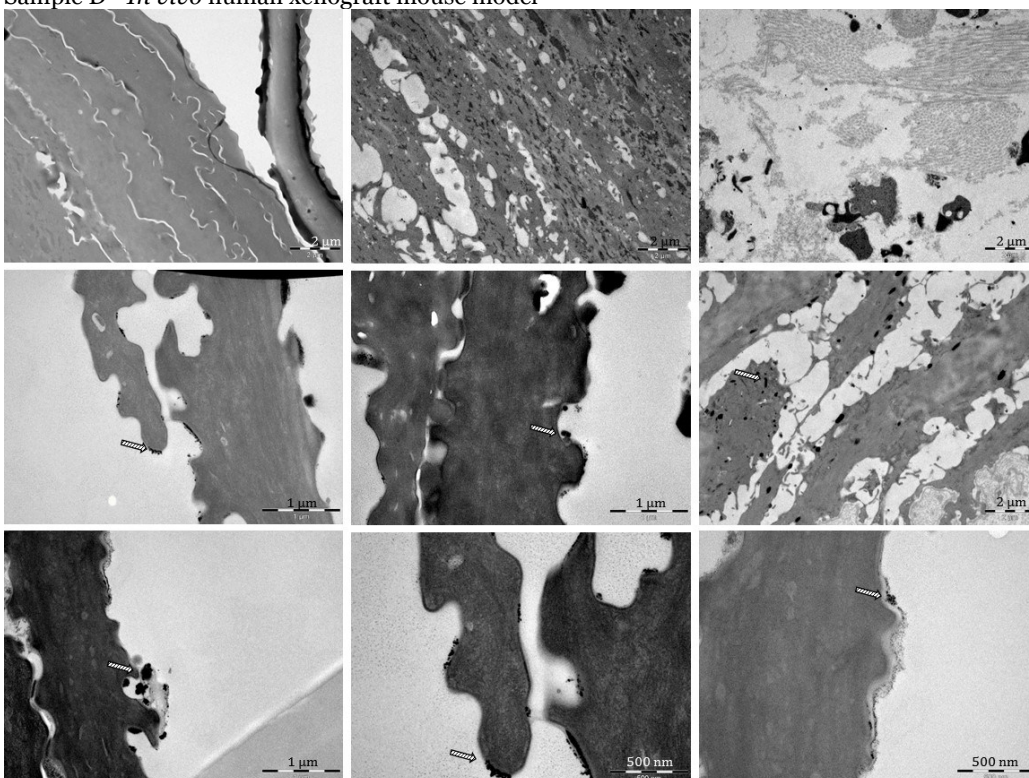
Sunscreen control - *In vivo* human xenograft mouse model



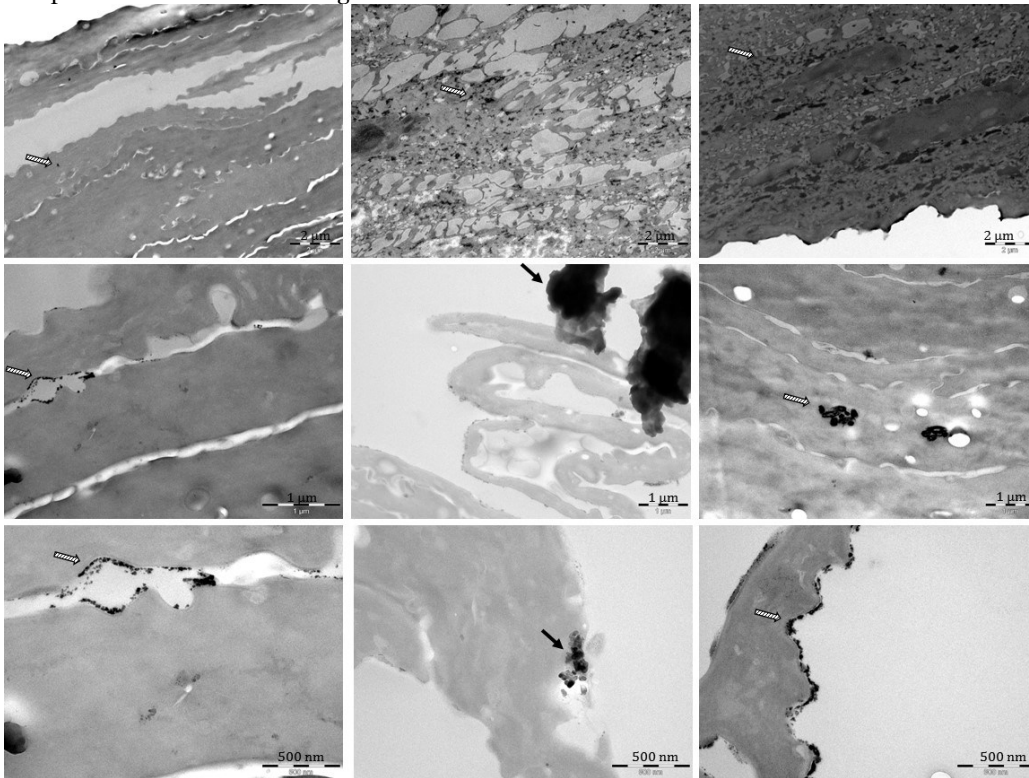
Sample C - *In vivo* human xenograft mouse model



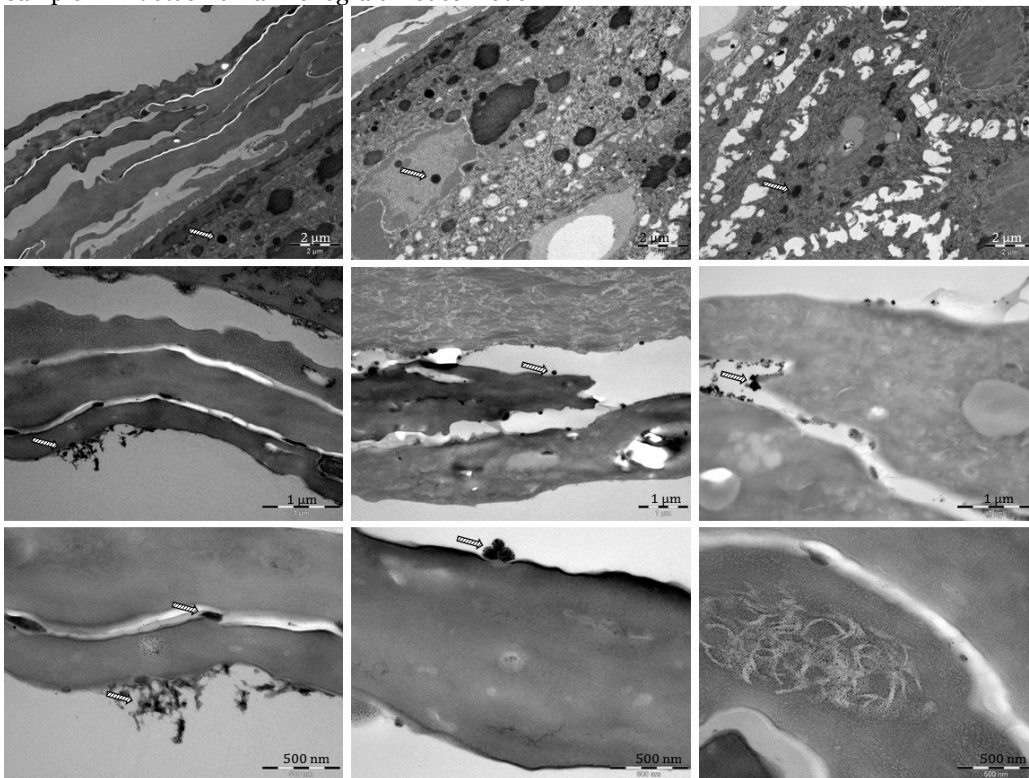
Sample D - *In vivo* human xenograft mouse model



Sample E - *In vivo* human xenograft mouse model



Sample F - *In vivo* human xenograft mouse model



Appendix 3: Weight and ear thickness in *in vivo* mouse model for acute irritant contact dermatitis after exposure to sunscreen with or without nanoparticles

		Day 1			Day 2			Day 3			Day 4			Day 8		
		Ear thickness			Ear thickness			Ear thickness			Ear thickness			Ear thickness		
Sunscreen	Treatment	Left	Right	Weight												
	TPA		0,21	0,22	20,10	0,56	0,50	21,20	0,60	0,58	20,50	0,57	0,64	20,50	0,49	0,45
		0,21	0,22	21,40	0,56	0,53	22,00	0,63	0,66	22,00	0,61	0,72	22,20	0,53	0,56	21,30
		0,21	0,22	21,60	0,58	0,70	21,40	0,53	0,69	22,00	0,54	0,64	22,10	0,48	0,52	21,10
Mean			0,22	21,03		0,57	21,53		0,62	21,50		0,62	21,60		0,51	20,90
SD			0,01	0,81		0,07	0,42		0,06	0,87		0,06	0,95		0,04	0,53
SEM			0,002	0,470		0,028	0,240		0,023	0,500		0,026	0,551		0,016	0,306
Untreated	Ace	0,22	0,22	22,80	0,22	0,22	23,10	0,23	0,22	22,30	0,22	0,22	23,00	0,24	0,22	22,80
	Ace	0,21	0,21	18,40	0,21	0,21	18,20	0,21	0,22	18,20	0,21	0,21	18,50	0,21	0,21	17,90
	Ace	0,22	0,22	23,30	0,22	0,22	22,90	0,23	0,23	23,00	0,22	0,21	23,30	0,21	0,21	22,30
	Mean		0,22	21,50		0,22	21,40		0,22	21,17		0,22	21,60		0,22	21,00
	SD		0,01	2,70		0,01	2,77		0,01	2,59		0,01	2,69		0,01	2,70
	SEM		0,002	1,557		0,002	1,601		0,003	1,497		0,002	1,552		0,005	1,557

		Day 1			Day 2			Day 3			Day 4			Day 8		
		Ear thickness			Ear thickness			Ear thickness			Ear thickness			Ear thickness		
Sunscreen	Treatment	Left	Right	Weight												
		TPA	0,22	0,22	23,60	0,66	0,67	23,30	0,56	0,46	21,90	0,61	0,50	21,90	0,99	0,87
	TPA	0,22	0,22	19,50	0,44	0,59	20,20	0,38	0,48	17,90	0,70	0,66	18,40	0,82	0,83	20,60
	TPA	0,22	0,21	21,30	0,46	0,74	21,60	0,41	0,58	19,80	0,55	0,47	19,40	1,25	0,98	21,70
	Mean		0,22	21,47		0,59	21,70		0,48	19,87		0,58	19,90		0,96	21,97
	SD		0,00	2,06		0,12	1,55		0,08	2,00		0,09	1,80		0,16	1,52
	SEM		0,002	1,186		0,049	0,896		0,032	1,155		0,037	1,041		0,066	0,876
B: Vehicle	Ace	0,21	0,23	23,00	0,21	0,22	23,60	0,21	0,22	20,60	0,22	0,23	21,90	0,60	0,64	23,20
	Ace	0,22	0,22	22,30	0,22	0,22	22,70	0,22	0,23	19,70	0,23	0,24	20,50	0,55	0,68	21,40
	Ace	0,23	0,24	22,40	0,22	0,22	22,70	0,24	0,27	21,40	0,22	0,23	21,70	0,60	0,58	22,50
	Mean		0,23	22,57		0,22	23,00		0,23	20,57		0,23	21,37		0,61	22,37
	SD		0,01	0,38		0,00	0,52		0,02	0,85		0,01	0,76		0,05	0,91
	SEM		0,004	0,219		0,002	0,300		0,009	0,491		0,003	0,437		0,019	0,524

		Day 1			Day 2			Day 3			Day 4			Day 8		
		Ear thickness			Ear thickness			Ear thickness			Ear thickness			Ear thickness		
Suns cree n	Treat ment	Left	Right	Weight												
		TPA	0,21	0,21	22,60	0,47	0,52	23,10	0,38	0,40	21,60	0,47	0,48	21,50	1,08	1,47
	TPA	0,22	0,22	21,50	0,53	0,48	21,20	0,38	0,38	20,20	0,54	0,73	20,10	0,99	1,14	21,90
	TPA	0,22	0,22	21,90	0,64	0,60	22,40	0,43	0,41	19,20	0,64	0,53	20,00	1,53	0,99	22,20
	Mean		0,22	22,00		0,54	22,23		0,40	20,33		0,57	20,53		1,20	22,53
	SD		0,01	0,56		0,07	0,96		0,02	1,21		0,10	0,84		0,24	0,85
	SEM		0,002	0,321		0,027	0,555		0,008	0,696		0,041	0,484		0,098	0,491
C: TiO ₂ 30 nm	Ace	0,22	0,23	21,70	0,22	0,23	21,50	0,22	0,22	19,70	0,23	0,23	20,20	0,69	0,52	22,10
	Ace	0,23	0,22	22,00	0,22	0,22	22,50	0,22	0,22	20,70	0,22	0,22	20,80	0,62	0,53	21,70
	Ace	0,21	0,20	21,50	0,21	0,21	22,40	0,21	0,21	19,90	0,22	0,20	19,00	0,68	0,64	22,00
	Mean		0,22	21,73		0,22	22,13		0,22	20,10		0,22	20,00		0,61	21,93
	SD		0,01	0,25		0,01	0,55		0,01	0,53		0,01	0,92		0,07	0,21
	SEM		0,005	0,145		0,003	0,318		0,002	0,306		0,004	0,529		0,030	0,120

		Day 1			Day 2			Day 3			Day 4			Day 8		
		Ear thickness			Ear thickness			Ear thickness			Ear thickness			Ear thickness		
Suns cree n	Treat ment	Left	Right	Weight												
		TPA	0,22	0,23	22,70	0,50	0,83	22,60	0,37	0,53	20,10	0,58	0,58	20,90	0,88	1,34
	TPA	0,21	0,23	20,10	0,69	0,68	20,70	0,40	0,48	18,20	0,46	0,52	18,30	0,99	0,73	20,70
	TPA	0,21	0,23	23,50	0,76	0,80	23,80	0,50	0,53	23,20	0,52	0,67	22,70	1,23	0,98	24,20
	Mean		0,22	22,10		0,71	22,37		0,47	20,50		0,56	20,63		1,03	22,70
	SD		0,01	1,78		0,12	1,56		0,07	2,52		0,07	2,21		0,22	1,80
	SEM		0,004	1,026		0,048	0,902		0,028	1,457		0,029	1,277		0,092	1,041
D: TiO ₂ 100 nm	Ace	0,22	0,22	21,00	0,22	0,23	21,30	0,24	0,25	19,60	0,24	0,31	19,90	0,75	0,64	22,50
	Ace	0,22	0,23	23,40	0,21	0,21	23,70	0,22	0,21	22,20	0,27	0,29	21,70	0,77	0,51	24,90
	Ace	0,21	0,23	21,10	0,21	0,22	20,60	0,22	0,22	18,20	0,25	0,27	18,70	0,74	0,69	20,80
	Mean		0,22	21,83		0,22	21,87		0,23	20,00		0,27	20,10		0,68	22,73
	SD		0,01	1,36		0,01	1,63		0,02	2,03		0,03	1,51		0,10	2,06
	SEM		0,003	0,784		0,003	0,939		0,006	1,172		0,010	0,872		0,040	1,189

		Day 1			Day 2			Day 3			Day 4			Day 8		
		Ear thickness			Ear thickness			Ear thickness			Ear thickness			Ear thickness		
Sunscre n	Treat ment	Left	Right	Weight												
		TPA	0,21	0,22	21,20	0,60	0,79	21,40	0,38	0,49	18,60	0,74	0,89	19,10	0,98	0,73
	TPA	0,21	0,22	20,90	0,53	0,82	21,10	0,36	0,63	20,00	0,48	0,57	19,10	0,74	0,98	21,40
	TPA	0,21	0,22	20,40	0,64	0,74	21,00	0,46	0,59	18,10	0,56	0,51	18,60	1,43	0,95	22,00
	Mean		0,22	20,83		0,69	21,17		0,49	18,90		0,63	18,93		0,97	21,77
	SD		0,01	0,40		0,11	0,21		0,11	0,98		0,16	0,29		0,25	0,32
	SEM		0,002	0,233		0,047	0,120		0,044	0,569		0,065	0,167		0,104	0,186
E: TiO ₂ silicone	Ace	0,22	0,22	21,70	0,22	0,22	21,80	0,23	0,23	19,20	0,28	0,23	19,40	0,76	0,70	20,90
	Ace	0,23	0,23	21,50	0,23	0,22	21,30	0,22	0,22	19,30	0,22	0,34	19,90	0,58	0,83	21,10
	Ace	0,21	0,21	21,00	0,21	0,22	22,50	0,21	0,22	18,90	0,21	0,28	18,60	0,58	0,76	21,10
	Mean		0,22	21,40		0,22	21,87		0,22	19,13		0,26	19,30		0,70	21,03
	SD		0,01	0,36		0,01	0,60		0,01	0,21		0,05	0,66		0,10	0,12

SEM 0,004 0,208 0,003 0,348 0,003 0,120 0,020 0,379 0,042 0,067

		Day 1			Day 2			Day 3			Day 4			Day 8		
		Ear thickness			Ear thickness			Ear thickness			Ear thickness			Ear thickness		
Suns cree n	Treat ment	Left	Right	Weight												
		TPA	0,23	0,23	21,70	0,64	0,69	22,20	0,45	0,38	19,70	0,66	0,63	19,20	1,28	1,02
	TPA	0,22	0,23	20,20	0,40	0,60	20,10	0,47	0,46	18,10	0,72	0,62	17,90	0,99	1,03	20,00
	TPA	0,22	0,22	20,90	0,78	0,76	21,90	0,43	0,46	19,30	0,64	0,53	19,30	1,26	1,04	20,10
	Mean		0,23	20,93		0,65	21,40		0,44	19,03		0,63	18,80		1,10	20,77
	SD		0,01	0,75		0,14	1,14		0,03	0,83		0,06	0,78		0,13	1,24
	SEM		0,002	0,433		0,056	0,656		0,014	0,481		0,025	0,451		0,053	0,717
F: TiO ₂ alumina	Ace	0,22	0,22	22,30	0,22	0,23	22,80	0,22	0,22	20,20	0,27	0,28	20,90	0,73	0,74	22,40
	Ace	0,21	0,22	21,40	0,21	0,22	21,30	0,21	0,22	19,40	0,27	0,25	19,90	0,74	0,72	22,20
	Ace	0,21	0,22	21,00	0,20	0,22	20,50	0,23	0,23	19,50	0,27	0,26	19,30	0,85	0,64	21,90
	Mean		0,22	21,57		0,22	21,53		0,22	19,70		0,27	20,03		0,74	22,17

SD	0,01	0,67	0,01	1,17	0,01	0,44	0,01	0,81	0,07	0,25
SEM	0,002	0,384	0,004	0,674	0,003	0,252	0,004	0,467	0,027	0,145

Appendix 4: Weight measurements in *in vivo* human xenograft skin model

		Day 1	Day 2	Day 3	Day 8	Comments
Sample	Mus	Weight	Weight	Weight	Weight	
Untreated	1	19.7	20	20.1	20	
	2	21.7	21.6	22.1	22.2	
	3	18.9	19.2	18.5	17.9	NB: Graft rejected
		Day 1	Day 2	Day 3	Day 8	Applied cream absorbed after 15 min.
Sample	Mus	Weight	Weight	Weight	Weight	
B: Vehicle	1	20.3	20.6	20.6	20.5	Removed collar between day 2 and 3
	2	21.6	20.8	20	20.5	
	3	18.3	18.5	18.8	19.2	NB: Graft rejected
		Day 1	Day 2	Day 3	Day 8	Cream dried out after 24 hours
Sample	Mus	Weight	Weight	Weight	Weight	
C: TiO₂ 30 nm	1	20.2	19	18.6	18.3	
	2	20.9	19.8	19.6	20.2	
	3	20.8	21	20.5	20.9	

		Day 1	Day 2	Day 3	Day 8	
						Cream dried out after 24 hours
Sample	Mus	Weight	Weight	Weight	Weight	
D: TiO₂ 100 nm	1	21.6	20.6	20.5	20.3	Removed collar between day 6 and 7
	2	20.3	19.3	19.1	19.8	Removed collar between day 6 and 7
	3	19.4	18.4	18.2	18.6	

		Day 1	Day 2	Day 3	Day 8	
						Cream dried out after 24 hours
Sample	Mus	Weight	Weight	Weight	Weight	
E: TiO₂ silicone	1	20.3	20.2	19.7	19.8	
	2	19.9	18.1	18.7	18.8	Removed collar between day 7 and 8
	3	22.6	21.3	21.1	22.1	

		Day 1	Day 2	Day 3	Day 8	
						Cream dried out after 24 hours
Sample	Mus	Weight	Weight	Weight	Weight	
F: TiO₂ alumina	1	21.3	20.4	20	21.7	
	2	21.3	20.3	20.1	20.3	
	3	20.2	18.5	19.4	19.6	Removed collar between day 7 and 8

Appendix 5: ICP-MS measurement data of medium below *in vitro* EpiDerm skin models and TEER of the tissues after 20h of exposure

Table A5.1: ICP-MS data for pooled medium of three EpiDerm skin model tissues taken directly after 20h exposure

Due to the high salt concentration of the medium the concentration for Ti had to be estimated (see materials and methods section). Therefore, also for the DMEM control a concentration of Ti is given although no Ti is present in these samples. The highest estimated Ti concentration for samples that do not contain Ti is 1.5. Samples that are above this value are marked with red.

Experiment	Sample	NP type	Upper limit for Ti [µg/L] measured	Ca [µg/L]	Zn [µg/L]	Ti [µg/L] estimated
	MilliQ water		0.04	73	0	0.0
	DMEM		2.21	52768	18	0.7
	DMEM		2.28	54053	18	0.8
	DMEM		2.46	54731	19	0.9
	DMEM		2.02	49388	18	0.6
	DMEM		1.43	50476	18	0.0
	DMEM		2.07	49574	21	0.7
Experiment 1	A	DMEM control	3.06	75991	26	0.9
Experiment 2	A	DMEM control	2.79	74905	23	0.7
Experiment 3	A	DMEM control	3.65	78997	26	1.4
Experiment 1	B	Sunscreen control	2.18	74025	34	0.1
Experiment 2	B	Sunscreen control	2.42	76441	35	0.3
Experiment 3	B	Sunscreen control	3.26	79745	42	1.0
Experiment 1	C	TiO ₂	2.56	74140	35	0.5
Experiment 2	C	TiO ₂	2.63	73852	37	0.5
Experiment 3	C	TiO ₂	2.65	76980	41	0.5
Experiment 1	D	TiO ₂	3.22	71852	33	1.2
Experiment 2	D	TiO ₂	3.50	75510	34	1.4
Experiment 3	D	TiO ₂	3.80	79154	43	1.6
Experiment 1	E	TiO ₂	3.16	76485	34	1.0

Experiment 2	E	TiO ₂	3.61	77631	35	1.4
Experiment 3	E	TiO ₂	3.00	81624	37	0.7
Experiment 1	F	TiO ₂	3.57	74815	34	1.5
Experiment 2	F	TiO ₂	3.76	77119	36	1.6
Experiment 3	F	TiO ₂	5.28	78991	54	3.0
Experiment 1	G	TiO ₂	3.09	75571	32	0.9
Experiment 2	G	TiO ₂	3.18	75421	35	1.0
Experiment 3	G	TiO ₂	5.22	81134	42	2.9
Experiment 1	H	TiO ₂	3.63	74860	34	1.5
Experiment 2	H	TiO ₂	3.61	74389	35	1.5
Experiment 3	H	TiO ₂	3.96	80956	41	1.7
Experiment 1	I	ZnO	3.22	76065	2395	1.1
Experiment 2	I	ZnO	3.32	78385	2859	1.1
Experiment 3	I	ZnO	2.38	82117	2980	0.1
Experiment 1	K	ZnO	3.20	79099	2320	1.0
Experiment 2	K	ZnO	3.73	77618	1599	1.5
Experiment 3	K	ZnO	3.09	81242	3398	0.8

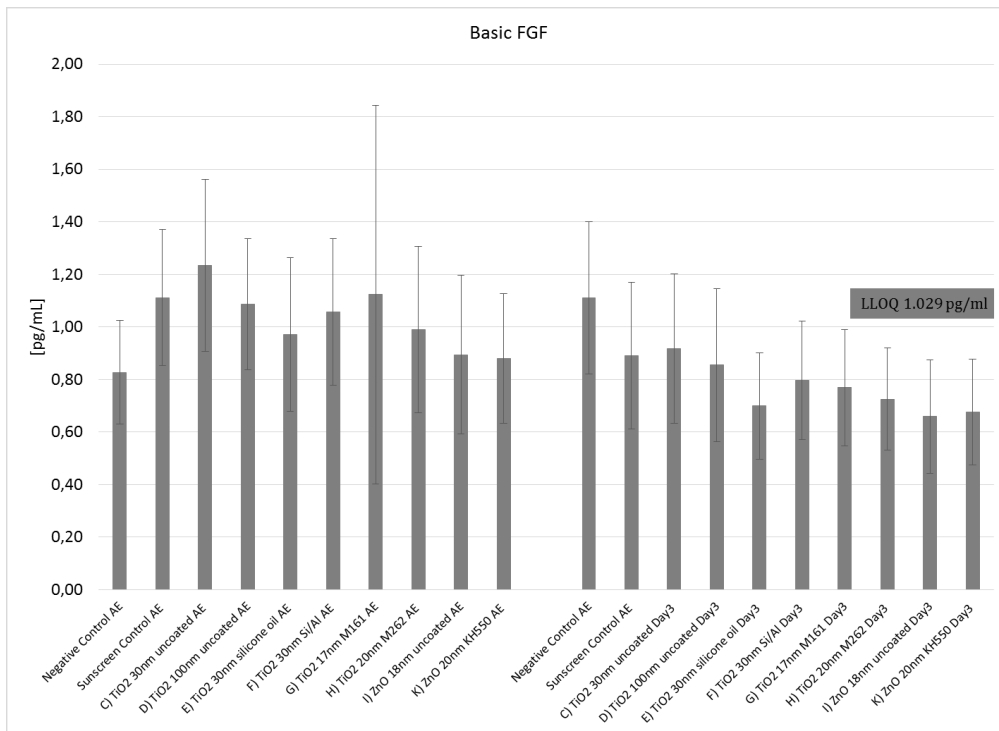
Table A5.2: TEER measurements of the tissues directly after 20h exposure, values below $510 \pm 120 \Omega/\text{cm}^2$ are considered as leaky and shown in red

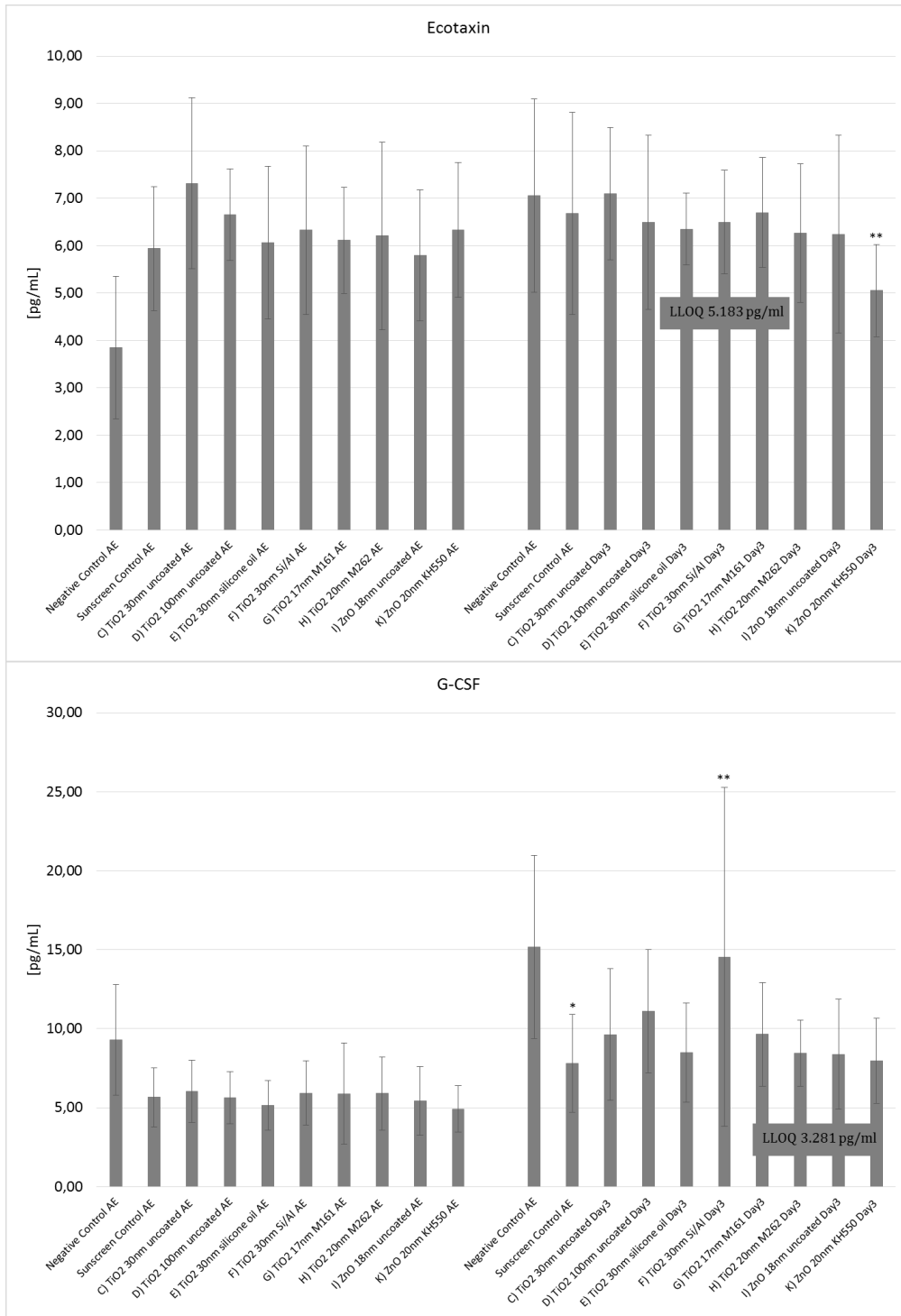
Sample	Sample code	TEER after 20h exposure [Ω/cm^2]		
		Exp 1	Exp 2	Exp 3
PBS		30	30	30
Membrane		102	101	101
Membrane		101	93	93
Negative Control 1	A)	1627	1256	1219
Negative Control 2	A)	1715	1360	1596
Negative Control 3	A)	1535	1421	1047
Sunscreen Control 1	B)	1013	872	465
Sunscreen Control 2	B)	682	884	745
Sunscreen Control 3	B)	953	880	487
TiO₂ 30nm uncoated 1	C)	670	827	663
TiO₂ 30nm uncoated 2	C)	922	859	538

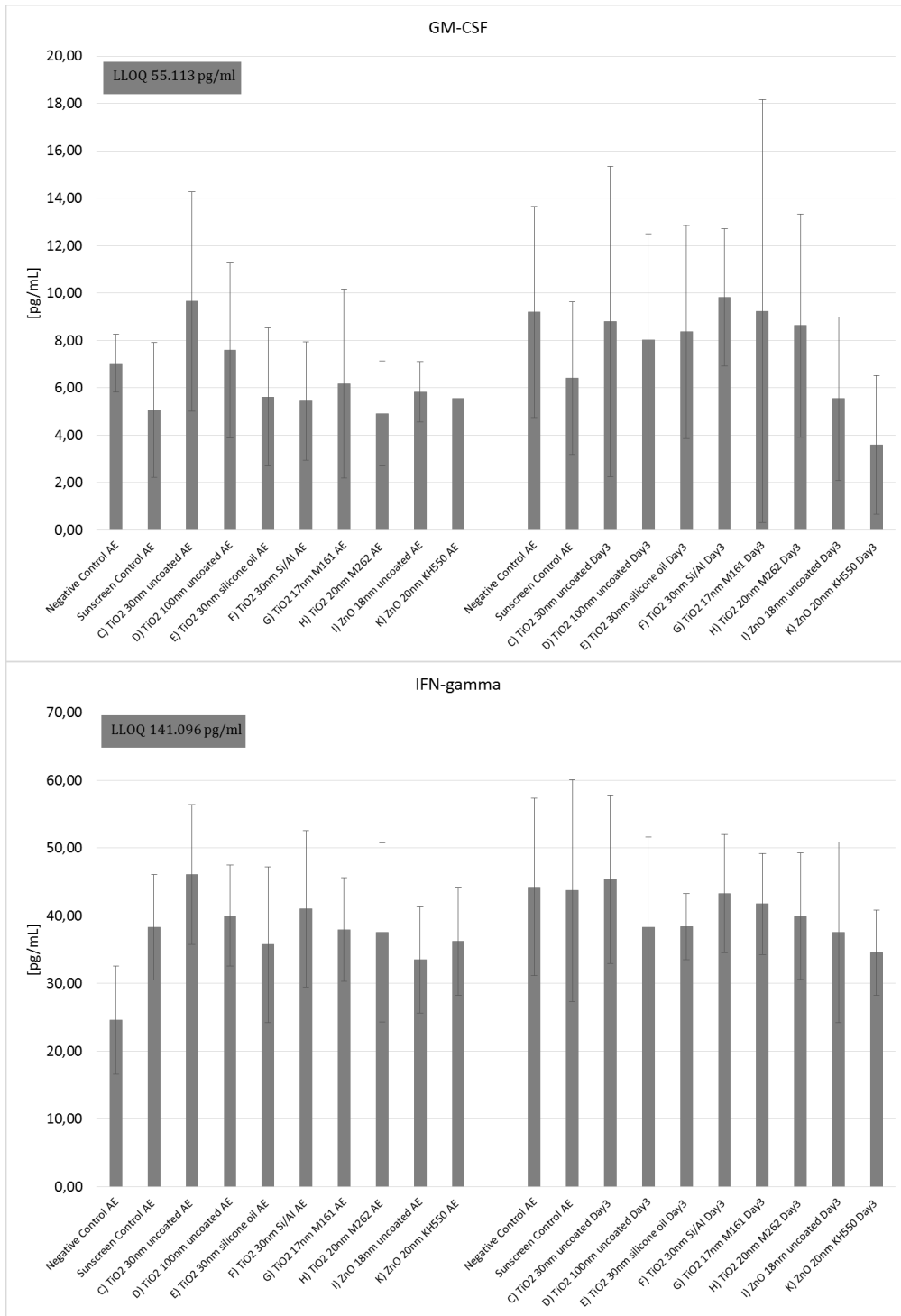
TiO₂ 30nm uncoated 3	C)	999	764	464
TiO₂ 100nm uncoated 1	D)	845	799	643
TiO₂ 100nm uncoated 2	D)	1051	530	464
TiO₂ 100nm uncoated 3	D)	781	752	810
TiO₂ 30nm, Silicone Oil 1	E)	947	890	1058
TiO₂ 30nm, Silicone Oil 2	E)	793	354	571
TiO₂ 30nm, Silicone Oil 3	E)	1253	657	1008
TiO₂ 30nm, Silicon/Al 1	F)	569	558	643
TiO₂ 30nm, Silicon/Al 2	F)	1136	1022	599
TiO₂ 30nm, Silicon/Al 3	F)	1019	513	641
TiO₂ 17nm M161 1	G)	643	527	743
TiO₂ 17nm M161 2	G)	1220	851	705
TiO₂ 17nm M161 3	G)	580	877	748
TiO₂ 20nm M262 1	H)	865	1003	844
TiO₂ 20nm M262 2	H)	835	640	976
TiO₂ 20nm M262 3	H)	622	755	799
ZnO 18nm uncoated 1	I)	433	497	532
ZnO 18nm uncoated 2	I)	859	688	694
ZnO 18nm uncoated 3	I)	1410	745	558
ZnO 20 nm KH550 1	K)	706	773	881
ZnO 20 nm KH550 2	K)	962	880	746
ZnO 20 nm KH550 3	K)	928	813	506

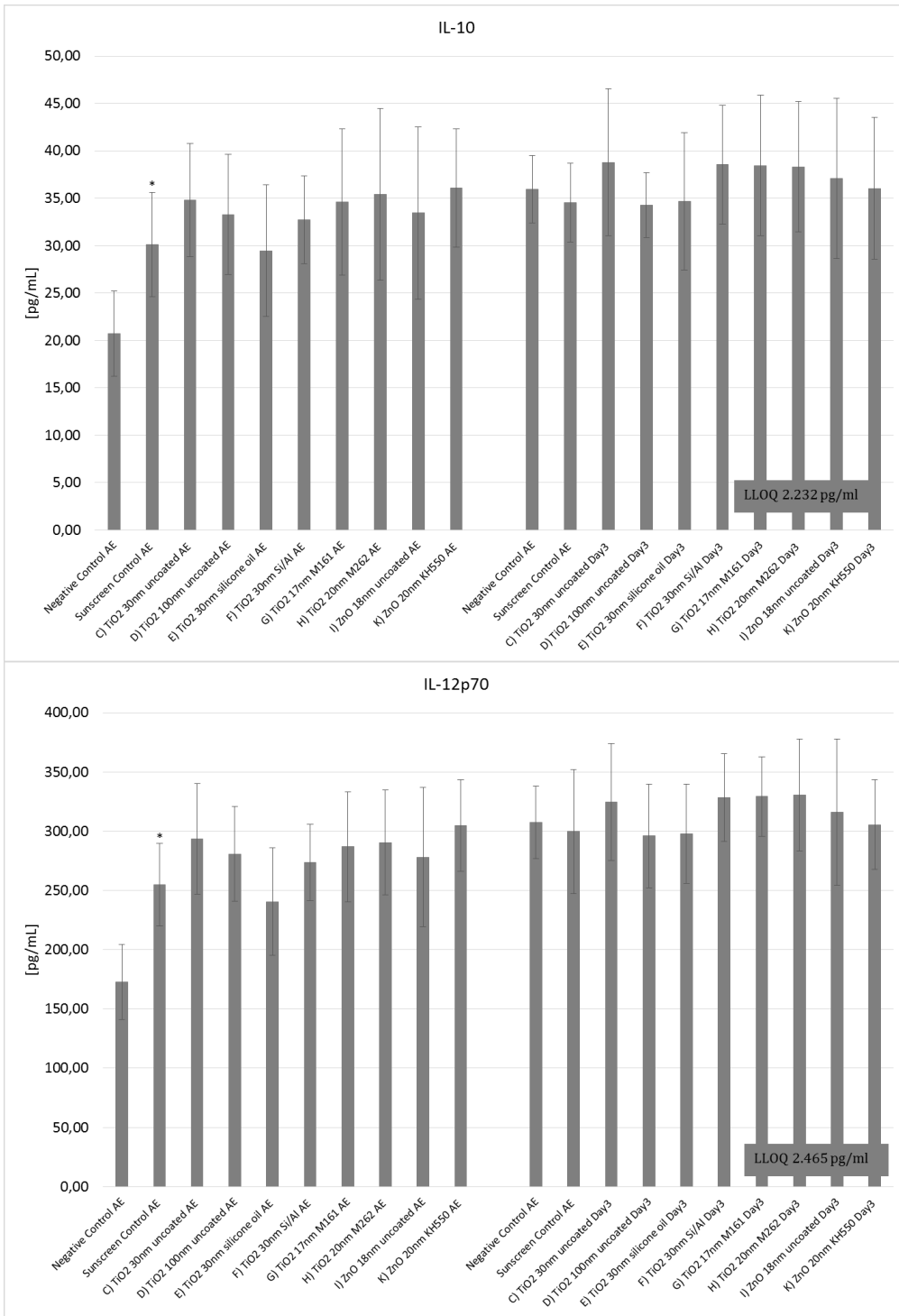
Appendix 6: Cytokine release of *in vitro* EpiDerm skin models after 20h exposure (AE) and 3 days after ended exposure

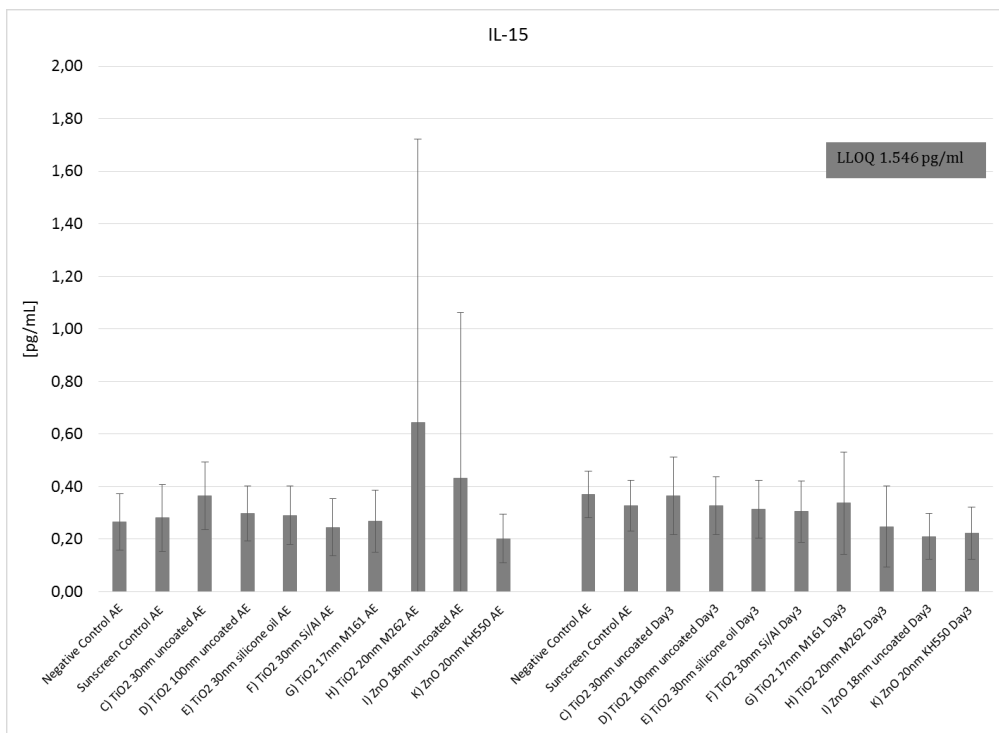
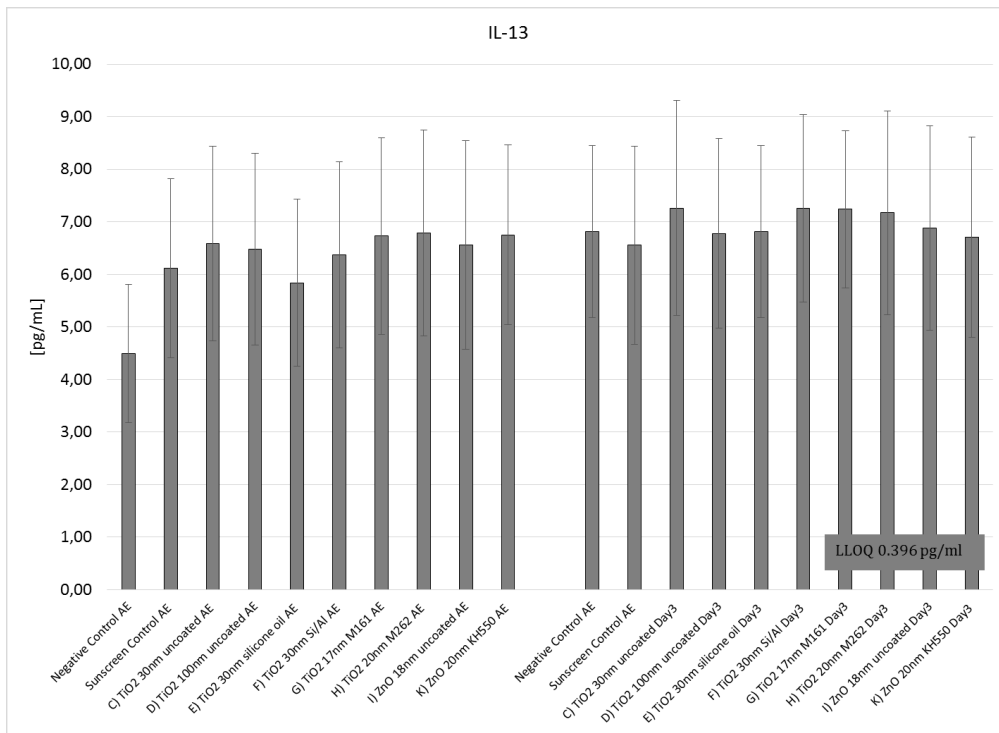
All graphs in Appendix 6 show the average of the cytokine release of nine independent EpiDerm skin models. Information on the Lower Limit of Quantification (LLOQ) is added for each cytokine. Data are expressed as mean \pm SD of nine independent tissues. Statistical significance compared to control was calculated by one-way analysis of variance (ANOVA) followed by Dunnett test and * depicts $p < 0.05$ when sunscreen control is statistically different from the negative control showing an effect of the sunscreen with no nanoparticles added. ** depicts $p < 0.05$ when the samples are statistically different from the sunscreen control showing an effect of nanoparticles added to the sunscreen.

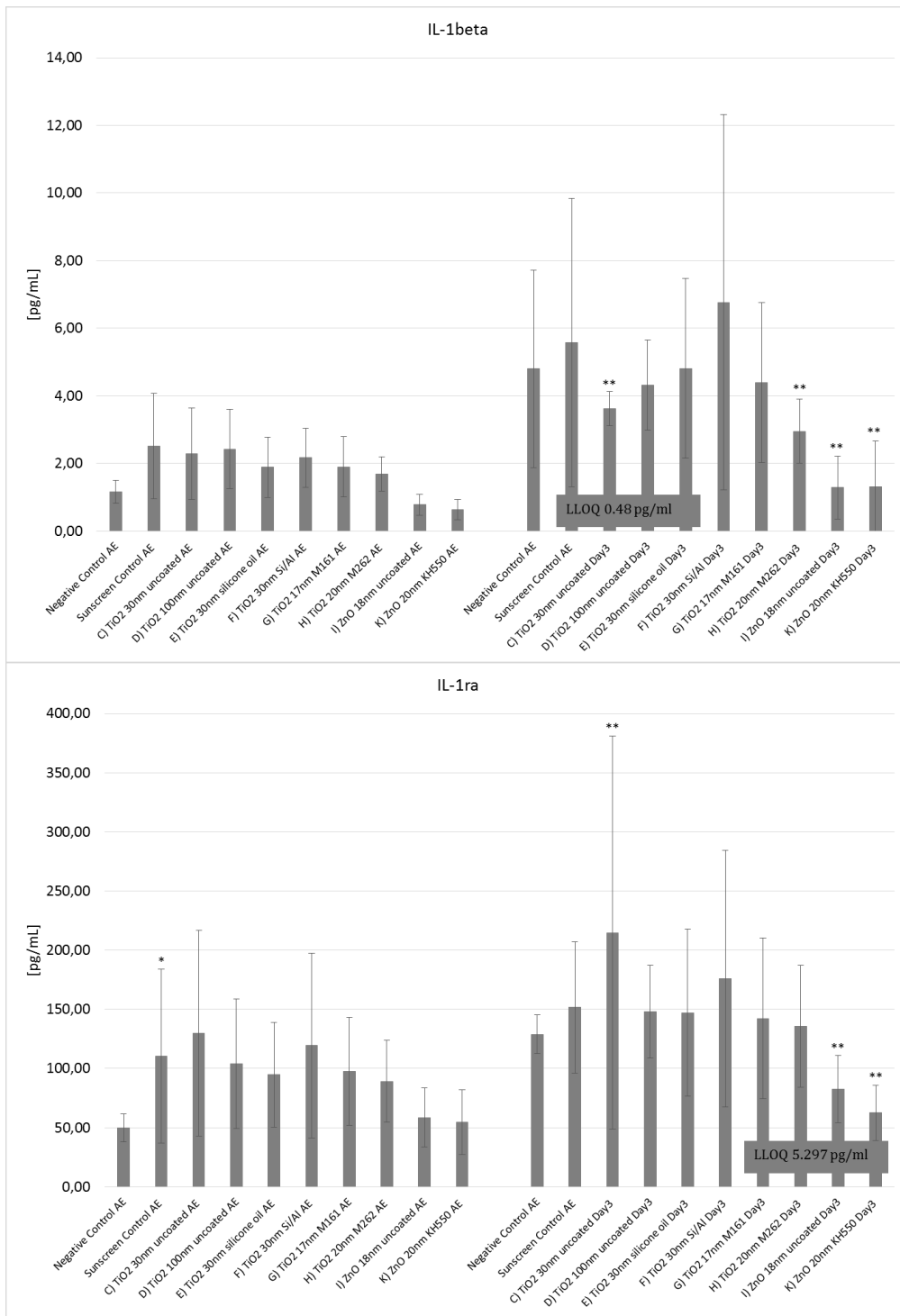


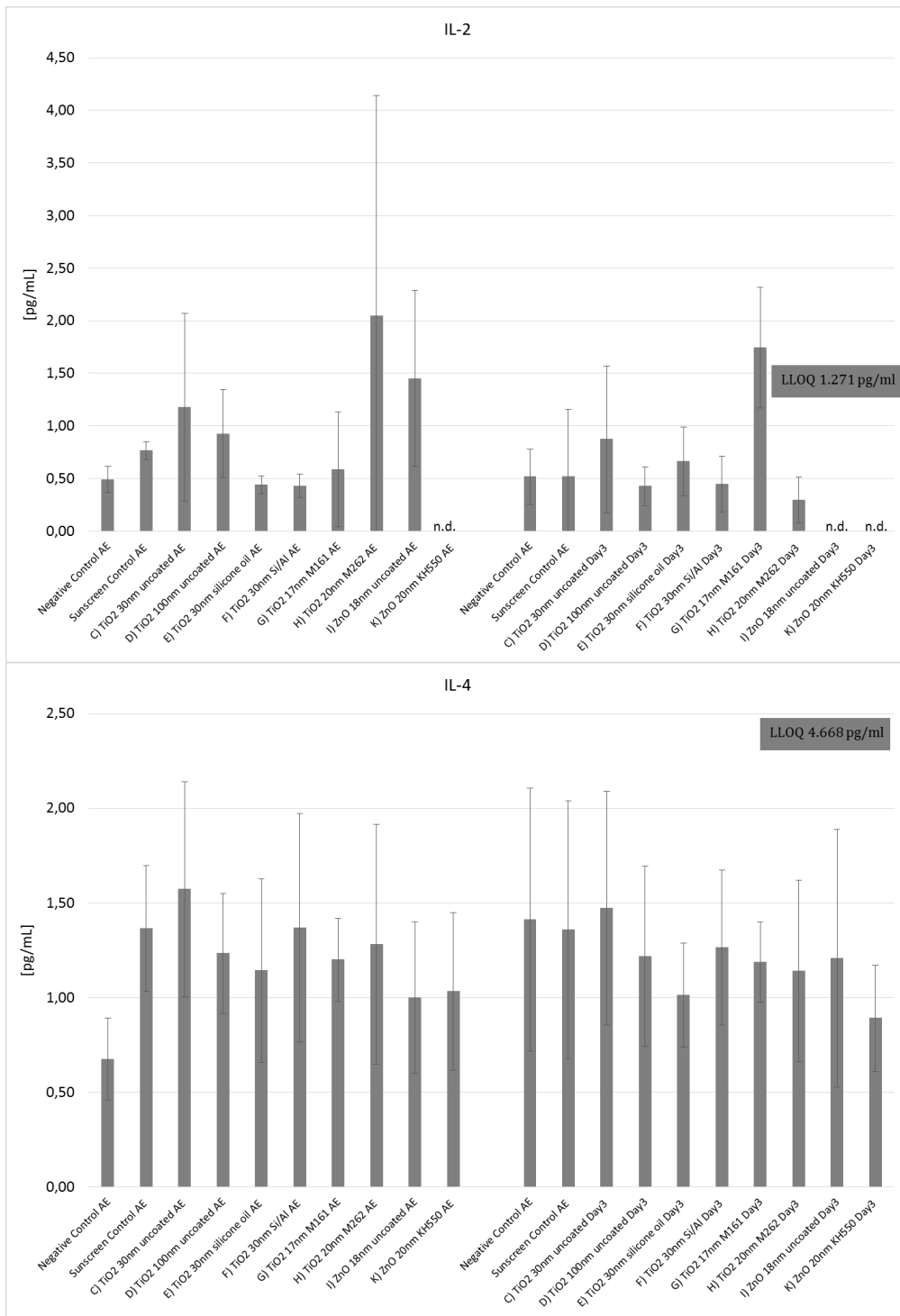


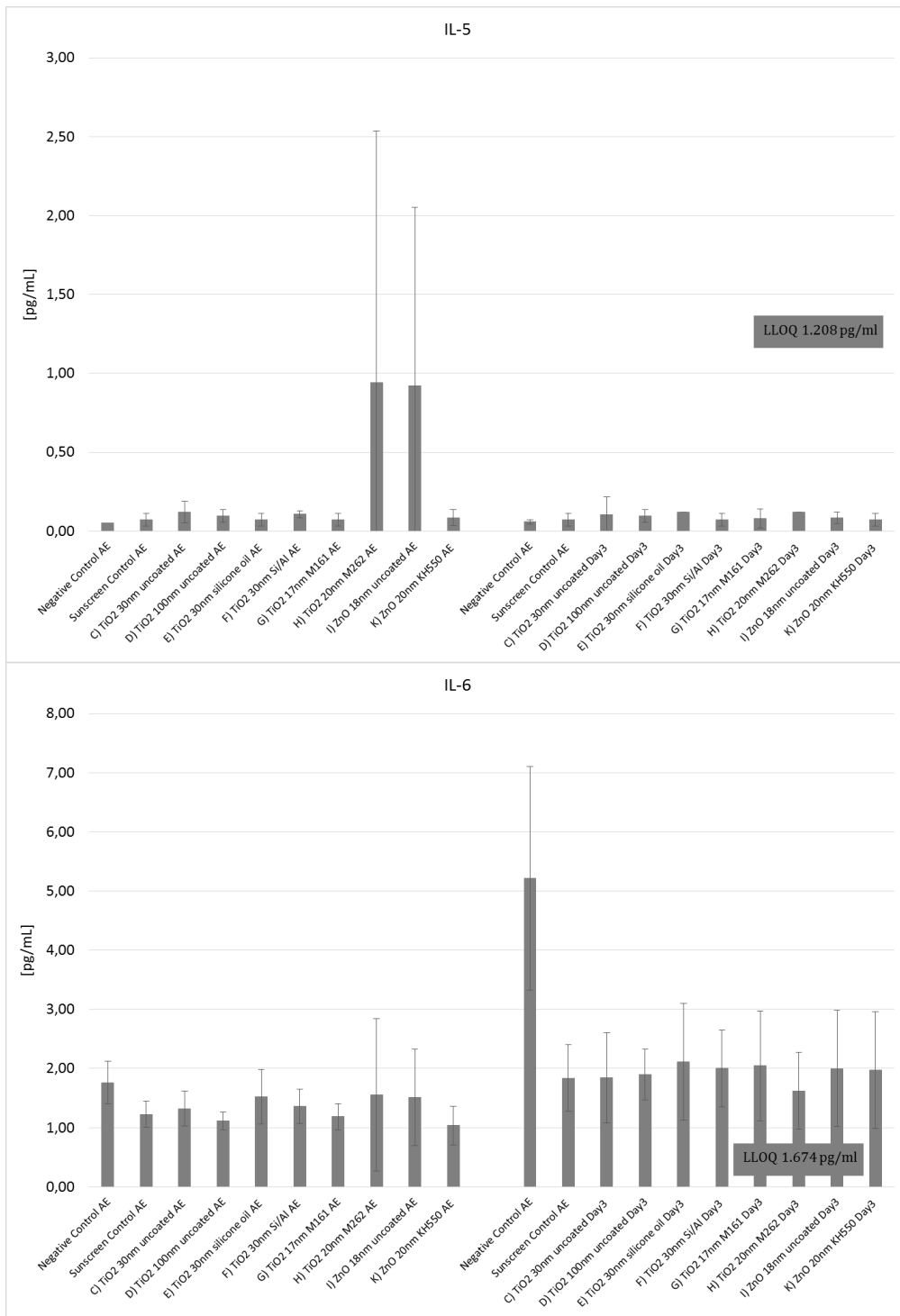


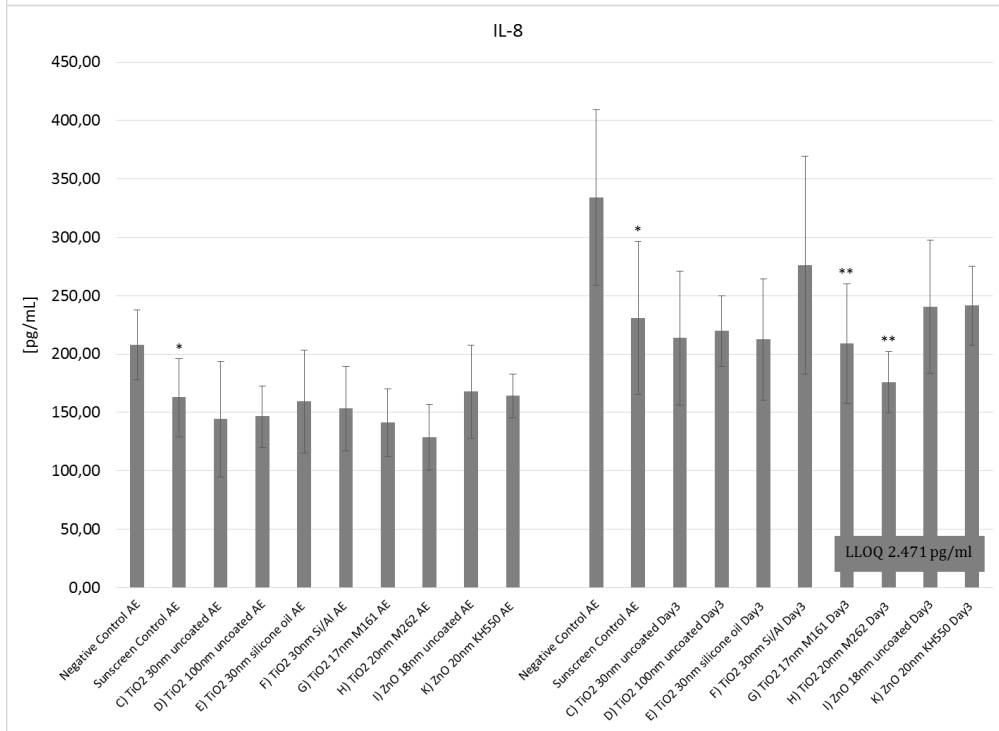
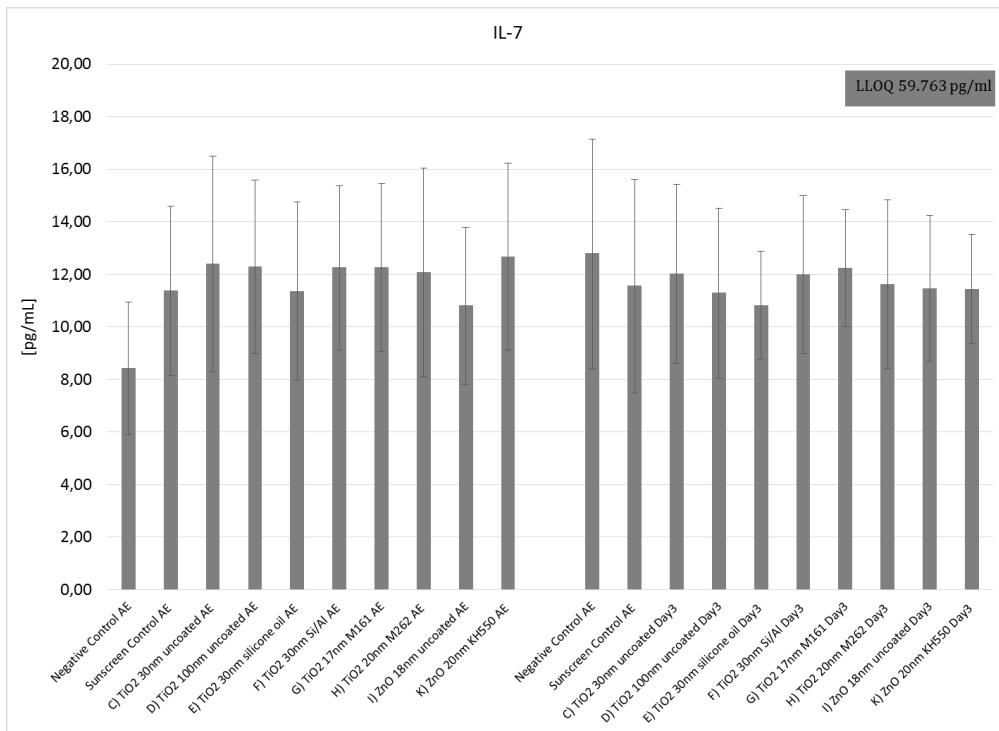


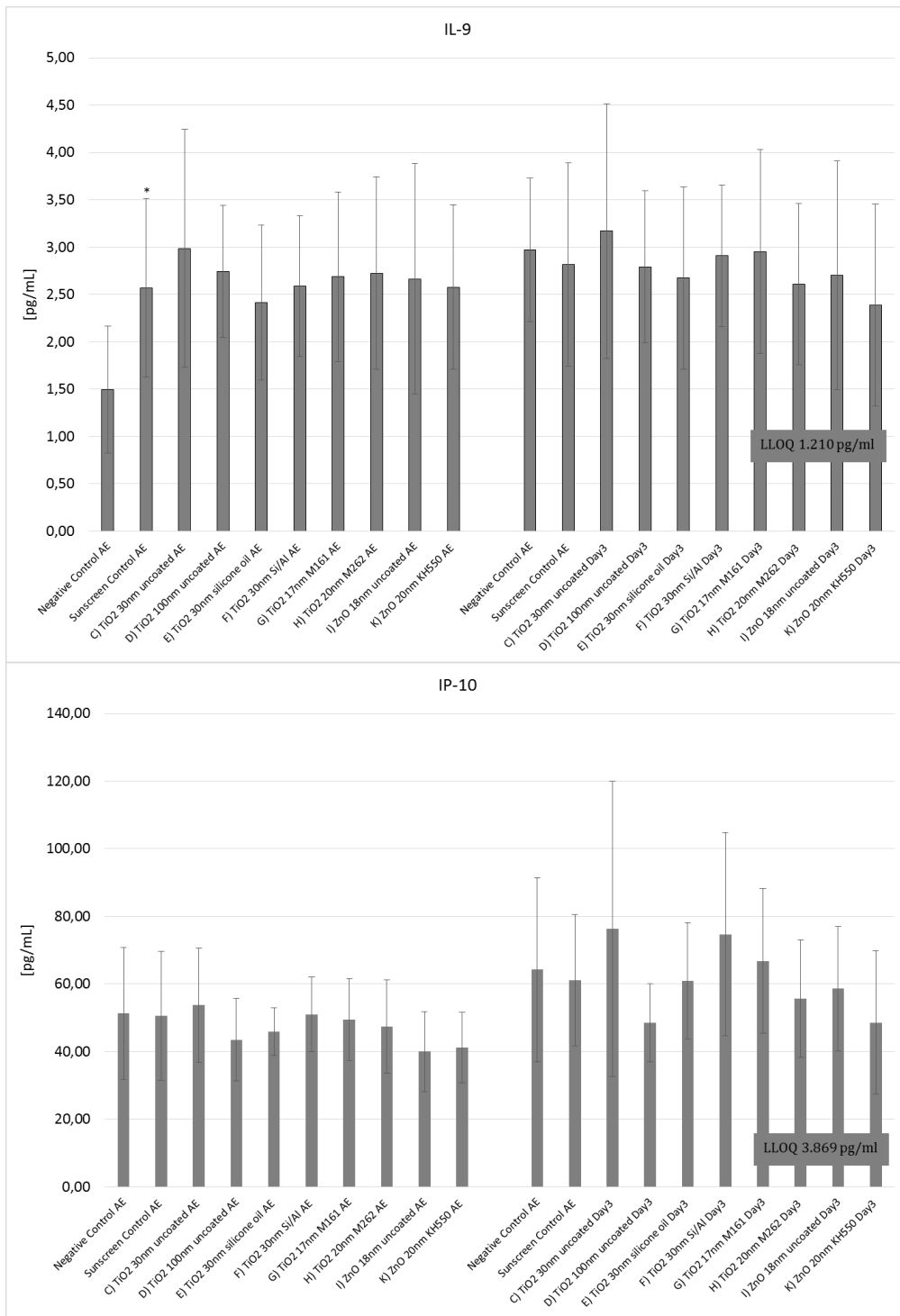


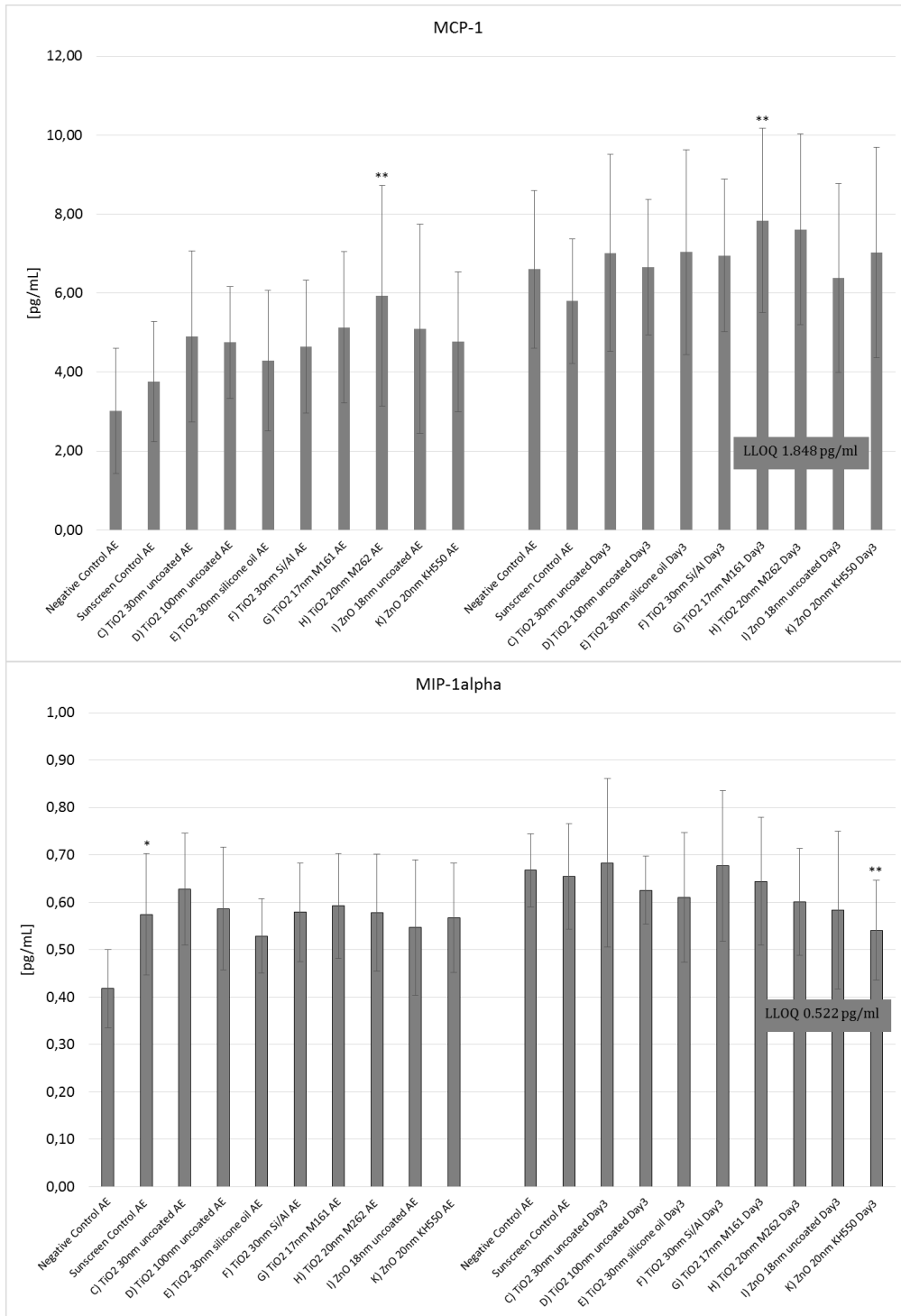


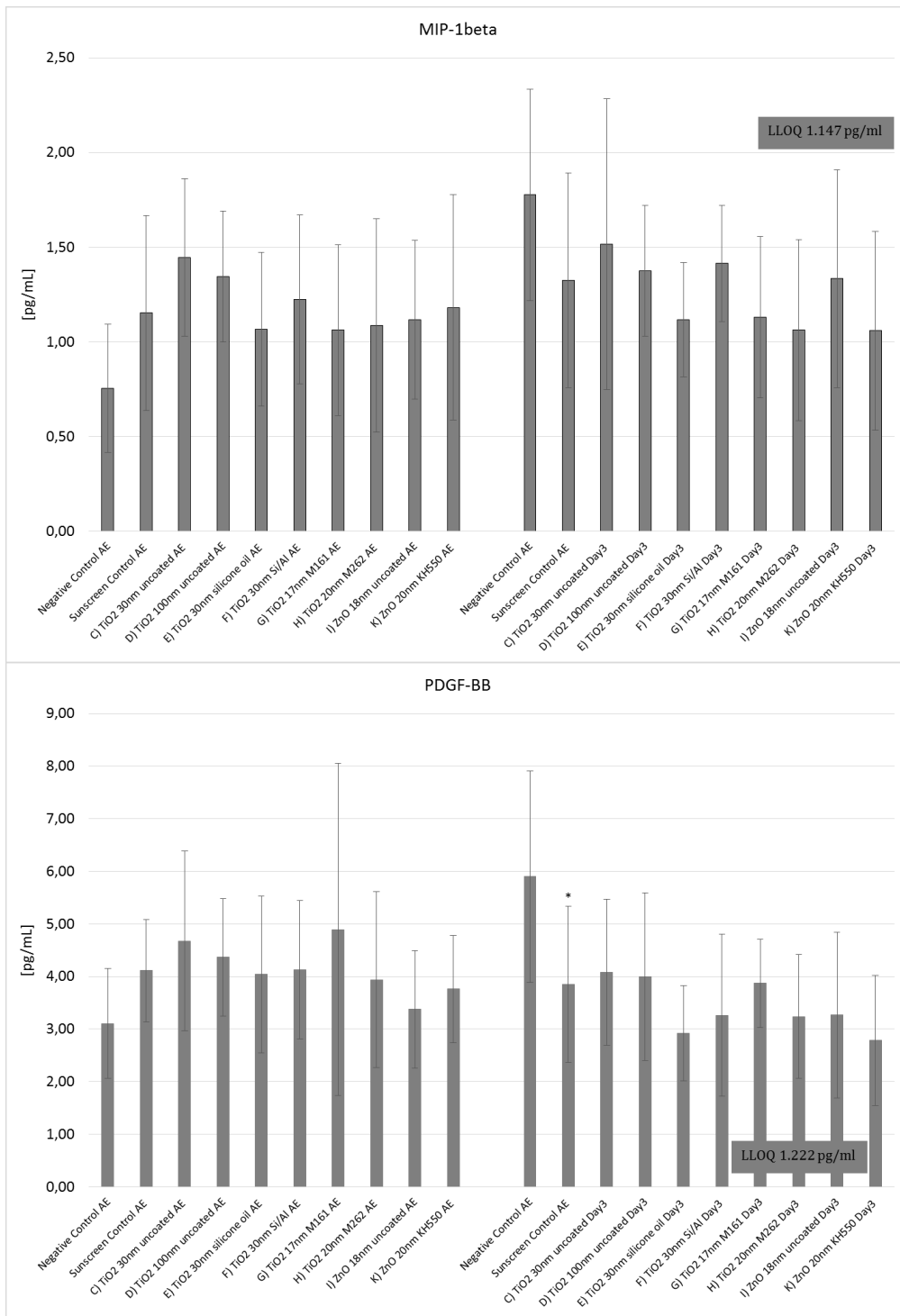


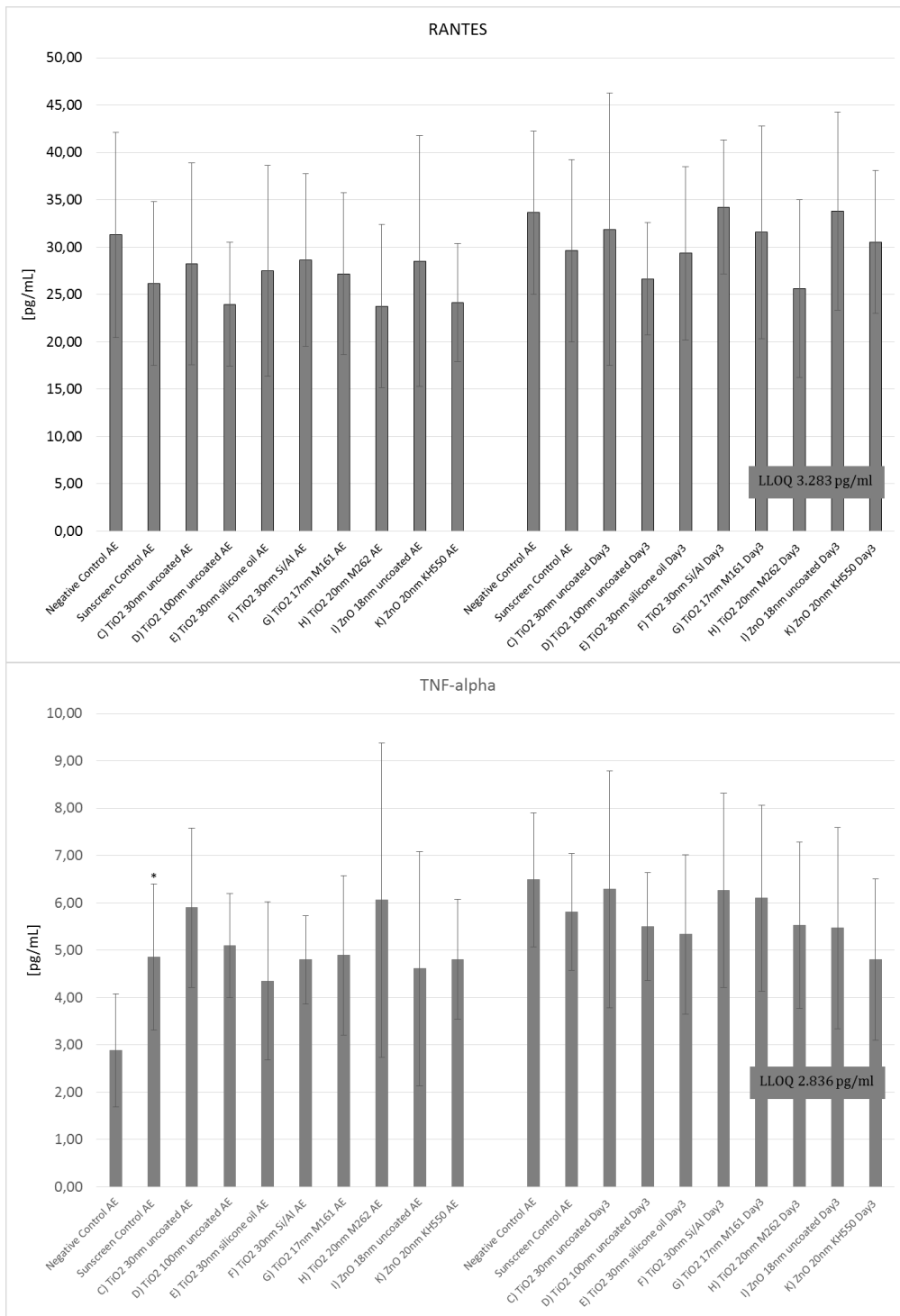


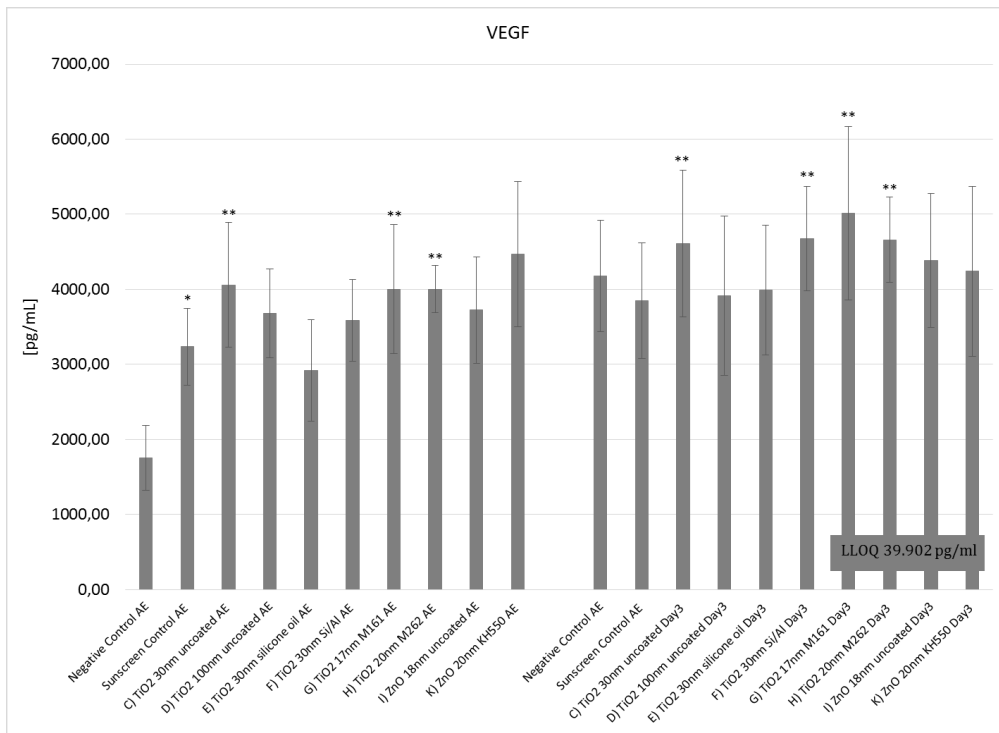












Appendix 7: Test report ICP-MS measurements of the *in vitro* and *in vivo* skin models: cell culture medium, mice ears and human skin

See next pages



Test Reg Nr 411



AARHUS
UNIVERSITET

DCE - NATIONALT CENTER FOR MILJØ OG ENERGI

Test report no. 802 Museører, hud og cellemedie

Customer: Christiane Beer

Sample collection: Christiane Beer

Sampling place: Unknown

Sampling time: Unknown

Sample type: Skin and media

Sampling performed by: Customer

Sampling methods: Unknown

Uncertainty in sampling: Unknown

Analyses performed by: University of Aarhus, Institute for bioscience
National Centre for Environment and Energy
Frederiksborgvej 399
4000 Roskilde

Date of analyses: October to December 2014

Analytical methods: Dissolution microwave Teflon bombs. Then ICP-MS

Uncertainty of measurement: The laboratory is by DANAK accredited to the uncertainties that are presented in the appendix.
The first line in the table is the “on the day” uncertainty calculated as 3 times the standard deviation of the blind measurements.

Notes: Blind values have been subtracted from all results.

Contact person: Gert Asmund

Appndix 1 :Uncertainties

Responsible for this report:

Gert Asmund, Senior scientist

Date: January 27 2014

The results represent only the samples that have been analysed

Underskrift

Media:

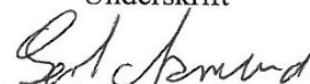
mikrogram/liter	Upper limit for Ti	Ca relativ	Zn	Ti Estimated
Reagensblind	2,02	49388	18	0,6
Reagensblind	1,43	50476	18	0,0
Reagensblind	2,07	49574	21	0,7
A1-3	3,06	75991	26	0,9
A4-6	2,79	74905	23	0,7
A7-9	3,65	78997	26	1,4
B1-3	2,18	74025	34	0,1
B4-6	2,42	76441	35	0,3
B7-9	3,26	79745	42	1,0
C1-3	2,56	74140	35	0,5
C4-6	2,63	73852	37	0,5
C7-9	2,65	76980	41	0,5
D1-3	3,22	71852	33	1,2
D4-6	3,50	75510	34	1,4
D7-9	3,80	79154	43	1,6
E1-3	3,16	76485	34	1,0
E4-6	3,61	77631	35	1,4
E7-9	3,00	81624	37	0,7
MilliQ	0,04	73	0	0,0
Reagensblind	2,21	52768	18	0,7
Reagensblind	2,28	54053	18	0,8
Reagensblind	2,46	54731	19	0,9
F1-3	3,57	74815	34	1,5
F4-6	3,76	77119	36	1,6
F7-9	5,28	78991	54	3,0
G1-3	3,09	75571	32	0,9
G4-6	3,18	75421	35	1,0
G7-9	5,22	81134	42	2,9
H1-3	3,63	74860	34	1,5
H4-6	3,61	74389	35	1,5
H7-9	3,96	80956	41	1,7
I1-3	3,22	76065	2395	1,1
I4-6	3,32	78385	2859	1,1
I7-9	2,38	82117	2980	0,1
K1-3	3,20	79099	2320	1,0
K4-6	3,73	77618	1599	1,5
K7-9	3,09	81242	3398	0,8

På grund af det høje indhold af Ca, Na, og Cl kan vi ikke måle Titan ordentligt. Vi kan med sikkerhed kun sige at det målte tal er det højeste titanindholdet kan være. Jeg har skønnet et titanindhold ved at antage at der ikke er titan i den laveste reagensblind og at interferensen er proportional med calciumindholdet. Det er selvfølgelig et meget usikkert skøn. Zink målingerne er alle langt over detektionsgrænsen på 1µg/L

Underskrift

Indvejning (g)	Prøveopløsning (g)	Indvejet (v/t)	Tørvægt%	Prøve		Ti (målt) mg/Kg tørt	Zn mg/Kg tørt	Ti (resultat) mg/Kg tørt
Detektionsgrænse (d.l.)					human hud		0,3	
0,06668	10,25	t	23,64	K1	Human hud	0,02	9,2	<0,15
0,02962	10,27	t	24,04	K2	Human hud	0,06	11,3	<0,34
0,06812	10,15	t	26,63	B1	Human hud	0,09	11,0	<0,15
0,08717	10,31	t	25,70	B2	Human hud	0,11	8,6	<0,11
0,11525	10,16	t	25,23	C2	Human hud	0,87	10,2	0,87
0,10335	10,23	t	25,16	C3	Human hud	0,21	9,4	0,21
0,10132	10,28	t	25,85	D2	Human hud	0,25	9,6	0,25
0,07586	10,21	t	25,98	D3	Human hud	0,32	9,6	0,32
0,06925	10,22	t	24,32	E1	Human hud	0,94	8,3	0,94
0,05521	10,26	t	29,07	E2	Human hud	0,30	9,0	0,30
0,12438	10,32	t	25,41	F1	Human hud	2,51	9,5	2,51
0,09362	10,3	t	25,29	F2	Human hud	1,80	9,1	1,80
Detektionsgrænse (d.l.)					museøre		0,6	
0,00622	10,39	t	82,32	UT1H	Museøre	-0,19	50,0	<1,6
0,00959	10,25	t	71,01	UT2H	Museøre	-0,08	38,5	<1,0
0,00465	10,19	t	69,46	UA1H	Museøre	4,49	35,7	4,49
0,00444	10,27	t	81,31	UA2H	Museøre	0,52	29,5	<2,3
0,00996	10,23	t	82,13	BT1H	Museøre	0,36	47,9	<1
0,02713	10,37	t	34,46	BT2H	Museøre	0,30	19,3	<0,4
0,0074	10,22	t	79,19	BA1H	Museøre	1,60	42,1	1,60
0,02075	10,22	t	40,92	BA2H	Museøre	0,25	21,6	<0,5
0,02008	10,39	t	55,28	CT1H	Museøre	17,62	32,5	17,62
0,01532	10,13	t	40,14	CT2H	Museøre	19,04	22,6	19,04
0,01773	10,29	t	50,99	CA1H	Museøre	12,97	22,9	12,97
0,00972	10,27	t	68,93	CA2H	Museøre	29,60	39,6	29,60
0,02602	10,34	t	38,51	DT1H	Museøre	6,40	20,3	6,40
0,02097	10,39	t	47,45	DT2H	Museøre	3,20	24,1	3,20
0,02355	10,28	t	41,10	DA1H	Museøre	19,54	22,1	19,54
0,01664	10,27	t	54,39	DA2H	Museøre	15,96	29,4	15,96
0,03018	10,23	t	34,72	ET1H	Museøre	16,42	20,1	16,42
0,02637	10,32	t	60,94	ET2H	Museøre	121,56	33,7	121,56
0,02127	10,28	t	37,19	EA1H	Museøre	57,92	20,7	57,92
0,01623	10,22	t	66,11	EA2H	Museøre	100,33	31,0	100,33
0,03027	10,2	t	35,12	FT1H	Museøre	32,04	19,7	32,04
0,02317	10,18	t	47,91	FT2H	Museøre	17,96	25,8	17,96
0,01469	10,4	t	58,68	FA1H	Museøre	27,10	33,3	27,10
0,01918	10,29	t	49,69	FA2H	Museøre	43,00	26,6	43,00
0,0204	10,19	v	86,57	Dolt-4	Ref.Mat.		99,6	
0,02283	10,36	v	86,57	Dolt-4	Ref.Mat.		106,5	
0,0199	10,24	v	86,57	Dolt-4	Ref.Mat.		102,8	
				<i>Certifikat</i>	<i>Ref.Mat.</i>		<i>100,4</i>	
0,02003	10,34	v	91,90	Tort-2	Ref.Mat.		167,3	
0,02146	10,27	v	91,90	Tort-2	Ref.Mat.		170,6	
				<i>Certifikat</i>	<i>Ref.Mat.</i>		<i>165,4</i>	

Underskrift



Appendix 1.

Accredited uncertainties for biota analyses. mg/Kg

Expanded uncertainty, k=2 (95% confidence)

Parameter	Detection limit on dry weight bases dl	Lower uncertainty U_{abs}	Upper Uncertainty U_{rel}
Cr	0,4	0,4	20%
Ni	0,3	0,3	15%
Cu	2	2	15%
Zn	5	5	15%
As	2	2	20%
Se	1	1	20%
Cd	0,1	6	15%
Pb	0,3	0,3	20%

Detection limit: The lowest result that is significant different from zero
The total uncertainty can be calculated from the formula:

$$U_C = \sqrt{U_{abs}^2 + U_{rel}^2 C^2};$$

For example: For a measurement of Se at 2 mg/Kg: $= U_C = \sqrt{0,2^2 + 0,10^2 2^2} = 0,3 \text{ mg/Kg}$

Where

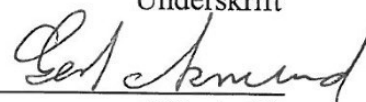
U_{abs} = Lower uncertainty: The absolute uncertainty dominating at the lower measuring level (Typically up to 5 times the detection limit This is the lowest uncertainty obtainable.

U_{rel} = Upper uncertainty: The relative uncertainty for samples with a high concentration. This is dominating when the concentration is more than 10 times the detection limit

Example: Calculate the uncertainty for a selenium measurement at 2mg/kg.

The formula gives $U_C = 2 \pm 0,3 \text{ mg/kg}$. This means that there is a 95% probability that the true result is between 1,7 and 2,3 mg/kg

Underskrift



Appendix 8: Certificate of analysis for the used lots of EpiDerm™ skin model

Certificate of Analysis



Product: EpiDerm™ Reconstructed Human Epidermis

Lot Number: 19645

Part#: EPI-200, EPI-212, EPI-218

Description: Reconstructed human epidermis tissue containing normal human keratinocytes. This product is for research use only. Not for use in animals, humans or diagnostic purposes.

I. Cell source

All cells used to produce EpiDerm™ are purchased or derived from tissue obtained by MatTek Corporation from accredited institutions. In all cases, consent was obtained by these institutions from the donor or the donor's legal next of kin, for use of the tissues or derivatives of the tissue for research purposes.

Keratinocyte Strain: 4F1188

II. Analysis for potential biological contaminants

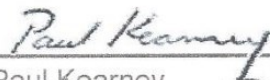
The cells used to produce EpiDerm™ tissue are screened for potential biological contaminants. Tests for each potential biological contaminant listed below were performed according to the test method given. Results of "Not detected" indicate that testing for the potential biological contaminant was not observed as determined by the stated test method.

HIV-1 virus – Oligonucleotide-directed amplification	Not detected
Hepatitis B virus – Oligonucleotide- directed amplification	Not detected
Hepatitis C virus – Oligonucleotide- directed amplification	Not detected
Bacteria, yeast, and other fungi – long term antibiotic, antimycotic free culture	Not detected

III. Analysis for tissue functionality and quality

Test	Specification	Acceptance criteria	Result and QA Statement	
Tissue viability	MTT QC assay, 4 hours, n=3	OD (540-570 nm) <1.0-3.0>	1.926 ± 0.051	Pass
Barrier function	ET-50 assay, 100 µL 1% Triton X-100, 4 time-points, n=3, MTT assay	ET-50 <4.77-8.72 hrs>	6.15 hrs	Pass
Sterility	Long term antibiotic and antimycotic free culture	No contamination	Sterile	Pass

Cell viability and the barrier function test are within the acceptable ranges and indicate appropriate formation of the epidermal barrier, the presence of a functional stratum corneum, a viable basal cell layer, and intermediate spinous and granular layers. Results obtained with this lot conform to the requirements of the OECD TG 431 and 439.


Paul Kearney
Quality Assurance Manager

June 18, 2014
Date

Initials: JK
Date: 18.06.2014

CAUTION: Whereas all information herein is believed to be correct, no absolute guarantee that human derived material is non-infectious can be made or is implied by this certificate of analysis. All tissues should be treated as potential pathogens. The use of protective clothing and eyewear and appropriate disposal procedures are strongly recommended.

MatTek In Vitro Life Science Laboratories, s.r.o

Mlynské Nivy 73, Bratislava - Slovak Republic
+421-2-3260-7401 | information@mattek.com

Certificate of Analysis

Product: EpiDerm™ Reconstructed Human Epidermis

Lot Number: **19650**

Part#: EPI-200, EPI-212, EPI-218

Description: Reconstructed human epidermis tissue containing normal human keratinocytes. This product is for research use only. Not for use in animals, humans or diagnostic purposes.

I. Cell source

All cells used to produce EpiDerm™ are purchased or derived from tissue obtained by MatTek Corporation from accredited institutions. In all cases, consent was obtained by these institutions from the donor or the donor's legal next of kin, for use of the tissues or derivatives of the tissue for research purposes.

Keratinocyte Strain: **4F1188**

II. Analysis for potential biological contaminants

The cells used to produce EpiDerm™ tissue are screened for potential biological contaminants. Tests for each potential biological contaminant listed below were performed according to the test method given. Results of "Not detected" indicate that testing for the potential biological contaminant was not observed as determined by the stated test method.

HIV-1 virus – Oligonucleotide-directed amplification	Not detected
Hepatitis B virus – Oligonucleotide- directed amplification	Not detected
Hepatitis C virus – Oligonucleotide- directed amplification	Not detected
Bacteria, yeast, and other fungi – long term antibiotic, antimycotic free culture	Not detected

III. Analysis for tissue functionality and quality

Test	Specification	Acceptance criteria	Result and QA Statement	
Tissue viability	MTT QC assay, 4 hours, n=3	OD (540-570 nm) <1.0-3.0>	1.837 ± 0.208	Pass
Barrier function	ET-50 assay, 100 µL 1% Triton X-100, 4 time-points, n=3, MTT assay	ET-50 <4.77-8.72 hrs>	6.74 hrs	Pass
Sterility	Long term antibiotic and antimycotic free culture	No contamination	Sterile	Pass

Cell viability and the barrier function test are within the acceptable ranges and indicate appropriate formation of the epidermal barrier, the presence of a functional stratum corneum, a viable basal cell layer, and intermediate spinous and granular layers. Results obtained with this lot conform to the requirements of the OECD TG 431 and 439.


Paul Kearney
Quality Assurance Manager

July 2, 2014
Date

Initials: **SK**
Date: **02.07.2014**

CAUTION: Whereas all information herein is believed to be correct, no absolute guarantee that human derived material is non-infectious can be made or is implied by this certificate of analysis. All tissues should be treated as potential pathogens. The use of protective clothing and eyewear and appropriate disposal procedures are strongly recommended.

MatTek In Vitro Life Science Laboratories, s.r.o

Mlynské Nivy 73, Bratislava – Slovak Republic
+421-2-3260-7401 | information@mattek.com

www.mattek.com

Certificate of Analysis



Product: EpiDerm™ Reconstructed Human Epidermis

Lot Number: 19661

Part#: EPI-200, EPI-212, EPI-218

Description: Reconstructed human epidermis tissue containing normal human keratinocytes. This product is for research use only. Not for use in animals, humans or diagnostic purposes.

I. Cell source

All cells used to produce EpiDerm™ are purchased or derived from tissue obtained by MatTek Corporation from accredited institutions. In all cases, consent was obtained by these institutions from the donor or the donor's legal next of kin, for use of the tissues or derivatives of the tissue for research purposes.

Keratinocyte Strain: 4F1188

II. Analysis for potential biological contaminants

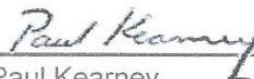
The cells used to produce EpiDerm™ tissue are screened for potential biological contaminants. Tests for each potential biological contaminant listed below were performed according to the test method given. Results of "Not detected" indicate that testing for the potential biological contaminant was not observed as determined by the stated test method.

HIV-1 virus – Oligonucleotide-directed amplification	Not detected
Hepatitis B virus – Oligonucleotide- directed amplification	Not detected
Hepatitis C virus – Oligonucleotide- directed amplification	Not detected
Bacteria, yeast, and other fungi – long term antibiotic, antimycotic free culture	Not detected

III. Analysis for tissue functionality and quality

Test	Specification	Acceptance criteria	Result and QA Statement	
Tissue viability	MTT QC assay, 4 hours, n=3	OD (540-570 nm) <1.0-3.0>	1.860 ± 0.276	Pass
Barrier function	ET-50 assay, 100 µL 1% Triton X-100, 4 time-points, n=3, MTT assay	ET-50 <4.77-8.72 hrs>	6.64 hrs	Pass
Sterility	Long term antibiotic and antimycotic free culture	No contamination	Sterile	Pass

Cell viability and the barrier function test are within the acceptable ranges and indicate appropriate formation of the epidermal barrier, the presence of a functional stratum corneum, a viable basal cell layer, and intermediate spinous and granular layers. Results obtained with this lot conform to the requirements of the OECD TG 431 and 439.


Paul Kearney
Quality Assurance Manager

August 6, 2014
Date

Initials: JK
Date: 06.08.2014

CAUTION: Whereas all information herein is believed to be correct, no absolute guarantee that human derived material is non-infectious can be made or is implied by this certificate of analysis. All tissues should be treated as potential pathogens. The use of protective clothing and eyewear and appropriate disposal procedures are strongly recommended.

MatTek In Vitro Life Science Laboratories, s.r.o

Mlynské Nivy 73, Bratislava - Slovak Republic
+421-2-3260-7401 | information@mattek.com

www.mattek.com

Dermal Absorption of Nanomaterials Titanium Dioxide and Zinc Oxide Based Sunscreen: Role of Size and Surface Coating

In this project, sunscreen containing nano TiO₂ was tested using in vitro and in vivo mouse and human skin models. Dermal penetration of TiO₂ and ZnO NPs did not occur at or above the limit of detection of the used experimental methods. This is in accordance with the conclusions that were made by the EU Scientific Committee on Consumer Safety that stated that both kind of nanoparticles are safe to use for dermal applications up to a concentration of 25% in cosmetic products [SCCS (Scientific Committee on Consumer Safety), 2012; SCCS (Scientific Committee on Consumer Safety), 2014].